New insights on the biogeochemical cycle of mercury in freshwater environments. Development and application of the DGT technique for bioavailability assessment and studies of methylmercury photodegradation

Cristal Fernández Gómez

UNIVERSITAT DE BARCELONA
UB

Facultat de Química

Departament de Química Analítica

Doctoral programme:

Química Analítica del Medi Ambient i la Pol·lució

Doctoral Thesis

New insights on the biogeochemical cycle of mercury in freshwater environments. Development and application of the DGT technique for bioavailability assessment and studies of methylmercury photodegradation

2014

Cristal Fernández Gómez

Directors

Prof. Josep M. Bayona Termens   **Dr. Sergi Díez Salvador**

Departament de Química Ambiental

Instituto de Diagnóstico Ambiental y Estudios del Agua (IDAEA)

Consejo Superior de Investigaciones Científicas (CSIC)

Tutor

José Fermín López Sánchez

Departament de Química Analítica

Facultat de Química

Universitat de Barcelona

Josep M. Bayona Termens, Professor d'Investigació del CSIC, i **Sergi Díez Salvador**, Científic Titular del CSIC, ambdós membres del Departament de Química Ambiental de l'Institut de Diagnosi Ambiental i Estudis de l'Aigua (IDAEA-CSIC),

CERTIFIQUEM

Que els estudis descrits a la present memòria que porta per títol, **"New insights on the biogeochemical cycle of mercury in freshwater environments. Development and application of the DGT technique for bioavailability assessment and studies of methylmercury photodegradation"** que presenta Cristal Fernández Gómez, Llicenciada en Ciències Ambientals, han estat realitzats sota la nostra direcció per optar al Títol de Doctor per la Universitat de Barcelona.

I perquè així consti, signem aquest certificat, amb el vistiplau del Tutor de la Universitat de Barcelona.

Barcelona , 7 de Març de 2014

Vist i plau
El tutor

Sergi Díez Salvador   Josep M. Bayona Termens   J. Fermín López Sánchez
Professor Titular
Departament de Química Analítica
Universitat de Barcelona

idÆa

C/ Jordi Girona, 18
08034 Barcelona. España
Tel. 93 400 61 00
Fax.: 93 204 59 04

ACKNOWLEDGEMENTS

En primer lugar, me gustaría expresarles mi agradecimiento a mis directores de tesis por su supervisión, consejos y correcciones durante estos 5 años, y sobre todo durante la redacción de la memoria. Al Prof. Josep M. Bayona quiero agradecerle que me haya permitido ser parte de su grupo de investigación, me haya ofrecido los medios para realizar este trabajo y haya mostrado siempre tan buena disposición para tratar los temas relativos a mi doctorado. A Sergi Díez, darle las gracias por "haberme fichado", por su cercana labor de dirección, su apoyo, su predisposición al diálogo y por haberme hecho sentir como en casa.

A mis compañeros del grupo de investigación, a los nuevos y a los viejos, darles las gracias de corazón por haber sido mi familia en el día a día, por aguantarme (que no es fácil), por ayudarme en tantos detalles dentro y fuera de lo profesional, por las charlas en la comida, y por nuestras salidas y actividades extracurriculares. A Luis agradecerle su labor mentora en mis comienzos en el mundo del mercurio. A Víctor, por su guía en mi breve incursión en el mundo de los compuestos orgánicos en el Guadalquivir. A Núria, por su cariño cuando yo no era más que la recién llegada. A Diana, a pesar de todo, decirle que fue un placer tenerla como compañera y amiga mientras duró. Carmen, mil gracias por tu alegría, por ser tan detallista y por ayudarme siempre a encontrar cualquier cosa en el lab 312. Gracias también por tus deliciosas y variadas tartas. Carolina, compañera de camino desde los inicios, te prometo que te iré a ver a Chile, amiga. Carla, tu llegada fue un soplo de aire fresco, y te convertiste en una gran amiga y confidente. Jagoš, gracias por tu ayuda informática y por preocuparte por mí. Sé que en ese chico de carácter cambiante venido de los Balcanes tendré un amigo para siempre. María, quién me iba a decir que aquella chica que me presentaron de pasada en León acabaría siendo mi compañera de trabajo en Barcelona! Ha sido un placer conocerte y tenerte con nosotros durante tus estancias y postdoc. Gracias por escucharme y brindarme tu amistad aún siendo las dos tan diferentes. Susana, gracias por las interminables charlas, los momentos reivindicativos, la aventura, los abrazos y por supuesto, la amistad. Ya lo sabía, pero ahora que escribiendo estas líneas se me humedecen los ojos, soy aún más consciente de lo importantes que habéis sido todos

para mí. Gracias también a Tami, Yolanda, Pablo, Cris, Wilkinson, Carles, Dani, Riccardo, a Inma por su ayuda en la sala de gases, a los miembros de otros grupos de investigación con los que tantas veces me he cruzado en los pasillos, Jornadas, pica-picas y calçotadas, y a muchos otros que han sido parte de mi periplo en el CSIC.

I feel really grateful for having the opportunity to do two research stays abroad. It is not only for what I learnt and the results I obtained, it is also for the fulfilling personal experiences that I had the chance to live. I would like to thank the research groups of Holger Hintelmann at Trent University, Ulf Skyllberg at SLU and Erik Björn at Umeå Universitet their help and support. To Holger, Ulf and Erik, thanks for accepting me to work with them, for their thorough supervision and for the facilities and resources they offered me. Joy Zhu, Brian Dimock, Andreas Drott, Solomon Tesfalidet, Lars Lambertsson, Rose-Marie Kronberg, Liem Nguyen, Vaughan Hurry and Bastiaan Brouwer deserve a special mention for their technical and research assistance. Thanks to Ana, Kyle, Emily and Jim, Tricia and the German girls for being my Canadian family; and to my buddy group, Nuria, the Czechs and IKSU frilufts crew for being my Swedish family. Thanks also to the rest of friends I made in Canada and Sweden, because you made me feel at home and you are undoubtedly part of this Thesis' story.

¿Y qué decir de mis amigos en Barcelona? ¡GRACIAS A TODOS POR HABER SIDO PARTE DE ESTA AVENTURA! Marta, nunca dejaré de agradecerte que decidieses ofrecerme tu amistad. Fuiste la primera persona que lo hizo en esta ciudad y te convertiste en un pilar fundamental en mi vida. Empezamos a coleccionar recuerdos en los cursos de doctorado, y ojalá sigamos coleccionándolos hasta el fin de nuestros días. Gracias a Porlad@s por las cenas, los cumpleaños y las escapadas. Gracias a mis amigos del Poliesportiu UPC por la energía, la locura, las fiestas y sobre todo porque un body pump o un body balance a vuestro lado y las charlas estirando o en el vestuario han sido la mejor terapia de desestrés. Gracias a mis compañeros de piso Edu, Jorge y María, porque también han sido mi familia. Gracias al Volley-team por la risoterapia y esos partidillos en la playa de Villa Olímpica me hacían salir de la rutina y pensar que vivir en Barcelona es un lujo. Mireia, gracias por tu espíritu todoterreno, aguantarme dentro y fuera del CSIC, por invitarme a tu casa, incluirme en tus planes e integrarme

entre tus amigos. Juani, me alegra que nuestra amistad creciese en los últimos años, me siento afortunada de tenerte como amiga. Gracias por tu espontaneidad, creatividad y generosidad. Mariana, me alegra que continúes en mi vida y seguir disfrutando de tu iniciativa y tus ganas de hacer cosas. Love u baby! Gracias también a Hade, Lisset, Cucu y las chicas de Filosofía Zen por estar ahí.

Aunque estén lejos, no quería olvidarme del resto de mis amigos. Sus llamadas, sus visitas, mis visitas, los comentarios en facebook, las conversaciones por whatsapp… hacen que de una forma u otra hayan estado presentes en esta etapa de mi vida. A mis amigos de Ferrolterra, darles las gracias por hacerme sentir que no ha pasado el tiempo, y Noe, gracias por las correcciones del resumen en gallego. A los de Celanova (mención especial a Nuria y Bea), por esas amistades de toda la vida. A los de León (residencia y carrera), por esos fuertes lazos que perduran a pesar del tiempo, y en concreto a León-as, por mantener ese grupo surgido en el Colegio Leonés hace ya más de 10 años, y a los miembros de Quintanilla 13 por seguir recibiéndome con los brazos abiertos. A mi familia Quetzal, ruteros y monis, porque han sido muy importantes para mí en este último año, y en especial a mis niñas del grupo 3, porque ya son como mis hermanas pequeñas.

No he sido capaz de empezar a escribir este párrafo sin antes ponerme a llorar como una magdalena. Gracias a mi pequeña pero muy unida familia por hacerme sentir tan querida. A mis abuelos, que afortunadamente aún a día de hoy me siguen regalando su amor y sabiduría. A mis tíos Gil y Eva, y mis primos Mario y Mireia, por abrirme las puertas de su casa en Huesca en cualquier momento y tenerme siempre presente en sus vidas. No tengo palabras para describir lo agradecida que les estoy a mis padres, José Manuel y Gisela. A vosotros os debo la vida, mi feliz e intensa infancia, el heredado carácter a veces complicado pero del que estoy orgullosa. Os agradezco vuestro amor incondicional, vuestra fe en mí, el hecho de jamás haberme condicionado en la toma de decisiones y nunca haberme pedido que me quedase cerca. Gracias por estar siempre por y para mí, por las largas conversaciones telefónicas a medianoche, por escucharme y animarme, por los paquetes, por darme alas y por ser el espejo en el que mirarme.

Creí que era una aventura y en realidad era la vida.

- Joseph Conrad-

TABLE OF CONTENTS

ABSTRACT

Mercury (Hg) is naturally present in the Earth's crust, however the historical use of this metal by the human being has spread and increased its presence in all types of environments. Both inorganic and organic species can be found in aquatic ecosystems, which are very sensitive to Hg pollution. In anoxic waters and sediments, sulphate-reducing bacteria can convert inorganic Hg into methylmercury (MeHg), a very toxic organic form which has the ability to bioaccumulate and biomagnify throughout trophic chains. Thus, to assess the risk associated to Hg, the development of techniques to monitor Hg levels in water is necessary, as well as investigating MeHg elimination pathways.

In this doctoral thesis, two aspects related to the biogeochemical cycle of Hg in freshwater are addressed. On one hand, a passive sampling technique –Diffusive Gradients in Thin films (DGT)– was developed both for determination of total Hg (THg) and MeHg in continental waters. Apart from providing a time-average Hg concentration, these samplers are able to measure the labile fraction of Hg, since they supposedly mimic biological membranes, and thus, the DGT technique is considered a good monitoring tool to estimate the bioavailability of Hg in water. On the other hand, MeHg photodegradation in freswhwaters dominated by dissolved organic matter (DOM) was studied.

Regarding the DGT technique, several preliminary tests were carried out both at the laboratory and in the field to test the validity of a commercial type of samplers (with thiol grups in the receiving gel) to measure the labile dissolved Hg in freshwater. Later, the performance of this commercial type was compared to that of two in-house manufactured samplers; both of them with the same receiving gel consisting of a resin with 3-mercaptopropyl groups embedded in a polyacrylamide gel, but one with an agarose gel (A-DGT) and the other with a polyacrylamide gel (P-DGT) as the diffusive layer. The uptake kinetics of Hg(II) and MeHg, both in the absence and in the presence of DOM, were studied. The diffusion coefficient, D, of Hg in the DGT diffusive layer varied among Hg species and also depended on the absence/presence of DOM in the

solution. This confirms the need to use the Hg species of interest and simulate the characteristics of the water to be sampled when performing the DGT calibration, if the aim is to accurately measure the labile Hg fraction. The P-DGT type was chosen as the most appropriate to determine both THg and MeHg in natural waters. Thereby, this type of sampler was used in a case study to assess the removal, methylation and lability of Hg(II) in a experimental scale plant for wastewater treatment consisting in several constructed wetlands with different conformation in series.

With respect to the MeHg photodegradation issue, this phenomenon was studied in waters from a lake-wetland gradient in boreal Sweden. The influence of the DOM on this process by attenuating light, forming reactive oxygen species and binding MeHg to its thiol groups to form complexes, was examined. It was observed that the desmethylation rate constant ($k_{pd\ Full\ Spectrum}$) varied significantly among the studied waters, but the wavelength-specific rate constants (k_{pdPAR}, k_{pdUVA} and k_{pdUVB}) were indistinguishable. Therefore, $k_{pd\ PAR}$, $k_{pd\ UVA}$ and $k_{pd\ UVB}$ can be considered universal, at least in waters dominated by DOM and in which MeHg is complexed by organic thiols, if the photon fluxes of PAR, UVA and UVB radiation are separately determined and the wavelength-specific light attenuation by DOM is corrected for. Furthermore, the relationship between the photodegradation and bioavailability of MeHg was examined in an experiment involving different types of natural and artificial freshwater and the DGT technique, but no apparent connection was observed between them.

RESUM

El mercuri (Hg) és un element present de forma natural en la escorça terrestre, tanmateix l'ús històric d'aquest metall per l'ésser humà ha estès i augmentat la seva presència al medi ambient. Tant les espècies inorgàniques com les orgàniques es poden trobar als ecosistemes aquàtics i afectar-los. En aigües i sediments anòxics, els bacteris sulfatreductors són els que majoritàriament poden metilar el Hg inorgànic a metilmercuri (MeHg), la forma orgànica més tòxica, que té la capacitat de bioacumular-se i biomagnificar-se al llarg de la cadena tròfica. Per tant, per avaluar el risc associat al Hg és necessari el desenvolupament de tècniques per controlar els nivells de les diferents especies de Hg al medi aquàtic, així com la determinació de la fracció biodisponible, i també l'estudi de les possibles vies d'eliminació de MeHg.

En aquesta tesi doctoral s'aborden dos aspectes relacionats amb al cicle biogeoquímic del Hg en aigües continentals. Per una banda, es va desenvolupar un sistema de mostreig passiu denominat gradients de difusió en capa fina (DGT), per la determinació del Hg total i del MeHg en fase aquosa. Aquests mostrejadors proporcionen la concentració mitjana de Hg durant el temps de mostreig i mesuren la fracció làbil de Hg, donat que mimetitzen les membranes biològiques. Per tant, la tècnica de DGT pot ser considerada una bona eina per avaluar la biodisponibilitat de Hg a l'aigua. D'altra banda, es va estudiar la fotodegradació de MeHg en aigües dolces amb un alt contingut en matèria orgànica dissolta (DOM).

Pel que fa a la tècnica DGT, es van dur a terme diverses proves preliminars tant al laboratori com en el camp per provar la validesa d'un tipus comercial de mostrejador (amb un agent lligant amb grups tiol) per mesurar el Hg dissolt i col·loidal làbil en aigua dolça. El seu funcionament es va comparar amb el de dos tipus de mostrejadors DGT manufacturats al laboratori; tots dos amb el mateix gel receptor format per una resina amb grups 3-mercaptopropil embegut en un gel de poliacrilamida i amb filtre de nylon, però amb diferent gel de difusió, un d'ells és d'agarosa (A-DGT) i l'altre de poliacrilamida (P-DGT). Es van estudiar les cinètiques d'acumulació de Hg(II) i MeHg de tots els mostrejadors, tant en absència com en presència de DOM. El coeficient de

difusió, D, de Hg en la capa de difusió de DGT varia entre espècies de Hg i, a banda d'altres factors, és molt depenent de la presència/absència de DOM en la dissolució. Això confirma la necessitat de calibrar els DGT rigorosament utilitzant la espècie de Hg d'interès i simular les característiques de l'aigua que posteriorment serà mostrejada. El P-DGT va ser escollit com el més apropiat per determinar ambdós THg i MeHg en aigües naturals. Així, aquest tipus de mostrejador va ser utilitzat en un estudi de cas per avaluar l'eliminació, metilació i labilitat de Hg(II) en una planta a escala experimental pel tractament d'aigües residuals urbanes que consisteix en diversos aiguamolls construïts amb diferent conformació en sèrie.

Pel que fa a la fotodegradació de MeHg, aquest fenòmen va ser estudiat en aigües d'un gradient llac-aiguamoll en la Suècia boreal. Es va estudiar la influència de DOM en aquest procés, be sigui atenuant la llum, tot formant espècies reactives d'oxigen o bé unint el seus grups tiol al MeHg per formar complexos. Es va observar que la constant de velocitat de fotodesmetilació ($k_{pd\ Full\ Spectrum}$) va variar significativament entre les aigües estudiades, però les constants de velocitat específiques per a cada longitud d'ona (k_{pdPAR}, k_{pdUVA} and k_{pdUVB}) van ser indistingibles per a les mateixes aigües. Per això, $k_{pdPAR,}$ k_{pdUVA} and k_{pdUVB} poden ser considerades universals. Això és cert en aigües amb un alt contingut en DOM i on el MeHg estigui complexat per grups tiols orgànics, sempre i quan els fluxes de fotons de PAR, radiació UVA i radiació UVB siguin determinats per separat i corregits per l'atenuació de la llum per DOM específica per a cada longitud d'ona. Finalment, amb la utilització de la tècnica DGT es va estudiar la possible influència que pot existir entre la fotodegradació i la biodisponibilitat de MeHg en diversos tipus d'aigues dolces naturals i artificials, però no es va observar cap connexió aparent entre elles.

RESUMO

O mercurio (Hg) atópase presente de forma natural na codia terrestre, non obstante o uso histórico deste metal polo ser humano estendeu e aumentou a súa presenza en todos os tipos de ambientes. Nos ecosistemas acuáticos, moi sensibles á contaminación por Hg, poden atoparse tanto especies inorgánicas coma orgánicas deste elemento. As bacterias redutoras de xofre, presentes en augas e sedimentos anóxicos, poden converter o Hg inorgánico en metilmercurio (MeHg), unha forma orgánica moi tóxica que ten a habilidade de se bioacumular e biomagnificar ó longo das cadeas tróficas. Estas son as razóns polas que se considera necesario o desenvolvemento de técnicas para controlar os niveis de Hg na auga, así como a investigación de vías de eliminación de Hg.

Nesta tese doutoural abórdanse dous aspectos relacionados co ciclo bioxeoquímico do Hg en auga doce. Por un lado, unha técnica de mostraxe pasiva para a determinación de metais en fase acuosa –Gradientes de difusión en capa fina (DGT)– desenvolveuse para medir Hg total (THg) e MeHg. Ademais de proporcionar a concentración media durante o tempo de mostraxe, estes mostradores miden a fracción lábil de Hg, xa que mimetizan as membranas biolóxicas, e polo tanto, a técnica DGT é considerada unha boa ferramenta para estimar a biodispoñibilidade do Hg na auga. Por outro lado, estudiouse a fotodegradación do MeHg en augas doces dominadas por materia orgánica disolta (DOM).

Polo que respecta á técnica DGT, diversas probas preliminares foron levadas a cabo tanto no laboratorio como no campo para probar a validez dun tipo comercial de mostrador (cunha resina con grupos tiol no xel receptor) para medir Hg en auga doce. Despois, o funcionamento deste tipo comercial foi comparado co doutros dous tipos de mostradores elaborados por nós facendo cinéticas de acumulación de Hg(II) e MeHg, tanto en ausencia coma na presenza de DOM. O coeficiente de difusión, D, do Hg na capa de difusión de DGT variou entre especies de Hg e tamén dependeu do feito de que houbese DOM en disolución ou non. Este feito confirma a necesidade de

empregar na calibración a especie de Hg de interese e simular as características da auga que logo será mostrada, co obxectivo de medir a fracción lábil de Hg con exactitude. O mostrador auto-elaborado (con xel de sílice funcionalizado con grupos 3-mercaptopropil coma axente ligante, e xel de poliacrilamida e un filtro de membrana de nailon coma capa de difusión; P-DGT) foi escollido coma o máis axeitado para determinar tanto THg coma MeHg en augas naturais. Deste xeito, P-DGT foi empregado nun estudo de caso para avaliar a eliminación, metilación e labilidade de Hg(II) nunha planta a escala experimental para o tratamento de augas residuais que consiste en varias brañas construídas en serie con diferentes configuracións.

En relación ó tema da fotodegradación do MeHg, este fenómeno estudiouse en augas dun gradiente lago-braña na Suecia boreal. Examinouse a influencia da DOM neste proceso ben sexa atenuando a luz, formando especies reactivas de osíxeno ou unindo os seus grupos tiol ó MeHg para formar complexos. Observouse que a constante de velocidade de fotodesmetilación ($k_{pd\ Full\ Spectrum}$) variou significativamente entre as tres augas estudiadas, pero as constantes específicas para cada lonxitude de onda (k_{pdPAR}, k_{pdUVA} and k_{pdUVB}) foron indistinguibles para as mesmas tres augas. Por iso, k_{pdPAR}, k_{pdUVA} and k_{pdUVB} poden considerarse universais, polo menos en augas dominadas por DOM nas cales o MeHg estea complexado por tioles orgánicos, se os fluxos de fotóns de PAR, radiación UVA e radiación UVB son determinados por separado e corrixidos pola atenuación por DOM específica para cada lonxitude de onda. Ademais, a relación entre a fotodegradación e a biodispoñibilidade do MeHg foi examinada nun experimento que implicou diversos tipos de auga doce natural e artificial con caracterísiticas diferentes, pero non se observou ningunha conexión directa entre elas.

LIST OF ACRONYMS

AAS	Atomic absorption spectrometry
AES	Atomic emission spectrometry
AFS	Atomic fluorescence spectrometry
AMA	Automatic mercury analyser
ANG	Ängessjön
AR	Aqua regia, 1:3 HNO_3:HCl
AS	Ascó
ATSDR	Agency for toxic substances and disease registry
A-DGT	In-house manufactured DGT sampler with agarose diffusive gel
BOD$_5$	biochemical oxygen demand over a 5-day period
BU	Búbal
CAR	Carboxen
CDOM	Chromophoric groups in dissolved organic matter
COD	Chemical oxygen demand
CRM	Certified reference material
CV	Cold vapour
CW	Constructed wetland
CVAAS	Cold vapour atomic absorption spectrometry
CVAFS	Cold vapour atomic fluorescence spectrometry
C-DGT	Commercial DGT sampler
D	Diffusion coefficient
DBL	Diffusive boundary layer
DET	Diffusive equilibrium in thin films
DGT	Diffusive gradients in thin films
DMA	Direct mercury analyser
DOC	Dissolved organic carbon
DOM	Dissolved organic matter
D$_{Hg(II)-DOM}$	Diffusion coefficient of Hg(II) in the DGT diffusive layer in the presence of DOM in solution

DHg^{2+}	Diffusion coefficient of Hg(II) in the DGT diffusive layer in the absence of DOM in solution
D_{MeHg}	Diffusion coefficient of MeHg in the DGT diffusive layer
$DMeHg^{+}$	Diffusion coefficient of MeHg in the DGT diffusive layer in the absence of DOM in solution
$D_{MeHg\text{-}DOM}$	Diffusion coefficient of MeHg in the DGT diffusive layer in the presence of DOM in solution
D_{THg}	Diffusion coefficient of THg in the DGT diffusive layer
DVB	Divinylbenzene
ECD	Electron capture detector
EPR	Electron paramagnetic resonance spectroscopy
EQS	Environmental quality standards
ETAAS	Electrothermal atomic absorption spectrometry
EtHg	Ethylmercury
EU	European Union
exp #1	MeHg photodegradation experiment with natural sunlight
exp #2	MeHg photodegradation with light from an artificial source with a higher proportion of UVB
FEP	Fluorinated ethylene propylene
FLX	Flix
FR	Flix reservoir
FW	Flix reservoir by high-load mercury sediments/wastes
FWS	Free water surface
GC	Gas chromatography
HF	Horizontal Flow
Hg^{0}	Elemental mercury
Hg^{2+}	Mercuric ion, free ionic inorganic mercury
Hg(II)	Inorganic mercury
Hg(P)	Mercury associated to particulate matter
HLR	Hydraulic loading rate
HPLC	High performance liquid chromatography

16

HS	Headspace
HRT	Hydraulic retention time
IARC	International Agency for Research on Cancer
IC	Ion chromatography
ICP	Inductively coupled plasma
ID	Isotope dilution
IHSS	International Humic Substances Society
IUPAC	International Union of Pure and Applied Chemistry
JB	Jabarrella
k_{pd}	MeHg photodegradation rate constant
KSN	Kroksjön
LDPE	Low-density polyethylene
LOD	Limit of detection
LOQ	Limit of quantification
MeHg	Methylmercury
MIP	Microwave induced plasma
MQO	MilliQ water (NaCl 0.01M, 10 mg OC L^{-1})
MQW	MilliQ water (NaCl 0.01M)
MS	Mass spectrometry
NaBEt$_4$	Sodium tetraethylborate
NaBPh$_4$	Sodium tetraphenylborate
NaBPr$_4$	Sodium tetrapropylborate
NH$_4$-N	Ammonium nitrogen
NRCC	National Research Council Canada
NS	7:3 HNO_3:H_2SO_4
OES	Optical emission spectrometry
OLR	Organic loading rate
PAR	Photosynthetically active radiation
PAR$_{IN}$	Photosynthetically active radiation measured inside the bottle
PDMS	Polydimethylsiloxane
PDY	Photodegradation yield

PET	Polyethylene terephthalate
PIMS	Passive integrative mercury sampler
PLM	Permeation liquid membrane
PTFE	Polytetrafluoroethylene, Teflon
P&T	Purge and trap
Py	Pyrolysis
P-DGT	In-house manufactured DGT sampler with polyacrylamide diffusive gel
QC & QA	Quality control and quality assurance
QFAAS	Quartz furnace atomic absorption spectrometry
RB	Riba-roja
ROS	Reactive oxygen species
RSD	Relative standard deviation
RSE	Relative standard error
RSH	Thiol group
SA	Sabiñánigo
SD	Standard deviation
SE	Standard error
SKM	Stor-Kälsmyran
SLM	Supported liquid membranes
SLMD	Stabilized liquid membrane device
SPME	Solid phase microextraction
SSF	Subsurface flow
S XANES	Sulfur X-ray absorption near-edge spectroscopy
TEMED	N,N,N',N'-Tetramethylethylenediamine
Tg	Teragram, 10^{12} g
THg	Total mercury
TOC	Total organic carbon
TON	Total organic nitrogen
TSS	Total suspended solids
TWA	Time-weighted average
UNEP	United nations environment programme

USEPA	United States Environment protection agency
UVA	Ultraviolet A (wavelength range: 320-400 nm)
UVB	Ultraviolet B (wavelength range: 208-320 nm)
VCM	Vinyl chloride monomer
VF	Vertical flow
WHO	World health organization

STRUCTURE OF THE THESIS

This thesis is organized in four parts. Part I includes two chapters: Chapter 1 and Chapter 2. Chapter 1 is the general introduction, and presents information that allows knowing more about Hg and its environmental problematic. Hg properties, applications, emission sources, biogeochemical cycle, toxicity and legal regulation, are described. In this first chapter, there is also one section focused on the analytical methodologies employed for Hg determination. A section discussing the concept of metal bioavailability was included to a better understanding of this thesis topic. Furthermore, another section on passive sampling and the DGT technique was considered necessary in order to introduce most of the work done within this thesis; and finally, the MeHg photodegradation issue was addressed. Chapter 2, in which we find ourselves, lists the objectives and describes the structure of the thesis.

The experimental work, results and discussion are reported in Part II and Part III. Part II is focused on the first general objective of the present thesis, and comprises three chapters: Chapter 3, Chapter 4 and Chapter 5. Chapter 3 reports the preliminary work and tests done with the DGT technique; Chapter 4, the further development of the technique to determine Hg(II) and MeHg; and Chapter 5, the application of the DGT technique in a specific study.

Part III, on the other hand, is focused on the second general objective, and contains two chapters: Chapter 6 and Chapter 7. Chapter 6 addresses a in-depth study on MeHg photodegradation in lake and wetland waters; and Chapter 7 reports a study aimed to examine the conection between photodegradation and bioavailability.

Part IV consists of an only chapter: Chapter 8, where the general conclusions are enumerated.

Finally, there is a summary of the thesis in Spanish and a section named Annexes, comprising Annex I, Annex II and Annex III. Annex I gives information about the methodology for analysis of MeHg in sediment samples. Annex II reports the additional

work performend to accomplish the study on Chapter 6. Eventually, Annex III contains a list of the papers related to the thesis content that were published in scientific journals.

PART I

Chapter 1

General Introduction

1   General Introduction

1.1   Mercury

1.1.1   Physicochemical properties

Mercury –Hg, Hydrargyrum (from the latinised Greek, "liquid silver")– is a heavy metal characterised for being the only one in liquid state at ambient temperature and pressure. It is a highly dense metal (density at 20 °C: 13.579 g cm^{-3}), with the lowest melting point among metals (-38.87 °C) and a boiling point of 356.58 °C.

Hg possesses widespread ubiquity on the Earth's surface, thus, any product, natural or artificial, will have at least Hg traces. This is due both to its capability of amalgamation with other metals and to the rest of physicochemical properties, among which its low specific heat (138 J kg^{-1} K^{-1}), low electrical resistivity (95.76 μohm cm a 20 °C), high thermal conductivity (8.34 W m^{-1} K^{-1}), high surface tension (480.3 din cm^{-3}), and high vapour pressure (0.16 Pa) can be highlighted.

Hg has seven stable isotopes (with an atomic weight of 196, 198, 199, 200, 201, 202, 204; whose percentage abundances in the environment are 0.146%, 10.02%, 16.84%, 23.13%, 13.22%, 29.80% and 6.85%, respectively) and four radioactive isotopes (194, 195, 197, 203). Moreover, it can appear in three oxidation states: elemental or metallic mercury (Hg^{0}), monovalent mercury (Hg(I), main inorganic form: mercurous ion, Hg$_2^{2+}$) and divalent mercury (Hg(II), main inorganic form; mercuric ion, Hg^{2+}). Except from the atmosphere, where most of the Hg is Hg^{0} vapour, in the rest of the environmental compartments, Hg is found essentially as inorganic salts (HgCl$_2$, Hg(OH)$_2$, HgS) and organic forms (methylmercury, MeHg^{+}; dimethylmercury, Me$_2$Hg; and to a lesser extent, ethylmercury, EtHg^{+}; and phenylmercury, PhHg^{+}) of Hg(II). However, Hg(I) is not quantitatively significant in nature.

In this doctoral thesis, the term inorganic Hg or Hg(II) is used to denote the Hg species with divalent oxidation state, without including the organometallic compounds. The expression Hg^{2+} can appear in some occasions referring only to the

inorganic mercury free ions. When talking about methylmercury, the expression MeHg is chosen. It includes both the free ions (MeHg$^+$) and the complexes with MeHg as central ion. The same criteria works for ethylmercury, hereafter referred as EtHg.

1.1.2 Applications

Hg and its principal mineral, cinnabar (HgS), are known and used since antiquity. Already in the Upper Paleolithic period (33,000-9,000 B.C.), vermilion (cinnabar powder) was employed as red pigment in cave paintings such those in Altamira or Lascaux. Civilisations like China, India, Egypt and Assyria, also used this mineral several millenniums before the Christian era. However, the uses of Hg have grown and diversified hugely since then. The most remarkable ones in recent times are listed below:

- Pigments and colourants
- Biocide in the paper industry, in paints and seeds deposits
- Fungicides and agro formulations
- Antiseptic in pharmaceuticals and cosmetics
- Gold and silver extraction (artisanal mining)
- Production of chlorinated solvents and other chlorine derivative products
- Catalysts employed in the synthesis of acetaldehyde and vinyl acetate, among other compounds
- Batteries and other components in electrical appliances
- Thermometers, barometers and manometers
- Fluorescent lamps
- Amalgams for dental fillings

1.1.3   Emission sources

1.1.3.1   Natural sources

Natural sources are those which release Hg with a geological origin through natural processes such as volcanic eruptions, geothermic activity, gradual degassing of soil systems or natural erosion of Hg enriched rocks (Table 1.1). The main complication when estimating emissions from natural sources is to distinguish primary emissions from re-emissions (Hg from former historical anthropogenic sources that is ultimately remobilised). Primary natural Hg emissions to the atmosphere have been estimated at 500 Mg yr^{-1} (Fitzgerald & Lamborg, 2004; Selin, 2009).

Table 1.1. Global Hg emissions by natural sources estimated for 2008 (Pirrone et al. 2010).

Source	Hg (Mg yr^{-1})	Contribution (%)
Oceans	2682	52
Lakes	96	2
Forests	342	7
Tundra/Grassland/Savannah/Prairie/Chaparral	448	9
Desert/Metalliferous/Non-vegetated zones	546	10
Agricultural areas	128	2
Evasion after Hg depletion events	200	4
Biomass burning	675	13
Volcanoes and geothermal areas	90	2
TOTAL	5207	100

1.1.3.2   Anthropogenic sources

1.1.3.2.1   Primary anthropogenic sources

These are those sources where Hg with a geologic origin is mobilised and released to the environment by the action of the human being. The principal types are mining (either Hg mining or when Hg is a by-product or a contaminant in the extraction of other minerals), extraction of fossil fuel where Hg is present as a trace pollutant,

cement production, and coal burning, which is the largest source of Hg to the atmosphere (Table 1.2). The current best estimates for total primary anthropogenic Hg emissions are in the 1960–2800 Mg yr^{-1} range (Selin et al., 2008; Pirrone et al., 2010; UNEP, 2013).

Figure 1.1. Sources of mercury (UNEP, 2008).

1.1.3.2.2 Secondary anthropogenic sources

In this type of sources, emissions occur due to an intentional use of Hg, e.g. products (described in section 1.1.2), industry or artisanal gold mining.

Concerning mercury-containing products, once they have been used, many of them are brought to landfills and incinerators, where their Hg content will be remobilised to different environmental compartments.

In regard to industry, several processes involving Hg are described below:

- Vinyl Chloride Monomer Production: Mercuric chloride is used as a catalyst in the production of vinyl chloride monomer (VCM), which is the precursor for PVC plastics. Global production of VCM in 2007 was almost 40 Tg. From 2004 to 2007, global consumption of VCM grew by about 5.5% per year as a result of strong demand for PVC, mainly for construction end-uses (Linak, 2009).

- Chlor-alkali Production: Chlorine and caustic soda are produced electrolytically by means of three different technologies; mercury-cell, diaphragm or membrane, but only the first one releases Hg to the environment and is the third largest consumer of this metal worldwide (UNEP, 2010). In recent years, governments have worked with industries to phase out the mercury based processes and to convert them over to the mercury-free alternative membrane processes. However, old chlor-alkali plants and other decommissioned industrial sites may constitute contaminated sites that continue to release Hg to the environment for many years.

Artisanal and small-scale gold mining is the largest Hg emission source by intentional use of this metal (the losses to the environment were estimated at 727 Mg in 2010) (UNEP, 2013) (Table 1.2). Moreover, a higher amount of Hg is used for this activity—an estimate of 1400 Mg in 2011—than for any other use of the metal (Telmer & Stapper, 2012). This practice consists in using Hg to amalgamate the gold and thus, separate it from other minerals and alluvial deposits. Subsequently, the amalgam is heated to recover the gold, and as a consequence the Hg is significantly released in the form of vapour to the atmosphere and the non gaseous fractions end up in piles of mining waste (tailings), soils, and waterways (Telmer & Veiga, 2009).

Table 1.2. Emissions from various sectors in tonnes per year (mean value and range), and as a percentage of total anthropogenic emissions (UNEP, 2013).

Sector	Emission (range)	Contribution
	(Mg yr^{-1})	(%)
By-product or unintentional emissions		
Fossil fuel burning		
Coal burning	474 (304 – 678)	24
Oil and natural gas burning	9.9 (4.5 – 16.3)	1
Mining, smelting and production of metals		
Primary production of ferrous metals	45.5 (20.5 – 241)	2
Primary production of non-ferrous metals	193 (82 – 660)	10
Large-scale gold production	97.3 (0.7 – 247)	5
Mine production of Hg	11.7 (6.9 – 17.8)	< 1
Cement production	173 (65.5 – 646)	9
Oil refining	16 (7.3 – 26.4)	1
Contaminated sites	82.5 (70 – 95)	4
Intentional uses		
Artisanal and small-scale gold mining	727 (410 – 1040)	37
Chlor-alkali industry	28.4 (10.2 – 54.7)	1
Consumer product waste	95.6 (23.7 – 330)	5
Cremation (dental amalgam)	3.6 (0.9 – 11.9)	< 1
TOTAL	1960 (1010 – 4070)	100

1.1.3.3   Remobilisation and re-emission

Remobilisation occurs when Hg that had been taking out of circulation is released again. In this case, the Hg released can be either of natural origin or coming from anthropogenic mercury releases historically deposited in soils, sediments, landfills, tailings dams and waste dumps. For instance, Hg accumulated in soils or sediments can be remobilized by rain or floods to enter the aquatic system. Hg uptaken by vegetation

can be re-emitted to the atmosphere during forest fires or biomass burning, and changes in land use affect the magnitude and the location of Hg releases. Unfortunately, it is not possible to experimentally distinguish the natural and the anthropogenic component of the re-emissions, but proportions are probably similar to those of the original emissions. Recent study suggests that the contribution of these historical or legacy Hg emissions to modern Hg exposure is much larger than previously thought (Amos et al., 2013). By modeling how 4000 years of historic Hg emissions propagate through Earth's surface reservoirs, it is estimated that legacy Hg constitutes 60% of modern Hg deposition.

1.1.4 Biogeochemical cycle

Hg occurs naturally in Earth's biogeochemical system, but centuries of human activities have been mobilizing increasing amounts of the element in the atmosphere, ocean, and terrestrial systems (Mason & Sheu, 2002). The continuous flux of this element between environmental compartments is called mercury cycle, and includes the processes schematized in Figure 1.2. Hg begins its biogeochemical cycle by emanating from the Earth's crust to the air, and then passing to the water and soils by means of wet and dry deposition. From there, the metal arrives to the different living organisms, and finally to the man through the food chain. Later, Hg continues the cycle in the inverse direction in diverse chemical and physical forms.

1.1.4.1 Atmospheric cycling

Hg is emitted from geological sources and from land and ocean surfaces in its elemental form, Hg^0, which is also released by anthropogenic sources such as coal-fired power plants. However, anthropogenic sources can also emit mercury in two other different forms: Hg(II) and mercury associated with particulate matter [Hg(P)]. Hg^0 is the most abundant form of Hg in the atmosphere, with a global mean concentration of about 1.6 ng m^{-3} in surface air and an atmospheric lifetime of about

0.5–1 year (Lin & Pehkonen, 1999). This long lifetime is the cause of the dispersion and distribution of Hg all around the globe.
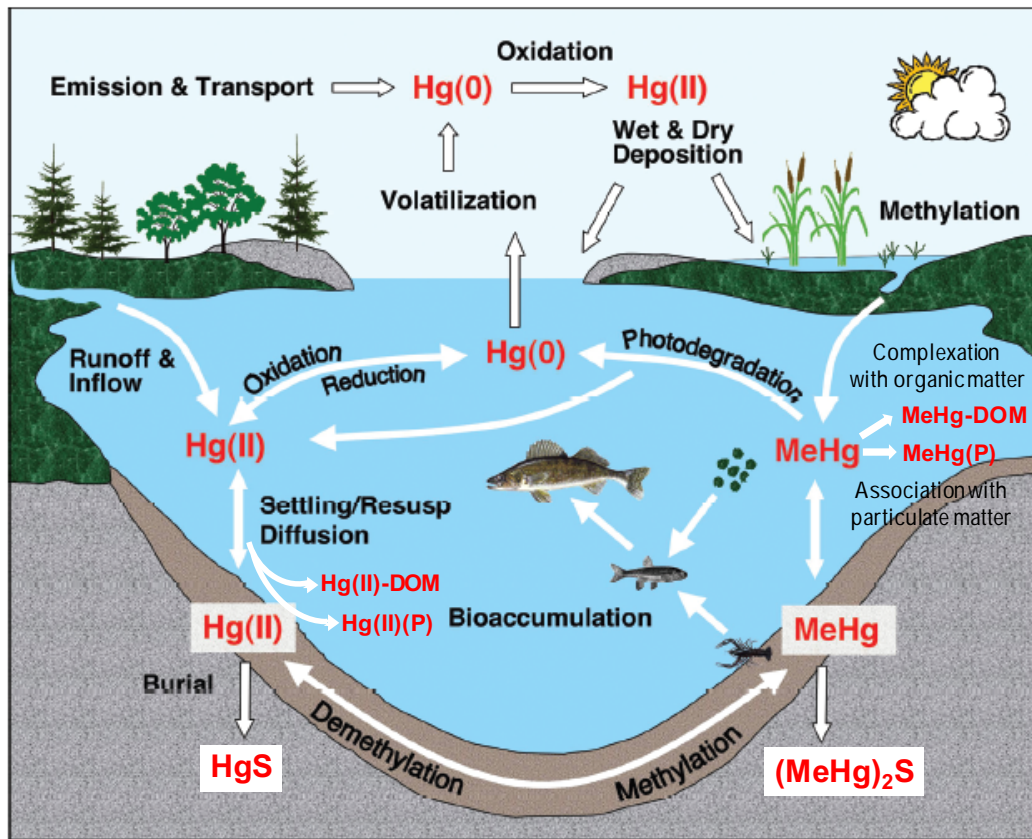
Figure 1.2. Mercury cycling in a lake and its watershed (Adapted from Engstrom, 2007). Resusp: resuspension.

Because Hg(II) and Hg(P) are more soluble in water than Hg^0, they are the predominant forms of Hg deposited to ecosystems through wet and dry deposition, and thus, they have a much shorter lifetime than Hg^0 in the atmosphere (days to weeks). Although total gaseous Hg is well mixed in the global atmosphere, concentrations are generally higher in the Northern Hemisphere since the majority of the emission sources are located there (Slemr & Langer, 1992; Slemr et al., 2003).

The main sink of Hg^0 in the atmosphere is oxidation to Hg(II). The chemical species involved in Hg^0 oxidation in the global atmosphere are not totally known. Traditionally, the most important global oxidant of Hg was thought to be O_3 or $\cdot OH$ (Hall, 1995; Pal &

Ariya, 2004). However, these reactions may not occur under atmospheric conditions, as some thermodynamic calculations and experimental measurements have recently shown (Calvert & Lindberg, 2005). On the other hand, atomic Br is today considered as a major oxidant for gaseous Hg^0 in the marine boundary layer and in the upper troposphere (Obrist et al., 2011; Lyman & Jaffe, 2012). Both Br and ·OH are photochemically produced, and thus, oxidation of Hg^0 to Hg(II) should be expected to have a diurnal cycle. This is what actually happens, as Hg(II) production peaks at midday and is at its minimum at night (Jaffe et al., 2005).

Summing up, the principal transformation reactions taking place in the atmosphere (mainly in the water drops of the clouds) are the following:

$$Hg^0 \text{ (g)} \rightarrow Hg^0 \text{ (aq)}$$
$$Hg^0 \text{ (aq)} + O_3/Br/\cdot OH \text{ (aq)} \rightarrow Hg^{2+} \text{ (aq)}$$
$$Hg^{2+} \text{ (aq)} + \text{particles or dust} \rightarrow Hg^{2+} \text{ (P)}$$
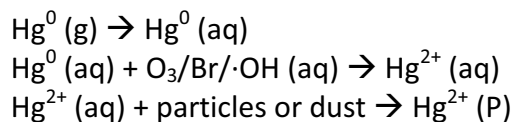
1.1.4.2 *Terrestrial cycling*

Aside from the geologically enriched areas, the majority of the Hg in the global land surface is deposited as Hg(II) from the atmosphere. After deposition, a portion of this Hg will rapidly revolatilise to the atmosphere. The remaining portion will be incorporated into the soil, where it can slowly (centuries to millennia) evade to the atmosphere. Newly deposited Hg has been shown to preferentially revolatilise, as evidenced by the METAALICUS experiment (Hintelmann et al., 2002), in which the radiolabeled Hg recently added to a watershed in eastern Canada was more available for reduction and subsequent emission as Hg^0 than the Hg originally present in the system. It has been estimated that from 5% to 60% of deposited Hg is quickly recycled to the atmosphere, depending on the surface characteristics (Hintelmann et al., 2002; Amyot et al., 2004; Ferrari et al., 2005). This mercury is also preferentially available for conversion into methylmercury (Hintelmann et al., 2002).

In soil, Hg occurs mainly in the form of inorganic compounds as $HgCl_2$ and $Hg(OH)_2$ or less reactive forms as HgS and HgO (also less prone to methylation) (Gaona, 2004).

Selenium is chemically similar to sulfur, so also HgSe complexes can be formed (mainly by a biologically mediated mechanism) enhancing Hg retirement (Hazen et al., 2012). Precisely, soil is the environmental compartment where most of the Hg in the terrestrial system (>90%) resides, binding strongly to reduced sulfur groups of organic matter (Skyllberg et al., 2003). In fact, it is the dissolved organic carbon (DOC) together with other dissolved species (e. g. S^{2-} and Cl^-) and the type of soil, the factors controlling the adsorption and desorption of Hg in soil systems (Gabriel & Williamson, 2004). Adsorbed Hg remains in the soil, while Hg in solution can undergo methylation or run off into a watershed.

Concerning vegetation, Hg in the aerial parts of plants is uptaken primarily from the atmosphere. Hg(II) deposits on leaves through wet and dry deposition, and uptake of Hg^0 is thought to occur through gas exchange at the stomata (Lindberg et al., 1992). On the other hand, Hg in roots comes from the pore water in soil (Obrist, 2007). Conversely, the Hg incorporated into the vegetation returns to the soil via throughfall and literfall (Grigal, 2002).

Hg returns to the atmosphere from soils by reduction to Hg^0 and subsequent diffusion. Although a recent study has shown that it could be partially controlled by microorganisms (Fritsche et al., 2008), this process is considered to be principally abiotic and mediated by agents such as Fe^{2+} and humic and fulvic compounds (Gabriel & Williamson, 2004). These reduction and volatilisation processes can be enhanced by temperature (Kim et al., 1995) and solar radiation (Gustin et al., 2002).

1.1.4.3 Aquatic cycling

The chemical species of mercury in oceans and freshwater are Hg^0, Hg(II), MeHg, Hg(P), colloidal Hg, and to a lesser extent, Me_2Hg and EtHg (Mason & Fitzgerald, 1993; Morel et al., 1998). Atmospheric Hg reaches the aquatic ecosystems by direct deposition (predominantly as Hg(II), as in terrestrial systems) to lake and ocean surfaces and through runoff from watersheds. Hg(II) can later reduce to Hg^0, which

may then volatilize to the atmosphere, as described also for soils. But also, a small portion of Hg(II) is converted to the more toxic form of MeHg.

The principal source of MeHg in aqueous environments is biotic methylation of Hg(II) by sulfate-reducing bacteria (Jensen & Jernelov, 1969; Compeau & Bartha, 1985) and, as shown more recently, by iron-reducing bacteria (Fleming et al., 2006; Kerin et al., 2006) and methanogens (Hamelin et al., 2011), in anoxic sediments. There are a number of environmental factors that affect the rate of MeHg production by influencing the supply of available Hg(II) for the methylating bacteria and/or the activity of the latter: sediment structure and composition, sulfide concentrations and organic carbon (Mason & Lawrence, 1999; Benoit et al., 2001). Apart from wetlands (Rudd, 1995) and sediments (Gilmour et al., 1992), MeHg production has also been measured in the water column of lakes (Eckley & Hintelmann, 2006). When speaking of marine environments, Hg methylation can occur in the sediments of the continental shelf (Hammerschmidt & Fitzgerald, 2006a) and estuaries (Heyes et al., 2006), within the water column (Monperrus et al., 2007), or in the deep ocean (Kraepiel et al., 2003). Although Hg methylation by microorganisms is known for more than 40 years, the exact mechanisms remain unrevealed. Two genes, hgcA and hgcB, that control anoxygenic Hg methylation in sulfate-reducing bacteria (Parks et al., 2013), have been recently discovered giving some light to this process.

On the other hand, MeHg can also be produced by abiotic methylation. The more common mechanism is the transmethylation by organometalic species of other metals as Pb, As or Sn (Ebinghaus et al., 1994). However, methyl donor compounds such as methylcobalamin, methyl iodide or methyltin compounds can also mediate this process (Thayer, 1989; Celo et al., 2006; Jimenez-Moreno et al., 2013).

The inverse process, demethylation, can also be biotic and abiotic. Biotic demethylation can be either oxidative or reductive. The former involves methanogenic bacteria and supposes the degradation of MeHg to CO_2, CH_4 and presumably, Hg(II) (Marvin-Dipasquale & Oremland, 1998). The reductive demethylation is carried out by the enzymes organomercury lyase (MerB) and mercury reductase (MerA). MerB breaks

the C-Hg bound in the MeHg molecule, giving CH_4 and Hg(II) as products. Later, Hg(II) is reduced to Hg^0 by MerA (Schaefer et al., 2004). Finally, the abiotic demethylation includes photodegradation (see section 1.5) and the reaction with sulphur to form Me_2Hg and HgS (Deacon, 1978).

Both MeHg and Hg(II) can be uptaken by living organisms and concentrated in their tissues (bioaccumulation), but only MeHg has the potential to biomagnify (Weiner et al., 2003) throughout the food chain as predators eat contaminated prey. This joint process of bioaccumulation and biomagnification can elevate MeHg concentrations in predatory fish relative to water by a factor of $\geq 10^6$ (Engstrom, 2007). It is often erroneously stated that MeHg biomagnifies while Hg(II) does not because the former is more lipophilic than the latter, when actually the major site of Hg accumulation in fish is the muscle rather than adipose tissue (Bloom, 1992). This indicates that lipid solubility is not the primary determinant of Hg biomagnification (Mason et al., 1995). In turn, Hg accumulates in muscle because this tissue is rich in proteins containing thiol (-SH) groups (Harris et al., 2003).

1.1.5 Toxicity to humans

The toxicity of Hg depends on its chemical form, thus, the symptoms and signs vary depending on whether the exposition is to elemental, inorganic or organic compounds. Chemical speciation is, therefore, the most important variable in Hg ecotoxicology.

1.1.5.1 Elemental mercury

Hg^0 is volatile at room temperature and its vapours may represent a hazard to humans, since its major exposure route is via inhalation. Such exposure may occur in laboratories, work places as well as in homes (broken thermometers containing Hg). Workplace exposure may occur in many types of industries: chlorine-alkali manufacture, dental amalgams, electronic switches, fluorescent lamps and artisanal gold mining (Syversen & Kaur, 2012).

Hg^0 vapour is readily uptaken through the lungs and about 74% is retained in the human body (Hursh et al., 1976), whereas the gastrointestinal absorption is very low (less than 0.1%) (Matheson et al., 1980). From blood, the Hg^0 distributes throughout all the tissues, as it easily passes through most cell membranes including the blood–brain barrier and the placenta because of its lipophilic character. The absorbed Hg has a body half-life of 58 days, although in the brain it is just of 21 days (Clarkson & Magos, 2006). This Hg can be eliminated through urine, and a small portion through the exhaleted air. However, in the tissues, the Hg^0 can be intracellularly bio-oxidated to inorganic Hg. Its partial conversion to $HgCl_2$ allows its retention by the kidneys and the central nervous system for years (ATSDR, 1999; UNEP, 2002; Tchounwou et al., 2003).

Inhalation of volatilized vapors of Hg^0 leads to chemical pneumonitis. Other symptoms are alopecia, salivation, insomnia, apathy, irritability, painful back spasms, urination, severe constipation and impotence (Clarkson, 1997).

1.1.5.2 Other inorganic compounds

Inorganic Hg presents a lower capacity of diffusion through the biomembranes than Hg^0 due to its hydrophilic character. These inorganic compounds have been used in a very extensive range of medical and cosmetic products; antiseptics, teething powders, skin-lightning creams, so accidental exposure to mercuric chloride has not been uncommon. Although only about 10% of ingested mercury salt is absorbed, it tends to be extremely caustic to the gastrointestinal tract. A small amount of dermal absorption occurs as well. In adults the half-life of ingested mercuric salt is about 40 days. Excretion is mostly fecal (Clarkson, 2002).

The toxicity of these inorganic Hg species is principally determined by their solubility. Consequently, the less soluble species, such as HgS or HgSe, are nearly non toxic, whereas mercury chloride salts are the most toxic. Nevertheless, inorganic salts as $HgCl_2$ do not accede to the brain so efficiently as MeHg and Hg^0 do (Jiménez-Moreno, 2008). In turn, they accumulate primarily in the kidney, followed by its accumulation in the liver.

The principal syndrome of acute mercury salt poisoning is stomatitis or digestive upset. Symptomatologies of chronic toxicity include progressive anemia, gastric disorders, salivation, metallic taste in the mouth, inflammation, and tenderness of gums and tremors (Hu, 2000). Central neuropathy can also occur from mercury salt exposure. On the other hand, the IARC (International Agency for Research on Cancer) general evaluation concludes that both Hg^0 and Hg inorganic compounds are not classifiable in terms of carcinogenicity for human beings (IARC, 1997).

1.1.5.3   Organic compounds

Organomercurials are lipophilic so they are absorbed more efficiently and go through the biological membranes more easily than inorganic Hg compounds, although they are excreted more slowly (UNEP, 2002; Tchounwou et al., 2003). These organic forms can be found as industrial compounds, primarily as biocides and as pesticides, but also in two once-common household antiseptics: mercurochrome (merbromin) and merthiolate (thimerosal) (Elferink, 1999; Clarkson, 2002). Nevertheless, consumption of contaminated fish and seafood is the primary route of human exposure to organic Hg (WHO, 1989).

The toxicity of organic Hg compounds depends on the specific compound, route of exposure, dose, and age of a person at the time of exposure. Alkylmercury compounds are considered to be similar regarding toxicity, whereas other organic compounds, such as phenylmercury, resemble more inorganic Hg (UNEP, 2002). MeHg occupies a distinct place among organomercurials since its toxicity is very well characterised and a big part of the population is exposed to it. If we are talking about oral exposure, the absorption from the intestine is practically 100%, even though the MeHg found in the food is bound to SH-groups. Furthermore, MeHg can be absorbed through skin (Aberg et al., 1969). This organomercurial rapidly goes through the placenta (and subsequently deposits in the fetus) and the blood-brain barrier. The brain has a stronger affinity for MeHg and the concentration of this species in this organ has been

reported to be 3–6 times higher that of the blood. In the blood MeHg has a mean half-life of 40–50 days (range: 20–70 days) for adults and 90% is excreted in feces through bile.

MeHg is a potent neurotoxic that can affect very negatively the central nervous system and the development of the brain (Wolfe et al., 1998). Exposure to high levels of this species causes mental retardation, cerebral palsy, seizures, and ultimately death (WHO, 1990). Other neurological problems such as tremors, insomnia, polyneuropathy, paresthesia, emotional lability, irritability, personality changes, headache, weakness, blurred vision, dysarthria or speech impairment, slowed mental response, and unsteady gait have been observed (Myers et al., 1995). In addition, IARC considers that MeHg compounds can be carcinogen for the human being (IARC, 1997).

1.1.6 Legal regulation in water

Laws and regulations are a major tool in protecting the environment. Water bodies are very sensitive ecosystems and the compartments where the first links on the trophic chains normally are. Therefore, Hg levels must be regulated in the aqueous media.

The Water Framework Directive (Directive 2000/60/EC of the European Parliament and of the Council of 23 October 2000 establishing a framework for Community action in the field of water policy) is a European Union directive which commits European Union member states to achieve good chemical and ecological status of all water bodies (including marine waters up to one nautical mile from shore) by 2021. It is a framework in the sense that it prescribes steps to reach the common goal rather than adopting the more traditional limit value approach. In 2008, the Directive 2008/105/EC of the European Parliament and the Council on environmental quality standards in the field of water policy was approved, amending Directive 2000/60/EC. However, the Directive 2013/39/EC was recently approved, amending the two previously mentioned directives. This directive replaced the list of priority substances in the field of the water policy, establishing limits on concentrations in surface waters for 45 substances. Hg

and its compounds were identified as priority hazardous substances and environmental quality standards (EQS) were established for them. The member states should ensure that the maximum allowable concentration of total Hg in inland surface waters (rivers and lakes and related artificial or heavily modified water bodies) and other surface waters is 0.07 μg L^{-1}. The Directive 2013/39/EC also established EQS for biota. For Hg and its compounds, the suggested EQS was of 20 μg kg^{-1} for fish (wet weight).

In 2011, the Royal Decree 60/2011 on the Environmental Quality Standards in the area of water policy, transposed to the Spanish legislation all the aspects contained in Directive 2008/105/EC. This Royal Decree maintained the EQS established by the European directive for Hg and its compounds in surface waters (annual average concentration of 0.05 μg L^{-1} and maximum allowable concentration of 0.07 μg L^{-1}) and biota (20 μg kg^{-1}).

Concerning drinking-water, in 1993 the World Health Organization (WHO) suggested European standards for different chemical compounds and parameters in this type of water (WHO, 1993). The health based guideline level for total Hg was 1 μg L^{-1}. In the same manner, the Directive 98/83/EC of 3 November 1998 on the quality of water intended for human consumption, set up a maximum allowable Hg concentration of 1 μg L^{-1}, to be adopted by the Member States. However, in 2008 WHO established a guideline level for inorganic Hg of 6 μg L^{-1}, since they claim that "it is unlikely there is any direct risk of the intake of organic mercury compounds, and especially of alkylmercurials, as the result of the ingestion of drinking-water" (WHO, 2008).

1.2 Determination of Hg in environmental samples

1.2.1 Sample collection and storage

Collection and storage of samples are critical steps in ultra trace Hg analysis (Leermakers et al., 2005) due to the risk of contamination and analyte losses caused by

the high volatility of some Hg species and the strong tendency of Hg^0 and inorganic Hg species to surface adsorption, as well as their permeability through some materials. These problems can be stressed by the extremely low concentrations in natural waters and by the minor contamination of the reagents used, storage containers or other tools. In addition, transpeciation (inter-conversion between Hg species) can occur during sample collection, pre-treatment and storage.

For all those reasons, a special care must be taken during these processes. Suitable sample collection and storage materials are polytetrafluoroethylene (PTFE), polyethylene terephthalate (PET), and glass (Yu & Yan, 2003). Acid or BrCl containing solutions are necessary for thoroughly cleaning PTFE and glass containers in order to reuse them, whereas PET vessels are disposable ware.

Natural waters are usually filtered immediately after collection to separate the dissolved and the particulate fractions. Different pore sizes and filter materials are used. PTFE, polycarbonate, Nylon, quartz or glass fibre are the most common materials (Tseng et al., 2000; Kotnik et al., 2007; Vermillion & Hudson, 2007; Leopold et al., 2009), and 0.45 µm is the most common pore size. Stabilization of water samples for total dissolved Hg determination is accomplished by addition of acid (e.g., HCl or HNO_3) or oxidant (e.g., BrCl) (Horvat, 1996; Yu & Yan, 2003).

When facing Hg speciation, different preservation strategies are applied. If the analytes of interest are volatile Hg species, they should be separated immediately after collection by purging them out of the water onto suitable traps. Other way to prevent losses is to store the sample in full glass bottles with PTFE lined caps (Parker & Bloom, 2005). If the target analyte is MeHg, acidification with HCl or deepfreezing the sample is recommended to preserve this species in water (Geerdink et al., 2007), and in the case of using glass vessels to collect and contain the sample, they should be amber to avoid photodegradation. Furthermore, no residual oxidant can remain from the cleaning of the vessels, as it causes decomposition of MeHg.

1.2.2 Determination of total mercury (THg)

Most of the conventional analytical techniques used for the determination of THg contents require the samples to be in liquid state and their organic matter to be destroyed before analysis. On the contrary, there are totally automatic techniques that allow THg determination without previous pretreatment of the sample. In the next two subsections, the procedures, reagents and equipments available for extraction and analysis of THg are described.

1.2.2.1 Solid samples

The determination of THg in solid matrixes such as soil and sediment is usually carried out by digestion with strong acids (HNO_3, HNO_3/HCl, $HNO_3/HCl/HF$ or HNO_3/H_2SO_4) (Pereira et al., 1998; Kocman et al., 2004; Canario et al., 2005), and by oxidant reagents (H_2O_2) (Ortiz et al., 2002) for biota. After this digestion step, solid samples are transformed into liquefied samples, thus, they will be subjected to the methods described in section 1.2.2.2. The detection systems more widely used are atomic absorption spectrometry (AAS), atomic fluorescence spectrometry (AFS), inductively coupled plasma atomic emission spectrometry (ICP-AES) and inductively coupled plasma mass spectrometry (ICP-MS) (Diez et al., 2007).

In general, the methodologies involving digestion of the sample are time-consuming and prone to analytical errors. As an alternative, THg in solid samples can be directly measured with automatic instruments (AMA-254 and DMA-80). These systems are based on the catalytic combustion of the sample, pre-concentration by amalgamation in a gold trap, thermal desorption and detection by AAS. The major advantage of these analysers is that sample pretreatment is not necessary, but it should be also noted that the analysis time is very short and the process is solventless.

1.2.2.2   Liquid samples

The most common detector system for the determination of THg in aqueous matrixes is CVAFS (Cold Vapour Absorption Fluorescense Spectrometry). As a pre-treatment, aqueous samples are digested to transform all Hg species to "reducible" Hg (free inorganic Hg(II) ions) by addition of a strong oxidant (BrCl, $KMnO_4$ or UV light). After pre-reduction of excess oxidant, Hg(II) is reduced to elemental Hg^0 generally by $SnCl_2$ o $NaBH_4$, which is then purged out of the reaction solution by an inert carrier gas. The Hg^0 vapour, called "cold vapour" (CV), is then either transported directly to the detector or pre-concentrated on a gold trap by formation of an amalgam (Fitzgerald & Gill, 1979). Subsequent heating of the gold trap releases the pre-concentrated Hg^0, which is then transported to the detection cell where Hg fluorescence is measured at a wavelength of 253.7 nm.

The general CVAFS procedure described above for THg determination in natural waters is recommended by regulatory bodies such as the USEPA (EPA 1631) and the EU (EN 13506), and it was the method chosen to analyse THg in part of the liquid samples of this thesis. Although its LOD is very low (pg L^{-1}), this method has considerable drawbacks such as the complex and long-lasting stages. An oxidative pre-treatment within an automated flow injection (FI) procedure (Wurl et al., 2000; Leopold et al., 2008) has been developed to simplify the former methods. These FI-CVAFS systems shorten analysis time, lower the contamination risk and are more reproducible than the manual procedure. Nevertheless, this method still presents limitations: the very extensive cleaning procedures required for the reagents used for oxidative digestion, the pre-reduction of oxidant excess and the reduction of Hg(II) to Hg^0.

On the other hand, the use of a high-intensity ultrasound (US) field in combination with CV generation, first reported by Capelo et al. (2000), enabled to work without reducing agents (Gil et al., 2006). This technique followed by amalgamation pre-concentration has been successfully applied to the determination of THg in estuarine, lake and river water (Fernandez et al., 2006; Ribeiro et al., 2007). In addition, the use of "in-atomizer" trapping in graphite furnace AAS after US-CV has been successfully

applied to the determination of Hg in natural waters (Gil et al., 2007). Another reagent-free method using nano-gold collectors and with high sensitivity (LOD = 80 pg L^{-1}) has been used for the decomposition and pre-concentration of Hg directly from natural waters (Leopold et al., 2009).

1.2.3   Chemical speciation

The definition of "speciation" accepted by the IUPAC refers to "the chemical form or compound in which an element occurs in both non-living and living systems. It may also refer to the quantitative distribution of an element" (de Bolster et al., 1997). The forms in which an element is present in the environmental systems affect to the mobility, bioavailability, bioaccumulation, and finally the ecotoxicological impact of the element rather than its total concentration. That is the reason why knowing which species and in what concentration they are present is crucial for the environmental assessment of a pollutant.

In this context, the term "speciation analysis" refers to the analytical activity of identifying and measuring species (Templeton et al., 2000). By "measuring" we understand the exact quantification in a real and representative matrix/sample. The addition of the quantities of single element species corresponds to the total element content in the sample.

The analytical methods aimed to speciation might comprise the following stages (Aguilar-Martínez, 2010):

1) **Extraction** of the target species from environmental samples, assuring both the integrity of the chemical form and the concentration of the species of interest. This stage is not necessary in the case of aqueous samples.

2) **Pre-concentration** of the species with the objective of reaching a final concentration detected by the chosen technique.

3) **Separation** of the species without varying their original relative concentrations.

4) Detection and individual determination of every species previously separated.

Furthermore, depending on the separation technique employed, an additional stage of **derivatisation** can be necessary to convert the non volatile Hg species in forms more suitable for their subsequent separation.

1.2.4 Determination of organic Hg species

1.2.4.1 *Extraction*

Ideally, the extraction must be performed in such a way that the analyte separates from the matrix without losses, contamination or interspeciation, and with the fewest possible interferences. The most commonly used techniques are acid or basic extraction, distillation and supercritical fluid extraction.

1.2.4.1.1 Acid extraction

Westoo (1966) developed a method to extract MeHg in the MeHgCl form using HCl and an organic solvent such as benzene, by means of an extraction involving several steps. This procedure has suffered improvements to selectively extract MeHg. The acidic medium can also contain NaCl, KBr or iodoacetic acid, and other organic solvents as toluene, chloroform or dichloromethane can be used (Hempel et al., 1992; Padberg et al., 1993; Rezende et al., 1993; Lorenzo et al., 1999; Abuin et al., 2000). On the other hand, solventless acid digestion is also used for Hg speciation. To accelerate the digestion process, the assistance of ultrasounds or microwaves is used. The acids frequently used as extractants are H_2SO_4, HNO_3 or a combination of the latter with HCl (Tseng et al., 1997; Dietz et al., 2001). For the particular case of some of this thesis' samples, another type of acid extraction was used. An aqueous solution of thiourea and HCl can be used to elute MeHg from thiol resins (Krishna et al., 2005; Clarisse & Hintelmann, 2006).

1.2.4.1.2 Basic extraction

The most commonly used alkaline extraction methods are those involving KOH-methanol (Cai & Bayona, 1995; Grinberg et al., 2003b) and tetramethylammonium hydroxide (Dietz et al., 2001; Park & Do, 2008) to release both MeHg and Hg(II) from biota and sediments. The application of ultrasounds or microwaves diminishes the extraction time and increases the efficiency. In many cases, alkaline extraction seems to be problematic as compared to the acidic ones, because basic solutions are much more difficult to get in pure form. Moreover, in subsequent steps, serious problems derived from the high levels of organic matter, sulphides or ferric ions co-extracted with the target species can be encountered (Horvat et al., 1993).

1.2.4.1.3 Distillation or acidic volatilisation

Another alternative to extract the organic species is to produce their volatile derivatives. The solid sample is treated with H_2SO_4 and NaCl or KCl with the aim of generating compounds of the type R-HgCl, which are volatile and thus easily separable by means of distillation using a nitrogen stream at 150 °C (Nagase et al., 1980). Although it is widely used, this technique has been criticised by the possible artificial formation of MeHg (Hintelmann et al., 1997a).

1.2.4.1.4 Supercritical fluid extraction

The application of this technology to Hg compounds extraction (Emteborg et al., 1996; Lorenzo et al., 1999) has not been fully developed, as evidenced by the poor recoveries (50-70%) achieved by the moment (Sun et al., 2001). However, this technique presents advantages as the low cost and toxicity of the employed reagents (especially CO_2) and a reasonably low extraction time.

1.2.4.2 Pre-concentration from liquid matrix

Traditionally, liquid-liquid extraction (Westoo, 1966; Horvat et al., 1990) and solid-phase extraction with different types of solid adsorbents as sulphydryl cotton fibers (Lee & Mowrer, 1989; Cai et al., 2000) or dithiocarbamate resins (Emteborg et al., 1995) were employed for Hg species pre-concentration. Nevertheless, analytical chemists have searched for alternatives that reduce costs and wastes. In this sense, the techniques explained below are more appropriate since they are solvent-free and easy to automate.

1.2.4.2.1 Solid-phase microextraction (SPME)

Developed by Arthur and Pawliszyn (1990), SPME is based on the non exhaustive extraction of volatile or semivolatile organic compounds from an aqueous or gaseous sample to a fused silica fibre coated with an appropriate stationary phase. While the fibre is exposed to the sample, the analytes diffuse from the matrix to the stationary phase until the equilibrium is reached (the quantity of the analyte extracted arrives to steady state). It is a simple, fast, solvent-free and easy to automate technique that allows the distinction between organic and inorganic forms of Hg (Diez & Bayona, 2008).

There are two modes of extraction: direct and headspace (HS). In the first mode, the fibre is immersed into the sample and the analytes are directly transported by diffusion to the stationary phase where they can be ad- or ab-sorbed depending on the polymer used. In the second, the fibre is located in a layer of air (the headspace) above the sample, through which the analytes are transported. When the matrix is not homogeneous or the pH or polarity of the medium is not compatible with the fibre coating, only the HS mode can be used. This is the most common mode and the one followed in the present thesis.

The type of material and the thickness of the stationary phase are possibly the most important characteristics that determine the selectivity and extractive capacity of SPME. Given their high stability, the most common fibres are those coated with polydimethylsiloxane (PDMS) (7-100 µm) (Carrasco et al., 2009). The use of fibres coated with polydimethylsiloxane/divinylbenzene (PDMS/DVB) (65 µm) (Mester et al., 2000), polydimethylsiloxane/divinylbenzene/carboxen (PDMS/DVB/CAR) (Centineo et al., 2004) and polydimethylsiloxane/carboxen (PDMS/CAR) (75 µm) (Jitaru et al., 2004) have also been described for the extraction of organic Hg species. The difference among these fibres lays on the mechanism of analyte partitioning: absorption in the case of PDMS, and predominantly adsorption in the case of PDMS/DVB, PDMS/DVB/CAR and PDMS/CAR.

1.2.4.2.2 Purge and trap (P&T)

This method enables the extraction and pre-concentration of organic Hg species by means of derivatisation and purge of the aqueous sample with a gas stream (generally nitrogen) that transports the volatile derivatives towards a column (trap) packed with an adsorbent (Tenax, Chromosorb or Carbotrap). The trap can be at room temperature or immersed in liquid nitrogen (cryogenic trapping) (Amouroux et al., 1998; Lambertsson & Bjorn, 2004; Stoichev et al., 2006). Later, the analytes can be desorbed by a quick and controlled heating of the trap. Temperature, purge time and gas flow rate are parameters affecting the efficiency of the process (Mao et al., 2008).

1.2.4.3 Derivatisation

The pre-concentration techniques more extensively described above (SPME and P&T), as well as the subsequent separation by gas chromatography, require the analytes to be volatile. Given that MeHg and other organic Hg species are not volatile, proceeding to their transformation is needed (Diez & Bayona, 2006).

50

The traditional derivatisation technique is the Grignard reaction, which allows the election among different alkyl groups to obtain the corresponding alkylated species. Nevertheless, buthylmagnesium chloride is generally used as the Grignard reagent (Cai et al., 1997). These reagents are very reactive to water, thus, the species of interest have to be extracted in anhydrous organic solvents. Consequently, the preparation of the sample is a long and tedious procedure. To solve some of the disadvantages of the Grignard derivatisation, the use of alternative methods has been spread. It is the case of hydride generation using $NaBH_4$ or aqueous phase alkylation (e.g., ethylation, propylation or phenylation using sodium tetraethylborate ($NaBEt_4$), sodium tetrapropylborate ($NaBPr_4$) or sodium tetraphenylborate ($NaBPh_4$), respectively).

The chemical reactions occurring during the derivatisation are the following:

$RHg^+ + NaBH_4 + 3\ H_2O \rightarrow RHgH + H_3BO_3 + 3\ H_2 + Na^+$ hydride generation

$RHg^+ + NaBEt_4 + 3\ H_2O \rightarrow RHgEt + BEt_3 + Na^+$ ethylation

$RHg^+ + NaBPr_4 + 3\ H_2O \rightarrow RHgPr + BPr_3 + Na^+$ propylation

$RHg^+ + NaBPh_4 + 3\ H_2O \rightarrow RHgPh + BPh_3 + Na^+$ phenylation
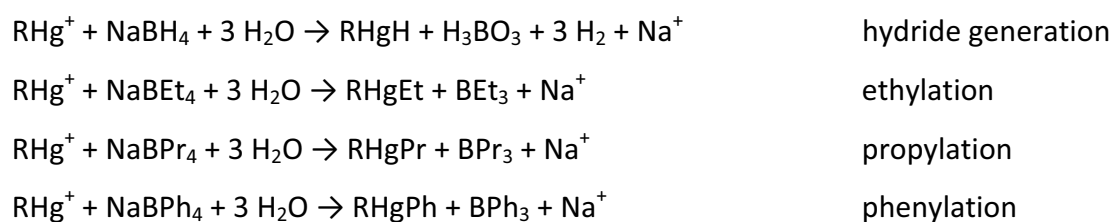
In all these cases, the reaction takes place in an aqueous medium, so the analysis time is shortened and the use of organic solvents is avoided. The most common reaction, due to its satisfactory results and its occurrence at room temperature, is ethylation (Cai & Bayona, 1995; Grinberg et al., 2003b). However, $NaBEt_4$ is very unstable in aqueous medium and ethylation cannot be used when trying to distinguish between EtHg and Hg(II), since the derivative of both compounds leads to the same product (diethylmercury). On the other hand, $NaBPr_4$ and $NaBPh_4$ present higher stability and easier handling for in situ derivatisation (Grinberg et al., 2003a). Although $NaBPh_4$ is the cheapest reagent, the phenylated species are less volatile than the ethylated or propylated and thereby, the equilibration time between the aqueous and the gas phase will be longer, and the temperature (to increase the concentration in the HS) higher. Provided that all the reagents show benefits and drawbacks, both $NaBPh_4$ and $NaBEt_4$ were selected for analysis performed within this thesis.

As the efficiency of the derivatisation reaction depends on the pH of the medium, acetic/acetate or citric/citrate solutions are employed to regulate and maintain it ca. 5 (Mao et al., 2008). Due to the variability caused by the matrix effect, the use of a recovery standard isotopically labelled or with a structure and reactivity similar to the analyte's is recommended.

1.2.4.4 Separation

Chromatograpy is the most widely employed technique for Hg speciation, since it provides higher resolution than non chromatographic methods. Nevertheless, there are some simple non-chromatographic approaches that adequately separate one or two species in a certain matrix.

1.2.4.4.1 Non-chromatographic methods

Non-chromatographic methods for Hg speciation in natural waters mostly determine only one species or one fraction rather than the simultaneous determination of all Hg species present. These methods are based on the different chemical or physical behaviour of the Hg species, i.e. on solubility, volatility, or redox potential.

Some of the previously described extraction and pre-concentration techniques, such as distillation or P&T, also serve to separate Hg species. Another technique is the selective reduction to Hg^0. Mild reduction conditions are used for determination of inorganic Hg and stronger conditions for the simultaneous reduction of inorganic and organic Hg species (i.e. determination of the total content of Hg). Formic acid or Sn(II) can be used as the selective reductant for inorganic Hg, while organic Hg compounds are decomposed and reduced to Hg^0 only by additional UV-irradiation (Zheng et al., 2005) or after ultrasonic decomposition (Capelo et al., 2000). Also, inorganic Hg can be detected by CVAAS and subsequently, organic Hg is photo-oxidized to inorganic Hg, allowing the determination of the total content of Hg (Atallah & Kalman, 1993). These

systems are simple, but methods involving differential calculation (obtaining the organic Hg fraction by subtracting the inorganic Hg fraction from THg concentration) are questionable.

Another approach is the use of different types of solid sorbent material and/or complexation reagents for the selective retention of either Hg(II) or MeHg or their complexes, i.e. the use of selective SPME. Selective retention of Hg(II) can be performed by complexation with pyrrolidine dithiocarbamate (Zachariadis et al., 2005), whereas MeHg can be selectively retained onto sulfydryl cotton (Jian & McLeod, 1992). Hg(II) can be separated from MeHg by using a simple anion exchange resin (Dowex M-41) (Sanz et al., 2004).

Additionally, the selective binding of MeHg to the yeast *Saccharomyces cerevisiae* receptors was taken advantage of to separate that organic species from Hg(II) (Madrid et al., 1995). Capillary electrophoresis has also been employed for Hg speciation in water samples (Yin, 2007; Fan & Liu, 2008). Eventually, an optic sensor has recently been developed to selectively determine Hg(II) in aqueous samples (Diez-Gil et al., 2011).

1.2.4.4.2 Chromatographic separation

Gas chromatography (GC) is by far the most commonly used separation technique for Hg speciation, because of its easy handling, high resolution power and easy coupling to a variety of detectors (e.g., AFS, AES, ICP-MS). In GC separation volatile Hg species are stripped from the sample solution or from a pre-concentration device (e.g., a trap or a SPME fibre) and transferred quantitatively to a column by the flow of a carrier inert gas (mobile phase) that is usually helium, argon or nitrogen. The column is a piece of glass or metal tubing containing a microscopic layer of liquid stationary phase which is adsorbed onto the surface of an inert solid. The gaseous compounds being analysed interact with the stationary phase on the walls of the column, which causes each compound to elute at a different time, known as the retention time of the

compound. The comparison of retention times is what gives GC its analytical usefulness.

Derivatisation is not necessary when the target analytes are the volatile forms (Amouroux et al., 1998). However, other Hg species, such as MeHg or EtHg, need to be derivatised and thus volatilised, to be transported into the GC column. Despite the derivatisation step, GC offers a quantitative transfer of the analytes to the detector and a high sensitivity (Diez & Bayona, 2008; Mao et al., 2008; Carrasco et al., 2009; Chung & Chan, 2011). There are three types of GC columns employed in the case of Hg speciation: packed, capillary and multi-capillary. Packed columns were the first ones employed (Bloom, 1989) and are still used for environmental studies (Heyes et al., 2006), although they can lead to severe tailing of the chromatographic peaks, low column efficiency or poor reproducibility (Alli et al., 1994). Capillary (Bulska et al., 1991) or multi-capillary GC (Rosenkranz & Bettmer, 2002) provides superior separation power and better detection limits, particularly the latter mode because of its higher sample capacity.

High performance liquid chromatography (HPLC) is a very suitable technique for polar, non volatile or ionic species separation. Thus, it is a good alternative to GC for Hg speciation. Usually, a reversed phase column based on alkyl-silica and a liquid mobile phase containing an organic modifier, a chelating agent or ion pair forming reagent, and in some cases a pH buffer, is usually used (Leermakers et al., 2005; Leng et al., 2013). HPLC offers a higher versatility than GC (Ramalhosa et al., 2001; Maldonado Santoyo et al., 2009; Moreno et al., 2013), but the sensitivity achieved with this separation technique is much lower due to the high solvent volumes employed and the dilution effect.

Another type of liquid chromatography, ion chromatography (IC), has also been used to separate Hg species (Park et al., 2011) on the basis of their interaction with the ion exchanger (typically a resin). This separation mode allows direct separation of ionic and very polar species, and thereby, sample pretreatment can be simplified.

54

1.2.4.5   Detection

The desirable features for an ideal detector to be used for trace element speciation are as following (Sánchez-Uria & Sanz-Medel, 1998):

- High sensitivity

- High elemental specificity

- Ability to interface to GC or HPLC

- On-line continuous operation with the separation column

- Real-time information on the analysed element

- Broad linear dynamic range

- Multi-element and multi-isotopic capacity

"Hybrid" techniques are preferred for speciation and, thus, the chosen detector should operate ideally on-line with the chromatographic column, providing continuous, real-time information on the trace element sought for speciation. In most cases of real-life analytical speciation, the most advantageous and thus, most frequent combination, is a chromatographic separation technique coupled to an atomic (element-specific) detector.

The first works on Hg speciation were carried out with an electron capture detector (ECD) (Horvat et al., 1990; Caricchia et al., 1997), which detects halogenated derivatives. However, the low selectivity of this detector leaded to its replacement by analytical plasmas, both at atmospheric or reduced pressure, which offer great analytical potential as element-specific detectors. The direct nebulisation of liquid samples into the inductively coupled plasma atomic emission spectrometry (ICP-AES) (Menendez-Garcia et al., 1996; Serafimovski et al., 2008) lacks the required sensitivity for real-life Hg speciation, favouring the extensive use of microwave induced plasma atomic emission spectrometry (MIP-AES) (Emteborg et al., 1996; Dietz et al., 2001).

Perhaps the atomic detector closest to the ideal features for speciation (listed above in this section) is the ICP-MS. Its importance in environmental analysis is

demonstrated by the increasing number of papers reporting the use of this detector for Hg speciation during the last years (Amouroux et al., 1998; Tseng et al., 2000; Qvarnstrom & Frech, 2002; Park & Do, 2008; Chung & Chan, 2011; Tjerngren et al., 2012a). ICP-MS also offers the possibility of working with different stable Hg isotopes (isotope dilution mass spectrometry) (Bjorn et al., 2007; Ma et al., 2014).

On the other hand, AFS is a much cheaper detection technique in comparison to the costly ICP-MS, and virtually keeps the same benefits of the latter in terms of sensitivity and selectivity. This is the reason why AFS is one of the most frequently used techniques for Hg speciation (Bloom, 1989; Cai et al., 2000; Diez & Bayona, 2002; Leopold et al., 2008; Carrasco et al., 2009; Leng et al., 2013) and also the type of detection employed in the major part of this thesis. It should be noted that only Hg^0 has fluorescence, then, all the Hg species have to be converted into Hg^0 by means of thermal decomposition in a pyrolyzer before detection.

Another common detector type is AAS in its different forms of "high sensitivity" measurements, namely cold vapor generation in flame quartz tubes (CVAAS) (Rezende et al., 1993; Krishna et al., 2005; Escudero et al., 2013), quartz furnace (QFAAS) (Deng et al., 2009) or electrothermal vaporization in a graphite furnace (ETAAS) (Sarica & Turker, 2012).

The performance of GC in combination with MIP-AES, MS, and AFS has been evaluated in a comparative study by Cai et al. (2000). Both GC-AFS and GC-MIP-AES offer the advantages of broad linear ranges and low costs for instrumentation and maintenance, whereas GC-MS is the preferred technique for identification and validation, particularly in conjunction with isotope dilution analysis.

1.2.4.5.1 Isotope dilution mass spectrometry

The application of isotope dilution (ID) analysis for the determination of metal speciation was first described by Heumann et al. (1994) using HPLC coupled to ID ICP-MS. ID consists in adding a known mass of an enriched isotope of the Hg species under

study to an aliquot of the sample prior to pre-treatment procedures and then, the ratio of the added isotope to the naturally occurring isotopes is measured. ID analysis is the most powerful technique for the optimisation of pre-treatment procedures and validation of speciation methods. It provides highly accurate analytical results because analyte losses occurring after the isotope equilibration have no affect on the final result, since the ratio mentioned above remains unchanged (Fischer et al., 2012; Ma et al., 2014). Apart from QC & QA, ID can also be used to investigate the dynamics of mercury cycling in the environment. In the METAALICUS project, ^{202}Hg was disseminated onto a boreal forest sub-catchment to study the fate of new Hg deposition and to distinguish it from historically deposited Hg in the ecosystem (Hintelmann et al., 2002).

This technique was used in this thesis due to its great capabilities. Two Hg isotopes were added to water samples to perform a study on MeHg photodegradation. One of them was used to rigorously track the photodemethylation of MeHg, and the other was used as internal standard.

1.3 Bioavailability concept

In order to carry out a risk assessment for any pollutant, knowing its bioavailable fraction instead of its total concentration is preferable. Metal "bioavailability" is a concept still hard to define. It may include 1) the physical-chemical availability of metals in the exposure medium, 2) the actual demand of biota, and 3) the toxicological behavior of metals inside the organisms' body (Landner & Reuther, 2004). The approach of the term varies from one author to another. Some of them define the term conceptually, whereas others give an operational definition.

1.3.1 Conceptual definitions

When speaking about bioavailable metals, Lee et al. (2000) refer to metals that are available from environmental media for bioaccumulation, whereas "bioaccumulation"

in turn is supposed to be an indicator of a particular metal dose. Moreover, Peijnenburg and Jager (2003) defined the bioavailability of metals as a phenomenon consisting of two discrete components: the physico-chemical component characterised by sorption/desorption processes, which control metal mobility in soils and determine the "chemical availability" of metals; and the biological component, characterised by a physiologically driven uptake process of a specific biological receptor. On the other hand, the US Environmental Protection Agency (USEPA) (McGeer et al., 2004) defines the bioavailability of metals as "the extent to which bioaccessible metals adsorb onto or absorb into and across biological membranes, during a given time and under defined condition". In this definition, the bioaccessible fraction is the portion of environmentally available metal that actually interacts at the organism's contact surface and is potentially available for absorption or adsorption (if bioactive upon contact) by the organism. The bioavailable fraction of a metal has thereby the potential for distribution, metabolism, elimination, and bioaccumulation. USEPA also claims that bioavailability is specific to the metal and its particulate size, the receptor and its specific pathophysiological characteristics, the route of entry, the duration and frequency of exposure, the dose, and the exposure matrix. Another definition is given by Gochfeld (2003), who, when speaks of bioavailability, refers to the ability of an organism to extract Hg from the environmental matrix (external bioavailability). This author claims that aquatic organisms readily uptake Hg from the water column, however, in higher organisms, that ingest Hg-containing food, bioavailability refers to processes within the gastrointestinal tract by which Hg is liberated from the matrix. Hg compounds that enter the gastrointestinal tract or the lungs do not necessarily gain access to the bloodstream or reach critical target organs. The amount that is transferred depends on both bioavailability and absorption.

1.3.2 Operational definitions

An operational definition is given when something is defined in terms of a process. In the case of metal bioavailability, the organisms and the effects of the metal on them, and/or the conditions, and/or the timeframe should be specified. Brun et al. (2001)

treat bioavailability as the portion of the total metal concentration (copper, in this case) in soil that can be uptaken by the roots of a given plant. Another restricted definition is given in Morton et al. (2000), who associate bioavailability with the amount of a metal that can be uptaken by certain microorganisms so that a physiological response is observable. It is generally agreed that a measure of the free metal ion represents the measure of the metal bioavailability (Peijnenburg & Jager, 2003; Worms et al., 2006), however, it is likely that bioavailable fraction includes more than just the free ion fraction (Brandt et al., 2008; Maderova et al., 2011). Brandt and co-workers' (2008) data provided evidence that Cu-DOM complexes derived from manure organic matter were bioavailable to *Pseudomonas* (i.e., able to induce expression of Cu-regulated genes). In this thesis, we consider bioavailability as a metal property that can be estimated and assessed by the Diffusive Gradients in Thin films (DGT) technique (introduced in the section below), a passive sampling technique that is supposed to mimic biological membranes and measure the labile fraction of dissolved metals (Conesa et al., 2010; Bade et al., 2012; Clarisse et al., 2012; Amirbahman et al., 2013; Han et al., 2013).

1.4   Passive samplers and the DGT technique

1.4.1   Passive sampling as a monitoring tool

The frequent need to monitor water for the presence of pollutants can cause ongoing challenges for the environmental and analytical scientist. Many of these compounds can pose a threat to both human and ecosystem health; therefore, they must be monitored to satisfy the requirements of legislative frameworks and directives. A large number of toxic compounds have been labeled as priority pollutants (e.g., those listed in the Water Framework Directive of the EU) and their measurement is required to ensure that water quality standards are maintained. Spot sampling followed by the measurement of a broad range of pollutants is the most common and widely accepted procedure used to monitor heavy metals and organometallic species in aquatic environments. The drawback of this strategy is that a relatively large number of samples must be taken from a given location along the monitoring period to

establish the quality of the water body. Therefore, this method reveals only instant levels at the time of sampling, which may not reflect the average conditions and may miss episodic peaks in discharge events. One solution to this problem is to increase the rate of sampling or to deploy automated sampling devices to collect a large number of water samples over a given time period. Nevertheless, as most pollutants are present at trace levels, often large volumes of water must be collected. As a result, this type of approach to aquatic monitoring programs is time consuming and could become very costly.

To overcome these shortcomings, new sampling procedures have recently been developed including online continuous monitoring, biomonitoring, sediment analysis, and passive sampling. Biomonitoring surveys are based on measurements of the accumulation of pollutants in the tissues of living organisms. These organisms can be deployed for extended periods of time, during which they can bioaccumulate pollutants from the surrounding water. The information obtained represents time-integrated concentrations for the period to which the test organisms are exposed and has the advantage over spot sampling that the aquatic environment is effectively sampled continuously throughout deployment. Nevertheless, the use of organisms as in situ samplers has its own challenges. Some compounds may not be accumulated because they are metabolized by the test organism. Tissue concentrations may differ among individuals of the same species because rates of bioaccumulation, depuration, metabolism, and excretion; as well as stress, viability, and general condition of the organism, can vary. Furthermore, a living organism will always have a pollution background before biomonitoring starts.

It has been suggested that concentrations in sediments could be used to estimate pollutant levels in water. Equilibrium distribution coefficients are applied to predict concentrations of dissolved analytes. However, this approach is limited by the need for equilibrium between sediments and the pore water, by the potential differences in organic carbon quality among sediments, and by the formation of non extractable sediment-bound residues that are not accounted for in current equilibrium–partition models (Vrana et al., 2005).

Therefore, passive sampling offers much potential as a low-tech and cost-effective monitoring tool (Table 1.3), avoiding many of the disadvantages of active sampling and associated sample preparation techniques. In addition, passive samplers measure only the freely dissolved fraction of an analyte (Kingston et al., 2000), whereas bioaccumulation depends not only on intake from dissolved waterborne material, but also reflects uptake from food (Namiesnik et al., 2005). In short, passive sampling has the benefit of (1) providing time-average concentrations of pollutants over deployment periods ranging from hours to weeks, (2) serving as an in situ enrichment procedure, and (3) protecting analytes against decomposition during transport and storage.

Despite its 20-year history, passive sampling continues to develop as a technique. Notable progress has been made in the past few years in device design, calibration methods, and implementation of quality assurance protocols. The growing number of publications devoted to this technique proves its large potential and testifies the increasing interest for environmental monitoring (Zabiegala et al., 2010). Passive sampling devices have been available for monitoring air quality since the early 1970s. Since then, the principles of passive dosimetry have been applied to monitoring in different environments: indoor and outdoor air, aquatic systems, sediment and soil (Vrana et al., 2005). However, the most dynamic development and greatest interest in the application of passive sampling are currently in water compartment monitoring (Figure 1.3).

Different designs of passive samplers and their application in environmental research have been described in several reviews (Kingston et al., 2000; Gorecki & Namiesnik, 2002; Namiesnik et al., 2005; Vrana et al., 2005; Kot-Wasik et al., 2007; Seethapathy et al., 2008; Zabiegala et al., 2010). Nevertheless, in this thesis we are going to focus only on passive sampling methods for measuring contaminants in water.

Table 1.3. Comparison of passive samplers with biosamplers and active sampling systems. Adapted from Zabielaga et al. *(2010)*

	Passive sampling	
	Advantages	**Drawbacks**
Biomonitoring		
- Mussels - Oysters - Fish: trout, carp	- Easier sample processing - Devices are not consumed and do not die - Can be used in all environments - Estimation of water concentration - Mimics bioconcentration	- Only estimates the water-soluble fraction - Changes in the uptake rates induced by environmental factors (water flow) - Ionic compounds are not always sampled - Biofouling can make it less effective
Active sampling		
- LLE (liquid-liquid extraction) - SPE (solid-phase extraction)	- Low-cost sampling - Does not need power supply - Good correlation between both - No maintenance required - Low-volume procedure - Determination of TWA concentration based only on exposure time (not sample volume)	- Unsuitable for monitoring short-term variations in contaminant concentrations - Lower enrichment efficiency - Complicated mathematical models – analyte sampling rate must be previously calculated - Usually impossible to automate - Indirect measurement - The number of compounds for which passive sampling can be used is limited - Does not provide direct or real-time data
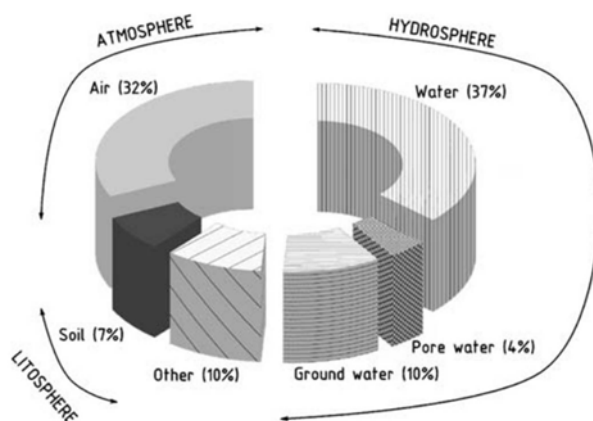
Figure 1.3. Main application areas of passive sampling used to monitor the quality of different environment compartments between 1999 and mid-2009 (Zabiegala et al., 2010).

1.4.2 Principles of Passive Sampling

Passive sampling can be defined as any sampling technique based on the free movement (by diffusion) of analyte molecules from the sampled medium to a receiving phase enclosed in a sampling device. This mass transfer is driven by differences in the chemical potential of the analyte in the two media. Sampling proceeds without the need for any energy source other than this chemical potential difference, and continues until equilibrium is established in the system, or until sampling is stopped (Gorecki & Namiesnik, 2002). Analytes are trapped or retained within the sampling device in a suitable medium, which is often referred to as the reference, receiving, or sorption phase and can be a solvent, chemical reagent, absorbent, or porous adsorbent material. The receiving phase is exposed to the water phase without attempting to quantitatively extract the dissolved contaminants. Instead, the information obtained as a result of the use of passive sampling technology depends on the accumulation regimes in which passive samplers operate during field exposure. Adsorption or absorption of pollutants from water into most passive sampling systems generally follows the profile shown in Figure 1.3.
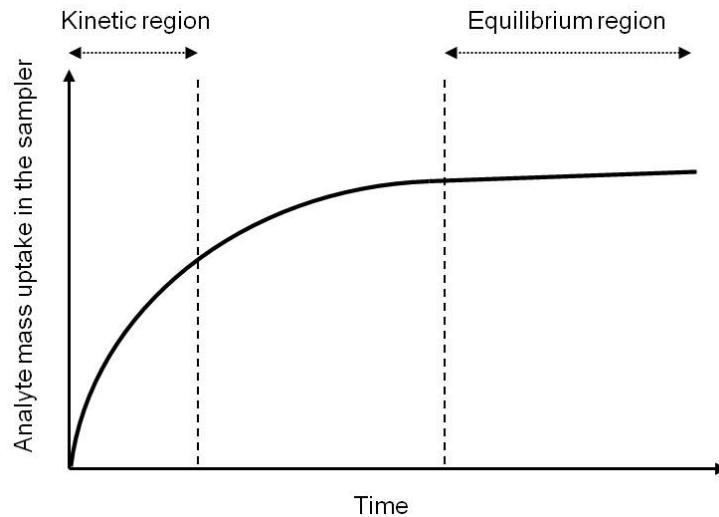
Figure 1.3. Analyte mass uptake profile of passive sampling devices that operate in two main regimes (kinetic and equilibrium).

The exchange kinetics between a passive sampler and the water phase can be described by a first-order, one-compartment mathematical model:

$$C_s(t) = C_w \frac{k_1}{k_2}\left(1 - e^{-k_2 t}\right) \qquad (1.1)$$

where $C_s(t)$ represents the concentration of the analyte in the sampler at exposure time t, C_w is the concentration of the analyte in the aqueous environment, and k_1 and k_2 are the uptake and offload rate constants, respectively. In general, a passive sampling device is designed to operate in two different modes: kinetic, time-integrative uptake or an at-equilibrium regime.

1.4.3 Sampler Design

Passive samplers are designed to maximise the amount of analyte sampled with the goal of detecting low levels of chemicals present in water, and at the same time ensuring a quantitative correlation between the collected mass of analyte and its average concentration in the sampled medium during the sampling period. Several important criteria must be taken into account in the design of an effective passive device. The device, commonly called sampler or dosimeter, should be:

- easy and not too expensive to manufacture

- easy to deploy, even by an untrained person

- small enough that it can be sent inexpensively to and from a remote location

- sensitive to the pollutants of interest

- not affected by any interfering matrix components such as humic material

Other possible advantageous properties that should be considered are the ability to withstand storage for an indefinite period before deployment and/or analysis, and the capacity to preconcentrate and/or extract the analyte without changing the concentration of the compounds sampled (Namiesnik et al., 2005).

1.4.4 Types of passive sampler devices

Several types of samplers that have been deployed in aqueous media to assess, screen, measure, and monitor inorganic pollutants are presented below to illustrate the wide range of applications of this technology. An overview of the passive sampling techniques used to measure inorganic contaminants in water is presented in Table 1.4. Whereas the other techniques are described briefly in the text, the DGT technique is treated more profoundly as this thesis focuses on it.

1.4.4.1 *Dialysis in situ*

In 1974, a method that enabled the determination of the concentration of dissolved forms of trace elements in natural waters, was described (Benes & Steinnes, 1974). The method avoids any substantial influence of adsorption on the walls of apparatus and vessels, and simplifies further analysis of the ionic and molecular forms of trace elements. It proceeds by immersing a dialysis bag filled with distilled water directly into the natural water. This sampling mode is based on the diffusive flux of species able to pass through the dialysis membrane toward a small volume of water as the acceptor solution, until equilibrium is reached. Following this pioneering study, equilibrium dialysis was considered to be a simple, size-based separation method applicable to the study of trace metal speciation (Truitt & Weber, 1981). Metals

associated with colloids and humic acid complexes that are larger than the pores of the membrane are excluded from sampling.

1.4.4.2 Dialysis with receiving resins

This technique has been used for determination of trace elements in seawater (Davey & Soper, 1975) and polluted waters (Morrison, 1987), and is considered to be a more sophisticated alternative to in situ dialysis, as the samplers employed also consist of a receiving phase (e.g., a chelating resin) with a high affinity for the target species (Figure 1.4). If a suitable chelating resin is selected, the bioavailable metal species can be separated and diffusion across the dialysis membrane may simulate metal transport processes across biological barriers. Often, Chelex 100 is used as the chelating resin facilitating uptake of the soluble fraction of Cd, Pb, Zn and Cu at low ambient water concentrations (Wu & Lau, 1996; Tao & Liang, 1997). The coefficients of variation are frequently lower than those obtained with biosentinels such as mussels, making this resin a promising acceptor phase for the measurement of dissolved metal species in seawater.
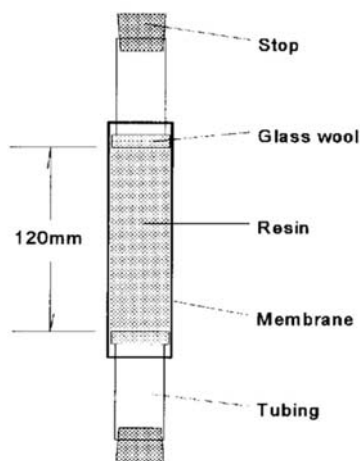
Figure 1.4. Schematic diagram of a resin-filled dialysis cell (Tao and Liang, 1997).

Table 1.4. Summary of passive sampling tecniques for inorganic contaminants in water. Adapted from Vrana et al. (2005).

Sampler name	Device design	Sampling aim	Analytes	Deployment period	Advantages	Drawbacks	Sample preparation	References
Dialysis in situ	Membrane housing in acceptor solution	Separation, determination of concentrations	Trace metals	Weeks	No reagents, versatile	Not selective	Direct analysis of the dialysis retentate	(Truitt & Weber, 1981)
Dialysis with resins	Membrane housing in solution with a receiving resin	Separation, pre-concentration, measuring concentrations	Trace metals	Weeks	No reagents, versatile	Low selectivity	Acid extraction	(Wu & Lau, 1996)
SLM (Supported liquid membrane)	Strip solution with a strong complexing agent separated from the test solution by a macroporous hydrophobic membrane	Integrative field sampling, pre-concentration, mimicking biological membranes	Doubly charged cations	Days	Versatile, selectivity can be adjusted		Direct analysis, can be coupled on-line for real-time monitoring	(Jonsson & Mathiasson, 1992)
PLM (Permeation liquid membrane)	Microporous hydrophobic support separating test solution from receiving solution	Measuring bioavailable metal species	Cu, Pb, Cd, Zn	Hours	Selectivity can be adjusted using an appropriate combination of carrier media and receiving phase	Complicated device preparation	Solvent extraction	(Slaveykova et al., 2004)

Sampler name	Device design	Sampling aim	Analytes	Deployment period	Advantages	Drawbacks	Sample preparation	References
SLMD (Stabilized liquid membrane device)	LDPE lay-flat tubing containing an acidic solution with high affinity for the target elements	Pre-concentration, sampling in situ, determination of labile metal ions	Divalent metal ions: Cd, Co, Cu, Ni, Pb, Zn	Days-weeks		Early development stage	Acid extraction	(Brumbaugh et al., 2002)
DGT (Difussive gradients in thin films)	Two layers of hydrogel (normally acrylamide) mounted in a plastic holder, one containing a binding agent and the other actin as a thin diffusion layer	Integrative sampling, screening, mimicking biological uptake, speciation	55 metalic elements, phosphorous, sulphide and ^{99}Tc	Weeks	Versatile, well documented	Complicated device preparation, biofouling	Acid extraction or direct analysis of the resin layer	(Davison & Zhang, 1994)
PIMS (Passive integrative mercury sampler)	LDPE lay-flat tubing	Preconcentration, screening	Neutral Hg species	Weeks-months	Membrane characteristics can be altered for control of sampling rates	Further development necessary for aquatic conditions	Direct analysis of the receiving phase	(Brumbaugh et al., 2000)
Chemcatcher	An inmobilized chelating resin on a PTFE base and a cellulose acetate membrane filter acting as a diffusion layer	Integrative in situ sampling, speciation	Cd, Cu, Ni, Pb and Zn	2-4 weeks	Selectivity can be adjusted using an appropriate combination of membrante and Empore disks, calibration data available for many chemicals		Acid extraction	(Persson et al., 2001)

1.4.4.3   Liquid membrane devices

Supported liquid membranes (SLM) preconcentrate trace elements from water and have been developed to mimic uptake across biological membranes. This system comprises a thin macroporous hydrophobic membrane (either as a flat sheet or as a hollow fiber with a small lumen) impregnated with an organic solvent containing a complexing agent that is selective for the target element (Figure 1.5). SLM devices have been used to measure Cd, Co, Cu, Ni, Pb, and Zn in natural waters. The utility of this technique for in-laboratory, pre-concentration/speciation of labile trace metals in bulk water samples has been demonstrated and effects of turbulence, pH, and concentration variations on the performance of SLM devices have been reported (Brumbaugh et al., 2002).
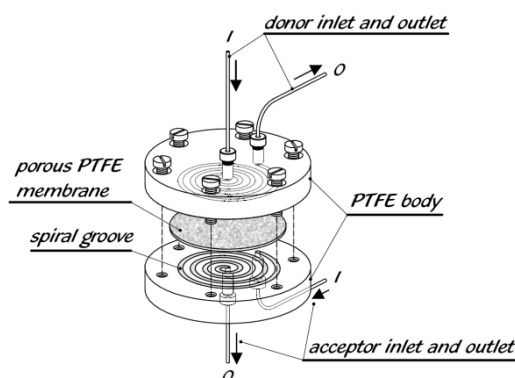
Figure 1.5. Design of a supported liquid-membrane device (Namiesnik et al., 2005).

The permeation liquid membrane (PLM) device is the result of further development of the SLM. The PLM technique is based on liquid–liquid extraction principles, taking advantage of a carrier-mediated transport of metals across a hydrophobic membrane (Buffle et al., 2000). The transport of Cu, Pb, Cd, and Zn complexes through a PLM with a neutral macrocyclic carrier and its capability for pre-concentration and speciation (both in one step) of trace metals was demonstrated using flat sheet as well as hollow-fiber support geometry (Slaveykova et al., 2009).

The stabilized liquid membrane device (SLMD) consists of a heat-sealed strip of low-density polyethylene (LDPE) layflat tubing containing an equal mixture of oleic acid and EMO-8Q. Each sampler is fabricated with a small loop on one end of the LDPE

tubing for attachment of a tether cord. The SLMD sampler is characterised by process-enhanced stability of the complexing media and is suitable for long-term, low-level in situ monitoring of labile forms of toxicologically important divalent metal ions (Cd, Co, Cu, Ni, Pb, and Zn). Field sampling was demonstrated for at least 9 days and, based on laboratory experiments, sampling intervals of up to several weeks seem possible (Brumbaugh et al., 2002).

1.4.4.4 Chemcatcher

The Chemcatcher is a passive sampling design developed by Kingston et al. (2000) for sampling of organic compounds from water. The device (Figure 1.6) consists of a two-piece polypropylene body housing the receiving phase, a diffusion-limiting membrane, and a protective open mesh. The design maintains a water tight seal.
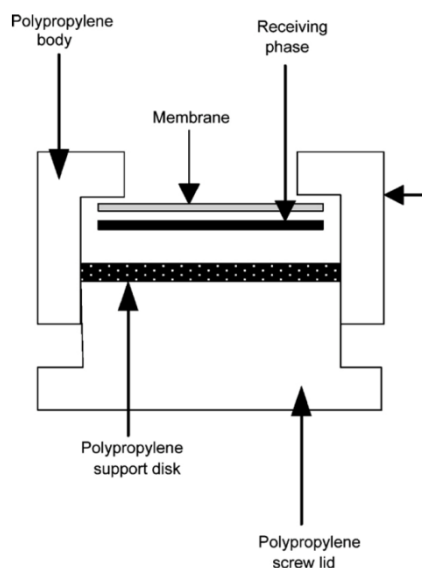
Figure 1.6. Design of the Chemcatcher passive sampler (Seethapathy et al., 2008)

A Chemcatcher variant has been developed for monitoring metals (Persson et al., 2001; Bjorklund Blom et al., 2003). This version is based on diffusion through a porous cellulose acetate membrane to a receiving Empore™ disk, which removes the analyte by chelation. In situ deployment of the passive sampler provided metal concentrations that corresponded to the electrochemically available fraction of total metal (Blom et al., 2002). Temperature and turbulence had a significant effect on sampling rates of

metals (Greenwood et al., 2007). Another Chemcatcher variation has been developed for the measurement of the time-weighted average (TWA) concentrations of organotin compounds (monobutyltin, dibutyltin, tributyltin, and triphenyltin) in water (Aguilar-Martinez et al., 2008).

1.4.4.5   Passive Integrative Mercury Sampler

Attempts have been made to use the passive integrative mercury sampler (PIMS), originally designed for air sampling, to sample neutral Hg species in water (Brumbaugh et al., 2000). The device consists of layflat LDPE tubing containing a reagent mixture of nitric acid and gold stock solution. PIMS does not require extraction for analysis, it is suitable for long-term (weeks to months) collection of dissolved gaseous Hg and neutral Hg species (e.g., $Hg(OH)_2$) from air or water, and the preconcentrating sampler design allows for convenient analysis by laboratories not equipped for low-level Hg determinations.

1.4.4.6   SorbiCell sampler

The SorbiCell sampler (Figure 1.7) can measure average concentrations over long periods of time (days to months) for various substances.
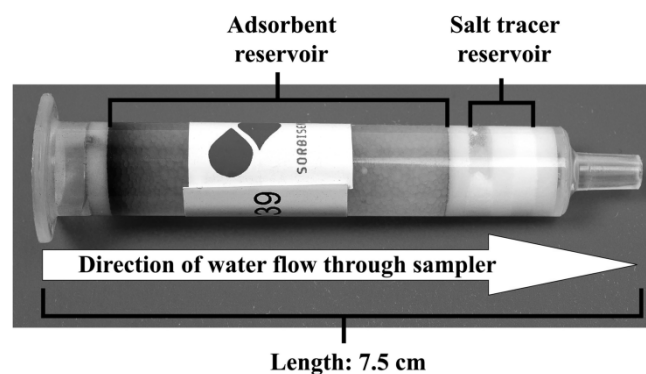
Figure 1.7. Design with basic components of a SorbiCell passive sampler (Rozemeijer et al., 2010).

The method is based on advective flow of water through the sampler, rather than establishing equilibrium or kinetic diffusion of analytes. To induce the water flow

through the samplers, they are typically placed on reservoirs with atmospheric pressure inside. Depending on the application, different mounting systems are used for sampling in groundwater wells, lakes, streams, and drain pipes, sewage pipes, or pressurized pipes. This sampler has been successfully applied for the sampling of nitrate, phosphate, and organics in groundwater, surface and drain water (De Jonge & Rothenberg, 2005; Rozemeijer et al., 2010). Based on field experiences, control of flow velocity and sample volume capacity were the most critical aspects and required careful optimization. Nevertheless, SorbiCell samplers proved to be a cost-effective alternative to grab sampling.

1.4.4.7   *Diffusive Equilibrium in Thin Films*

The Diffusive Equilibrium in Thin films (DET) principle, developed by Davison et al. (1994), is similar to dialysis except that the chamber volumes are filled with a gel instead of water. Solutes in the surrounding solution diffuse into the gel until the concentrations in the gel and in the water are equal. Compared with dialysis, this technique presents the advantage of relatively fast response times (within a day) and the ability to perform measurements at detailed spatial resolution (up to 0.1 cm). Similar to DGT (section 1.1.4.8), the DET principle is based on diffusion of target molecules into the gel. However, there is no resin where these target molecules are accumulated. The DET technique is an equilibration technique and was originally limited to the measurements of Fe, Mn, and other major anions and cations in the environment (Zhang et al., 1999). However, the advent of highly sensitive, multielement analytical instruments such as ICP/MS has opened up the technique to a large range of metals (Fones et al., 2001).

1.4.4.8   *Diffusive Gradients in Thin films*

Diffusive Gradients in Thin films (DGT) devices were first used in the mid-1990s as an in situ technique for determination of kinetically labile metal species in aquatic systems by Davison and co-workers (Davison & Zhang, 1994; Zhang & Davison, 1995).

Since then, it has been developed as a general monitoring tool for a wide range of analytes. In addition to the transition and heavy metals measured originally, major cations such as Ca^{2+} and Mg^{2+} (Dahlqvist et al., 2002), stable Cs and Sr isotopes (Chang et al., 1998), phosphates (Zhang et al., 1998) and sulphides (Teasdale et al., 1999) have been analyzed. In a comprehensive study, Garmo et al. (2003) demonstrated the capabilities of DGT to measure 55 elements with a resin gel based on Chelex 100.

The DGT technique is based on the diffusive transport of solutes across a well-defined concentration gradient, typically established within a layer of hydrogel and outer filter membrane, making it possible to obtain quantitative data on concentration and speciation over relatively short time periods (from hours to weeks). DGT units comprise a binding agent, which is separated from the solution to be analyzed by an ion-permeable gel and a filter membrane, all assembled into a plastic sampling device consisting of a piston base and a cap (Figure 1.8).
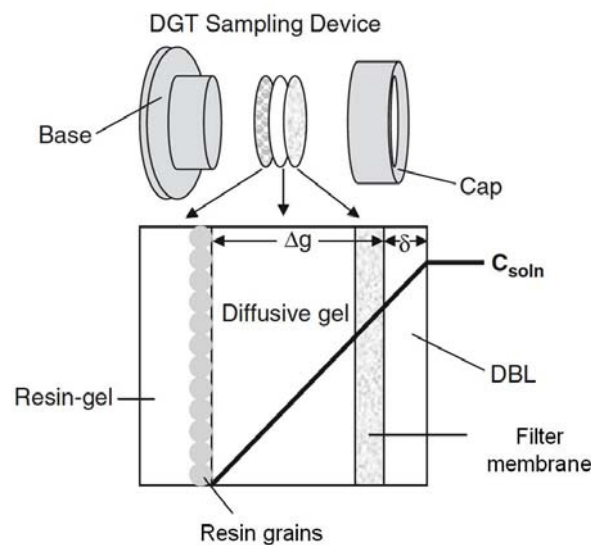
Figure 1.8. Design of a DGT sampling device. The schematic drawing shows the main parts: a base and a cap, which contains the filter, the diffusive gel and the resin or receiving gel. The diffusive boundary layer (DBL) extends out from the device face into the bulk water with a concentration (C_{soln}) (Adapted from Warnken et al. (2007)).

The cap has an opening or window that uncovers a known area of the filter, which is exposed directly to the deployment solution and acts as a protective layer for the diffusive gel. Once diffusing through these outer layers, solutes are irreversibly removed from the solution and chelated by a selective binding agent, which is

immobilized in a second layer of hydrogel. The hydrogels used in DGTs are typically made of polyacrylamide, which can be fabricated with a range of properties, including almost unimpeded diffusion due to the gel having a water content as high as 95% (Zhang & Davison, 1999). However, some studies have demonstrated the usefulness of agarose gel as a diffusive gel for certain compounds (e.g., Hg species) (Docekalova & Divis, 2005).

Based on Fick's first diffusion law, the mass of analyte (M) accumulated by the resin inside the DGT unit depends on its concentration in solution (C), its diffusive coefficient (D) in the diffusive gel, and some physical properties of the diffusive gel layer itself, such as thickness (Δg), surface area (A), and deployment time (t) of the DGT device in solution.

$$M = \frac{DAtC}{\Delta g} \qquad (1.2)$$

Species accumulated by the resin are extracted in the laboratory and the absolute mass M then yields the dissolved concentration.

$$C = \frac{DAtM}{\Delta g} \qquad (1.3)$$

The theoretical basis for the use of DGTs in aqueous solutions has been systematically developed in the past decade (Lehto et al., 2006). Improvements in design and the broad range of inorganic pollutants that can be sampled contributed to the versatility and widespread use of the DGT technique. It is possible to sample any labile species for which a suitable binding agent can be embedded into the receiving phase gel. Heavy metals are usually measured using Chelex 100 as a binding layer (resin gel). Chelex 100 is an ion-exchange resin, selective for divalent and trivalent metal ions. However, other kinds of even more selective resins have been used, including thiol groups specific for Hg species (Clarisse & Hintelmann, 2006; Clarisse et al., 2009), ferrihydrite for phosphates (Zhang et al., 1998; Santner et al., 2010), silver iodide for sulfide (Devries & Wang, 2003) and ammonium molybdate or copper ferrocyanide for Cs (Murdock et al., 2001).

Preliminary experiments are usually conducted prior to deployment in the environment to establish specific DGT performance characteristics, including the diffusion coefficients of metals and their complexes (Scally et al., 2006), the capacity of the resin layer, the elution factor of metal ions from the resin-gel (Zhang & Davison, 1995) and the effects of solution composition, pH dependence, and flow and deployment time (Gimpel et al., 2001).

Applications of the DGT technique in waters, soils, and sediments were reviewed in 2000 by Davison et al. Further development and applications in aqueous systems, which include its use for (1) speciation measurements, (2) bioavailability studies, and (3) routine environmental monitoring, were reviewed in 2007 by Warnken and collaborators.

This technique was chosen to be developed for labile Hg species determination in freshwater as part of this thesis' work. The reason was that it appeared to be a promising monitoring tool for metals, but still little developed for Hg measurements.

1.4.5 Calibration and Environmental Factors Affecting Passive Sampling

Theoretical and experimental approaches are used to calibrate passive sampling devices. In a theoretical approach, the kinetic parameters characterizing the uptake of analytes are estimated using semi-empirical correlations between mass transfer coefficients, diffusivities in various media, and hydrodynamic parameters. Nevertheless, it is often difficult to estimate uptake parameters because of the complexity of the water flow around sampler devices during exposure. Substance-specific information such as the distribution coefficient K, which characterises the affinity of a pollutant to the receiving phase relative to water, is usually available from the literature.

For practical purposes, calibration of passive sampling exchange or uptake kinetics is performed in the laboratory at known exposure concentrations (Harper et al., 1998).

Knowledge of the uptake rates of specific analytes under different environmental conditions is required, and those rates depend not only on the physicochemical properties of the chemicals, but also on the design of the device and environmental variables, such as water temperature, water turbulence, and biofouling. If significant alterations in uptake rates occur due to changes in temperature and turbulence, then laboratory-derived calibration data must be adjusted to compensate for the effect of the environmental variable on the sampler performance. Water turbulence affects the thickness of the diffusive boundary layer (DBL) of water that is part of the diffusion-limiting barrier close to the surface of the sampler, and accordingly affects the mass transfer of the analytes. Nevertheless, in the case of DGT, the effect of the turbulence is negligible since the diffusive layer is what controls the diffusion. The dynamic viscosity changes greatly with temperature. Thus, the diffusion coefficient also changes with temperature. It is therefore necessary to determine the temperature during sampling, which is often accomplished by measuring the initial and final temperature (Zhang & Davison, 2000). Several methods have been developed to compensate for the effect of environmental variables in sampler performance.

A potentially serious challenge, especially for long-duration deployments of passive samplers in natural waters, is that of biofouling, or colonization by bacteria and various flora and fauna on the active sampler surface that may ultimately form a biofilm. Algal films typically limit metal transport based on molecular diffusion. The primary effect of such growth arises from its influence on the DBL. Biofouling can affect the overall resistance to mass transfer by increasing the thickness of the barrier and by blocking any water-filled pores in the DBL. In addition, the colonizing organisms may also damage the surface of membranes. Given the same membrane, the composition of biofilms varies significantly depending on the aquatic system and even from exposure to exposure (e.g., season, time). If long-term deployments in productive waters are expected, it is prudent to deploy multiple configurations of samplers in order to correct for any deviation in DBL thickness. Biofilms can also serve as sorption sites for dissolved metals (Tien & Chen, 2013), and, as a result, may lead to an underestimation of the free metal ion concentration predicted by passive samplers. The problem of biofouling in passive sampling devices may be reduced by careful selection of suitable

materials. For example, polyethersulfone used in one design of the Chemcatcher is less prone to fouling than the polyethylene used in semipermeable membrane devices (Alvarez et al., 2005). Furthermore, certain membrane devices are protected from fouling by slow seeping of a fouling-inhibiting solvent (e.g., n-hexane) from the sampler during exposure. Protection by screens made of metal (e.g., copper or bronze) has also been shown to inhibit biofilm growth (Vrana et al., 2005). However, the choice of such screens excludes the measurement of heavy metals with these samplers.

On the other hand, in a biofouling protection approach adopted by Björklund Blom et al. (2003), a thin surface coating of Nafion was applied to the diffusion-limiting membrane (e.g., cellulose acetate) of a passive sampler system, which to some extent prevented periphyton growth on the sampler. Also, the addition of AgI or CuI_2 to the membrane filters was shown to help prevent the formation of biofilms on the surface of polysulfone membranes (Pichette et al., 2007). The two metals appeared to be more effective than antimicrobial agents (chloramphenicol and glutaraldehyde) in limiting algal growth, and, in contrast to AgI, CuI_2 does not appear to interfere with DGT measurements.

1.4.6   Other utilities of passive samplers

DGT is the passive sampling technique chosen to be developed and applied in the studies that are the object of this thesis. Thereby, this section is centred on this technique.

1.4.6.1   *Physicochemical speciation*

With regard to environmental contaminants speciation, not only chemical speciation (see section 1.2.3) (trace metals are present in water in several forms such as hydrated ions, and inorganic and organic complexes) is taken into account, but also physicochemical speciation of the forms in which analytes are present in the sampled matrix (e.g., freely dissolved, colloidal, and particle-bound forms). Species associated with heterogeneous colloidal dispersions may be present, and the particulate phase

also contains elements in different states of chemical association, ranging from weak adsorption to binding in the mineral matrix. These species coexist, although they may not necessarily be in thermodynamic equilibrium. The fractionation of species is considered a key step in assessing bioavailability and toxicity in water.

Speciation measurements must preserve the integrity of chemical species, which can be a challenge, considering that equilibria may change after sample collection due to adsorption or desorption of analytes to particulate and colloidal surfaces. In addition, the low levels of the contaminants typically present in natural waters make it difficult to differentiate the various species. Therefore, characteristic values are difficult to establish via conventional sampling procedures in environments where concentrations may oscillate. In the case of metals, passive sampling has been shown to be a useful tool for the further understanding of their species in the aquatic environment.

Speciation of metals using DGT devices depends on two effects: the difference in diffusion coefficients and the difference in affinity to the binding agent among species to be characterised. It is possible to distinguish between inorganic labile species and organic labile species by using a systematic variation of diffusion gel pore sizes, resulting in a size-discriminating uptake in a similar manner to voltammetry. However, diffusion coefficients have to be determined individually to make accurate concentration measurements of the labile species (Zhang & Davison, 2000).

According to Persson et al. (2001), different metal species may vary in their ionic radius, affecting both the calculated diffusion coefficient and the measured concentrations. Hence, exact knowledge of metal species passing through the porous membrane is critical; for example, metal–organic complexes may predominate under natural conditions in the field, while free ions and hydroxides are the species of interest present in the laboratory. Clearly, measured diffusion coefficients will depend on metal speciation and should be determined for different types of water. Depending on the environment, deployment times may also be optimized for different aquatic systems (e.g., river water, wastewater, or even industrial effluents). An exhaustive

calibration database for known metal concentrations in different aquatic environments will be a prerequisite for further development of the passive sampling system.

DGT was also used to differentiate metal–DOM complexes by size using two different types of DGT gels, which are commonly referred to as the open pore gel and the restricted gel (Warnken et al., 2008). The latter has much smaller pore size, allowing only the penetration of free metals ions; the former has large pores that are permeable to high molecular weight compounds and complexes. However, other authors caution that humic and fulvic acids will also accumulate in DGT/DET devices, i.e., metal–DOM associated metals are not strictly excluded by these passive samplers and only careful DGT/DET comeasurement and interpretation of data may allow the estimation of free ion metals in the presence of DOM (Van der Veeken et al., 2010).

1.4.6.2   *Assessing bioavailability*

The biological availability and therefore the toxicity of metals in aquatic systems strongly depend on the species in which the metal is present in water. However, it is a perennial challenge for environmental chemists to determine the speciation of metals in situ. Although DGTs and other passive sampling devices do not provide information regarding the species distribution of metals (when using only one sampler conformation), they are deemed to respond to the labile fraction (species which are unstable, likely to change and react with other compounds) of dissolved metals in water. Lability has been correlated with metal bioavailability (Jansen et al., 2002), which is the starting point for many researchers to consider the DGT technique as tool to estimate the bioavailable fraction of metals in aqueous media.

A number of studies have been conducted to evaluate the usefulness of DGT measurements to predict the availability of metals for plants in soils and soil solutions. Plant uptake of three metals (Ni, Cd, and Zn) correlated with the uptake of these metals into DGT, suggesting that DGT may be useful in assessing the potential biovailability of metals in soils (Huynh et al., 2010). Furthermore, most of the dissolved

Zn and half of the dissolved Cu in runoff from road sites was potentially bioavailable according to DGT measurements (Munksgaard & Lottermoser, 2010).

DGTs have also been used to estimate the bioavailability of metals in aquatic ecosystems. Bradac et al. (2009) related the increased uptake of Cd in peryphyton to the concentration of labile (DGT determined) Cd, rather than total free Cd. A significant relationship was also found between metal (i.e. Cu, Pb) accumulation in DGT and bioaccumulation in chironomids (Roulier et al., 2008). When monitoring the water quality in the presence of suspended particles, DGT samplers were found to be less sensitive to variations in metal concentrations compared with amphipods (Stark et al., 2006). However, DGT determined Cd concentrations were reasonably close to modeled Cd concentrations and had good predictive capability for Cd uptake into amphipods (Pellet et al., 2009). Similarly, the bioavailability of Cu in water containing natural DOM, expressed as the fraction binding to fish gills, correlated well with the DGT Cu concentrations (Luider et al., 2004). Laboratory experiments with saltwater clams exposed to MeHg under varying conditions of salinity, temperature, and DOM concentrations resulted in a linear relationship between MeHg uptake into clams and DGT (Clarisse et al., 2010). The authors suggested that DGT devices may serve as a viable sentinel for bioavailable MeHg. As a consequence of all these studies, the DGT technique has been promoted as a suitable and promising monitoring tool to predict metal bioavailability.

1.5   Methylmercury photodegradation in water

Due to the high toxicity and the bioaccumulation and biomagnification capacity of MeHg, the study of its elimination pathways is crucial to control its presence in aquatic environments. MeHg can be demethylated either by the action of microorganisms in the water column (Matilainen & Verta, 1995; Schaefer et al., 2004) or by photodegradation in superficial waters (Sellers et al., 1996). However, the latter has been proven to be the principal mechanism of MeHg removal in oligotrophic lakes (Sellers et al., 2001; Hammerschmidt & Fitzgerald, 2006b; Lehnherr & Louis, 2009).

Although direct photolysis was also observed by Inoko (1981) in an MeHgCl aqueous solution irradiated at the wavelength of Hg absorption (253.7 nm), visible and ultraviolet (UV) radiation have the capacity of decomposing MeHg essentially by indirect photolysis involving reactive oxygen species (ROS) (e.g. hydroxyl radical, ·OH; singlet oxygen, $^1O_2$) (Suda et al., 1993; Gardfeldt et al., 2001; Chen et al., 2003; Zhang & Hsu-Kim, 2010b) formed by solar light shining on the water and its DOM.

To better understand these processes, a summary of the mechanisms of MeHg decomposition and the kinetic parameters of MeHg photodegradation is reported below.

1.5.1 Factors affecting MeHg photodegradation

All the studies mentioned above illustrate diverse environmental factors competing and influencing the MeHg photodegradation rate in surface waters. Among those factors, we can find MeHg concentration, intensity and wavelength range of the solar radiation, filtration of the water, and the type and concentration of DOM.

1.5.1.1 MeHg concentration

The relationship between the MeHg photodegradation rate in surface water and the initial concentration of that Hg species is lineal as demonstrated by Sellers and co-workers (1996) and Hammerschmidt and Fitzgerald (2006) in the experiments performed at the Experimental Lakes Area (ELA, Ontario) and at an artic lake (Toolik Lake, Alaska), respectively. In both studies, the photodegradation rate increased with MeHg initial concentration.

1.5.1.2 Radiation intensity

In those two studies (Sellers et al., 1996; Hammerschmidt and Fitzgerald, 2006), it was observed that both the daily average photosynthetic active radiation (PAR) and

the MeHg decomposition rate decreased exponentially in relation to the water depth. Thus, MeHg photodegradation rate is positively correlated with PAR intensity. At Toolik Lake, this correlation occurs in all the depths except from the surface. The fact that MeHg degraded faster in the water surface can be attributed to the additional influence of the UV light (UVA and UVB, 280-400 nm), that is more intensely attenuated with depth than PAR in surface lacustrian waters (Morris et al., 1995).

1.5.1.3 Radiation wavelength

Various studies have demonstrated that the UV radiation is the main responsible for MeHg photodegradation in surface waters. Those works showed that in samples incubated in the dark or exposed to visible light, there is no significant MeHg degradation ($p > 0.1$), whereas in samples exposed to full sunlight (UVB+UVA+visible) or to UVA+visible radiation, an important degradation is observed (Lehnherr and Louis, 2009; Li et al., 2010). In the experiment carried out at ELA, Canada, the photodegradation constant corresponding to the samples exposed exclusively to visible light was 7-12 times lower than in the case of samples exposed to the full solar spectrum radiation, and 5-8 times lower than in the case of those exposed to UVA+visible light (Lehnherr and Louis, 2009).

1.5.1.4 Filtration

Sellers and collaborators (1996) proved that the use of 0.45 μm pore size filters (which remove all the photonsyntetic organisms and most of the bacteria) to filter the water, has no effect on the MeHg photodegradation rate. The fact that the reaction takes place in filtered water suggests that demethylation is fundamentally abiotic. Sterilisation seems not to inhibit photodegradation either. Ten years later, these premises were confirmed when it was observed that the degradation of MeHg was very similar for non-filtered and filtered-sterilised waters, both from an artic lake and from the Everglades (Florida), incubated under environmental conditions of temperature and light (Li et al., 2010).

1.5.1.5 Dissolved organic matter

DOM concentration could be one of the key factors controlling MeHg degradation in waters with levels of organic matter from moderate to high, since UV light attenuation in this type of waters depends on it. In addition, it should be highlighted that DOM could affect the MeHg photodegradation by means of other processes. For instance, laboratory studies have shown that some ROS, specially ·OH (Chen et al., 2003) and $^1O_2$ (Zhang and Hsu-Kim, 2010), could have a crucial role in MeHg photolysis; and it is known that DOM, among other compounds (e.g., nitrate, iron and carbonate) (Mopper & Zhou, 1990; Zepp et al., 1992a; Brezonik & Fulkerson-Brekken, 1998; Liao et al., 2001), has a relevant role in the regulation of the cycle of ROS in water. In fact, Black et al. (2012) found that an increase in DOM concentration implies a slight decrease in the MeHg photodegradation rate, but in a magnitude lower to that expected taking into account only light attenuation, suggesting a complex role of DOM in demethylation. Furthermore, Zhang and Hsu-Kim (2010) reported that MeHg species bound to thiol-containing ligands (e.g., glutathione, mercaptoacetate, and humics) are degraded faster than unreactive MeHg-chloride complexes. Also, quinones have been proposed as agents that facilitate photooxidation in the aqueous media, with the consequent production of ·OH (Alegría et al., 1997). So determining is the organic matter for MeHg photodegradation, that Fleck and collaborators (2013) postulated that optical measurements of DOM may provide a useful tool for understanding factors controlling MeHg photodemethylation in situ.

1.5.2 Kinetic parameters of MeHg photodegradation

The MeHg photodegradation rate constant (k_{pd}) is obtained from an incubation temporal series by fitting the MeHg concentration data on the basis of a first order chemical kinetics:

$$\ln[MeHg_t] = \ln[MeHg_0] - kt \tag{1.4}$$

where [MeHg$_t$] and [MeHg$_0$] are the MeHg concentrations at time t and time 0, respectively, and k is the first order rate constant. Nevertheless, for a photochemical process, the photon flux density predicts the reaction progress better than the reaction time itself. Thereby, if ln[MeHg$_t$] is plotted versus the cumulative radiation (photosynthetic active radiation –PAR– or full spectrum radiation), k_{pd} is obtained as the slope of the regression line of this first order kinetics:

$$\ln[MeHg_t] = \ln[MeHg_0] - (k_{pd} \times \text{cumulative radiation photon flux}) \qquad (1.5)$$

In general, all the k_{pd}s obtained in field studies coincide, but they were procured by using Teflon® FEP bottles (Sellers et al., 1996; Sellers et al., 2001; Hammerschmidt & Fitzgerald, 2006b; Lehnherr & Louis, 2009). It should be noted that FEP material is not completely transparent to the UV radiation and, thus, the k_{pd} values obtained with this type of bottles are probably subestimating the real k_{pd}s.

Although Lehnherr and Louis (2009) determined that the 79% of visible light, the 51% of UVA and the 30% of UVB are transmitted by the FEP material; the previously reported values of 99%, 82% and 66% for visible light, UVA and UVB, respectively (Amyot et al., 1997), are more widely accepted since there were obtained under more realistic conditions (under sunlight exposure and the sensor measuring the irradiance inside the bottle). These percentages of radiation attenuation due to FEP material (and also due to the water's DOM) should be always measured and applied to the correction of the k_{pd}.

For instance, the similar k_{pd} found in the water of lake 979 (ELA) (3.69×10^{-3} m^2 E^{-1}) (Lehnherr and Louis, 2009) and a lake in the Alaskan tundra (3.72×10^{-3} m^2 E^{-1}) (Hammerschmidt & Fitzgerald, 2006b) could infer that MeHg photodegradation kinetics are not influenced by the site characteristics and thus, k_{pd} might be universal for freshwater, as suggested (Sellers et al., 1996; Hammerschmidt & Fitzgerald, 2006b). However, the k_{pd} obtained in water from the Everglades, a subtropical wetland with a high content of DOM, was reported to be 13.67×10^{-3} m^2 E^{-1}, substantially higher than those described before. In all those three cases k_{pd} was calculated as a function of PAR

alone (ignoring UVA and UVB, more potent in MeHg degradation), and attenuation of light by FEP and DOM was not considered. This proves the need to consider the mentioned aspects to be able to compare k_{pd}s and explore if they can be universal.

Chapter 2

Objectives of the thesis

2 Objectives of the thesis

Given the marked polluting role of Hg in the environment and especially in aquatic ecosystems, its worldwide distribution, and the increasing scientific and social interest on the issue, this thesis establishes the following **general objectives**:

- To develop the DGT (Diffusive Gradients in Thin films) technique for labile Hg determination in water, and thus, for assessment of the bioavailability of this metal in aqueous systems.

- To study the photodegradation of MeHg in aquatic environments and its possible relationship with the bioavailability of this Hg species.

Within this context, the **specific objectives** listed below are set up:

- To test the validity of commercial DGT devices for Hg measurements under laboratory conditions.

- To examine the performance of these commercial DGT samplers under environmental conditions, in order to measure in situ the labile Hg concentration in the Gállego River and the Ebro River.

- To search for the most efficient DGT sampler components for THg and MeHg determination in freshwater by comparing three different types of DGT units (one commercial and two in-house manufactured), both in the absence and in the presence of DOM.

- To assess the Hg removal efficiency of an alternative wastewater treatment system consisting of three different small-scale constructed wetlands (CWs) in series, and to examine Hg methylation in the different treatment steps.

- To determine the labile fraction of Hg and MeHg in the water along the treatment line by means of the DGT technique and to compare to the direct measurement of Hg and MeHg in the water.

- To determine rates of MeHg photodegradation in DOM dominated (humic) waters along a forested wetland – freshwater lake gradient in boreal Sweden, and to calculate wavelength-specific first-order photodegradation rate constants ($k_{pd\ PAR}$, $k_{pd\ UVA}$, $k_{pd\ UVB}$), corrected for the light attenuation by DOM.

- To study the photodegradation of MeHg in different natural and artificial freshwaters and to assess the MeHg bioavailability by measuring its labile fraction by means of the DGT technique.

PART II

Chapter 3

Assessment of the DGT technique for dissolved mercury monitoring in natural freshwaters

3 Assessment of the DGT technique for dissolved mercury monitoring in natural freshwaters

3.1 Objectives of the study

The first aim of the work included in this chapter was to validate a type of commercial DGT samplers for Hg determination under laboratory conditions. Once the performance of the DGT samplers was tested, the next objective was to obtain the diffusion coefficient of this Hg species in the diffusive layer of our DGT units. Later, we wanted to check the uptake efficiency of the DGT technique under environmental conditions. For that purpose, we set the aim of determining an accurate field diffusion coefficient for all the Hg species present in river water. Another objective was to measure in situ Hg concentration in certain stretches of the Gállego River and the Ebro River, both carrying a long history of Hg pollution episodes.

3.2 Experimental Methodology

3.2.1 Materials and general procedures

The ready-to-use DGT-Hg units used for these experiments were purchased from Exposmeter AB (Tavelsjö, Sweden). Each DGT unit consists of a plastic piston and a plastic cap with a window 2 cm in diameter (the diameter of the whole assembly is 4 cm and its height 1.7 cm), a Spheron-Thiol resin (with –SH groups) immobilised in a layer of polyacrylamide gel as the binding agent, an agarose gel diffusive layer with a thickness of 0.76 mm on the top of the resin layer, and a 0.45 μm pore size filter membrane with a thickness of 0.1 mm covering the latter. DGT units, kept in a zip lock polyethylene bag containing a few drops of 0.01 M NaNO$_3$ solution, were stored in a refrigerator at 4 °C before deployment. During storage, the units were checked once a week to make sure they were under moist conditions. DGT deployment involved the immersion of the sampler in an aqueous solution in the case of laboratory assays or in river water in the case of field studies. The sampling devices used in every case to hold and suspend the DGT units varied depending on the environmental conditions

(described below in the corresponding sections). After retrieval, the DGT devices were rinsed with Milli-Q water and kept in clean polyethylene bags for transport to the laboratory and storage at 4 °C. Prior to analysis, DGT units were dismantled, resin gels were extracted and the amount of Hg was detected by AAS by means of an AMA-254 spectrometer, manufactured by Altec (Prague, Czech Republic) and distributed by Leco Corp. (St. Joseph, MI, USA).

In the laboratory assays, THg was determined in the spiked water solution before and after DGT deployment by taking a 5 mL aliquot and analysing it immediately using the AMA-254. In the field studies, a volume of 100 mL of water was collected at the beginning and the end of the DGT deployment, acidified to 0.4% with concentrated HCl and stored at 4 °C until analysis.

The pH in the solutions was measured using a pH meter GLP 22 with a pH electrode 52-02 (Crison Instruments, Barcelona, Spain). A Multi Probe System YSI 556 MPS (YSI Inc., Yellow Springs, OH, USA) was used to measure temperature and conductivity in situ in natural waters. Mercury solutions were prepared from an MeHgCl (99%) standard from Strem Chemicals (Newburyport, MA, USA). Sodium chloride GR for analysis was purchased from Merck (Darmstadt, Germany). For dilutions and test solutions, high-purity demineralised water provided by a Milli-Q Plus filter apparatus (Millipore, USA) was used.

3.2.2   Analytical determination of THg

THg in resin gels was measured using an Advanced Mercury Analyzer, model AMA-254, that uses catalytic combustion of the sample, pre-concentration by gold amalgamation, thermal desorption and detection by AAS. After the sample (in this case, the entire resin gel) is placed in a nickel boat, the instrument automatically introduces it into a quartz combustion tube and self-seals. Immediately, oxygen starts to flow over the sample at 200 mL min^{-1}. Subsequently, the sample is dried at 120 °C and thermally and chemically decomposed at 550 °C. Gaseous combustion products

are carried in a oxygen stream through the catalytic furnace (kept at 550 °C), where a Mn_3O_4/CaO-based catalyst allows complete oxidation of the sample and halogens, nitrogen and sulphur oxides are trapped. At the same time, the high temperature enables the conversion of the different Hg species into Hg^0 vapour. Hg^0 and the remaining decomposition products are carried into a tube containing gold-coated sand, which works as an amalgamator and selectively traps Hg. During a pre-specified time interval (normally 45 seconds), Hg remains amalgamated while the other products are flushed out of the system. Then, the gold-based trap is heated to 700 °C in order to release the trapped Hg and blown it to an AAS detector with a low-pressure Hg vapour lamp working at 253.65 nm. The total anyalisis time of one sample is roughly 5 minutes (Diez et al., 2007). A schematic diagram of the AMA-254 instrument is shown in Figure 3.1.
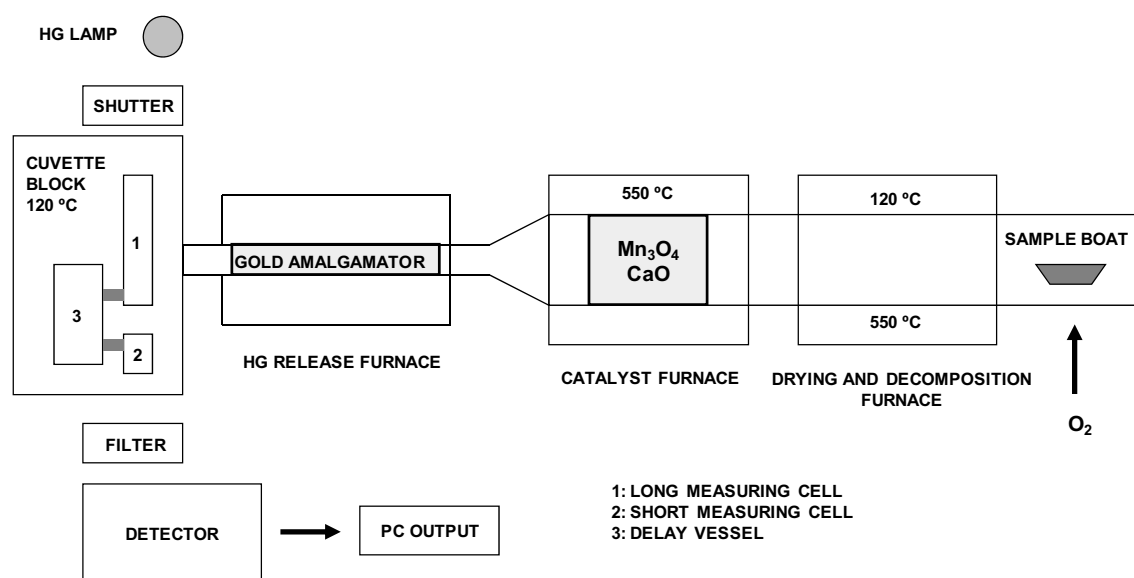
Figure 3.1. Diagram of the Advanced Mercury Analiser AMA-254.

The entire analytical procedure was validated by analyzing DORM-2 certified reference material consisting of dogfish (*Squalus acanthias*) muscle from the National Research Council of Canada (NRCC, Ottawa, Ontario), with an Hg certified value of 4.64 $\pm$ 0.26 mg kg^{-1}. This reference material was analyzed in triplicate at the beginning and end of each set of (usually 10) samples, thereby ensuring that the instrument remained calibrated throughout the study. The detection and quantification limits (0.2

and 0.7 ng g^{-1} ww of Hg, respectively) were calculated based on blank measurements (Navarro et al., 2009).

To determine THg concentrations in water, also the AMA-254 was used, but in this case a 1 mL sample aliquot was put in a nickel boat (1 mL maximum capacity) and the drying time was adjusted by a simple calculation: number of microliters of sample × 0.6 = seconds of drying time (AMA-254 Operating Manual, Leco Corp., St. Joseph, MI, USA). Because of the low concentration of Hg in water, the pre-concentration mode proposed by the AMA-254 was used for direct measurement of THg in water samples. The limit of detection (LOD) and the limit of quantification (LOQ) were calculated as 3 times and 10 times the standard deviation of the blank (0.042 ± 0.005 ng mL^{-1}, n = 6) respectively, resulting in LOD = 0.016 ng mL^{-1} and LOQ = 0.054 ng mL^{-1}.

3.2.3   Preliminary laboratory test

This first laboratory assay had the objective of assessing the repeatability of the method. For that purpose, two amber glass bottles were filled with 1L of 0.1M NaCl solution prepared in Milli-Q water. An MeHgCl standard (in acetone) was added to one of them in order to obtain a 5 ng mL^{-1} MeHg solution. The other bottle was kept as an Hg-free solution in order to obtain the experimental blank. Both solutions were left to homogenise overnight while being stirred. Subsequently, three DGT units were immersed in each bottle for 24 h, suspended and attached to the top by a nylon string. During the experiment, the temperature of the solution was maintained at 25 °C.

3.2.4   Time series experiment and calibration

A solution of MeHgCl (5 ng mL^{-1} as Hg, 0.01M NaCl), which was left to homogenise overnight, was used to perform a time series experiment in order to obtain the diffusion coefficient of this Hg species in agarose diffusive gel. Six DGT devices were submerged into the stirred solution (kept at 25 °C) for different periods of time (i.e., 8, 24, 32, 48, 54 and 120 h). At each sampling interval, a DGT unit was removed from the

solution and the mass of THg complexed by the resin was determined. Also, the remaining concentration in solution was measured in triplicate in order to monitor THg levels during the whole length of the experiment. Resin gel discs with a high load of Hg (those deployed for 32 hours and longer) were cut into smaller pieces for measurement. Then, the total amount of Hg in each disc was calculated as the addition of Hg masses in all these pieces.

3.2.5 Ebro River basin and its mercury pollution

The Ebro River basin is located in the NE quadrant of the Iberian peninsula covering an area of 85,362 Km^2, from which 445 Km^2 are in Andorra, 502 Km^2 in France and the rest in Spain. It is the largest basin in Spain, representing the 17.3% of the total area of the country. This catchment is drained by the Ebro River, the longest river in the country with a length of 910 km, that flows in NW-SE direction from Peñalabra (a mountain located in the border between Cantabria and the province of Palencia) (Romaní et al., 2011) towards the Mediterranean Sea.

At its mouth, the Ebro forms a 320 km^2 delta of high ecological, agricultural and recreational value. Part of the delta territory was declared Natural Park in 1983 and extended in 1986 due to its ornithological importance. In fact, a part of the Ebro Delta was included as a wetland of international importance in the list of the Ramsar Convention in 1993 (site 593). Furthermore, the maritime zone surrounding the delta is one of the richest fishing areas of the Western Mediterranean.

Apart from the intense agricultural and urban activity (2,800,000 inhabitants populate this extensive territory), the industrial activity is also remarkably high in the whole basin. For instance, three (in Sabiñánigo, Monzón and Flix,) out of the eight chlor-alkali plants currently existing in Spain (Figure 3.2) are located within the Ebro catchment. The method of the mercury cell, which releases Hg to the environment, is still employed for the production of chlorinated compounds in these plants. The great environmental problem derived from that aroused the interest of the scientific

community, and consequently the first publications on Hg pollution in the Ebro River basin date back to the 90s (Raldua & Pedrocchi, 1996; Ramos et al., 1999). The impact of Hg pollution in local populations of mollusks, fish and birds has been evaluated in the last years (Lavado et al., 2006; Carrasco et al., 2008; Navarro et al., 2009; Cotin et al., 2012). High concentrations of Hg were found in all the tested species indicating that the surrounding areas of chlor-alkali factories are likely the major point sources of Hg pollution in the Ebro River basin. In addition, it is suspected that substantial amounts of Hg might be transported downstream from the chlor-alkali plants dumping points towards the Ebro Delta where a wildlife reserve and a Ramsar site are located. This suspicion is supported by the report of progressively increasing levels of THg in kidney and muscle of common carps fished from a site next to Flix factory to a point 37 km downstream (Navarro et al., 2009).
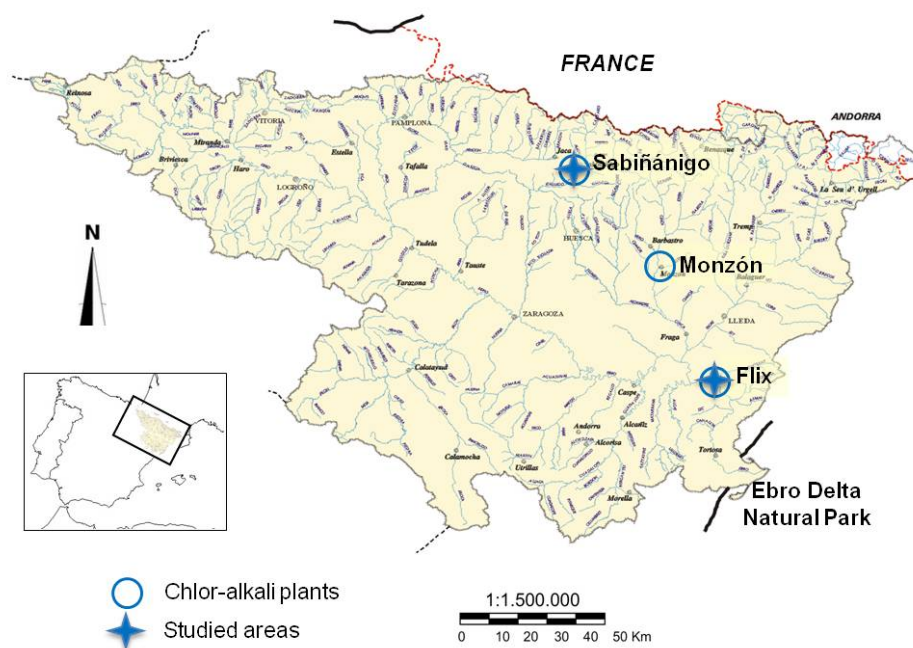
Figure 3.1. The Ebro River basin geographical area and the location of chlor-alkali plants and the areas studied in this chapter.

Apart from the knowledge that the water has substantial Hg levels, there is another reason why we selected the Ebro River and its tributary the Gállego River to test the Hg monitoring potential of the DGT technique. Once it is fully developed, this technique should be applied at theses locations, since controlling Hg concentrations

there is crucial due to the sensitive land and river uses (protected natural areas, fishing, etc.) of part of the basin.

The first testing area was a stretch of the Gállego River close to Sabiñánigo (Huesca, Spain), where a chlor-alkali factory with a capacity of 25×10^3 Mg chlorine yr^{-1} is located. The second testing area was located on the lower Ebro River, in the vicinity of the town of Flix (Tarragona, Spain), where the Erkimia chlor-alkali plant (Ercros S.A. Group) has been operational since 1899. The chlorine production of this factory is currently the highest in Spain, with a capacity of 15×10^4 Mg yr^{-1}. At present, the major concern here is a 35×10^4 Mg deposit of hazardous industrial solid waste, occupying an area of 4.2 Ha and containing high concentrations of Hg (170 µg g^{-1}) in the surface sediments and up to 440 µg g^{-1} at 1 m depth.

3.2.6   Test in the Gállego River

The DGT technique was used in the Gállego River (July 2009). Three sampling sites were selected along the river: one at the Sabiñánigo reservoir (SA), in front of the chlorinated solvent factory and close to the waste dumping point (42° 30' 47"N, 0° 21' 07"W); another at the Jabarrella reservoir (JB), located 6 km downstream from site SA (42° 28' 27"N, 0° 23' 13"W); and the last one at the Búbal reservoir (BU), 22 km upstream from site SA, acting as the control site (42° 42' 52"N, 0° 18' 10"W).

Three DGT units were deployed at each sampling point, approximately 50 cm above the sediment-water interface. The sampling device used to hold and suspend the samplers consisted of a homemade double methacrylate plate with three round holes attached to two iron sticks by a nylon string (Figure 3.3). The whole device was stuck on the sediment and the DGT units were exposed for eight days. A conductivity of 150, 300 and 250 µS cm^{-1} was measured in the river water at the beginning and the end of the experiment at the BU, SA and JB sites, respectively. Similar pH values (pH=8.3) were obtained at the BU and JB sites and pH=8.0 at the SA site. Water temperature was monitored during the experiment with average values of 19, 15 and 13 °C at the BU, SA and JB sites, respectively. Sediment was also collected at each

sampling site and THg and MeHg concentrations were determined (see Annex I). Finally, after retrieval of the DGT units, THg was analysed in the resin gels.
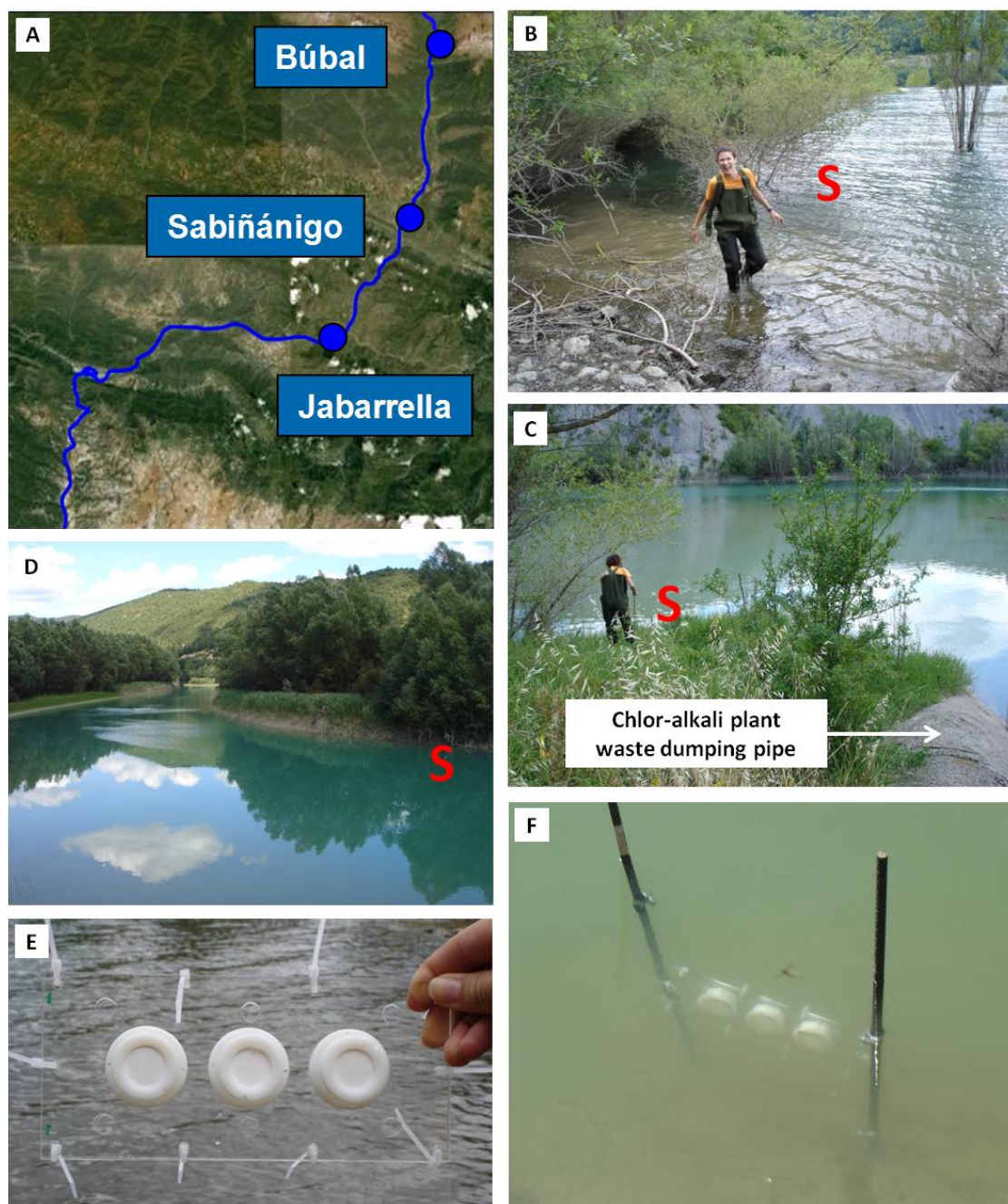
Figure 3.3. Sampling campaign in the Gállego River: (A) map of the sampling sites (for location in the basin, see Figure 3.2), (B) Búbal reservoir, (C) Sabiñánigo reservoir, (D) Jabarrella dam, (E) DGT sampler triplicate in the methacrylate plate and (F) sampling device driven into the river bed. The red S letters mark the sampling points.

3.2.7 Time series experiment in the Ebro River

The Flix Reservoir (FR) was the location within the Ebro River chosen to perform a time series experiment under environmental conditions in October-November 2009. The samplers were placed close to a chlor-alkali plant, 100 m downstream from the waste dumping point (41° 13' 56"N, 0° 32' 47"E). On the other hand, a point at Riba-roja (RB), 8 km upstream from the source of Hg pollution, was used as the control site (41° 14' 49"N, 0° 28' 40"E).

The experiment timeframe was extended in contrast with the duration of the previous test; eight days proved to be too short an exposure period in these low Hg-level natural waters, since the mass of Hg accumulated in the resin was very low. DGT units were deployed in triplicate for 2, 4, 6 and 8 weeks in FR at approximately 1–2m above the sediment-water interface. A triplicate of samplers was also deployed for eight weeks at RB as a control. The sampling device used to hold and suspend the DGT units consisted of a homemade cylindrical basket made of a plastic net for housing a double methacrylate plate with three round holes. A DGT sampler fit in each hole. Finally, the basket was anchored to a rope with a weight on one end and a buoy on the other (Figure 3.2). A similar conductivity of 1500 μS cm^{-1} was found in the river water of the control and the hot spot sites at the beginning and at the end of the experiment. A very reproducible pH value of 8.0 was measured at both sites, and the water temperature was monitored, with an average temperature of 18 °C throughout the experiment.

3.2.8 DGT measurements above sediments in the Ebro River

In November 2009, another test was performed also in the same area of the Ebro River where the previous experiment took place. The objective of this test was, in the light of the previous results, to check if these commercial DGT units are able to accumulate a significant amount of Hg in natural waters when the deployment time is shorter and the Hg concentration is supposedly higher.
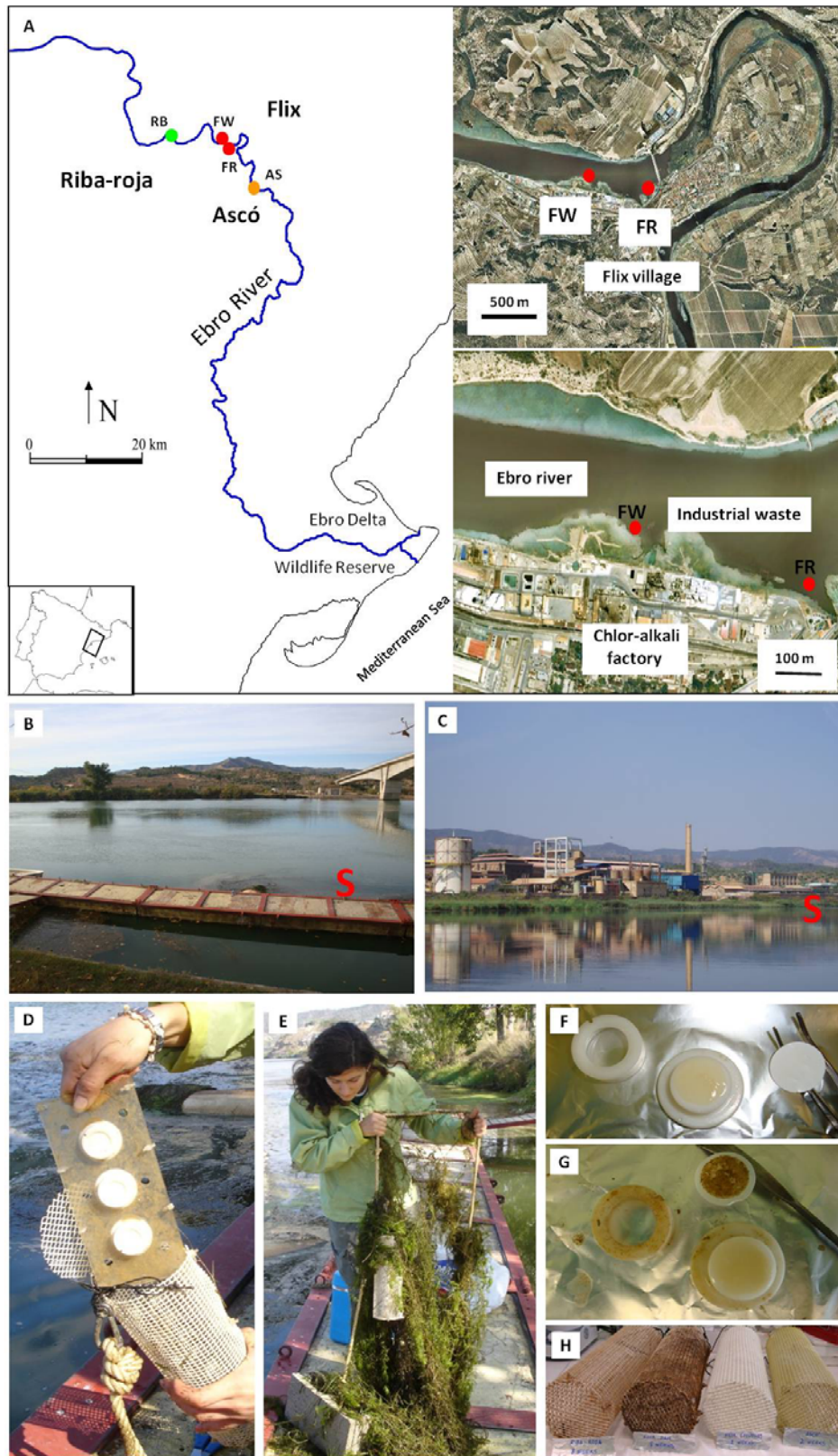
Figure 3.2. Sampling campaign in the Ebro River: (A) map of the sampling sites, (B) RB site, (C) Chlor-alkali plant by the Flix Reservoir (FW site), (D) DGT sampler triplicate in the methacrylate plate and the protective basket, (E) macrophytes covering the sampling device, (F) DGT unit blank, (G) DGT unit deployed at Flix and (H) baskets covered with biofilm and particulate matter after 8 weeks deployment at RB (first from the left) and FR (second), and 2 weeks at FW (third) and AS (fourth). The red S letters mark the sampling points.

Two sampling sites were selected for this assessment: another location in Flix Reservoir (FW) (41° 13' 56"N, 0° 32' 47"E), where the samplers were deployed over the high Hg-load sediments, and Ascó (AS) (41° 11' 1"N, 0° 34' 16"E) (Figure 3.2).

Three DGT units were deployed in each sampling point approximately 50 cm above the sediment-water interface. The DGT units were suspended in triplicates only for 2 weeks, because the previous experience demonstrated that a longer deployment time results in the formation of biofilm preventing the proper operation of DGT devices. The sampling device used for this test was basically the same as for the previous study, but in this case the basket was attached to two iron bars that were fixed into the sediment. An average conductivity of 1660 and 1630 μS cm^{-2} was measured in the water at the beginning and the end of the experiment in FW and AS respectively. pH was measured in the laboratory, obtaining a value of 8.1 at both sites. Water temperature was monitored during the experiment and an average temperature of 16 °C was measured in FW and 17 °C in AS. Finally, sediment was collected at each sampling site and both THg and MeHg concentrations were determined (see Annex I).

3.3   Results and discussion

3.3.1   Preliminary laboratory test

The THg detected in the experimental blank (DGT units deployed in an Hg-free aqueous solution) was 1.34 ± 0.05 ng. The amount of THg measured in the triplicates deployed in the 5 mg L^{-1} MeHg solution was 160 ± 6 ng. Thus, the relative standard deviation was 3.6%, a low value which proves the good precision of the technique plus the followed methodology. The value of direct measurement of THg in the spiked solution before and after DGT deployment was 4.79 ± 0.13 mg L^{-1} and 4.39 ± 0.08 ng mL^{-1}, respectively. THg concentration in the solution might have declined due to adsorption on the walls, apart from DGT uptake; however, that drift was not a trouble for this test.

3.3.2 Time series experiment and calibration

Knowing the mass of Hg accumulated by the DGT units and the volume of solution (1 L), the effect of the DGT uptake on Hg concentration in solution was estimated and those levels compared to the actual Hg concentration at every sampling time (Figure 3.3). Mass balance was calculated, and it was proven that the amount of MeHg accumulated by the sampler was equal to that lost in the solution at every time interval.
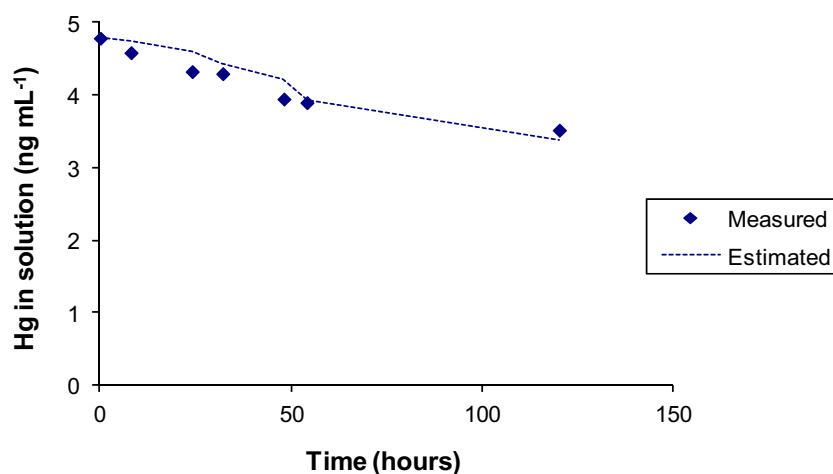
Figure 3.3. Comparison of MeHg concentration measured in the solution at every sampling time (dots) and the estimated concentration calculated by taking into account the effect of the DGT uptake.

In accordance with the DGT principle (Equation (3.1)), the mass of Hg accumulated in the resin (M) is proportional to the exposure time (t), as shown in Figure 3.4. Owing to the variable Hg concentration in solution (C) during the experiment, the mass in the figure is expressed as MC^{-1}.

The diffusion coefficient of MeHg in the agarose gel was calculated on the basis of Fick's law from the slope (s) (cm^3 s^{-1}) of the relationship between the amount of Hg accumulated by the DGT units (normalised for Hg concentration in solution) and the deployment time. Then, according to that relationship and Equation (3.1) (further explained in section 1.4.4.8, Equation 1.2), the slope could be calculated using Equation (3.2).

$$M = \frac{DAtC}{\Delta g} \qquad (3.1)$$

$$s = \frac{DA}{\Delta g} \qquad (3.2)$$

Thereby, the diffusion coefficient (D) of MeHg in the diffusive layer can be calculated with the Equation (3.3).

$$D = \frac{s\Delta g}{A} \qquad (3.3)$$

Previous studies using the DGT technique showed a good agreement between the D of Hg in water and in agarose gels (Docekalova & Divis, 2005). If the latter happens, the diffusion coefficient at any temperature, D_T, can be calculated applying the Stokes–Einstein equation (Equation (3.4)) (Zhang & Davison, 1995), where D_{25} is the diffusion coefficient of ions in water at 25 °C.

$$\log D_T = \frac{1.370223(T-25)+8.36\times10^{-4}(T-25)^2}{109+T} + \log\frac{D_{25}(273+T)}{298} \qquad (3.4)$$

The D of MeHg in the agarose gel (8.50×10^{-6} cm^2 s^{-1} at 25 °C) can be compared with that of MeHg in polyacrylamide gel (5.1×10^{-6} cm^2 s^{-1} at 20 °C) (Clarisse & Hintelmann, 2006) or that of Hg(II) in agarose gel (8.86×10^{-6} and 9.08×10^{-6} cm^2 s^{-1}) (Docekalova & Divis, 2005). This proves that different ionic Hg species have similar diffusion coefficients. In the case of our experiment, the calculated coefficient was also found to be very similar to that reported for Hg(II) in water (8.47×10^{-6} cm^2 s^{-1} at 25 °C) (Lide, 2004-2005). In this manner, D was calculated for a wide range of temperatures as shown in Figure 3.5. Hence, knowing the diffusion coefficient and applying the temperature correction, the concentration of MeHg in aqueous solution can be calculated from the measured mass of MeHg accumulated by the resin. The results of this time series experiment confirm the validity of the basic DGT principles and thus, this type of commercial DGT device can be used for reliable MeHg measurements and, by extension, of other ionic Hg species.
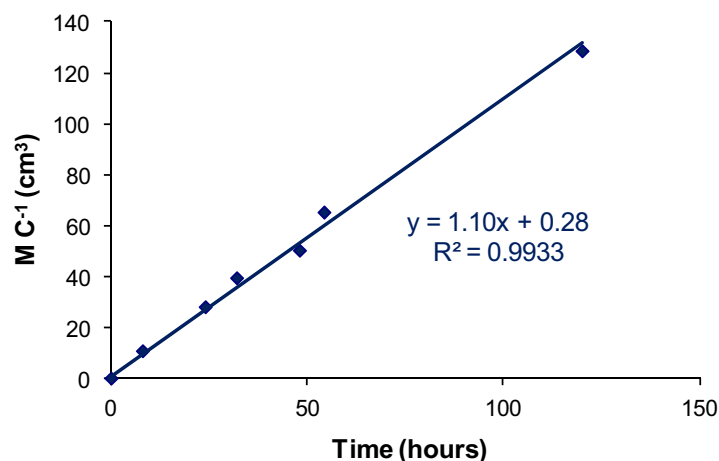
Figure 3.4. Measured mass (M) of accumulated Hg normalized for MeHg concentration in solution (5 ng mL^{-1}) for various periods of time (n = 7, p < 0.001).
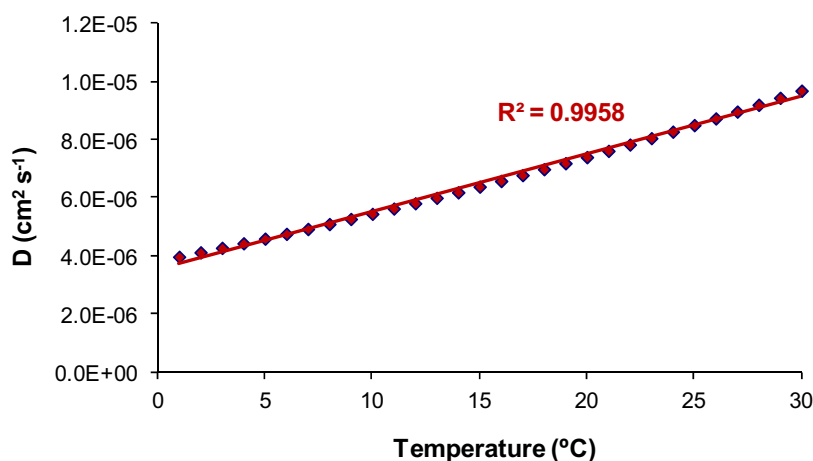
Figure 3.5. Diffusion coefficient of MeHg in the agarose gel calculated on the basis of Fick's law for a wide range of temperatures (n = 30, p < 0.001).

3.3.3   Test in the Gállego River

From now on, the concentration calculated from the mass of MeHg accumulated in the DGT will be referred as labile or DGT-labile MeHg concentration, since DGT technique determines the labile dissolved and colloidal species.

THg was determined in the resin gels of the three DGT units deployed at each sampling site giving rise to a mass of 1.5 ± 0.4 ng at BU, 5.4 ± 1.0 ng at SA, and 2.3 ± 0.6

ng at JB. The D obtained from the time series experiment in the laboratory is strictly valid only for MeHg, however we assumed that the diffusivity of all the Hg species was similar enough to use that D for the determination of all the species present in the river water. The D was corrected for the average temperature measured at BU, SA and JB, and values of 7.19×10^{-6} cm^2 s^{-1}, 6.38×10^{-6} cm^2 s^{-1} and 5.99×10^{-6} cm^2 s^{-1} were used for the DGT calculation, respectively. The three DGT devices deployed at SA site (close to the Hg pollution source) provided the highest labile Hg concentration (36 ± 7 ng L^{-1}), which was about 2.3 and 4 times higher than the concentrations downstream at JB (16 ± 4 ng L^{-1}) and upstream at BU (9 ± 2 ng L^{-1}), respectively, and higher than most Hg levels reported for river water worldwide (Bisinoti et al., 2007; Kehrig et al., 2009; Ridal et al., 2010; Zierhut et al., 2010). The high dispersion values (relative standard deviation of 24%, 19% and 25% at BU, SA, and JB respectively) may be attributed to the fact that environmental conditions are much more variable than laboratory conditions. The value of direct measurement of Hg in water from SA (89 ± 31 ng L^{-1}) was 2.5 times higher than the DGT-labile concentration (36 ± 7 ng L^{-1}). This difference may be explained by the fact that DGT measures only ionic Hg and labile Hg species, while inert organic species, large colloids and the Hg associated to the particulate phase are excluded. Furthermore, these low DGT values may be attributable to the fact that the previously determined diffusion coefficient is strictly valid only for MeHgCl under controlled laboratory conditions. In natural waters, MeHg and other ionic Hg species are partially complexed by dissolved organic matter (DOM), and those complexes are expected to diffuse at a lower rate through the diffusive gel. The use of a higher diffusion coefficient corresponding to smaller species will contribute significantly to an underestimation of the labile fraction.

In addition, sediment was collected from each sampling site and THg was analysed. Hg in sediments can be present as Hg^0, HgS, and other compounds which are assumed to consist mainly of organically bound Hg(II). HgS and Hg^0, stable and mostly insoluble, are usually the predominant forms (above the 80% of the total Hg) of Hg in river sediments (Biester et al., 2000; Shi et al., 2005). However, the mobility and bioavailability of Hg in aquatic ecosystems is affected by DOM, which can also enhance the solubility and dissolution of cinnabar (Ravichandran, 2004; Waples et al., 2005).

Thus, even though most of the Hg present in the sediments is unavailable and immobile, there can be an exchange of bioavailable species between sediment and water (Shi et al. (2005) reported a percentage of exchangeable or water soluble Hg in sediments of 0.1–4.6%).
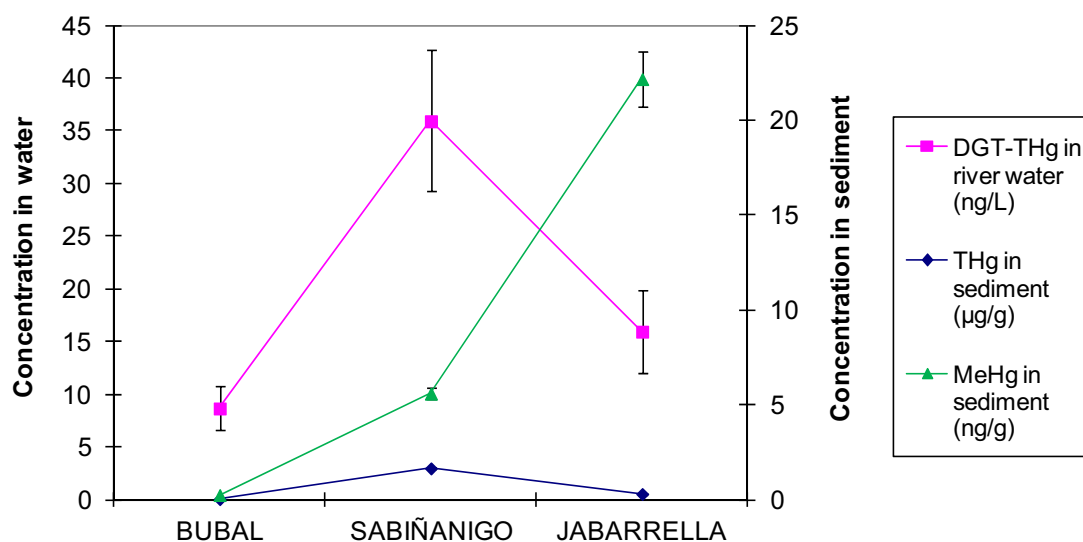
Figure 3.6. THg and MeHg concentration in sediment and labile THg concentration in water measured by the DGT technique at the three sampling points

Interestingly, the THg concentration was also higher in the sediments located just below the DGT units at the SA site (1.66 ± 0.04 µg g^{-1}) versus those at the JB and BU sites (0.31 ± 0.01 µg g^{-1} and 0.038 ± 0.001 µg g^{-1}, respectively), following the same pattern as the labile Hg measured in water by DGT, as shown in Figure 3.6. Nevertheless, the highest MeHg concentration in sediment corresponded to JB site, downstream from the hotspot.

3.3.4 Times series experiment in the Ebro River

The measured mass of Hg in the DGT devices deployed at FR for 2, 4, 6 and 8 weeks was 1.2 ± 0.2, 1.1 ± 0.2, 1.4 ± 0.3 and 1.2 ± 0.2 ng, respectively. Therefore, the DGT units deployed for eight weeks presented nearly the same mass of Hg as the units deployed for two weeks. The Hg detected in the DGT units deployed at RB was 1.2 ± 0.3 ng. The values obtained at FR were statistically not different from the values

obtained in RB and the DGT blank (1.34 ± 0.05 ng) (t-test, p > 0.05) and in one case was even lower than the blank. This means that Hg was not significantly accumulated in the DGT devices during deployment. This may be explained by the fact that a thick brownish-gray layer of particulate organic matter and microorganisms such as algae or bacteria covered the filter of the DGT units (Figure 3.2). This biofilm layer might have blocked the membrane filter, preventing Hg species from diffusing through it. Another possible explanation could be that the low level of labile Hg in the river water, combined with the unexpected levels of Hg found in the blanks, made it difficult to quantify the net Hg concentration accumulated in the resin and, further, to distinguish it from the Hg already present in the DGT. It is expected that the Hg captured by DGT corresponds with all Hg labile species; from aqueous Hg(II) and MeHg ions and small inorganic complexes with comparable diffusion coefficients, to bigger complexes with DOM which have much lower diffusivity (Zhang & Davison, 1999). However in the Ebro River water (approx. 2 mg DOC L^{-1}, measurements made for other studies), complexes with DOM as a ligand should be predominant. This might be another reason why such a low amount of Hg was retained in the resin. In light of these results, it does not make sense to calculate the Hg concentration provided by DGT. Nevertheless, the levels of THg in the river water were measured directly obtaining a value of 55 ng L^{-1} at FR and 23 ng L^{-1} at RB. The relatively high nitrates level measured by the Ebro Hydrographic Confederation at Flix (9.8 mg L^{-1}) during the experiment indicate the eutrophic nature of this river water in comparison to the water at Sabiñánigo and Jabarrella, which turned out to be much more oligotrophic, with nitrate levels of 2.4 and 2.1 mg L^{-1}, respectively. Also, conductivity can be used as a trophic state indicator (Kelly & Whitton, 1995; Menetrey et al., 2008), since an increase of this parameter means an increase of dissolved nutrients, as long as there is no marine influence. Conductivity values measured at the Flix reservoir (FR and FW) (1500 µS cm^{-1}) versus values detected at Sabiñánigo (SA) and Jabarrella (JB) (≤ 300 µS cm^{-1}) might also indicate a higher eutrophication of the Ebro River in comparison with the Gállego River, since water bodies having conductivity values greater than 500 µS cm^{-1} have been classified as eutrophic (Olsen, 1950). This could be the reason why DGT resins at FR barely accumulated Hg, since eutrophic waters favour algal growth and, consequently,

biofouling phenomena. These results demonstrate the limitations of the DGT technique in non-oligotrophic natural waters.

3.3.5 DGT measurements above sediments in the Ebro River

The measured mass of Hg in the triplicate of DGT devices deployed for two weeks at FW was 2.5 ± 0.2 ng, while at AS was 1.7 ± 0.3 ng. These values are still low and close to the blank (1.34 ± 0.05 ng), but higher than it; so in this case the labile Hg concentration can be calculated from the DGT data after subtracting the blank value. The DGT-labile Hg concentration at FW was 4.0 ± 0.7 ng L^{-1}, while at AS was 1.2 ± 0.9 ng L^{-1}. The direct measurement of THg for FW was 174 ng L^{-1} and for AS was lower than the LOQ. One more time, concentrations provided by DGT were much lower than those measured directly. As we said before, particles cannot go through the DGT filter, while direct measurements include both the dissolved and the particulate phase. In the case of AS, the amount of Hg accumulated in the resin was so similar to the blank that the standard deviation of the calculated labile concentration had the same magnitude as the concentration itself.

The percentage of labile Hg in relation to the Hg measured directly in water was lower for FW (2.3%) than that found by Docekalova and Divis (2005) in the Svitava River (Brno, Czech Republic) (13%) (6.4 ± 0.2 mg DOC L^{-1}). On the other hand, the THg concentration in the sediment was 49 ± 2 and 1.05 ± 0.04 µg g^{-1} at FW and AS, respectively. The much higher level in the sediment at FW showed the high Hg loading in that deposit of hazardous industrial solid waste in front of the chlor-alkali plant mentioned in the introduction of this chapter. Nevertheless, given the very high THg level found in the FW sediments in comparison with AS sediments, the labile Hg concentration in the water immediately above them would be expected to be higher than it was. A brownish-gray layer was also observed on the filter surface of these DGT units, but subtler than for the DGT units deployed for more than 2 weeks (previous experiment). In any case, it remains unclear if the cause of such a low measurements of the labile Hg concentration is this proliferation of biofilm and deposition of

particulate matter on the filter, the low levels of labile Hg in the river water or a selection by the diffusive layer of the species that are able to reach the resin gel.

3.3.6   General discussion

This study has demonstrated the ability of commercial specific-for-Hg DGT devices to measure the concentration of dissolved labile Hg in water. Basic laboratory assays verified the validity of the DGT principles for this type of DGT unit. The determined diffusion coefficient of MeHg in the diffusive layer (8.50×10^{-6} cm^2 s^{-1}) was found to be very similar to that of Hg(II) in water (8.47×10^{-6} cm^2 s^{-1}). Nevertheless, although the technique worked perfectly under laboratory conditions; under environmental conditions, and mainly in eutrophic waters, some problems were found, such as the presence of biofouling and particulate matter, which can clog the filter. As the concentration of labile Hg in river water is usually low, a long deployment time is needed. Even so, when deploying DGT devices for more than a week, a biofilm layer appears on top of the filter preventing Hg species from diffusing through it. Also, it has been demonstrated that the DGT technique performs fairly well in oligotrophic waters; however, it does not work properly in eutrophic river water, where biofouling phenomena can occur. Further experiments are needed in order to solve the problem of algal growth on the filter surface, since this issue seems to be crucial to the normal diffusion of Hg species through DGT and consequently to the accurate determination of Hg concentration. Moreover, the need for a diffusion coefficient for Hg species complexed by DOM has been identified. These big molecules are supposed to diffuse at a lower rate through the diffusive gel, thus, future studies should address the calibration of the DGT units in the presence of DOM, so that the labile Hg fraction will not be underestimated.

Chapter 4

Development of the DGT technique for the determination of mercury in freshwater: Comparison of three types of samplers in laboratory assays

4 Development of the DGT technique for the determination of mercury in freshwater: Comparison of three types of samplers in laboratory assays

4.1 Objective of the study

This study was carried out with the first aim of assessing the rate of Hg uptake by three types of DGT samplers (one commercial and two in-house manufactured) and obtaining the diffusion coefficient of Hg(II) in the respective diffusive gel layers, both in the absence and in the presence of DOM. By doing these tests we could decide which DGT type was the most suitable one for Hg determination in freshwater. Later, a step forward was taken. It consisted of assessing the MeHg uptake rate of the two types of in-house manufactured DGT devices and obtaining the diffusion coefficient of MeHg in their respective diffusive layers, also both in the presence and in the absence of DOM.

4.2 Experimental methodology

4.2.1 Preparation of gels and assembly of samplers

4.2.1.1 Materials and equipments

Three types of DGT samplers were used; one commercial and two in-house manufactured.

- C-DGT: The commercial DGT units (Exposmeter AB, Tavelsjö, Sweden) consisted of a Spheron-Thiol resin immobilised in a layer of polyacrylamide gel as the binding agent, a 0.76 mm thick agarose gel as the diffusive layer and a 0.1 mm thick, 0.45 μm pore size filter membrane to protect the diffusive gel.

- A-DGT: This type of in-house manufactured DGT devices had 3-mercaptopropyl functionalized silica gel embedded in a polyacrylamide gel as the binding agent, a 0.5 or 0.76 mm thick agarose gel as the diffusive gel, and a 0.1 mm thick 0.45 μm pore size Nylon filter membrane.

- P-DGT: This type of in-house manufactured DGT devices had the same components as A-DGT but with the only difference that its diffusive gel is a 0.4 mm thick polyacrylamide gel.

The reagents and materials employed for the preparation of the in-house manufactured DGT gels were acrylamide solution (40%), electrophoresis grade (Fisher Scientific); DGT gel cross-linker, 2% aqueous solution (DGT Research Ltd., Lancaster, UK); ammonium peroxydisulfate, certified A.C.S, 99% (Fisher Scientific); N,N,N′,N′-tetramethylethylenediamine, ReagentPlus, 99% (Sigma-Aldrich); 3-mercaptopropyl-functionalized silica gel (Sigma-Aldrich); agarose, LE, analytical grade (Promega) for Hg(II) experiments and Type I, low EEO (Sigma-Aldrich) for MeHg experiments; high-purity demineralised 18.2 MΩ.cm Milli-Q water (Millipore, USA) and 0.25, 0.50 and 0.76 mm thick skived PTFE films (CS Hyde company, USA) as spacers. Whatman 0.45 μm pore size, 25 mm in diameter nylon membranes were used as filters to protect the diffusive gel, and plastic DGT solution deployment mouldings (3.14 cm^2 window) (DGT Research Ltd.) were used to support and enclose all the layers.

4.2.1.2 Diffusive gels

4.2.1.2.1 Polyacrylamide gels

A procedure used by Clarisse and Hintelmann (Clarisse & Hintelmann, 2006) was followed for preparing polyacrylamide gels. A gel solution in Milli-Q water consisting of 15% (v/v) acrylamide and 0.3% (v/v) cross-linker was firstly prepared. Subsequently, polymerization was initiated by adding 7 μL of freshly prepared 10% (w/v) ammonium persulfate and 2 μL of N,N,N′,N′-Tetramethylethylenediamine (TEMED) catalyst per each millilitre of the gel solution. After mixing, the solution was immediately cast between two glass plates separated by a 0.25 mm thick Teflon spacer and kept in the oven at about 44 ± 2 ºC for 45 min. After being taken out from the glass plates using plastic tweezers, the gel sheet was hydrated in Milli-Q water for at least 24 h before use. During this hydration step the gel expanded to its stable dimension while impurities within the gel were able to diffuse out. Given its swelling factor (1.6) (Zhang

& Davison, 1999), the final thickness of the polyacrylamide gel was 0.4 mm. The gels were stored in Milli-Q water until assembly.

4.2.1.2.2 Agarose gels

Preparation of these gels followed the procedure used by Dočekalová and Diviš (Docekalova & Divis, 2005). A diffusive gel containing 1.5% agarose was prepared by dissolving the agarose in an appropriate volume of 80 °C warm deionised water. The mixture was placed in a boiling water bath and gently stirred until all the agarose was dissolved and the solution became transparent. The hot gel solution was immediately pipetted between two preheated glass plates separated by a 0.5 or 0.76 mm Teflon spacer and left to cool down to its gelling temperature (36 °C or below). The gel sheet was cut in discs immediately afterwards, since it would not expand (the expansion factor of agarose gel is 1) (Zhang & Davison, 1999), and the discs were stored in Milli-Q water.

4.2.1.3 Resin gels

The binding layer, also known as the resin gel, consisted of a thiol resin embedded in a polyacrylamide gel. It was prepared by mixing 1.2 g of 3-mercaptopropyl functionalized silica gel with each 10 mL of gel solution (the same as used for polyacrylamide diffusive gels). Polymerization was also initiated by adding 7 μL of freshly prepared 10% (w/v) ammonium persulfate and 2 μL of TEMED per each millilitre of the gel solution. The same casting, heating and hydration procedure as for polyacrylamide diffusive gels was used.

4.2.1.4 Assembly

A plastic mould based on a simple tight-fitting piston design with a 2 cm diameter window was used to support the gels and to ensure that only a known surface of the DGT unit (area = 3.14 cm^2) was in contact with the solution. A disc of resin gel was placed on top of the cylindrical piston, with the side containing the gravity-deposited

resin beads facing upward. That side of the gel was identified by observing it thoroughly with a magnifying glass. A disc of diffusive gel (polyacrylamide or agarose) was placed on top of the resin gel, followed by a 0.1 mm thick, 0.45 µm pore size nylon filter membrane for protection. Care was taken to exclude air bubbles between each layer by keeping the layers wet during assembly. The front cap was pressed down tightly, ensuring a good seal between the cap and the membrane surface. The filter has been found to behave as an extension of the diffusive gel layer and to allow the free diffusion of ions (Zhang & Davison, 1999).

4.2.2   General procedures

DGT units were assembled one or two days before deployment and stored until use in a plastic container containing a 0.01 M NaCl solution in Milli-Q water. The DGT deployment involved the immersion of the sampler, suspended by a nylon string, in a stirred aqueous solution. Prior to analysis, DGT units were dismantled, resin gels were extracted and subjected to the corresponding pre-treatment depending on the subsequent analysis (THg or MeHg). Also, a 5 mL aliquot of solution, to which DGT units were exposed to, was taken before and after DGT deployment, acidified to 0.4% with concentrated HCl and stored at 4 °C until analysis.

4.2.3   Hg(II) assays
4.2.3.1   Materials and equipments

Mercury standards and test solutions were prepared from a 1000 mg L^{-1} Mercury Standard for ICP (NIST- and BAM-CRM traceable, FLUKA) in HNO_3 12%. High-purity demineralised 18.2 MΩ·cm Milli-Q water (Millipore, USA) was used for dilutions and test solutions. The Tekran® Series 2600 system (Tekran Instruments Corp., Knoxville, TN, USA) was used for the analysis of ultra-trace levels of total mercury (THg) in liquid samples. This instrument is capable of providing a fully automated implementation of the USEPA method 1631 (USEPA, 2002), with a detection limit lower than 0.5 ng L^{-1}. A Varian Cary 50 Bio UV-visible spectrophotometer (Varian, USA) was used to measure

the DOC in the solutions. The system was calibrated for the range from 1 to 20 mg L^{-1}, and the absorbance was measured at 254 nm (Mattson et al., 1974). The pH in the solutions and samples was measured using a Consort C535 multi-parameter analyser with an accumet® accu·pHast® electrode (Fisher Scientific).

4.2.3.2   *Optimization of the method for resin gel digestion*

Three acid solutions were tested to digest the resin gels prior to THg analysis: hydrochloric acid (conc., HCl), aqua regia (1:3 HNO_3:HCl, AR) and 7:3 HNO_3:H_2SO_4 (conc., NS). 12 resin gel discs were placed individually in 40 mL glass vials; nine of them were spiked with 10 ng of Hg(II) (50 μL of 200 ng mL^{-1} $HgCl_2$ standard) and the remaining three were used as resin blanks. Mercury was left to equilibrate with the gel matrix for 3 hours at room temperature and then overnight in the refrigerator. Spiked resin gel discs were treated in triplicate with 5 mL of each acid solution. In addition, one resin blank and one solution blank were also recorded for each acid. Vials were covered with an acid washed marble to avoid excessive evaporation but to enable the release of reaction fumes. Samples were left to react at room temperature for 1 h, after which they were placed in a heating block, where the temperature was raised over one hour to 110 °C (pre-digestion step). Then, samples were heated at 110 °C for 5 h (digestion step) (Lomonte et al., 2008). Once the digestion was completed every sample was reconstituted to 10 mL with Milli-Q water and the digests were stored in the refrigerator until analysis.

Recoveries of 54 ± 3, 86 ± 7 and 75 ± 18 % were obtained for HCl, AR and NS acid solutions and digestion in polypropylene vials, respectively. Digestions conducted in glass vials resulted in recoveries of 97 ± 12 and 92 ± 7 % for AR and NS, respectively. The amount of mercury in the resin blank digested with AR (0.03 ng) was lower than that in the resin blank digested with NS (0.16 ng). In the light of these results, aqua regia was chosen as the most suitable acid solution for resin gel digestion.

4.2.3.3 Analytical determination of THg

The resin gel digests were diluted 40 times with a solution consisting of 0.4% HCl (v/v) and 0.5% BrCl (v/v) in polypropylene and glass vials. Water samples (previously acidified to 0.4% HCl) were added BrCl to 0.5% (v/v). Prior to analysis, excess BrCl was removed by adding 0.1% $NH_2OH \cdot HCl$ (w/v). The dilutions were analysed for THg by dual stage gold pre-concentration (after reduction by $SnCl_2$) and CVAFS (Tekran® Series 2600 system) following the USEPA method 1631 and performing a calibration curve with standards at 1, 2.5, 5, 10, 25 and 100 ng L^{-1}. The LOD, which was calculated three times the standard deviation of the blank, was 0.01 ng, and LOQ, considered 10 times the standard deviation of the blank, was 0.04 ng. The repeatability of the method was confirmed (RSD < 3%, n = 3).

4.2.3.4 Time series experiments in the absence and in the presence of DOM

Two time series experiments –one in the absence and in the other in the presence of DOM– were performed using three types of DGT devices (C-DGT, A-DGT and P-DGT). 8 L of Hg(II) solution (1 µg L^{-1}, 0.01 M NaCl) was prepared in both cases, but in one of them organic matter from a Nordic Reservoir (IHSS, 1R108N) was added to obtain 10 mg L^{-1} of DOC. The pH was adjusted to 7 using NaOH and HCl 1M. Afterwards, the solution was left to equilibrate for 24 h while being stirred. Four DGT devices each were submerged in each solution (containing and not containing DOM) which was stirred with a magnetic stirring bar and held at a temperature of 20-22 °C. DGT samplers were retrieved after 4, 8, 24 and 32 h. Controls consisted of units that were not deployed at all (DGT blank) and units which were deployed in a 0.01 M NaCl solution during the whole length (32 h) of the experiment (experimental blanks).

In this occasion, we had 5 experimental blanks that accumulated 0.03 ± 0.02 ng (n = 5) in the case of A-DGT, 0.02 ± 0.01 ng (n = 5) in the case of P-DGT and 0.21 ± 0.04 ng (n = 3) in the case of C-DGT. From these data we can calculate the LOD and the LOQ for the experimental methodology as three times and ten times the standard deviation of the blank respectively. For A-DGT, the LOD was 0.06 ng and the LOQ was 0.20 ng; for P-

DGT, the LOD was 0.03 ng and the LOQ was 0.10 ng; and for C-DGT, the LOD was 0.11 ng and the LOQ was 0.37 ng. Also, at each sampling interval, 5 mL of Hg solution were sampled as well to monitor the Hg concentration remaining in solution.

4.2.4   MeHg assays

4.2.4.1   *Materials and equipments*

The two in-house manufactured DGT devices (A-DGT and P-DGT, defined in section 4.1.1) were used. Thiourea (ACS, ≥ 99.0%), purchased from Fluka (Steinheim, Germany) and hydrochloric acid fuming 37% (ACS, ISO), purchased from Merck (Germany), were used to prepare an acid thiourea solution for MeHg elution from resin gels. Methylmercury chloride (MeHgCl) –CH_3HgCl, 99%– was obtained from Strem (Newburgport, MA, USA), and ethylmercury chloride (EtHgCl) –CH_3CH_2HgCl– from Alfa Aesar (Karlsruhe, Germany). Stock standard solutions were prepared at 1000 mg L^{-1} (as Hg) in acetone and stored in the freezer. Working solutions were prepared weekly by diluting the stock solutions with acetone to a range of 0.02-500 µg L^{-1} (as Hg).

Sodium tetraphenylborate ($NaBPh_4$, ACS, 99.5%) was obtained from ABCR (Karlsruhe, Germany). A fresh $NaBPh_4$ solution of 1% (w/v) was daily prepared in Milli-Q water and stored at 4 °C. ACS reagent sodium citrate tribasic dihydrate (99.0%) and citric acid monohydrate (99.0-102%) were obtained from Sigma–Aldrich. Citric buffer (pH 4.5–5) was prepared by mixing in Milli-Q water citric acid monohydrate (0.1M) and sodium citrate dihydrate (0.1 M). High-purity demineralised 18.2 MΩ·cm Milli-Q water (Sartorius stedim Arium 611, Goettingen, Germany) was used for dilutions and test solutions. The SPME fiber holder for manual use and the silica fiber coated with 100 µm thickness of PDMS were obtained from Supelco (Bellefonte, PA, USA). An ETS-D4 fuzzy thermometer and a digital RCT hot plate stirrer, purchased from Ika Labortechnik (Staufen, Germany), were used to control the temperature and stir the sample during the MeHg extraction.

Gas chromatography coupled to atomic fluorescence spectrometry via a pyrolytic reactor (GC-Py-AFS) was used for the analysis of MeHg in water samples and DGT resin

gel eluates. The GC analysis was accomplished with a prototype system formed by a Thermo trace GC ultra (Milan, Italy) gas chromatograph interfaced to an AFS Tekran Model 2500 (Toronto, Canada) detector via a 18 cm × 23 cm × 18 cm pyrolyzer (Hg-800, Rektorik R&D Chromatography, Meyrin, Switzerland) (Carrasco et al., 2009). A split/splitless injector was used in the splitless mode (3 min). To overcome MeHg decomposition (Diez & Bayona, 2002), the injector temperature was maintained at 180 °C. A 15 m × 0.32 mm I.D. fused-silica column coated with a 0.25 μm film thickness of BP1 (SGE, Ringwood, Victoria, Australia) was used as analytical column. The initial column temperature was held at 50 °C for 3 min, programmed at 7 °C min^{-1} to 150 °C, and then at 80 °C min^{-1} to 250 °C. This latter temperature was held for 2min. After the different Hg forms had been separated in the GC column, they were converted into Hg^0 by thermal decomposition at 750 °C in the pyrolyzer and finally detected by AFS. Ar 5.0 grade gas was used as the carrier gas (2 mL min^{-1}) and also as make-up gas (6 mL min^{-1}) for the AFS detector connected to the system before it was connected to the pyrolyzer. All the tubing was made of PTFE. Finally, data were acquired and processed by Chrom-Card software (Milan, Italy). The pH in the solutions and samples was measured using a GLP 22 CRISON pHmeter (Barcelona, Spain).

4.2.4.2 Analytical determination of MeHg

After being retrieved from the DGT assembly, every resin gel disc was placed in a glass vial using hydrochloric acid (10%) cleaned tweezers. 2 mL of a freshly prepared thiourea acid solution (1.3 mM thiourea, 0.1M HCl) were added to each vial, which was wrapped with aluminium foil to prevent photodegradation and left at room temperature for the elution to take place. After 24 hours, the vials were stored in the fridge (4 °C) until analysis (within a week).

A 250 μL aliquot of resin extract was placed in a 6 mL glass vial with PTFE-coated silicone rubber septum containing 3 mL of citric-citrate buffer (pH = 4.5-5). 10 μL of EtHgCl (230 pg mL^{-1} as Hg) in acetone were also added to the vial as instrumental standard. Once the vial was covered, placed in a water bath at 70 °C and being stirred

at 1200 rpm –using an ETS-D4 fuzzy thermometer and a digital RCT hot plate stirrer working at 1200 rpm, both purchased from Ika Labortechnik (Staufen, Germany) –; 50 µL of 1% NaBPh$_4$ aqueous solution were added as derivatizing agent to the mixture through the septum. After a five-minute derivatization step, extraction was accomplished for 27 minutes by headspace solid-phase microextraction (HS-SPME) using a 100 µm PDMS fiber. The final detection was carried out using a gas chromatograph interfaced to an atomic fluorescence spectrometer via a pyrolytic reactor (GC-Py-AFS).

Three resin gels were spiked with 3 ng of MeHg in order to calculate the recovery of the method, which was 65% (RSD = 4%, n = 3). This value was later used to correct the results. The repeatability of the methodology was tested by analysing the same sample three times every time the instrument was switched on to run a set of samples, and yielded an RSD of less than 5% (n = 3), which proves the robustness of the analytical procedure. A six-point calibration curve was performed in the range from 29 to 1180 pg of MeHg (as Hg). The LOD was calculated as the mean of the method blanks plus 3 times their standard deviation, and the LOQ as the mean of the method blanks plus 10 times their standard deviation, resulting in 5.8 and 19 pg, respectively.

In the case of the water samples, the methodology was basically the same but with two differences: the EtHgCl was added as internal standard right after taking the samples and before storing them to correct for any possible loss of MeHg during storage or due to adsorption on the vial walls, apart from detector variations; and the aliquot of sample for HS-SPME was 1 mL and the volume of citric-citrate buffer was 2 mL.

4.2.4.3   *Time series experiments in the absence and in the presence of DOM*

Two time series experiments –in the presence and in the absence of DOM– were carried out under controlled laboratory conditions using the two types of in-house manufactured DGT devices (A-DGT and P-DGT). Two MeHg solutions (1 µg L^{-1} MeHgCl,

0.01 M NaCl), one with organic matter from a Nordic Reservoir (1R108N, IHSS) (10 mg L^{-1}) and the other one without it, were prepared in 5 L amber glass bottles. The pH was adjusted to 7 using NaOH and HCl 2M and 0.5M. Afterwards, the solution was left to equilibrate overnight while being stirred with a magnetic stirring bar. Ten A-DGT and ten P-DGT devices were submerged in each solution, whose temperature was controlled and kept at 25.5 ± 0.5 °C. Duplicates of DGT units were retrieved after 2, 4, 8, 14 and 24 h. A duplicate not deployed at all was considered as DGT blank (i.e. 0 h). At each sampling interval, 5 mL of each MeHg solution were collected and acidified to 0.4% with HCl to monitor the MeHg concentration remaining in solution, and 10 mL were taken only from the DOM containing solution to measure DOC. Both the DGT units and the water samples were stored in the fridge until analysis.

4.3 Results and discussion

4.3.1 Hg(II) assays

4.3.1.1 Uptake of Hg(II) in the absence of DOM

In accordance with the principle of DGT (Equation (4.1), further explained in section 1.4.4.8, Equation (1.2)),

$$M = \frac{DAtC}{\Delta g} \qquad (4.1)$$

the mass of Hg accumulated in the resin (M) is proportional to the exposure time (t), as shown in Figure 4.1. To account for the decrease in Hg concentration in solution (C) during the experiment, caused by the DGT uptake and the adsorption on the container wall, the mass of accumulated Hg is normalized by the solution concentration of Hg. The three types of DGT performed well, as evidenced by the regression coefficients of the three linear curves ($R^2 > 0.96$), although the regression of the P-DGT and C-DGT curves ($R^2 > 0.98$) is better than that of the A-DGT curve ($R^2 = 0.966$). Nevertheless, the C-DGT blank (0.19 ng) was much higher than the A-DGT and P-DGT blanks (0.02 and 0.03 ng). The three curves have similar slopes, although A-DGT

showed the fastest uptake rate (the greatest slope), followed by P-DGT and finally, C-DGT.
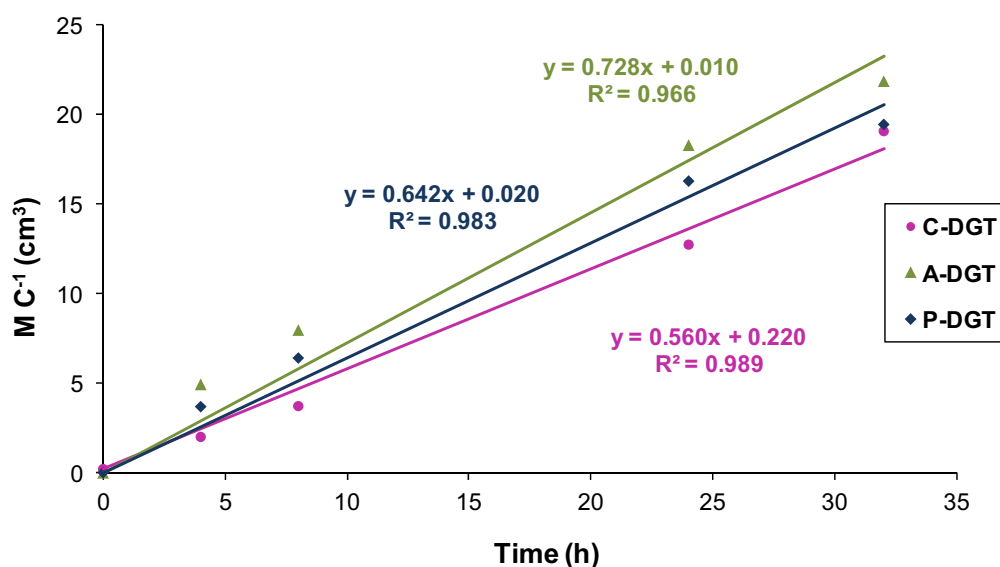
Figure 4.1. Time-series experiment. Mass of mercury accumulated in the resin (M) normalized by the Hg(II) concentration in the solution for various periods of time and for the three DGT types.

The diffusion coefficient (D) of Hg(II) in the diffusive layer can be calculated from the slope (s) of the relationship between the amount of Hg accumulated by the DGT units (normalised for Hg concentration in solution) and the deployment time (Equation (4.2), also Equation (3.3) in section 3.3.2).

$$D = \frac{s \Delta g}{A} \qquad (4.2)$$

The diffusion coefficient of Hg(II) ($D_{Hg^{2+}}$) in the agarose diffusive gel of the C-DGT, in the agarose diffusive gel of the A-DGT and in the polyacrylamide diffusive gel of the P-DGT were calculated on the basis of Fick's law as 4.41×10^{-6}, 3.86×10^{-6} and 2.84×10^{-6} cm^2 s^{-1} respectively at 21.5 °C, and can be compared with that of MeHg in polyacrylamide gel (5.1×10^{-6} cm^2 s^{-1} at 20 °C) (Clarisse & Hintelmann, 2006) or that of Hg(II) in agarose gel (8.86×10^{-6} and 9.08×10^{-6} cm^2 s^{-1}) (Docekalova & Divis, 2005).

Previous studies using the DGT technique showed a good agreement between the diffusion coefficient of metals in water and that in agarose or polyacrylamide gels (Zhang & Davison, 1999; Docekalova & Divis, 2005). In this context, the diffusion coefficient of free ionic Hg(II) at any temperature, $D_{Hg^{2+}T}$, can be calculated applying the Stokes-Einsten equation (Equation (4.3), also Equation (3.4) in section 3.3.2) (Zhang & Davison, 1995), where $D_{Hg^{2+}25}$ would be the diffusion coefficient of Hg(II) ions in water at 25 ºC.

$$\log D_t = \frac{1.370223\,(t-25)+8.36\times10^{-4}\,(t-25)^2}{109+t} + \log \frac{D_{25}\,(273+t)}{298} \qquad (4.3)$$

Our D_{Hg2+} experimental values were found to be fairly similar to that reported for Hg(II) in water (8.47×10^{-6} cm^2 s^{-1} at 25 °C) (Lide, 2004-2005). Then, $D_{Hg^{2+}25}$ was calculated firstly substituting the $D_{Hg^{2+}}$ previously obtained at 21.5 °C into Equation (4.3). Then, D_{Hg2+} was calculated for a wide range of temperatures as shown in Figure 4.2. Hence, by applying this temperature correction, the concentration of Hg in aqueous solution can be calculated from the measured mass of Hg accumulated by the resin.

Figure 4.2. Diffusion coefficient of Hg(II) in absence of DOM ($D_{Hg^{2+}}$) in the three different diffusive layers calculated on the base of Fick´s law for a wide range of temperatures.

The results of this time series experiment confirm that these three DGT type comply with the basic DGT principles, and thus they can be used for Hg(II) measurements under the studied conditions.

4.3.1.1.1 Assessment of Hg(II) accumulation by the diffusive gel

The diffusive gel of the three DGT units were analysed for THg to test if they were able to accumulate inorganic Hg, preventing its free diffusion and collection on the resin gel. In contrast to previous studies (Docekalova & Divis, 2005), no Hg accumulation on the polyacrylamide diffusive gel was observed, since the measured Hg mass after a 32-hour deployment was 0.07 ng. This amount of Hg corresponds to a concentration of 0.54 µg L^{-1} in the diffusive gel disc, which is lower than the Hg concentration present in the solution (1 µg L^{-1}). In the case of the agarose diffusive gel of A-DGT, 0.13 ng of Hg were found in the diffusive gel disc after 32 h deployment in the Hg solution, corresponding to a concentration of 0.83 µg L^{-1} in the disc, which is nearly the same concentration of the test solution. However, C-DGT presented higher amounts of Hg in their diffusive gels (from 0.94 to 4.07 ng in the samplers deployed for 4 to 32 h respectively, that correspond to concentrations in the gel of 3.9 to 17 µg L^{-1}). Thus, it was confirmed that the polyacrylamide diffusive gel, apart from not trapping MeHg –as Clarisse and Hintelmann (2006) showed–, has no specific affinity to inorganic Hg. Consequently, this gel is considered suitable to be used as a diffusive layer in the DGT technique for measuring both organic and inorganic Hg species. In-house manufactured agarose diffusive gel is also appropriate for that purpose, whereas the agarose diffusive gel used in the C-DGT units does accumulate Hg, which is not advisable if we want to avoid the competition with the resin for binding Hg.

4.3.1.2 Uptake of Hg(II) in the the presence of DOM

In natural waters, Hg speciation is considered to be dominated by DOM (Hintelmann et al., 1997b; Amirbahman et al., 2002). Those Hg-DOM complexes are expected to diffuse at a lower rate through the diffusive layer, since the diffusion of a

metal bound to humic substances was reported to be 10-20 times slower than the diffusion of the free ionic form of the same metal (Zhang & Davison, 2000). In addition, the resin is assumed to bind exclusively with the free Hg ions, so the measurement of an Hg-complex only occurs if it can dissociate during the measurement time (Zhang & Davison, 2000). The determination of all potential ligands present in natural waters and their associated diffusion coefficients is a limitation for the applicability of the DGT technique as a monitoring tool. For this reason all Hg-DOM complexes are typically represented by a mean diffusion coefficient (Clarisse et al., 2009). Indeed, DOM complexes are mostly humic substances, whose diffusion coefficients have been shown to be similar in spite of their different origins (Lead et al., 1999).

As shown in the Figure 4.3, P-DGT performed very well (Hg uptake was linear with time, R^2 = 0.989) and A-DGT performed acceptably well (R^2 = 0.965), whereas the accumulation of Hg in C-DGT throughout time was negligible (R^2 = 0.33). A-DGT showed again the fastest uptake rate, as suggested by the highest regression line slope.

The diffusion coefficients of Hg(II) bound to DOM ($D_{Hg(II)-DOM}$) in the diffusive gel of P-DGT and A-DGT were calculated from the slope of the regression lines and their values were 5.78×10^{-7} (at 22.8 °C) and 8.03×10^{-7} $cm^2 \, s^{-1}$ (at 20 °C), respectively. These are similar to the diffusion coefficient of MeHg bound to DOM from the Nordic Reservoir (7×10^{-7} $cm^2 \, s^{-1}$ at 20 °C) reported elsewhere (Clarisse et al., 2009). Values of $D_{Hg(II)-DOM}$ for a broad range of temperatures (Figure 4.4) were calculated using the Equation (4.3). These values are roughly five times lower than those in absence of DOM, which demonstrates that the rate of diffusion of Hg is lower when it is complexed with organic matter.
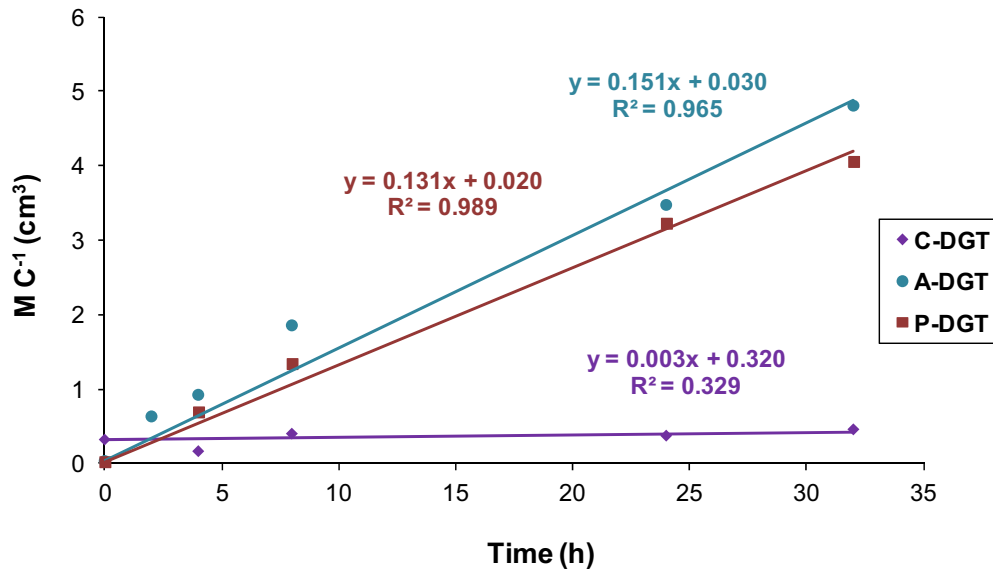
Figure 4.3. Time-series experiment with DOM. Mass of mercury accumulated in the resin (M) normalised by the Hg(II) concentration in the solution (C) for various periods of time and for the three DGT types.
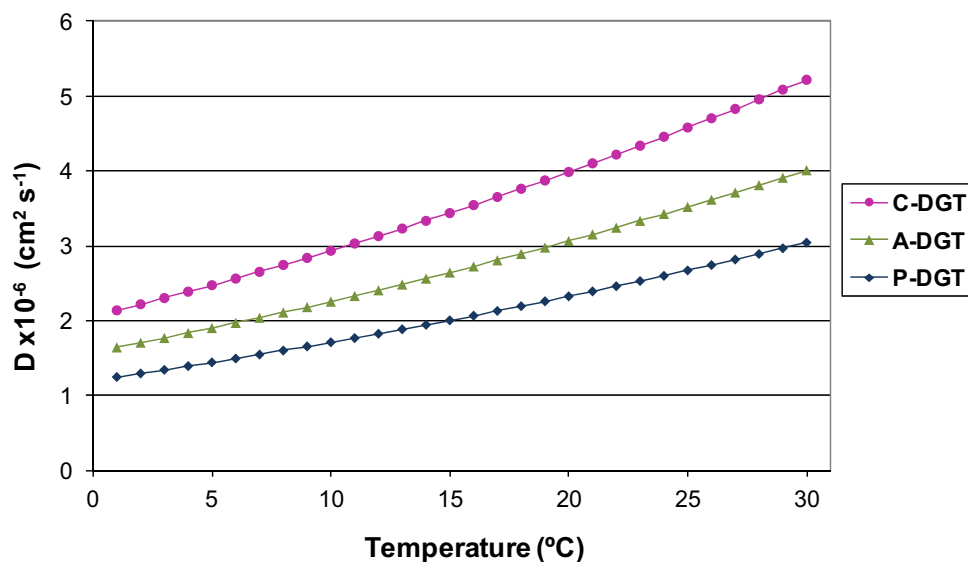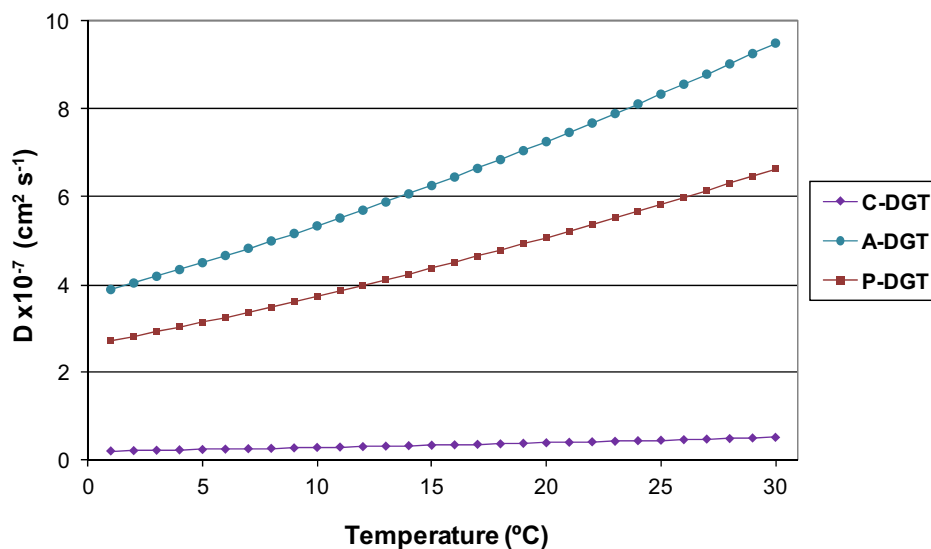

Figure 4.4. Diffusion coefficient of Hg(II) in presence of DOM ($D_{Hg(II)-DOM}$) in the three different diffusive layers calculated on the base of Fick´s law for a wide range of temperatures.

To calculate $D_{Hg(II)-DOM}$ for C-DGT did not make sense, since this DGT type showed no substantial Hg accumulation along time and the linearity of its uptake kinetics was very poor. This could explain the low mass of Hg accumulated when this type of DGT devices was deployed in previous field tests (section 3.3.4), and thus, in waters with presence of DOM.

4.3.2   MeHg assays

4.3.2.1   *Effect of DOM on the MeHg uptake rate*

The performance of the P-DGT type to measure MeHg had been previously tested by Clarisse and Hintelmann (2006) to measure MeHg, however, according to our knowledge, this is the first time that A-DGT devices have been calibrated to measure the uptake of MeHg with and without of DOM in solution, to better simulate natural water conditions in the field. The results of these calibration experiments showed that both DGT types, in the presence and the absence of DOM, proportionally accumulate MeHg in relation to exposure time, as evidenced by the regression coefficients of the four linear curves (R^2 > 0.99) (Figure 4.5). When comparing the slopes of those four curves, we see that they are significantly different among each other (t-student), except for P-DGT DOM and A-DGT DOM (see nomenclature in the figure legend). This means that as long as there is DOM in solution (specifically 10 mg L^{-1}), both DGT types could be used indistinctly.

As the other Hg species, the diffusion coefficient (D) of MeHg in the diffusive layer can be calculated from the slope (s) of the relationship between the mass of MeHg accumulated by the DGT units and the deployment time (Equation (4.2)). When the analyte concentration in the solution varies, the mass accumulated in the DGT resin gel should be normalised for it. In this experiment we worked with quite a high volume of solution (5 L), MeHg concentration barely decreased because of DGT uptake or adsorption on the container wall. However, here, MC^{-1} is represented versus exposure time to continue with the same criterion as in Figure 4.1 and Figure 4.3. The difference between the slopes of the uptake kinetics curves (Figure 4.5), and therefore between the diffusion coefficients of MeHg in the DGT diffusive gels in the presence ($D_{MeHg-DOM}$) and in the absence of DOM (D_{MeHg^+}) was bigger for P-DGT than for A-DGT. This suggests that P-DGT is more appropriate to measure MeHg since it discriminates better between the MeHg species in solution, i.e. free MeHg ions or MeHg bound to DOM. This higher differentiation could imply a more accurate labile MeHg concentration determination when using a D matching the water DOM level. D_{MeHg^+} and $D_{MeHg-DOM}$ in A-DGT were 3.2 × 10^{-6} and 2.7 × 10^{-6} cm^2 s^{-1} at 25 °C, respectively; and D_{MeHg^+} and

$D_{MeHg-DOM}$ in P-DGT were 2.5 × 10^{-6} and 1.7 × 10^{-6} cm^2 s^{-1} at 25 °C (Table 4.1). Applying the Stokes–Einstein equation (Zhang and Davison, 1995) (Equation (4.3)), D at any temperature can be calculated (Figure 4.6) and consequently contrasted with those D obtained in previous studies.

Our D_{MeHg^+} and $D_{MeHg-DOM}$ in A-DGT (3.2 × 10^{-6} and 2.7 × 10^{-6} cm^2 s^{-1} at 25 °C, respectively) can be compared to D_{MeHg^+} and $D_{MeHg-DOM}$ obtained in agarose gel (5.26 × 10^{-6} and 3.57 × 10^{-6} cm^2 s^{-1} at 25 °C) by Hong et al. (2011). These authors saw a negligible effect of ionic strength and agarose grade on the effective D, thus none explanation for the difference between the two D_{MeHg^+} can be given in this case. In addition, when calculating $D_{MeHg-DOM}$, both in Hong and co-workers' and in our experiment, the same DOC concentration was used (10 mg L^{-1}). However, the DOM source was different: the other authors used Suwannee River DOM, also from IHSS.
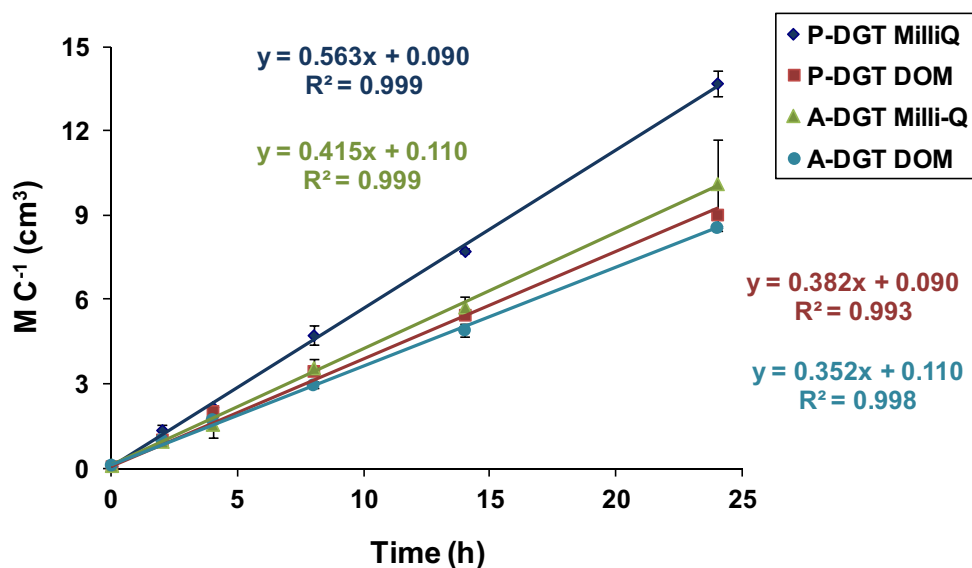
Figure 4.5. Time-series experiment. Mass of methylmercury accumulated in the resin (M) at different deployment times for the two DGT types (A-DGT and P-DGT), both in the absence (MilliQ) and in the presence (DOM) of DOM.
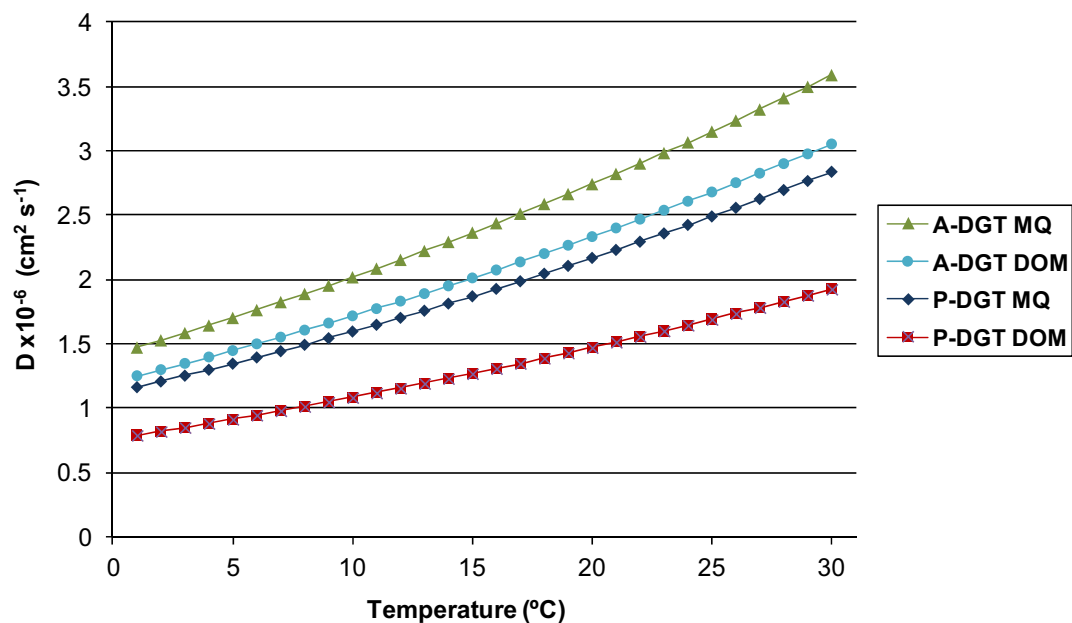
Figure 4.6. Diffusion coefficient of MeHg in the two different diffusive layers (A-DGT and P-DGT) in the absence (MQ) (D_{MeHg^+}) and in the presence (DOM) of DOM ($D_{MeHg-DOM}$), calculated on the base of Fick's law for a wide range of temperatures.

At 20 °C, the calculated D_{MeHg^+} and $D_{MeHg-DOM}$ in P-DGT were 2.2×10^{-6} and 1.5×10^{-6} cm^2 s^{-1}. These values can be compared to D_{MeHg^+} (5.1×10^{-6} cm^2 s^{-1} at 20 °C) (Clarisse and Hintelmann, 2006) and $D_{MeHg-DOM}$ (0.7×10^{-6} cm^2 s^{-1} at 20 °C) (Clarisse et al., 2009) in polyacrylamide gel. The only reason why the D_{MeHg^+} determined by Clarisse and co-workers differs from ours could be that the concentration of NaCl was 0.1 M in the first case and 0.01 M in the second, although the DGT uptake is supposed to be independent of ionic strength (Zhang & Davison, 1995; Hong et al., 2011). Apart from that, there were no remarkable differences between the two experiments. Concerning $D_{MeHg-DOM}$, we determined it submerging the DGT units in a 10 mg DOC L^{-1} solution whereas the other authors performed their experiment in a solution of MeHg saturated with DOM, using in both cases the same type of organic matter (IHSS, 1R108N). This leaves proof of the importance of calibrating the DGT units in a solution with similar characteristics to those of the water where DGT will be deployed.

Table 4.1. Diffusion coefficients of different Hg species in the DGT diffusive layer.

	Origin	A-DGT	P-DGT
$D_{Hg^{2+}}$ (25 °C)	Hong et al. (2011)	4.02×10^{-6}	-
$D_{Hg(II)\text{-}DOM}$ (25 °C)	Hong et al. (2011)	2.16×10^{-6}	-
$D_{Hg^{2+}}$ (22 °C)	This study	3.9×10^{-6}	2.8×10^{-6}
$D_{Hg(II)\text{-}DOM}$ (23 °C)	This study	0.80×10^{-6}	0.58×10^{-6}
$D_{MeHg^{+}}$ (25 °C)	Hong et al. (2011)	5.26×10^{-6}	-
$D_{MeHg\text{-}DOM}$ (25 °C)	Hong et al. (2011)	3.57×10^{-6}	-
$D_{MeHg^{+}}$ (20 °C)	Clarisse and Hintelmann (2006)	-	5.1×10^{-6}
$D_{MeHg\text{-}DOM}$ (20 °C)	Clarisse et al. (2009)	-	0.7×10^{-6}
$D_{MeHg^{+}}$ (25 °C)	This study	3.2×10^{-6}	2.5×10^{-6}
$D_{MeHg\text{-}DOM}$ (25 °C)	This study	2.7×10^{-6}	1.7×10^{-6}

4.3.3   General discussion

3-mercaptopropyl functionalized silica gel was satisfactorily used as the binding agent in the DGT resin gel for THg measurements –it had been tested previously only for MeHg measurements by Clarisse et al. (2006, 2009)–. Polyacrylamide diffusive gel was shown not to compete with the resin for binding Hg(II) ions and was therefore considered appropriate to be used as the diffusive layer in the DGT technique for measuring inorganic Hg species (previously, this diffusive gel was only used to determine MeHg by Clarisse and Hintelmann (2006)).

From these studies it can be concluded that P-DGT seems to be the best choice to measure THg, considering that polyacrylamide diffusive gel did not accumulate Hg, the rate of uptake in the resin gel was the most linear with time (R^2 = 0.983 and 0.989 with and without DOM, respectively) and its resin blanks were one of the lowest, resulting in low limits of detection (reported in section 4.2.3.4). However, if monitoring very low Hg concentrations in water, A-DGT may be the most suitable type due to its slightly larger uptake rate and its low resin blanks. When it comes to measuring MeHg, it was

shown that P-DGT is more suitable to measure MeHg since it showed a higher uptake rate and a higher discrimination ability between the MeHg species (of different lability) in solution. In conclusion, the polyacrylamide gel can be considered the best diffusive gel for THg and MeHg determination by the DGT technique.

The diffusion coefficients of Hg(II) in the presence ($D_{Hg(II)-DOM}$) and in the absence of DOM ($D_{Hg^{2+}}$) were determined and compared (Table 4.1). When there is DOM in the solution, Hg-DOM complexes dominate the speciation of Hg(II). As a result, $D_{Hg(II)-DOM}$ is one order of magnitude lower than $D_{Hg^{2+}}$. This demonstrates the need of accurately simulating the natural water conditions when calibrating the DGT devices. The results of subsequent field monitoring campaigns will strongly depend on the validity of the diffusion coefficient used for the DGT calculations.

On the other hand, our values of diffusivity for MeHg in the DGT diffusive layer in the absence and in the presence of DOM, D_{MeHg^+} and $D_{MeHg-DOM}$, were not so different from each other as $D_{Hg^{2+}}$ and $D_{Hg(II)-DOM}$, in spite of using solutions with the same properties and DGT units manufactured with the same additives (Table 4.1). Also, the absolute value of $D_{MeHg-DOM}$ is higher than $D_{Hg(II)-DOM}$. This might suggest that MeHg–DOM complexes are more labile than Hg(II)–DOM complexes, which means that the MeHg-DOM molecule dissociates faster and easier than the Hg-DOM molecule, letting MeHg behave similarly as when its freely dissolved in pure water. Supporting this assumption, Cattani et al. (2009) postulated that MeHg has a higher lability than Hg(II). MeHg is considered to have a lower affinity for the thiol functional groups in organic matter than Hg(II) because the attachment of the methyl functional group reduces the affinity of the Hg atom to thiols. This implies that MeHg-DOM complexes are more labile than Hg(II)-DOM complexes and have a higher dissociation rate constant (Warnken et al., 2007).

Injection of Hg(II) in a pilot scale constructed wetland for wastewater treatment and application of DGT samplers to assess mercury methylation

5 Injection of Hg(II) in a pilot scale constructed wetland for wastewater treatment and application of DGT samplers to assess mercury methylation

5.1 Constructed wetlands as an alternative for wastewater treatment

Constructed wetlands (CW) are natural or passive wastewater treatment systems consisting of shallow ponds or channels (depth < 1m) planted with vegetation typical of wet areas (aquatic macrophytes), and where removal processes occur by means of interactions between water, solid substrate, microorganisms and vegetation (Garcia et al., 2010). The components of the CWs are: water, granular media, biofilm and plants; and the wetland bed is usually waterproofed with geotextile-geomembrane or compacted clay, in order to avoid the aquifer contamination.

Seidel was the first who in 1952 performed experiments aimed to study the treatment capacity of wetland systems (Seidel, 1966). In the next decade, Seidel and Kickuth developed a treatment system later known as Root-Zone Method (Brix, 1987), consisting of a subsuperficial flow wetland with clay as substrate. However, this technology began to lose popularity since using soil as substrate brought adverse phenomena such as clogging. With the objective of guaranteeing a proper hydraulic conductivity, in 1990, gravel was started being used as a substrate. From that moment, wetlands started to gain popularity and a big number of systems were built all over the world. In fact, the creation of handbooks providing information about design, management, operation and maintenance of wetlands has widely spread the implementation of this technology (Vymazal et al., 1998; USEPA, 2000). Indeed, it has been successfully used for the treatment of domestic (Mburu et al., 2013; Sani et al., 2013) and industrial wastewaters (Dotro et al., 2012; de la Varga et al., 2013), landfill leachates, run-off waters, etc. because of their high contaminant removal efficiency and their low operation and maintenance costs. Currently, the efforts are centred on the development of new configurations or designs (flow type, presence or absence of substrate, vegetation type) to optimize the contaminant removal efficiency.

The CWs are designed for removing suspended solids and organic matter but also nitrogen, phosphorous and pathogens can be removed by means of mechanisms of bacteria dying off, filtration, sedimentation, plant uptake, volatilisation and chemical precipitation (Garcia et al., 2010). The removal efficiency of priority and emerging pollutants was studied since the middle of the last decade. Various and numerous studies show the efficacy of these systems to eliminate pharmaceuticals and personal care products (Reyes-Contreras et al., 2012), antibiotics (Hijosa-Valsero et al., 2011), nitrobenzene (Lv et al., 2013), pathogens (Azaizeh et al., 2013), benzothiazoles and benzotriazoles (Matamoros et al., 2010) and metals (Alvarez et al., 2013; Arroyo et al., 2013).

Removal of heavy metals from wastewater in CWs occurs mainly by 1) binding to soils, sediments and particulate matter; 2) precipitation as insoluble salts; and 3) uptake by bacteria, algae and plants (Bhatia & Goyal, 2014). Because of their positive charge, heavy metals are readily adsorbed, complexed and bound with suspended particles, which subsequently settle on the substrate. The precipitation of metals as insoluble salts (e.g., carbonates, bicarbonates, sulfides and hydroxides) is another process that leads to their long term removal (Sheoran & Sheoran, 2006). Finally, some wetland plant species have been found to have a property of heavy metal tolerance and remediation potential, for example, *Typha* sp., *Spartina* sp. and *Phragmites australis* (Cambrolle et al., 2008; Hegazy et al., 2011; Anjum et al., 2012).

A few studies on Hg removal in CWs have been carried out (Dombeck et al., 1998; King et al., 2002; Stamenkovic et al., 2005; Gustin et al., 2006; Rumbold & Fink, 2006; Chavan et al., 2007; Fay & Gustin, 2007; Kropfelova et al., 2009; Vymazal et al., 2009; Vymazal et al., 2010; Sinclair et al., 2012). One example of the previous work on the topic is the use of mesocosm CWs with different combinations of sediments (clean or Hg contaminated) with water (also, clean or Hg contaminated) to assess the potential for MeHg and THg removal or attenuation (Gustin et al., 2006). These mesocosms behaved as a sinks for N, P, suspended particles, and THg, but as a source of MeHg. Also, Chavan et al. (2007) performed an evaluation of a small-scale CW for nutrient removal and Hg transformation, observing that the wetland system behaved as a sink

for MeHg during the winter months and as a source for MeHg during summer months. In the same manner, Kropfelova and collaborators (2009) measured the removal of 34 trace elements at three full-scale horizontal-flow CWs in the Czech Republic designed to treat municipal wastewater, recording THg removal in all the three cases. Sinclair and co-workers (2012) studied MeHg in sediment, water, and invertebrates in Canadian created wetlands of various ages. They found that newly created wetlands had a strong ability to produce and accumulate MeHg within their saturated sediment. These studies were mostly performed at mesocosm scale or individual full-scale wetlands, thus, there are still more complex designs and multiple configurations that have not been assessed yet.

5.1.1 Types of constructed wetlands

CWs can be classified according to the various design parameters, but the three most important criteria are hydrology (free water surface flow and subsurface flow), type of macrophytic growth (emergent, submerged and free-floating) and flow path (horizontal and vertical) (Vymazal, 2011) (Figure 5.1).
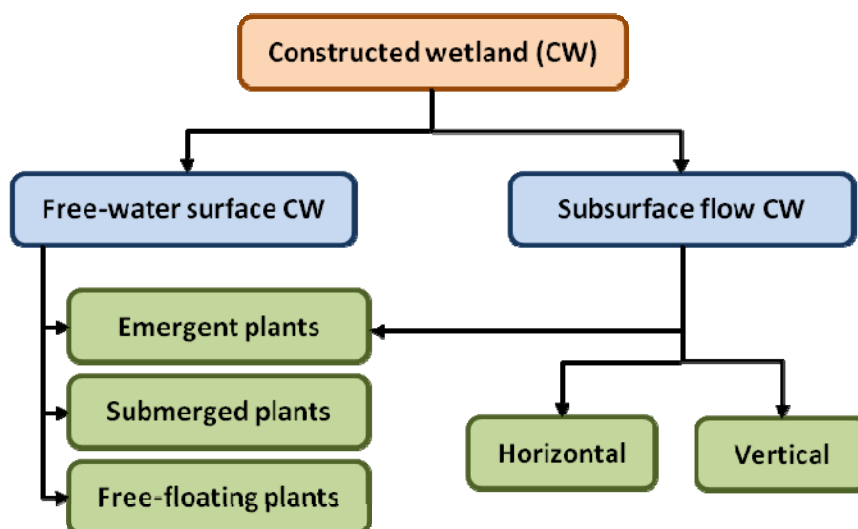
Figure 5.1. Classification of constructed wetlands according with the flow pattern.

Since only the CWs consisting of emerged rooted macrophytes are those used in the study contained in this thesis, their characteristics are described below (Figure 5.2).
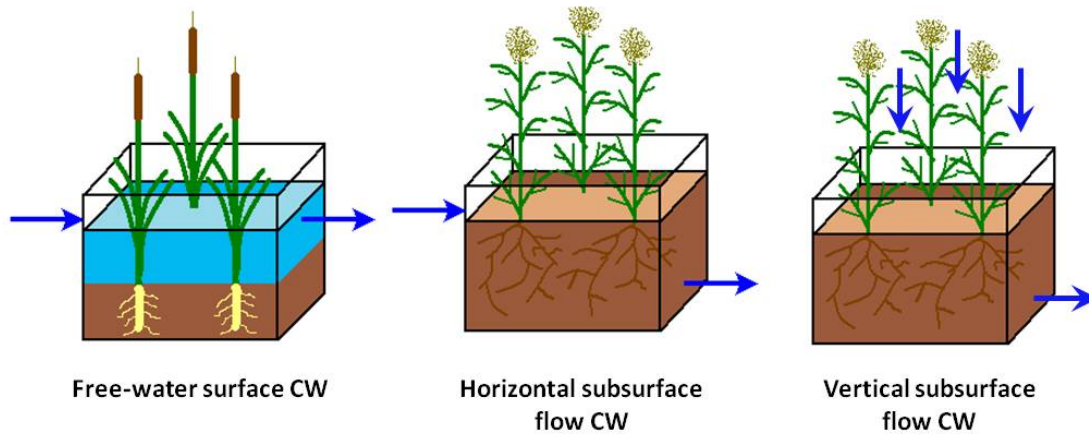
Figure 5.2. Three constructed wetland types. The blue arrows point the influent and effluent of water (Drawings ceded by M. Hijosa-Valsero).

Free water surface constructed wetland (FWS-CW): Also known as surface flow constructed wetland, it is a shallow system where the water is directly exposed to the atmosphere and circulates around the stems and leaves of the plants. The thickness of the water sheet varies between 0.3 and 0.4 m and the feeding is continuous. Leaves, stems and roots (alive or dead) serve as support for adhesion of the bacterial film responsible of biodegradation processes, predominating the aerobic processes. The reason is that these systems are usually supersaturated with oxygen in the surface, the oxygen concentration decreases with depth and anoxic conditions can be reached in the water-granular media interphase. These CWs are designed to treat waters coming from a secondary treatment (García & Corzo, 2008).

Subsurface flow constructed wetland (SSF-CW): In this type of wetland, water circulates through a granular medium of enough permeability to permit the contact of the water with the roots and rhizomes of the plants. The water sheet thickness is 0.3-0.9 m, but never reaching the wetland surface. The biofilm in charge of the treatment processes grows attached to the granular material, roots and rhizomes. Generally, these have a smaller surface area than the FWS-CWs and are usually used for the wastewater treatment generated by settlements with less than 2000 p.e. (population

equivalent), as secondary treatment. These CWs present a higher tolerance to temperature changes than FWS-CWs, there are neither generation of bad odours nor proliferation of mosquitoes. The main disadvantages are the high footprint, the high construction cost (due to the acquisition of the granular material), and their tendency to suffer clogging, which reduces the efficiency for contaminants removal. According to the wastewater circulation, these CWs can be classified in two subtypes.

- **Horizontal subsurface flow constructed wetland (HF-CW):** In this type of wetland the water circulates horizontally through the granular medium by the action of the gravity. These HF-CWs operate permanently flooded with organic loading rates (OLR) around 2-4 g BOD m^{-2} d^{-1} and hydraulic retention times (HRT) of several days. Typical hydraulic loading rates are 0.05-0.1 m below the surface of the granular medium, which must be homogeneous in size and long-lasting, with an average diameter of 5-8 mm. Due to the generation of anoxic ambient in this type of wetlands, the denitrification reaction occurs, eliminating the nitrogen from nitrified effluents.

- **Vertical subsurface flow constructed wetland (VF-CW):** The water circulation is vertical by gravity and the feeding is intermittent, so that the granular medium is not permanently flooded and the oxygen supply is guaranteed. There are periods of feeding, reaction and discharge. The feeding is carried out with a pipe system on top of the wetland surface, where the water seeps in through the substrate (gravel, sand, etc.). Then, it is collected by means of a drainage system in the bottom of the wetland bed. The depth of the granular medium fluctuates between 0.5 and 0.8 m, the operational OLR is around 20 g BOD m^{-2} d^{-1} and the HRT is usually of hours. This CW type has a higher treatment capacity than the HF-CW, producing effluents with a higher oxygenation level.

5.1.2 Advantages and disadvantages

García et al. (1997) describe the main advantages and disadvantages of the CWs versus the conventional treatment systems:

- **Advantages**

    1. Easily operated; qualified staff is not required
    2. Low energy consumption, since waters can circulate by the action of gravity
    3. Low waste generation
    4. Low running and maintenance costs
    5. Greater tolerance to variations of flow and organic loading, as they present high hydraulic retention times
    6. Integration in the environment and low noise impact
    7. The FWS-CWs make the creation and restoration of wet zones possible, enhancing wildlife habitats, environmental education and recreation areas.

- **Disadvantages**

    1. A large land surface is necessary for its implementation
    2. Long start-up stage
    3. Difficult to be designed due to the complexity of the contaminants removal processes
    4. Water losses by evapotranspiration
    5. Possible occurrence of illness vectors (mosquitoes) in the FWS-CWs
    6. Propensity to clogging of the granular media in the SSF-CWs
    7. Generation of greenhouse gases, mainly CH_4 and N_2O in the SSF-CWs

5.2 Objectives of the study

This study was performed with the aim of assessing the efficiency of an alternative wastewater treatment system consisting of three different experimental-scale CWs in series to remove Hg. Examining Hg methylation in the different treatment steps was

another important objective, since wetlands are known to be sites where MeHg can be produced by Hg biomethylation (Morel et al., 1998).

Besides, another objective was to determine the labile fraction of Hg and MeHg in the water along the treatment line by means of the DGT technique and compare it to the Hg and MeHg measured directly in the water (total Hg and total MeHg). The interest lays on the fact that the labile fraction is that which is susceptible to be uptaken by living organisms, and therefore important once the treated wastewater is discharged to rivers or reused.

5.3   Description of the experimental wetland

The experimental treatment plant is set outdoors at the experimental facility of the GEMMA's group (Department of Hydraulic, Maritime and Environmental Engineering of the Universitat Politècnica de Catalunya - BarcelonaTech, Spain). The system started operation in May 2010. All of the elements of the treatment system are integrated on two 11 m^2 skids, which can be easily transported. Urban wastewater is pumped directly by means of 2 pumps from a nearby municipal sewer. Firstly, the wastewater is coarsely screened and subsequently conveyed to a 1.2 m^3 polyethylene storage tank, which is continuously stirred and completely integrated in the experimental plant. Subsequently, the water is diverted by means of peristaltic pumps into an Imhoff tank (0.2 m^3) with a nominal design an HRT of 24 h (for a design flow of 200 L d^{-1}). Its effluent then flows into a 0.25 m^3 stirred storage tank and from this point water flows into 3 stages of different CW configurations. These are two vertical flow (VF) beds alternating its operation followed by a horizontal flow (HF) wetland and a free-water surface (FWS) wetland operating in series. The treatment line can be seen in Figure 5.3.

The two VF-CWs have a surface area of 1.5 m^2 each and operate alternatively in cycles of 3.5 days. This alternation of phases of feed and rest allow for controlling the growth of the attached biomass, to maintain aerobic conditions within the filter bed and to mineralize the organic deposits accumulated on the bed surface (Molle et al.,

2008). VF-CWs are intermittently fed from a 0.25 m^3 stirred storage tank by means of hydraulic pulses so as to improve oxygen renewal. For this purpose two pressure pumps work alternatively, depending on the day of the cycle, to feed each of the VF-CW beds. Each of these pumps is ruled by a level float switch, which is programmed so as to provide about 13 pulses per day. Every time the level float activated the pump, a volume of approx. 15 L (from a stirred storage tank) is discharged on a VF bed during about 10 s. A polyethylene pipe distributes the pumped water 0.1 m above the top of the bed. This pipe contains 5 perforations with diffusers that provide a true 360° radial horizontal water pattern, thus ensuring an evenly distribution of the wastewater over the whole surface of the filter. Moreover, each VF container has a metalic tramex 0.1 m above floor level and a number of holes situated underneath it so as to allow for passive aeration of the bed.
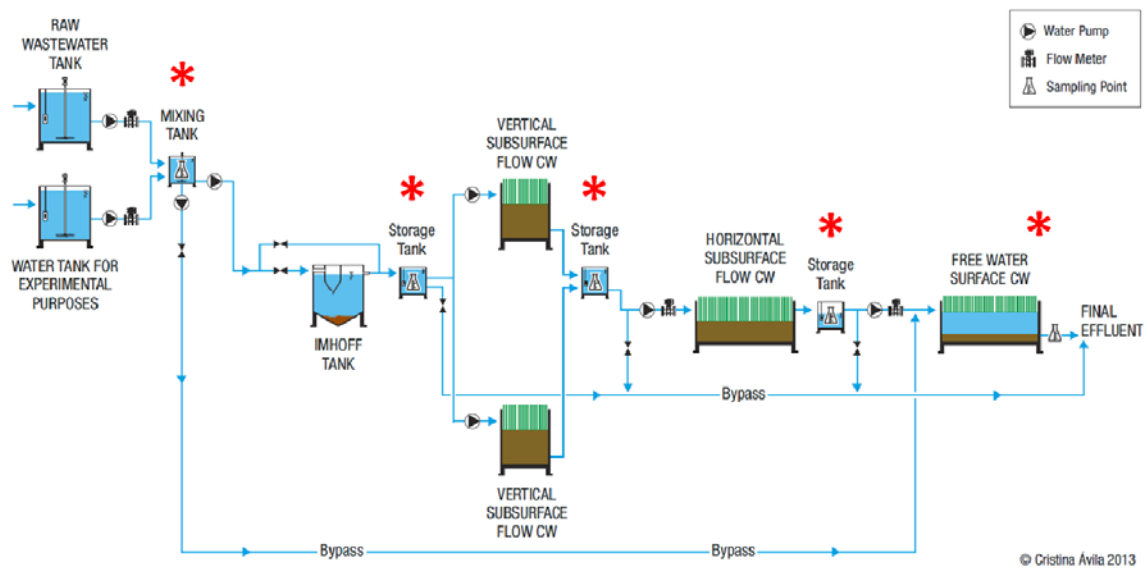
Figure 5.3. Layout of the hybrid constructed wetland system (Avila et al., 2014). Sampling locations are indicated with a red asterisk.

Effluent of the VF beds –regardless of the one in operation– is accumulated in a 0.25 m^3 tank and sent to the second stage of wetlands, which consists of a 2 m^2 HF-CW. Finally, the effluent of this unit is collected in another 0.25 m^3 storage tank and subsequently pumped into a 2 m^2 FWS-CW to complete the treatment and to produce an effluent of quality for its further reuse. Feeding of the HF and FWS CWs is in a continuous mode and is done by means of peristaltic pumps. To this regard, the above-

mentioned intermediate 0.25 m³ storage tanks are necessary for sampling of the effluents as well as for overall functioning of the treatment system. These are not exposed to light. All CWs were constructed on polypropylene and were planted with *Phragmites australis*. Vegetation was well established in all VF and HF CWs at the time of monitoring. Only about a third of the area of the FWS-CW was covered with vegetation in order to allow for sunlight penetration.
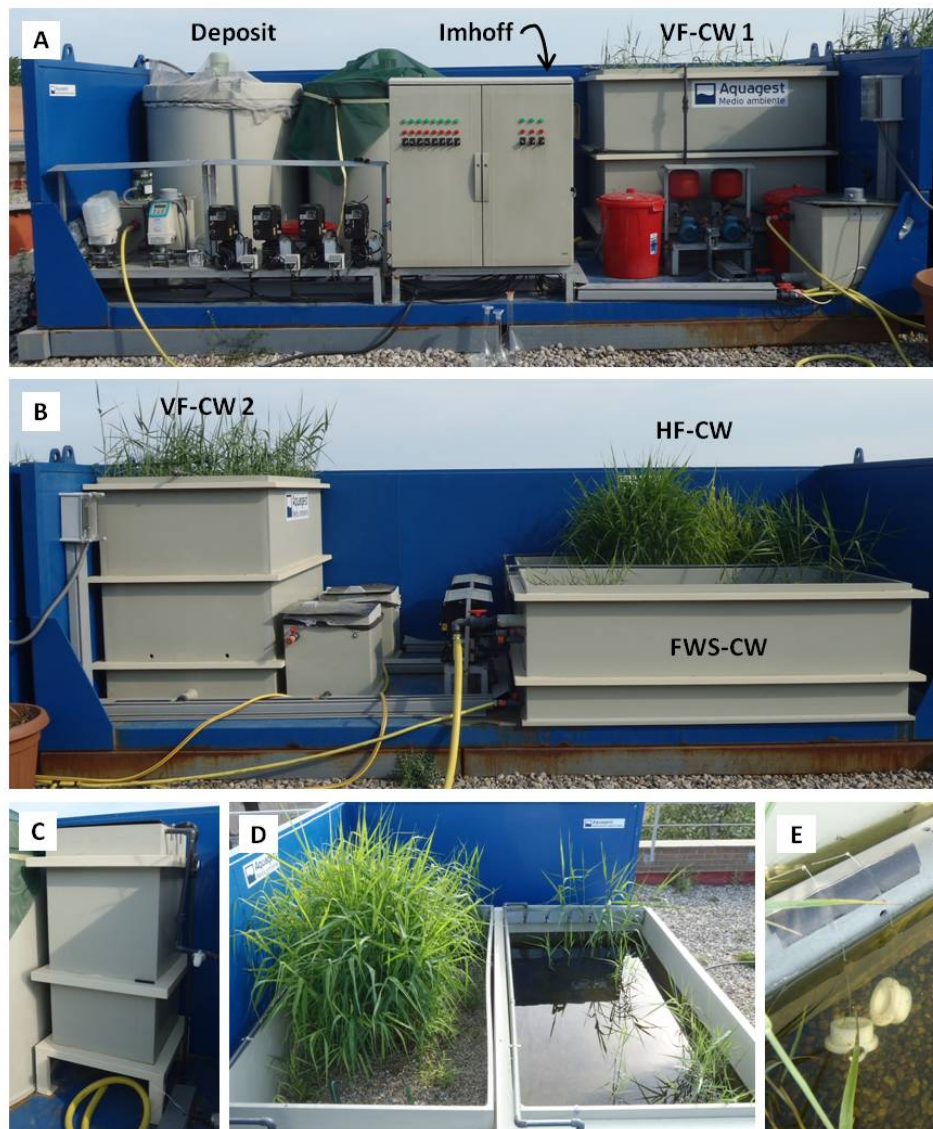
Figure 5.4. Pictures of the experimental constructed wetland. (A) Front view of the treatment line, (B) Back of the treatment line, (C) Imhoff tank, (D) HF-CW and FWS-CW and (E) DGT samplers submerged next to the way out of the FWS-CW effluent.

Several electromagnetic flow meters (SITRANS F M MAGFLO®) are installed along the treatment system to assist on the follow up of the flow values entering the

treatment system as well as the evaluation of flow fluctuations due to evapotranspiration or storm events during experimental setups. Further system features are detailed in Table 5.1.

Table 5.1. Main characteristics of the hybrid treatment system based on CWs.

Parameter	Unit	Value
Average Inflow	L d^{-1}	550
Dimensions VF-CWs	m (W x L x D)	1.0 x 1.5 x 1.3
VF-CW filling media	Depth of layers: m	Upper layer: 0.1 m of sand (1-2 mm)
	Grain size Ø: mm	Bottom layer: 0.7 m of fine gravel (3-8 mm)
Dimensions HF-CW	m	1.0 x 2.0 x 0.3
HF-CW water level	m	0.25
HF-CW filtering media	Main media: mm	Main media: 0.3 m of gravel (4-12 mm)
	Inlet and outlet: cm	Inlet and outlet: stone (3-5 cm)
Dimensions FWS-CW	m	1.0 x 2.0 x 0.5
FWS-CW free water column	m	0.3

5.4 Experimental methodology

5.4.1 Materials and equipments

The same materials and equipments as in section 4.2.1.1 were used. Regarding the DGT materials, the only difference is that only the P-DGT (a DGT sampler with polyacrylamide as diffusive gel, further defined in section 4.2.1.1) type was employed. Furthermore, 125 mL Teflon® FEP bottles (Thermo Scientific-Nalgene) were used for

water sampling, $HgCl_2$ (99.9995%, Strem Chemicals) was used to spike the solution for injection into the treatment line and KBr (Sigma-Aldrich) was used as a tracer.

Physicochemical parameters in the water of the experimental treatment plant were measured with different instruments water temperature, dissolved oxygen, pH and conductivity were measured onsite by using a Checktemp-1 Hanna thermometer, a EutechEcoscan DO6 oxymeter, a Crison pH-meter and a EH CLM 381 conductivity meter, respectively. Redox potential was also measured in situ by using a Thermo Orion 3 Star redox meter. COD, total suspended solids (TSS) and ammonium nitrogen (NH_4-N) were determined by using Standard Methods (APHA, 2001). BOD_5 was measured by using a WTW®OxiTop®BOD Measuring System.

5.4.2 Analytical determination of THg

THg was determined with the AMA-254 in water and resin gels as previously described in section 3.2.2. Aliquots of 1 mL were analysed in the case of the water samples and half the resin disc (the other half was used for MeHg determination) in the case of the DGT resin gels. The LOD and LOQ for the THg analysis of half the resin gel disc were 0.06 and 0.20 ng, respectively.

THg in the particulate phase was measured by cutting the nylon filter discs used to filter the water in four even pieces and putting one of those pieces in the nickel boat to be directly introduced into the AMA-254.

5.4.3 Analytical determination of MeHg

After being retrieved from the DGT assembly, every half-resin gel disc was treated and analyzed as explained in section 4.2.4.2. Given the lower MeHg concentrations of the water where the DGT samplers were deployed, several adjustments were necessary. The aliquot of resin extract for HS-SPME was 500 µL and the volume of citric-citrate buffer (pH = 4.5-5) added was 2.5 mL. Additionally, the six-point

calibration curve (R^2 > 0.99) was performed in the range from 6.5 to 590 pg of MeHg (as Hg).

In the case of the water samples, the methodology was basically the same except from the fact that the aliquot of sample for HS-SPME was 3 mL (its pH previously adjusted using HCl and NaOH with a larger amount of sample) and no citric-citrate buffer was added to the SPME vial.

5.4.4 DGT calibration in wastewater

A time series experiment was performed with the aim of obtaining the diffusion coefficient, D, of THg and MeHg in the diffusive layer of P-DGT deployed in wastewater. 1.5 L of wastewater collected in the experimental treatment plant (a mix of the effluent of the Imhoff tank and the VF wetland) was introduced in a amber glass bottle and spiked with 3 pg of MeHg and 15 pg of Hg(II) to obtain concentrations in water of 2 and 10 ng mL^{-1} respectively. Afterwards, the solution was left to equilibrate overnight while being stirred. Fifteen P-DGT devices were submerged in the solution, which was stirred with a magnetic stirring bar and held at a temperature of 30 °C. Three DGT samplers were retrieved after 3, 6, 10, 25 and 32 h of deployment time. The DGT blanks consisted of three units that were not deployed and kept in the fridge. At each sampling interval, 3 mL of wastewater were sampled and acidified to 0.4% with HCl, to monitor the THg and MeHg concentration remaining in solution. The results of the calibration can be seen in Figure 5.5 and the D was calculated as explained in section 3.2.4.

D_{THg} in P-DGT diffusive layer in our study wastewater was 4.48 × 10^{-7} cm^2 s^{-1} and D_{MeHg} was 2.23 × 10^{-6} cm^2 s^{-1}, both at 30 °C. On the other hand, D_{THg} and D_{MeHg} were calculated for a wide range of temperatures applying the Stokes-Einsten equation (Equation 3.3) as shown in Figure 5.6. As the average temperature of the water during the DGT deployment was 19 °C, the D_{THg} and D_{MeHg} employed for DGT calculations in order to obtain the labile Hg concentration were 3.32 × 10^{-7} cm^2 s^{-1} and 1.65 × 10^{-6} cm^2 s^{-1}, respectively.

150
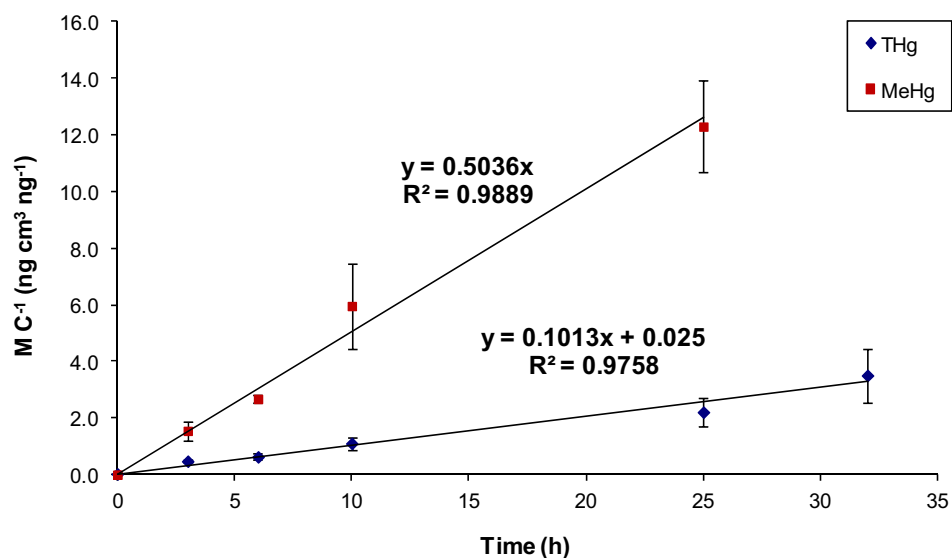
Figure 5.5. Calibration of the P-DGT units in wastewater. Mass of mercury accumulated in the resin (M) normalised by the mercury concentration in the solution for various periods of time and for THg and MeHg.
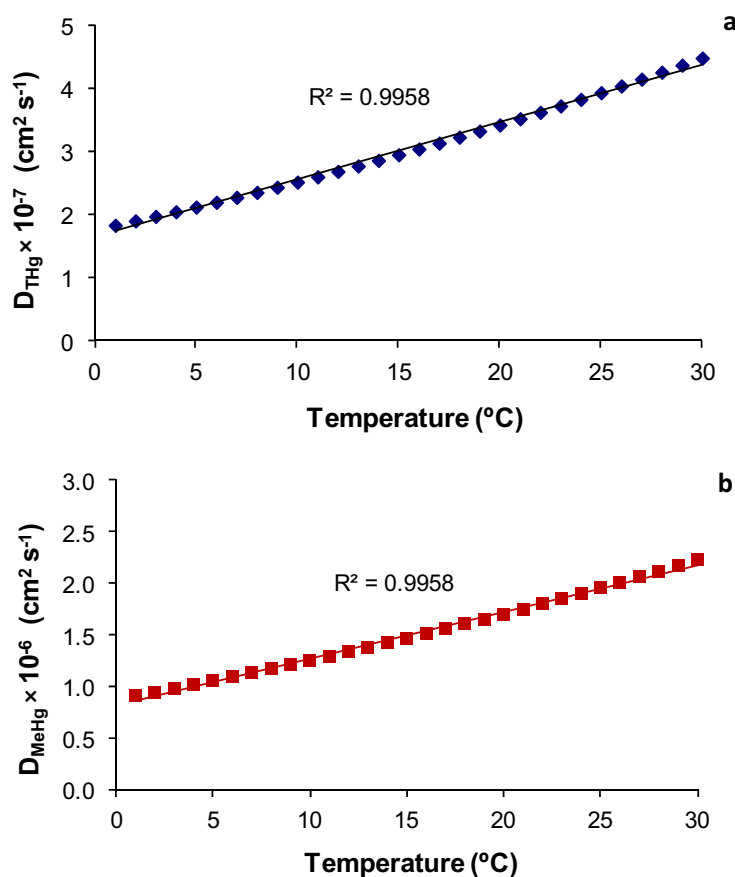
Figure 5.6. Diffusion coefficient of (a) THg (D_{THg}) and (b) MeHg (D_{MeHg}) in the polyacrylamide diffusive layer in wastewater calculated on the basis of Fick's law for a wide range of temperatures (n = 30, p < 0.001).

151

5.4.5 Experimental design and sampling

The injection experiment lasted 11 days in April 2011. Twenty litres of distilled water contained in a glass bottle protected from sunlight were spiked with Hg(II) together with potassium bromide (KBr), used as a conservative tracer. This blend was homogenized and injected into the storage tank located in the treatment line between the Imhoff tank and the VF wetlands by means of a peristaltic pump, obtained from Gilson (Middleton, WI, USA), that supplied a flow rate of 9 L d^{-1} (6.25 mL min^{-1}), synchronized with the discharge of the effluent from the Imhoff tank. This flow rate was selected so as to synchronize the duration of the injection of the doped solution to that of the wastewater, and therefore to obtain a homogenous mixture at the wetland influent. The concentration of the doped solution (670 μg L^{-1} of Hg and 800 mg L^{-1} of KBr) was adjusted in order to obtain the desired influent concentration of Hg (~10 μg L^{-1}) and the tracer (KBr = 12 mg L^{-1}). Those Hg concentrations corresponded to those reported in industrial effluents (petroleum, paper, resin or chlor-alkali industry among others), in the range 3-9600 μg L^{-1} as total Hg (von Canstein et al., 1999; Rezaee et al., 2005; Rehman et al., 2010; Safavi et al., 2010). Given the high flow entering the treatment plant and the considerable duration of the injection experiment, a total of 6 bottles with 20 L of doped solution had to be prepared.

DGT sampling started only when Br$^-$ concentrations at the effluent of the treatment line reached steady state conditions, to obtain a more reliable estimation of the removal efficiency of the system. That happened four days after the beginning of the injection experiment. At the fifth day of injection, 20 P-DGT samplers were deployed in the experimental treatment plant for five days, four replicates in each of the five points of interest: i) the mixing tank, ii) the storage tank receiving the effluent of the Imhoff tank, iii) the storage tank receiving the effluent of the VF-CWs, iv) the storage tank receiving the effluent of the HF-CW and v) the final effluent (after FWS-CW treatment) (see Figure 5.3). All the samplers were hung from the wall of the tank using a nylon string ensuring they were continuously completely submerged in the water. Another four DGT units were stored in the fridge in the laboratory during the length of the experiment as DGT blanks.

Water samples were collected at three different times: (a) right before the Hg injection started to obtain the wastewater blanks, (b) when the DGT samplers were deployed and (c) when they were retrieved. The sampling points were the same five locations were the DGT units were deployed. All samples were collected in 125 mL FEP bottles and brought to the laboratory where they were immediately filtered (Nylon filters, 47 mm diameter, 0.45 μm pore size). The filters were wrapped with aluminium foil and stored in the freezer, and the filtered water samples were acidified with concentrated HCl to reach a concentration of 0.4% (v/v) and stored in the fridge at 4 °C until analysis, which took place within one week time span. Samples were analyzed for THg and MeHg, except from the particulate phase on the filters, which was analyzed only for THg. In addition, water physicochemical parameters were daily measured during the Hg injection.

5.5   Results and discussion

5.5.1   Physico-chemical parameters

During the Hg injection study (April 2011), the vegetation was well developed in both VF and HF CWs. The average values of physicochemical parameters of the water during the study are presented in Table 5.2. The COD, TSS and NH_4-N concentrations detected in the influent (deposit or mixing tank) and the effluent of the Imhoff tank were in agreement with the values described for urban wastewaters.

The organic load entering the VF-CW was 161 g COD m^2 d^{-1}. The study VF-CWs were designed to be operated in intermittent mode (feeding-repose), which permits a high oxygen transfer that facilitates the organic matter removal, as can be observed from the increase of the redox potential and the dissolved oxygen concentration in the VF-CW. In general, a decrease of the levels of TSS, COD, BOD_5 and NH_4-N was observed. The system was designed to operate under an hydraulic loading rate (HLR) of 200 L d^{-1}, but during this Hg injection study, the system was functioning with a HLR of 550 L d^{-1}, 2.75 times as high as the former one. When forcing the system to operate at loadings higher than the design HLR, it is generated a higher feeding frequency and

a reduction of the HRT in the system. Consequently, the oxygen concentration decreases in the VF-CWs, affecting the efficiency of organic matter removal and nitrification in the wetlands beds (Torrens et al., 2009).

Table 5.2. Water quality parameters obtained for the different treatment steps (data provided by C. Ávila – GEMMA-UPC–).

	Imhoff	**VF-CW**	**HF-CW**	**FWS-CW**
pH	7.54 ± 0.02	7.80 ± 0.06	7.57 ± 0.08	7.58 ± 0.01
Temperature (°C)	18.6 ± 1.3	18.8 ± 1.3	19.4 ± 1.5	18.3 ± 1.4
Turbidity (NTU)	96 ± 15	29 ± 10	5.7 ± 3.4	4.0 ± 2.0
Conductivity (mS cm^{-1})	2.0 ± 0.3	2.0 ± 0.3	1.9 ± 0.1	2.0 ± 0.1
Redox potential (mV)	-168 ± 17	110 ± 19	-115 ± 42	156 ± 23
Dissolved oxygen (mg L^{-1})	0.24 ± 0.04	2.67 ± 0.27	0.30 ± 0.21	3.71 ± 0.35
COD (mg L^{-1})	868 ± 146	354 ± 100	177 ± 54	74 ± 17
BOD$_5$ (mg L^{-1})	178 ± 101	93 ± 32	14 ± 5.3	18 ± 5.5
TSS (mg L^{-1})	60 ± 12	17 ± 10	2.7 ± 1.3	2.91 ± 1.6
NH$_4$-N (mg L^{-1})	43 ± 9	15 ± 7	12 ± 3	6 ± 1

Due to the continuous feeding of the HF-CW, this operates under saturated conditions, which implies a decrease of the redox potential and the dissolved oxygen concentration, and consequently the reduction of the organic matter removal efficiency and limitation to the denitrification processes. Finally, the oxic conditions were restablished in the FWS-CW, thus the system removes successfully the organic matter and the NH$_4$-N. Commonly, this wetland type is used in order to obtain water of a higher quality, which can be reused for other purposes.

In general, it was observed that this treatment system is able to remove the organic matter and enables the development of nitrification-denitrification processes, permitting the removal of NH$_4$-N.

5.5.2 THg and MeHg

Before the injection of Hg(II) in the experimental treatment plant, THg levels measured in the wastewater were very low (0.03-0.08 ng mL^{-1}) and in the last treatment steps even lower than the LOQ of the THg determination methodology (0.054 ng mL^{-1}). At the time of the DGT deployment, five days after the start of the Hg(II) injection, the THg concentration in the water in the storage tank (where the injection took place) receiving the effluent of the Imhoff tank was 0.99 ng mL^{-1}, as shown in Figure 5.7; whereas the level in the previous step, the deposit (labelled as mixing tank in Figure 5.3), was still 0.07 ng mL^{-1}.

Figure 5.7. THg concentration in the dissolved phase of the water; measured directly before Hg(II) injection and right before and after DGT deployment, and determined from the DGT measurements (labile concentration). Every group of bars corresponds to every storage tank, ordered as their position in the treatment line.

Logically, THg level diminished along the treatment line (from 0.99 to 0.24 ng mL^{-1}, see the blue bars in Figure 5.7) as the injected Hg(II) should be adsorbed on the wetlands gravel or uptaken by the vegetation. However, at the time of the DGT retrieval, 10 days after the beginning of the injection, the decrease of THg concentration in water along the treatment line was not so strong (from 0.65 to 0.49 ng mL^{-1}, see the purple bars in Figure 5.7). This might be due to the fact that the system could be reaching the saturation of Hg –the particulate matter covering the gravel probably may have had already a high load of Hg and all the present sulphides

could be bound to Hg species forming insoluble HgS– and consequently poorly removing Hg from the water.
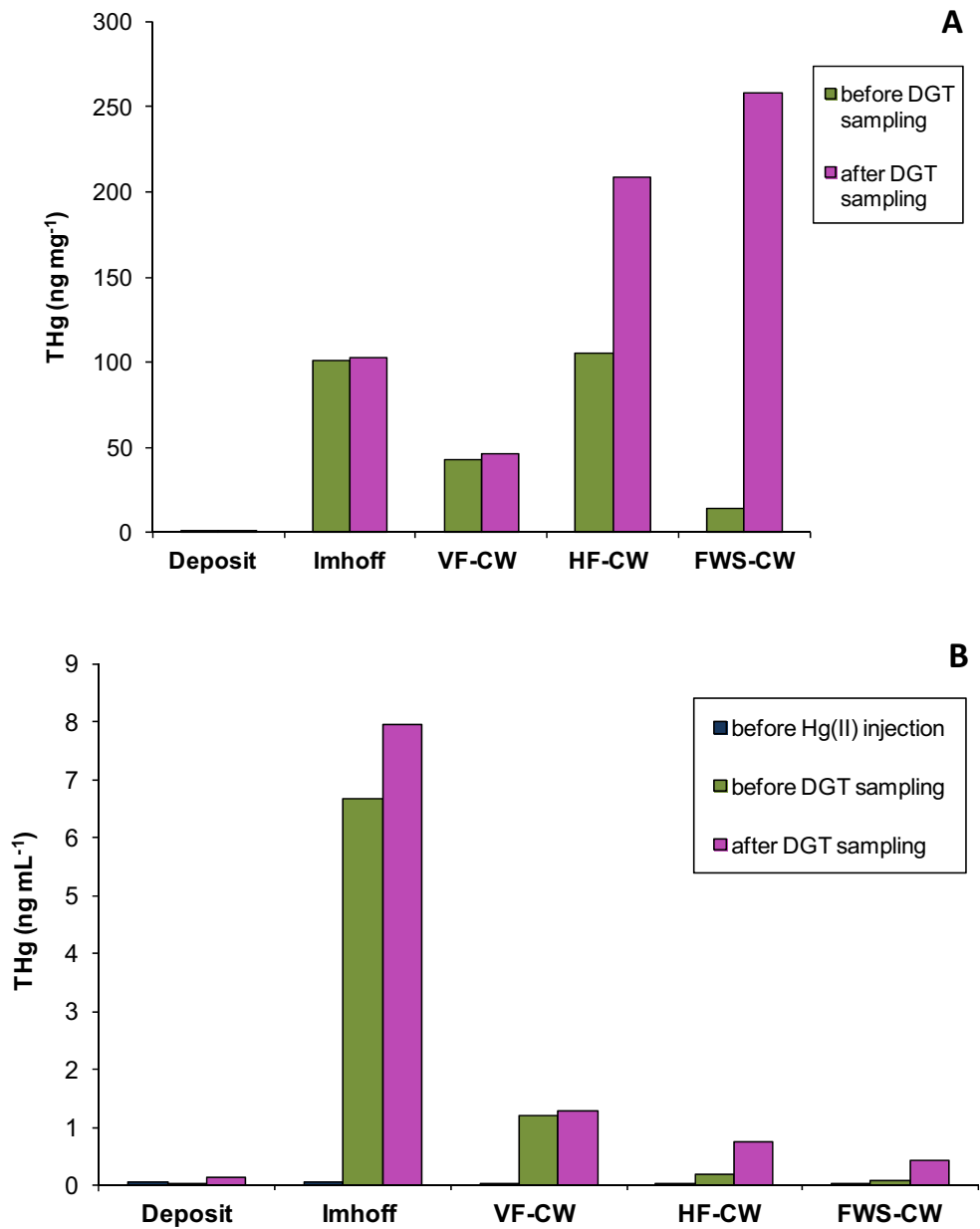
Figure 5.8. THg in the particulate phase of the water: A) THg per mass of particulate matter in 1 mL of water, B) THg per volume of water.

It also should be noted that at the end of the experiment, THg concentration in the particulate matter of the water rose importantly in the HF and FWS CWs (Figure 5.8 A). There is a lower amount of particulate matter in the water of these two last treatment

steps (TSS, Table 5.2) and thus, all the present Hg susceptible to be bound to the particles will be concentrated in that little matter.

Concerning the DGT-labile THg concentration (RSD < 30%, n = 4), it was roughly twice higher than the THg concentration directly measured in the water at the Imhoff and VF-CWs storage tanks, since it should be lower or at most equal to the directly measured concentration. The reason could be that the direct measurements correspond to spot samples, whereas the DGT units were deployed for five days recording the average concentration during the deployment time. In the case of VF-CW, the presence of a gelatinous microbial colony found covering the DGT units could have thickened the DGT diffusive layer, which means a longer residence time for Hg-DOM complexes, facilitating dissociation and accumulation. Nevertheless, the decrease of the labile THg concentration showing values closer to the direct measurements as we move forward along the treatment line, make these results credible and reliable.

Although the amount of Hg(II) injected was such to obtain a concentration of 10 ng mL^{-1} in the Imhoff's storage tank, the actual level in the water dissolved phase was about 10 times lower. This can be explained by a THg concentration in the particulate phase of 6.7-7.9 ng mL^{-1} (Figure 5.8 B), as most of the Hg tends to bind to fine clay-sized particulate matter (Brown et al., 2005). The THg concentration estimated when adding the THg concentration in the dissolved phase and in the particulate phase (expressed as mass of THg per volume of water) was 8 ng mL^{-1}, both before and after DGT deployment. There are still 2 ng mL^{-1} missing to reach those theoretical 10 ng mL^{-1} injected. That amount of Hg could have been lost by adsorption in the injection pipes and tanks walls or bound to sulphides and particle matter settled in the bottom of the storage tank.

Methylation of Hg occurred in the storage tank receiving water from the Imhoff (Hg (II) injection spot), as proven by a high MeHg level at that sampling point (Figure 5.9) in contrast with the very low level found in the raw wastewater, and that was very likely because of the anoxic conditions in the layer of sludge at the bottom of the tank (see

the negative redox potential and the low dissolved oxygen concentration in Table 5.2). It can be noted that after DGT deployment (10 days after the injection started) the MeHg level measured directly in the water was threefold the level before DGT deployment. This might have happened because of the fact that the longer Hg(II) was injected, the longer the methylation process took place, and therefore more MeHg was accumulated in the layer of sludge settled in the bottom of the tank, being susceptible of exchange between the particulate and the dissolved phase.
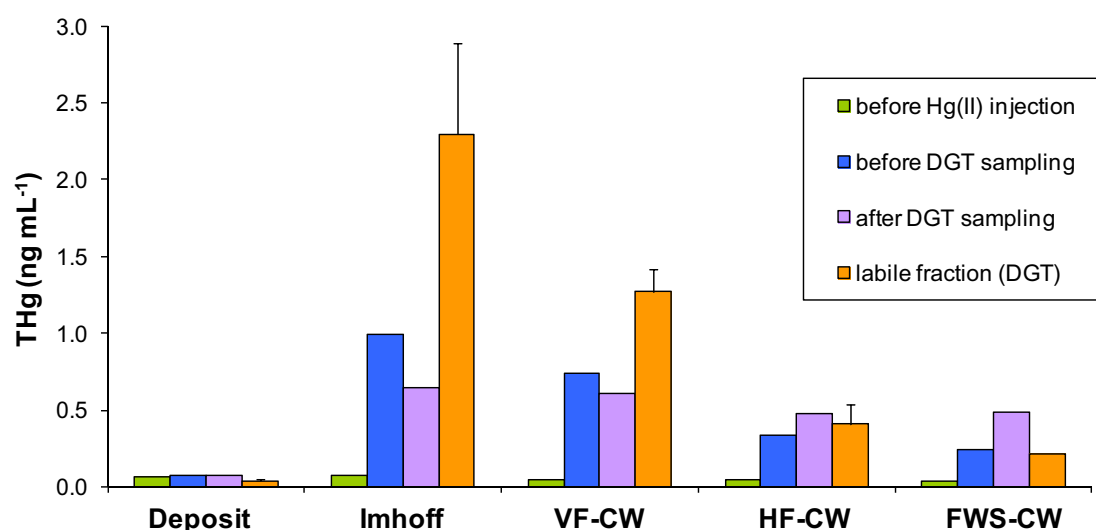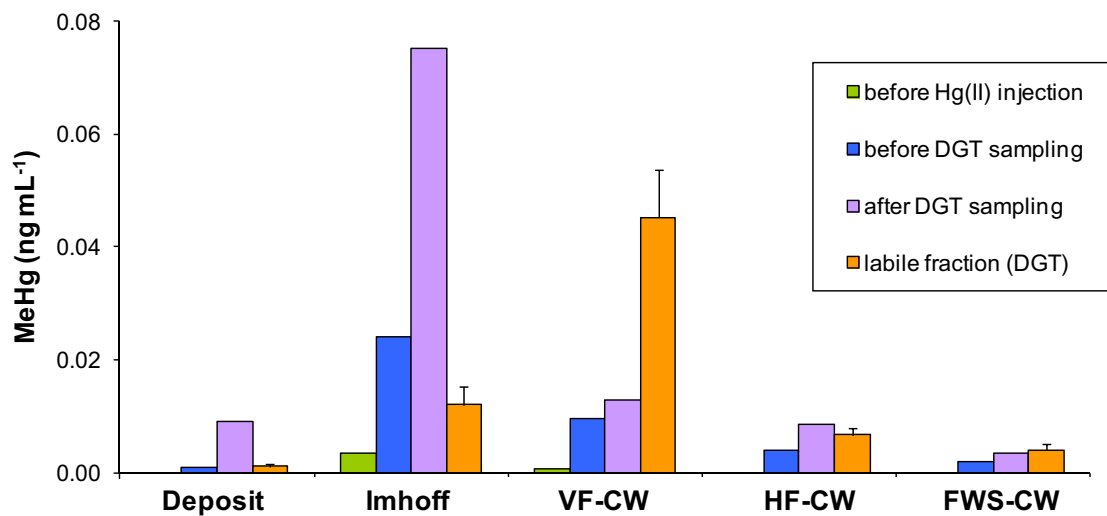

Figure 5.9. MeHg concentration in the dissolved phase of the water; measured directly before Hg(II) injection and right before and after DGT deployment, and determined from the DGT measurements (labile concentration).

Directly measured MeHg level clearly diminished throughout the treatment line, however that did not occur in the case of DGT-labile level. In this case, an increase of 277% from the Imhoff to the VF-CW storage tank was observed (Figure 5.9, yellow bars). The only explanation that can be given for that high MeHg concentration measured by the DGT samplers is that the gelatinous colony of microorganisms mentioned before could have participated in the methylation process, or thickened the DGT diffusive layer (which means a longer residence time for MeHg-DOM complexes and thus, more dissociation, more accumulation, and a higer D).

An increase of MeHg in relation to THg towards the end of the experiment duration can also be observed in Figure 5.10 (the percentage of Hg as MeHg was higher after

DGT deployment than before it in all the sampling points except the last one, even in the raw wastewater –deposit–). The fact that the percentage of Hg as MeHg was higher for DGT-labile concentrations than for those directly measured in some sampling points (VF-CW and FWS-CW) can be related to the fact that MeHg is more labile than Hg(II) (Cattani et al., 2009).
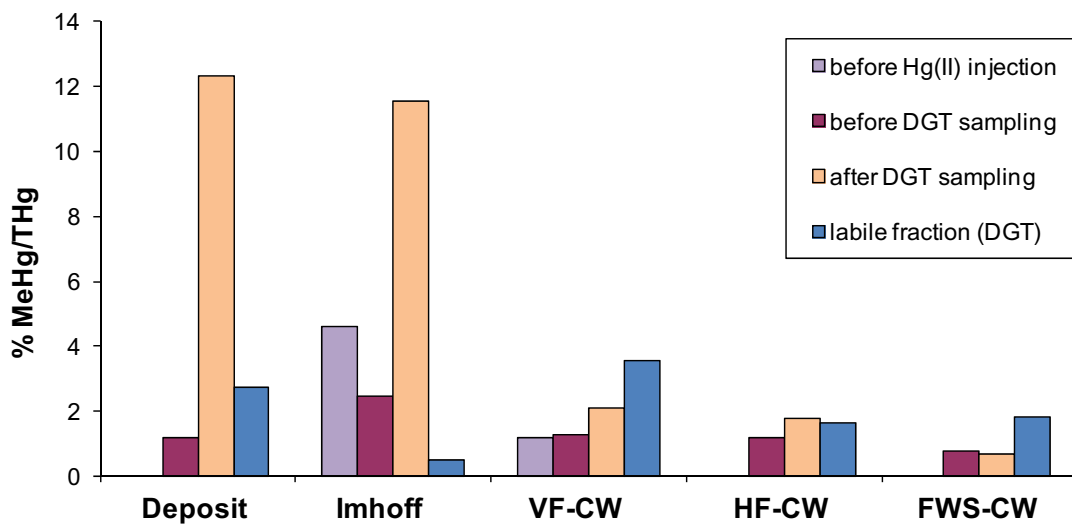
Figure 5.10. Percentage of MeHg to THg in the dissolved phase of the water

5.5.3 General discussion

The experimental treatment plant seems to effectively remove the THg present in the wastewater as proved by the 75% removal five days after the beginning of the injection of Hg(II) (see blue bars in Figure 5.7). In contrast, five days later, the percentage of removal was only 25% (see purple bars in Figure 5.7). This could be caused by the system breakthrough (particulate matter on the gravel and the scarce vegetation, mainly) since its dimensions are small and the amount of Hg injected was too high for an urban wastewater, which is the type of wastewater the plant was designed for. These values can be compared to other previously reported: 39 ± 9 % for three horizontal-flow CWs (Kropfelova et al., 2009) or 78 ± 7.5 % for another small-scale CW design (Chavan et al., 2007). However, the latter was attributed to high TSS removal since most of the THg was in particulate form (THg was measured in unfiltered water, whereas our results correspond only to the dissolved phase). THg in the particulate phase is not a problem in the effluent of our treatment plant, since both

the TSS concentration in the wastewater and the whole THg amount bound to the particles were very low at the last treatment step. The removal percentage of labile THg was 90% (see yellow bars in Figure 5.7), which is a very high efficiency and good news since that fraction of Hg is the most worrying for being the fraction susceptible to be uptaken by biota.

With regard to MeHg, we can observe that the percentage of removal was high both five and ten days after the start of the injection of Hg(II) (92% and 96%, respectively) (blue and purple bars in Figure 5.9), while it was lower in the case of the labile MeHg (66%) (yellow bars). These results contrast with those previously reported by Gustin et al. (2006) and Chavan et al. (2007), who observed a higher MeHg concentration in the effluent than in the influent of their small-scale CWs. However, it should be taken into account that Gustin et al. (2006) claimed that water chemistry is thought to be an important factor influencing MeHg production. They observed a higher methylation using clean water (4-16 ng Hg L^{-1}) instead of Hg contaminated water (25-320 ng Hg L^{-1}), however that clean water differed from the contaminated water in many parameters (higher SO_4^{2-}, TOC and temperature and lower pH among others). Also, it should be noted that Chavan et al. observed how their wetland system behaved as a sink for MeHg during the winter months and as a source for MeHg during the summer, when using water with a high load of Hg (25-320 ng Hg L^{-1}). Higher MeHg concentrations in summer are attributed to increased microbial activity, when higher temperatures and plant exudates stimulate sulfate reducing bacteria (Ullrich et al., 2001), while lower temperatures and senescent vegetation during winter may lower overall microbial activity and reduce methylation (Gilmour et al., 1998). Thus, seasonality could be also observed in the MeHg levels of the effluent of our study wetland. Unfortunately, the present study was performed only and entirely in April, therefore we cannot discuss the effect of the season on the Hg removal efficiency. It should be noted that the design of our treatment plant, involving several treatment steps in series, is more complex than those of previous studies.

In any case, the results obtained in this study confirm the Hg removal capacity of this CW design, although several adjustments should be done depending on the Hg load of the influent. For such a high Hg load as the one entering the treatment line in

this study (not only the Hg concentration was high, also the hydraulic loading was 2.75 times as high as that for which the plant was designed) for an extended period of time, the dimensions of the CWs should be bigger or the inflow lower to avoid saturation. In addition, the periodical cleaning and drainage of the system to eliminate the saturated particulate matter would be recommended. However, with the Hg loads commonly found in urban wastewater, this CW design could work suitably for long periods of time.

On the other hand, there are significant uncertainties with respect to the use of small-scale systems, such as the one applied here, to predict how a large-scale system might behave. Spatial heterogeneity typical of large wetlands was not the case in our system of study and the hydrologic setting applied may not be representative of a large-scale system.

PART III

Chapter 6

MeHg photodegradation in the water phase along a lake-wetland gradient in Boreal Sweden

6 MeHg photodegradation in the water phase along a lake-wetland gradient in Boreal Sweden

6.1 MeHg photodegradation in lakes and wetlands

As MeHg is a potent neurotoxin with the ability to pass biological membranes and to bioaccumulate and biomagnify throughout the aquatic food web (Mergler et al., 2007; Scheulhammer et al., 2007; Diez, 2009), determination of rates of production and degradation of MeHg in soils, sediments and waters, as well as identification of factors in control of the rates, is crucial for our understanding of the toxicity of mercury in the environment. On the landscape scale, lakes are often sinks for MeHg. MeHg may be degraded in sediments by the action of microorganisms (Matilainen & Verta, 1995; Schaefer et al., 2004), but most importantly it is decomposed by abiotic, light driven processes in the water column (Sellers et al., 2001; Lehnherr & Louis, 2009), which may consume the 80% or more of MeHg total inputs, including internal production (Hammerschmidt et al., 2006; Hines & Brezonik, 2007). As a consequence, drainage lakes receiving runoff from wetlands may be important sinks for MeHg in forested-wetland landscapes (Sellers et al., 2001; Watras et al., 2005). Photolysis of MeHg in open water should also be considered an important process to mitigate formation of MeHg during wetland restoration (Tjerngren et al., 2012b).

Several mechanisms have been suggested to be involved in MeHg photolysis in water, all relying on a first step of formation of reactive oxygen species (ROS) through the action of light absorption by either chromophoric groups in humic substances (such as quinones) (Alegria et al., 1997; Grandbois et al., 2008) and/or redox active inorganic components such as e.g. nitrate (Zepp et al., 1987) and iron (Hammerschmidt & Fitzgerald, 2010). Once formed, ROS are protected by rapid oxidation by hydrophobic moieties in humic substances (Latch & McNeill, 2006). In the second step, energy from ROS is transferred to the MeHg molecule resulting in a cleavage of the C-Hg bond leading to the formation of Hg(II) or Hg^0. Certain studies have provided evidence for the involvement of hydroxyl radicals (·OH) (Hoigne & Bader, 1978; Suda et al., 1991; Gardfeldt et al., 2001; Chen et al., 2003) and singlet

oxygen ($^1O_2$) (Suda et al., 1993; Zhang & Hsu-Kim, 2010b). Other studies have dismissed the action of these radicals and suggested multi-reaction pathways (Black et al., 2012).

Apart from providing the formation and protection of ROS, the importance of DOM in the MeHg photolysis process has been highlighted in many studies (Black et al., 2009). The wavelength-specificwavelength-specific light attenuation by DOM is well-known and controls the spectral composition in many surface waters (Morris et al., 1995; Williamson et al., 1996). Furthermore, DOM controls the chemical speciation of MeHg, through complexation with thiol (RSH) groups (Miller et al., 2009). In the study of Zhang and Hsu-Kim (2010) it is shown that the strong complexation of MeHg to organic thiol groups in well-defined organic molecules highly enhanced the photolysis of MeHg, as compared to complexation by carboxyl groups or inorganic ligands like Cl^-.

There are a number of studies in which the rates of MeHg photodegradation in natural waters have been determined (Sellers et al., 1996; Sellers et al., 2001; Hammerschmidt et al., 2006; Hines & Brezonik, 2007; Lehnherr & Louis, 2009; Black et al., 2012; Lehnherr et al., 2012). These studies show a progress, with the relative importance of different light wavelengths in the MeHg photolysis processes as perhaps the most important insight. Recent studies suggest that light with shorter wavelength (UV) is more efficient than photosynthetically active radiation (PAR) in the degradation of MeHg (Lehnherr & Louis, 2009; Black et al., 2012). However, results of the relative role of UVA and UVB diverge (Lehnherr & Louis, 2009; Hammerschmidt & Fitzgerald, 2010; Black et al., 2012).

Because of the different ways to conduct experiments and report data, published photodegradation rate constants (k_{pd}) are site and method specific and very difficult to compare. When derived from photon flux (E m^{-2}), k_{pd} in most studies is calculated as a function of incident PAR (Sellers et al., 1996; Sellers et al., 2001; Hammerschmidt et al., 2006; Hines & Brezonik, 2007; Lehnherr & Louis, 2009; Lehnherr et al., 2012) despite acknowledging the impact of the full solar spectrum for the process. Methodological effects like actinic flux (light scattering by reaction vessel material), correction for the

refractory index of water in contact with the optics, and the light attenuation by the reaction bottle material have been handled in different ways, or not at all. Finally, because of the strong wavelength-specific attenuation of light by DOM, k_{pd} determined in waters with different concentrations and quality of DOM cannot be easily compared.

6.2 Objective of the study

The aim of this study was to determine rates of MeHg photodegradation in DOM (humic) dominated waters from three sites along a forested wetland-freshwater lake gradient in boreal Sweden. We combined data from experiments using different spectral composition: natural sunlight and an artificial UV source, to calculate wavelength-specific first-order photodegradation rate constants ($k_{pd\ PAR}$, $k_{pd\ UVA}$, $k_{pd\ UVB}$), corrected for the light attenuation by DOM. We employed electron paramagnetic resonance spectroscopy (EPR) and sulfur X-ray absorption near-edge spectroscopy (S XANES) to quantify the formation of radicals and organic thiol groups, respectively.

6.3 Description of the study water bodies

Rates of MeHg photodegradation were determined in organic rich surface waters taken along a lake-wetland gradient in a Boreal coniferous forest area with mixed ombrotrophic-minerotrophic mires, situated 40 km north of Umeå, Sweden. The area is covered by glacial till developed from gneissic bedrock. Soils are dominated by Iron Podzols (Spodosols) in recharge areas, grading into Humic Podzols and Histosols and Gleysols in discharge areas. Norway spruce (*Picea abies*) dominates most upland soils and slopes of discharge areas, whereas Scots pine (*Pinus silvestris*) dominates on wetter areas covered by Histosols/Gleysols. pH in wetlands and surface soils fall in the range 3.8-4.5, but can be substantially higher (5.5-6.5) in lakes which receive a mixture of humic rich waters from discharge areas and ground water from the upland soils (Tjerngren et al., 2012a).

Three sites (Figure 6.1) were included in the study: a dystrophic lake: Ängessjön (ANG) (64°2'56''N 20°50'17''E), a mixed *Sphagnum/Carex* peatland – dystrophic lake with approximately 30% open water: Kroksjön (KSN) (63°57'8''N 20°38'13''E), and a riparian zone wetland created by artificial damming of a small stream: Stor-Kälsmyran (SKM) (63°56'52''N 20°38'48''E). The ANG lake has an average water depth of about 2-2.5 m and more than 50 cm deep organic sediments. About 30% of the shores are covered by peatland and 70% by shallow mineral soils. The KSN site is dominated by floating mats and islands of *Sphagnum/Carex* peat mixed with small areas with open water having a maximum water depth of about 1 m. The level of surface water was raised by approximately 40 cm in June 2008, by damming of the outlet. The SKM riparian zone wetland consists of *Polytrichum spp*. hummocks mixed with small hollows that fill with water during periods with high precipitation. These three sites were selected because they span a range in physicochemical characteristics typical for humic lakes and wetlands in boreal Sweden. The KSN and SKM sites were included in the study of Tjerngren et al. (2012b), where a more detailed description of the sites is presented.

Figure 6.1. Study sites: (A) ANG, (B) KSN and (C and D) SKM.

6.4   Experimental methodology

6.4.1   Acid cleaning procedure for Teflon bottles

The bottles and their lids (Thermo Scientific/Nalgene®) were washed in the washing machine with alkaline detergent. Afterwards, they were rinsed three times with Milli-Q water and immersed in an acid solution (2% HCl and HNO_3). The bottles were kept in the acid bath for 72 hours, the solution being changed after approximately 36 hours, and thoroughly rinsed with Milli-Q water before use.

6.4.2   Water sampling

Surface water was collected at 20 cm depth in the middle of the lake ANG, at 20 cm depth in the open clear water area of KSN and at 20 cm depth at the dam located in the outlet of site SKM. Samples were taken in acid-washed 25 L plastic containers with gloved hands (Figure 6.1 D) and kept stored in darkness and at 4 °C until use in the experiments.

6.4.3   Chemical analyses

pH, TOC and specific UV absorbance (SUVA) were measured immediately after sampling. pH was measured using a SevenMultiTM pH meter with an InLab Science pH electrode (Mettler Toledo). Absorbance at 254 nm was measured using a 1 cm quartz cell and a UV/VIS 920 spectrophotometer (GBC Scientific Equipment, Australia). SUVA, reflecting the aromaticity of natural organic matter, was calculated as the absorbance at 254 nm corrected for the absorbance by total dissolved Fe (Weishaar et al., 2003) divided by TOC (mg L^{-1}). DOC was analyzed using a Shimadzu TOC-5000 analyser (Schimadzu Company, Japan) and concentrations of Cl, F, Br, SO_4, NO_3 and PO_4 were analyzed using anion-exchange HPLC with conductivity detection (IC-Dionex 4000i, Dionex Corporation, USA). Concentrations of Ca, Fe, Mg, Mn, Na and total S were determined by ICP-OES (Spectro Ciros Vision, Spectro Analytical Instruments,

Germany). The water was not filtered prior to analysis, but given the very small contribution from particles larger than a 0.45 μm cutoff filter (< 10% of TOC) in previous studies at these particular sites (Tjerngren et al., 2012b), TOC can be considered as practically equivalent to DOC. Also, one liter of water sample was freeze dried from each of the three sites. This material was used to determine concentrations of organic radicals by EPR and sulfur speciation by S K-edge XANES, as described in detail in annex II (section II.1 and II.2, respectively).

6.4.4 Analytical determination of MeHg

The total concentration of MeHg in water, as well as the concentrations of Me^{204}Hg and Me^{198}Hg isotopes, were determined following the procedure of Lambertsson and Bjorn (2004). Samples were acidified to 0.5% (w/w) by HCl, Me^{200}Hg was added as internal standard and then kept stored at -19 °C in darkness until analysis.

After thawing, a 40 mL aliquot of the sample was poured into a 125 mL silanised glass flask along with 1 mL of 5M acetic acid/acetate buffer (pH 4.9) followed by addition of 100 mL 1% NaBEt$_4$ in Milli-Q water. Ethylated Hg species were then transferred onto quartz tubes packed with Tenax TA, mesh 60-80 (Supelco, Bellefonte, PA, USA) by purging with N$_2$ for 8 min at a flow rate of 80 mL min^{-1}.

The analyte was finally detected after thermal desorption to GC-ICP-MS. Thermal desorption and separation of collected Hg species was done using an in-house built thermal desorption station and an Agilent 6890 Gas Chromatograph connected to an Agilent 7500a ICP-MS via a commercial interface (Yokogawa Analytical Systems). Hg species collected on Tenax TA® traps were desorbed by heating to 250 °C and injected to an Agilent HP-1 fused silica column (15 m × 0.53 mm I.D. × 3 μm film thicknesses) at a gas flow rate of 25 mL min^{-1} (He) during 15 seconds after 45 seconds of heating. Hg species were separated using an initial GC temperature of 80 °C for 1 min followed by a 50 °C min^{-1} ramp to 250 °C which was kept for 1 min. Data were collected by monitoring m/z 198, 200, 202 and 204 at a 0.1 s integration time per point.

Concentrations of ambient MeHg and MeHg isotope tracer species were calculated using isotope dilution analysis (Qvarnstrom & Frech, 2002). For every batch of samples, triplicate blanks were analyzed and blank correction was performed. The detection limit was ~0.015 ng L^{-1}.

6.4.5 Determination of wavelength-specificwavelength-specific light attenuation by DOM

The transmission of light in the three water samples was determined by scanning the samples in the spectral range 250 to 700 nm by a step of 0.16 nm in 1-cm quartz cuvettes, using a UV/VIS 920 spectrophotometer (GBC, Scientific equipment, Australia). In addition to the specific water samples used in each of the two experiments, samples diluted in Milli-Q water were measured in order to establish light attenuation as a function of concentration of TOC (Figure 6.2). Geometric, average transmission values were calculated for PAR (400-700 nm), UVB (280-320 nm) and UVA (320-400 nm). The wavelength-specific attenuation coefficient normalized to 1 m, K_d (λ), m^{-1}, was calculated as K_d = ln (I_0/I)/-0.01, where I_0 and I is incident and transmitted radiation through the 0.01 m path length of the cuvette, respectively.
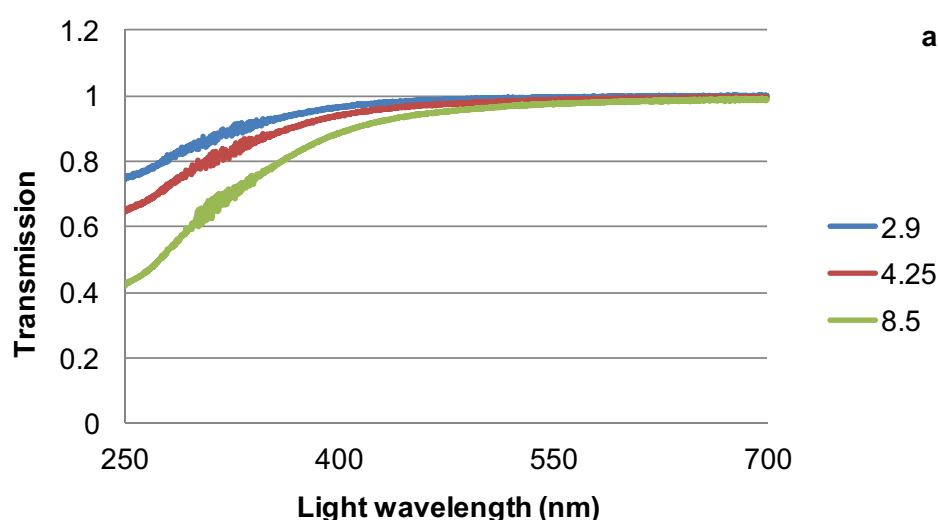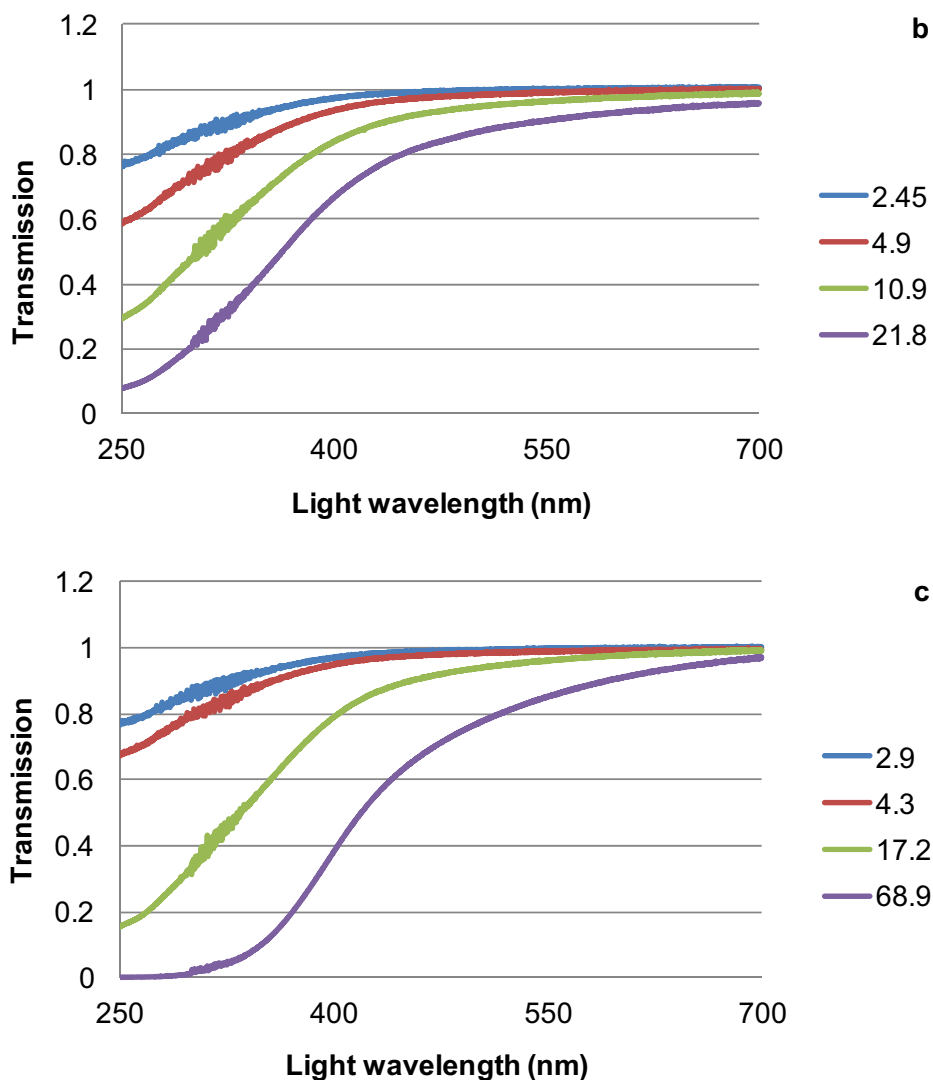
Figure 6.2. Transmission of 250-700 nm light by water at site ANG (a), KSN (b) and SKM (c), diluted by Milli-Q water to give a range of DOC concentrations (mg L^{-1}), as specified in the legend.

6.4.6 MeHg photodegradation experiments

All experiments were conducted with non-filtered water in acid-washed (following a trace-metal clean procedure described in section 6.4.1) 250 mL Teflon® FEP bottles (Nalgene). Methyl mercury was added as an isotope enriched tracer (Me^{198}Hg in exp #1 and Me^{204}Hg in exp #2) to all bottles, resulting in concentrations similar to ambient MeHg (~0.5 ng L^{-1}). All bottles were filled to the top to avoid any headspace, and weighed. No precautions were taken prior to and during experiments to avoid contact with air. A strict time of pre-equilibration (in darkness) was not applied, but in reality it

took about 30 min until the samples were exposed to light. Because of the single bond formation between MeHg and RSH (thiol) groups in DOM (Qian et al., 2002), a shorter time can be expected for MeHg-SR complexes to establish equilibrium than the ~10 hours suggested for Hg(II) to find its strongest association with presumably two RSH groups (Miller et al., 2009). The fact that our determined MeHg degradation rate constants remained the same, irrespective of whether the second sampling time data points in exp #1 and or #2 were omitted from the linear regressions or not, demonstrates the insignificant effect of adsorption kinetics on the reported results.

The bottles were either exposed to natural sunlight (exp #1) or to light from an artificial source (lamp) with a higher proportion of UVB (exp #2). PAR was measured inside and outside the bottles during the whole length of the exposure using a Quantum Meter MQ-200 Series (Apogee). PAR was measured inside the bottles (PAR_{IN}) to avoid uncertainties associated with the scattering of light by the bottles that need to be considered if the incident light is measured. To account for the change in light sensors response due to the different refractory index of water in contact with the optics, measured PAR_{IN} was multiplied by a water immersion factor of 1.35 (Zibordi et al., 2004). The bottles were placed horizontally in relation to the light source. To stop the photodegradation process, samples were immediately frozen at -19 °C in darkness, after addition of HCl (corresponding to a final concentration of 0.5%, w/w) and Me^{200}Hg as an internal standard, to correct for possible losses during storage.

6.4.6.1 *Experiment #1: MeHg photodegradation in original water samples by natural sunlight*

A total of 63 FEP bottles (21 from each or the three sites) were added original water spiked with Me^{198}Hg. Three samples from each site were immediately frozen (-19 °C) (representing time zero) and the rest were exposed to natural sunlight at the roof of the building of the Swedish Agricultural University (63° 49' 22"N, 20° 17' 25"E) (Figure 6.3). Serving as dark controls, three bottles from each site were double wrapped with aluminium foil, but otherwise treated the same as the light exposed

bottles. In order to estimate the spectral composition of the incident sunlight in terms of the contribution by PAR (400-700 nm), UVA (320-400 nm) and UVB (280-320 nm) to the radiation received at the surface, we performed radiative transfer calculations (Lindfors et al., 2009). The radiative transfer model was set up to represent Umeå during the period of measurement in October 2011. The resulting radiation spectra give a relative photon flux of PAR, UVA and UVB of 92.3%, 7.5% and 0.17%, respectively. The average sunlight spectrum, the input parameters used in the model and its uncertainties are reported in Annex II, section II.3. All bottles were placed on the side, avoiding shading. Triplicates from each site were retrieved at five different occasions, corresponding to a cumulative PAR_{IN} of 29, 64, 138, 213, 283 E m^{-2} for ANG; 24, 54, 118, 182, 242 E m^{-2} for KSN and 19, 43, 94, 144, 192 E m^{-2} for SKM.
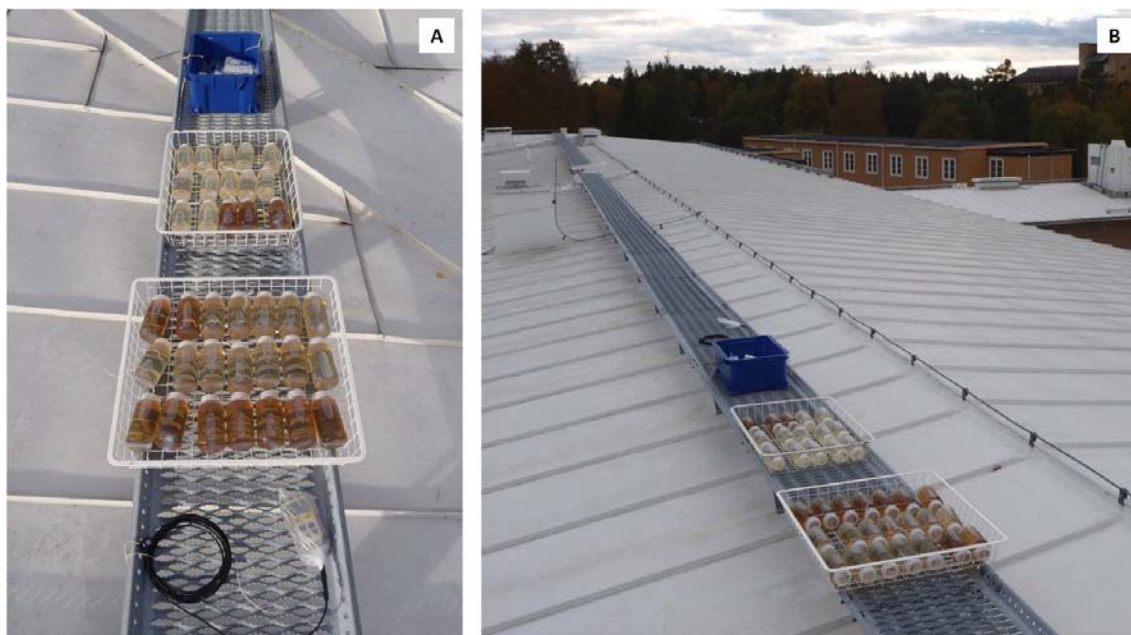
Figure 6.3. Position of the bottles and the light meter in Experiment #1 (A) and their location on the university roof (B).

6.4.6.2 *Experiment #2: MeHg photodegradation in diluted water samples by artificial light*

Water samples from the three sites were diluted by Milli-Q water to a final concentration of ~2.5 mg DOC L^{-1}, and poured into four FEP bottles for each site. The four bottles of each site were added $Me^{204}Hg$ corresponding to 0.6, 6.3, 43 and 677

nM, respectively. The bottles were exposed to artificial light from a Repti Glo 10.0 UVB, 20 W, lamp (Exoterra) having about tentimes higher relative photon flux of UVB than natural sunlight: 91.6% PAR, 6.3% UVA and 2.1% UVB, as determined by a ILT 900-R spectroradiometer (Peabody, MA, USA). The spectrum is shown in Figure II.4, Annex II. The lamp was placed at about 20 cm distance from the bottles in a closed box with white walls. Before starting the irradiation, and at six time intervals (4, 12, 24, 35, 52 and 75 h), 10 mL of sample were retrieved from each bottle for MeHg determination and another 10 mL were taken for measurements of pH and $SUVA_{254nm}$ (values shown in Figure II.5, Annex II). PAR_{IN} was measured along the experiment in the centre of the bottles.

6.4.7 Calculation of overall and wavelength-specific MeHg photodegradation rate constants

Photodegradation rate constants (k_{pd}) were calculated from first-order decay kinetics as the slope of the negative linear relationship between the natural logarithm of the quotient between the concentration of MeHg at the sampling occasion and the initial concentration, $-\ln([MeHg]/[MeHg]_0)$, and the cumulative photon flux (E m^{-2}). The latter was expressed as PAR and as the full light spectrum (280-700 nm) photon flux.

In order to calculate the full spectrum photon flux (PAR+UVA+UVB) reaching the middle of the bottles, the UVA and UVB light attenuation by the Teflon material (FEP) and DOM need to be considered. The effect of FEP was established by measuring PAR outside and in the centre of the bottles filled with distilled water. Our values on PAR attenuation agreed with the result reported by Amyot et al. (1997) (0.7%) and therefore their reported results on the relative attenuation of UVA (18%) and UVB (34%) could be adopted.

The light attenuation by DOM was accounted for by using the wavelength (λ) specific attenuation coefficient, $K_d(\lambda)$, as determined for the three wavelength regions (PAR: 400-700 nm, UVA:320-400 nm and UVB: 280-320 nm) for the water samples (see

section 6.4.5). The regression equations in Figure 6.4 were used to calculate values on $K_d(\lambda)$ valid for the concentrations of DOC in the water samples used in exp #1 and #2. In exp #2, the high UVB intensity caused a loss of absorbance at 254 nm during the course of the experiment amounting to 10-15% (Figure II.5, Annex II), which suggests a decrease in light attenuation by DOM over time. Considering the decreased bleaching with increasing wavelength (Bertilsson & Tranvik, 2000) the downwelling irradiance was corrected for an average of 7.5% loss of UVB and 2.5% loss of UVA in exp #2. We anticipate no significant loss of PAR attenuation over time, neither in exp #1 nor in exp #2, and no loss of UVB and UVA attenuation over time in exp #1.
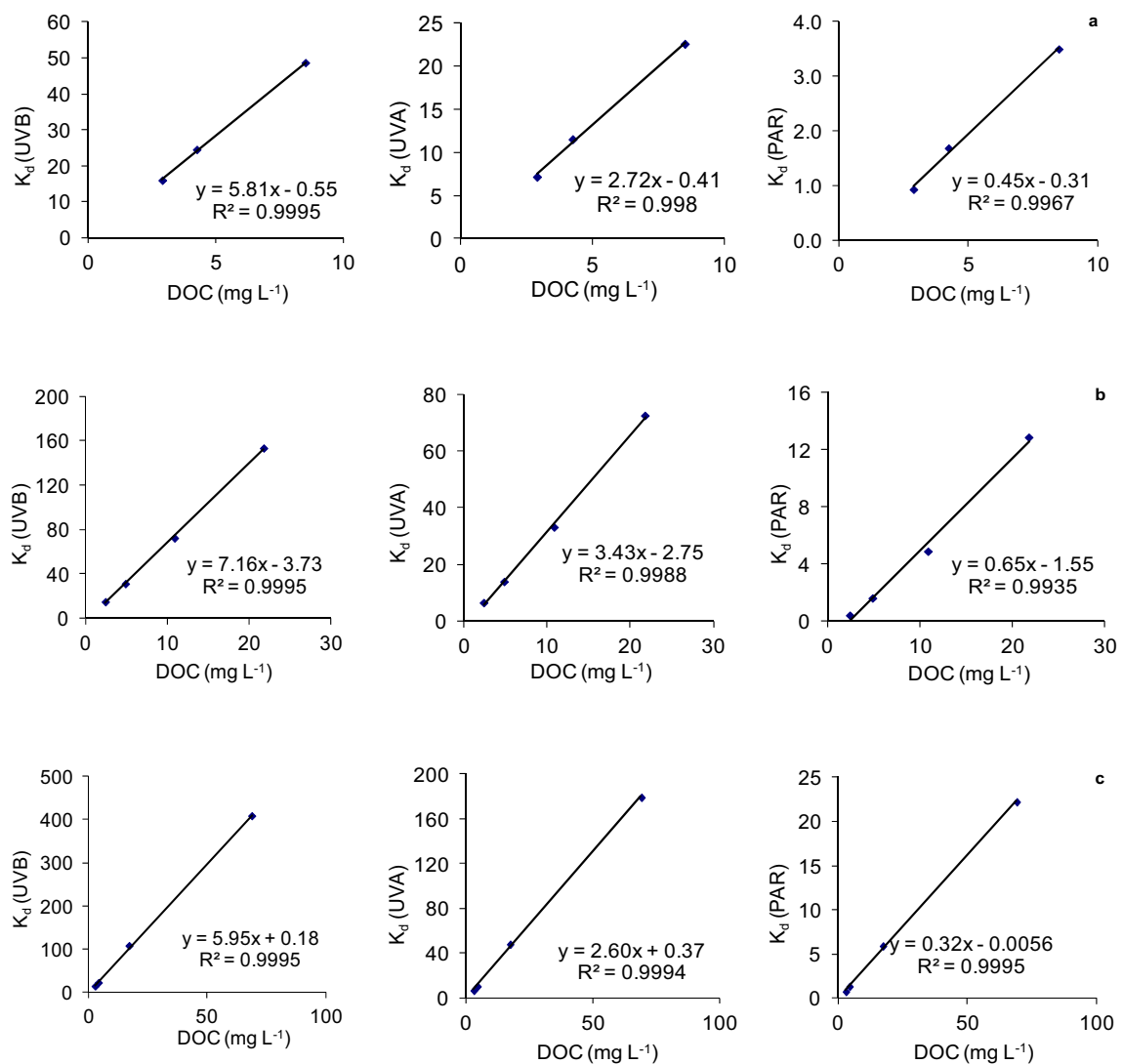
Figure 6.4. Relationships between TOC (denoted DOC) and wavelength-specific light attenuation coefficients (Kd, m^{-1}) calculated from measured wavelength-specific light transmission in water samples from sites ANG (a), KSN (b) and SKM (c).

The ratio of the downwelling irradiance travelling the distance between the inside of the bottle wall and the middle of the horizontally placed Teflon bottle (which corresponds to a distance of half the bottle diameter, 8/2 = 4 cm), i.e. the light transmission, is in agreement with Kirk (1994) calculated by Equation (6.1):

$$E_4/E_0(\lambda) = \exp(-K_d(\lambda) \times 0.04) \qquad (6.1)$$

The total wavelength dependent light transmission, taking into account the attenuation by FEP and DOM, could be expressed as $T_{PAR} = 0.99 \times E_4/E_0(PAR)$, $T_{UVA} = 0.82 \times E_4/E_0(UVA)$ and $T_{UVB} = 0.66 \times E_4/E_0(UVB)$.

The full spectrum photon flux reaching the middle of the bottles was calculated from Equation (6.2):

$$\text{Full spectrum photon flux (E m}^{-2}) = I_f(PAR_{IN} + T_{UVA}/T_{PAR} \times F_{UVA}/F_{PAR} \times PAR_{IN} + T_{UVB}/T_{PAR}$$
$$\times F_{UVB}/F_{PAR} \times PAR_{IN}) \qquad (6.2)$$

where I_f is the water immersion factor (1.35), the parameters F_{PAR}, F_{UVA} and F_{UVB} are the fractions of PAR, UVA and UVB in incident light, and PAR_{IN} is the measurement of PAR in the middle of the bottles. The $k_{pd\ Full\ Spectrum}$ constant was determined as the slope of the relationship between $-\ln([MeHg]/[MeHg_0])$ and the cumulative full spectrum photon flux (Figure 6.7). In the final step, wavelength-specific photodegradation constants ($k_{pd\ PAR}$, $k_{pd\ UVA}$ and $k_{pd\ UVB}$) were calculated from the $k_{pd\ Full\ Spectrum}$ constants determined in exp #1 and #2, and the following three equations, by an iterative procedure:

$$k_{pd\ Full\ Spectrum} = k_{pd\ PAR} \times f_{PAR} + k_{pd\ UVA} \times f_{UVA} + k_{pd\ UVB} \times f_{UVB} \qquad (6.3)$$

$$k_{pd\ PAR}\ (\text{site ANG}) = P_1 \times k_{pd\ PAR}\ (\text{site KSN}) = P_2 \times k_{pd\ PAR}\ (\text{site SKM}) \qquad (6.4)$$

$$k_{pd\ PAR}\ /\ k_{pd\ UVA}\ /\ k_{pd\ UVB}\ (\text{site ANG}) = k_{pd\ PAR}\ /\ k_{pd\ UVA}\ /\ k_{pd\ UVB}\ (\text{site KSN})$$
$$= k_{pd\ PAR}\ /\ k_{pd\ UVA}\ /\ k_{pd\ UVB}\ (\text{site SKM}) \qquad (6.5)$$

The parameters f_{PAR}, f_{UVA} and f_{UVB} ($f_{PAR} + f_{UVA} + f_{UVB} = 1.0$) denote fractions of the full light spectrum represented by PAR, UVA and UVB light, respectively, reaching the middle of the Teflon bottles. These are in turn calculated as

$$f_{PAR} = (F_{PAR} \times T_{PAR})/(F_{PAR} \times T_{PAR} + F_{UVA} \times T_{UVA} + F_{UVB} \times T_{UVB}),$$

$$f_{UVA} = (F_{UVA} \times T_{UVA})/(F_{PAR} \times T_{PAR} + F_{UVA} \times T_{UVA} + F_{UVB} \times T_{UVB}), \text{ and}$$

$$f_{UVB} = (F_{UVB} \times T_{UVB})/(F_{PAR} \times T_{PAR} + F_{UVA} \times T_{UVA} + F_{UVB} \times T_{UVB}). \tag{6.6}$$

As described by Equation (6.5), the model was constrained by assuming the quotients of the wavelength-specific rate constants were the same at all sites. This was primarily done to lower the number of fitting parameters, but as will be shown by the results, it may be also reasonable from a mechanistic point of view. Absolute differences in the three wavelength-specific rate constants among the three sites were expressed by the proportionality factors P_1 and P_2 in Equation (6.4). The three equations were solved for data collected from all three sites in experiment #1 and at the lowest MeHg/TOC ratio in experiment #2, taking advantage of the difference in incident light spectral composition in the two experiments. Thus, in total six versions of Equation (6.3) (three sites and two experiments), were combined with Equation (6.4) and Equation (6.5) to calculate the five unknown parameters: $k_{pd\ PAR}$, $k_{pd\ UVA}$ and $k_{pd\ UVB}$ and the proportionality factors P_1 and P_2 by an iterative procedure.

The uncertainty in k_{pd} constants, as determined from the slopes of the relationship between $-\ln([MeHg]/[MeHg_0])$ and the respective photon flux (E m^{-2}), are reported as standard errors (SE). These errors, being on the order of 3-5% relative SE (RSE), are largely associated with MeHg determinations and estimates of the PAR and full spectrum photon flux (Equation (6.2)). Uncertainties in the calculated wavelength-specific k_{pd} were determined by propagating estimated RSEs of $k_{pd\ Full\ Spectrum}$ (±4% exp #1 & #2), f_{PAR} (±2% exp #1 & #2), f_{UVA} (±10% exp #1, ±5% exp #2) and f_{UVB} (non-significant exp #1, ±5% exp #2) in Equation (6.3), following the rules of Taylor, 1982. The calculated RSE was ±9% for $k_{pd\ PAR}$, ±24% for $k_{pd\ UVA}$ and ±19% for $k_{pd\ UVB}$.

6.5   Results and discussion

6.5.1   Chemical characterization and light absorption by water from the lake-wetland gradient

Organic horizons of Podzols and wetland soils in the study area generate runoff with a pH in the range 3.5-4.5 and TOC > 100 mg L^{-1}, as opposed to deeper soil and groundwater with a pH of 5.5-6.5 and a TOC concentration in the range 1-10 mg L^{-1} (Williamson et al., 1996). Therefore, the decrease in pH (6.6 > 5.1 > 3.8) and increase in TOC (17.5 < 27 < 81 mg L^{-1}) along the lake-wetland gradient ANG, KSN and SKM (Table 6.1) reflects a change from mineral soil drainage to increasing influence of organic surface soil and wetlands.

The lower $SUVA_{254nm}$ and TOC/TON ratio in the ANG lake reflects a larger contribution from in-lake (aquatic) production of more labile organic matter with less aromatic (terrestrial) character. When normalized to TOC, the concentration of organic radicals (spins per g) as determined by EPR (Figure II.1, Annex II), and the concentration of organic thiol groups (RSH) as estimated by S XANES (Figure II.2, Annex II) decreased in the order ANG > KSN > SKM (Table 6.1). The devoid of hyperfine splitting of the single, broad EPR peak, the spectroscopic splitting constant g of 2.00442, 2.00436 and 2.00436 for spectra of ANG, KSN and SKM, respectively, and the number of spins per gram TOC in the range 5.5–13 × 10^{17} are measurements well in agreement with previous studies consistent with semi-quinones as the primary radical forming chromophoric groups in DOM (Senesi & Schnitzer, 1977; Scott et al., 1998; Polewski et al., 2005). Relatively high concentrations of Fe in all three waters in addition suggest that hydroxyl radicals were formed through the photo-Fenton reaction (Zepp et al., 1992b), while the nitrate concentration was likely too low to be important (Table 6.1).

Table 6.1. Chemical characteristics of original water (used in exp #1) from the three sites. Total MeHg includes 0.5 ng L^{-1} of MeHg isotope tracer addition.

		ANG	KSN	SKM
wetland influence		low	high	intermediate
surface forest soil influence		intermediate	low	high
aquatic/deeper groundwater influence		high	intermediate	low
	pH	6.6	5.1	3.8
	ionic strength (mM)	0.44	0.21	0.22
	ambient MeHg (ng L^{-1})	0.16	0.70	0.27
DOM quantity	TOC (mg L^{-1})	17.5	27	81
DOM quality	SUVA$_{254nm}$ (L mg^{-1} m^{-1})	3.3	4.2	4.1
	TOC/TON (g g^{-1})	24	49	64
organic radical formation				
	spins/L	2.3×10^{16}	2.3×10^{16}	4.5×10^{16}
	spins/g TOC	1.3×10^{18}	8.5×10^{17}	5.5×10^{17}
	ambient MeHg/spins (µmol mol^{-1})	19	85	17
	total MeHg/spins (µmol mol^{-1})	74	140	45
chemical complexation of MeHg				
	RSH (mg L^{-1})	0.026	0.037	0.039
	RSH/TOC (mg g^{-1})	1.5	1.4	0.5
	ambient MeHg/RSH (µmol mol^{-1})	0.91	2.8	1.0
	total MeHg/RSH (µmol mol^{-1})	3.5	4.6	2.7
potential ROS forming components				
	NO$_3$ (µM)	< 0.08	< 0.08	< 0.08
	Mn (µM)	0.15	0.33	0.29
	Fe (µM)	16	21	38

Although the light absorption (250-700 nm, Figure 6.2) was quite similar in the three water samples, KSN showed a systematically higher attenuation of PAR, UVA and

UVB, as reflected by larger slopes of the relationships between the wavelength-specific light attenuation coefficient, $K_d(\lambda)$, and TOC (Figure 6.4). Consequently, K_d values calculated to represent 10 mg TOC L^{-1} were the highest for the KSN sample (Table 6.2). The ratios of light attenuation: UVB/PAR, UVA/PAR and UVB/UVA were very similar for ANG and KSN, in fair agreement with the average reported for a set of 65 temperate lakes (Williamson et al., 1996). Slightly less attenuation of PAR at site SKM resulted in higher UVB/PAR and UVA/PAR ratios at this site.

Table 6.2. Wavelength-specific light attenuation coefficients K_d (m^{-1}) measured and calculated for 10 mg TOC L^{-1} at the three sites in this study, as well as values derived from equations representing data sets of 65 temperate lakes (Morris et al., 1995) (PAR = 400-700 nm, UVA = 320-400 nm, UVB = 280-320 nm).

	ANG	KSN	SKM	Morris et al.
PAR	4.2	4.9	**3.2**	2.2
UVA	27	31	26	12 (380 nm)
UVB	58	67	60	28 (320 nm)
UVB/PAR	13.8	13.5	**18.5**	12.5
UVA/PAR	6.5	6.2	**8.2**	5.5
UVB/UVA	2.1	2.2	2.3	2.3

6.5.2 MeHg photodegradation in water samples by sunlight

Dark control samples showed no degradation of MeHg (Figure 6.5), demonstrating that the degradation was entirely caused by the action of light. At site KSN, having the highest concentration of ambient MeHg (0.7 ng L^{-1}) of the three sites, k_{pd} values determined from spiked Me^{198}Hg and ambient MeHg were not significantly different (Figure 6.6). This agrees with a previous study using a similar isotope addition methodology (Lehnherr & Louis, 2009), suggesting that isotope labelled MeHg tracers are expected to quantitatively reflect photodegradation of ambient MeHg. At sites ANG and SKM concentrations of ambient MeHg were too low to get reproducible results.
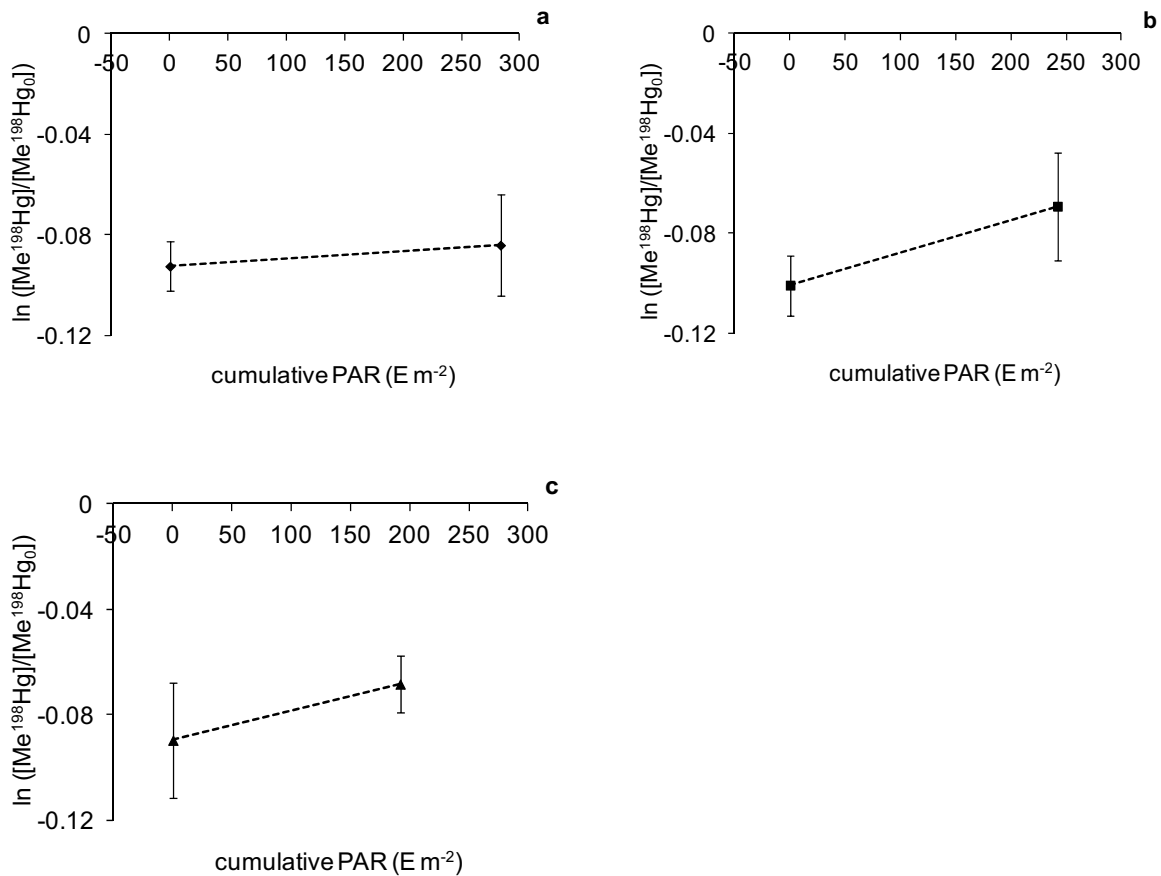
Figure 6.5. Relationships between ln([MeHg]/[MeHg₀]) and cumulative photon flux of PAR for dark controls in experiment #1. Error bars denote ±SD for triplicates. (a) ANG, (b) KSN, (c) SKM.
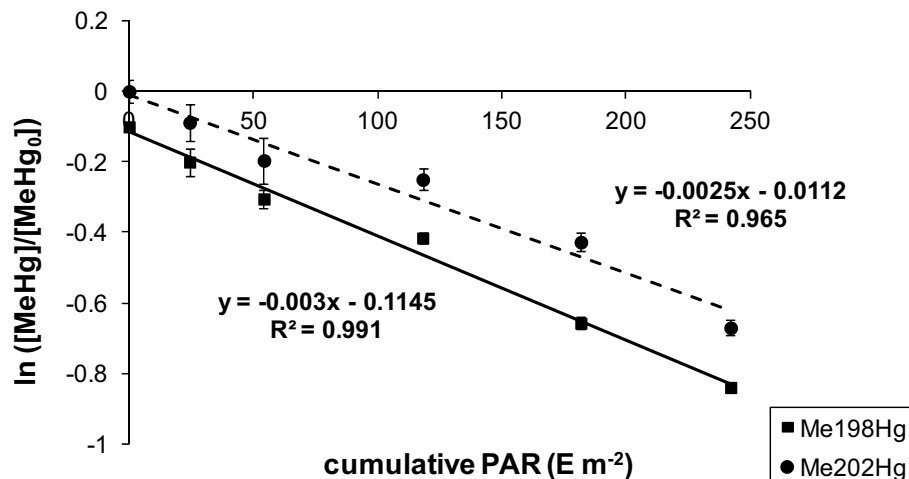
Figure 6.6. Relationships between $ln([MeHg]/[MeHg_0])$ and cumulative PAR photon flux for ambient MeHg ($Me^{202}Hg$) and $Me^{198}Hg$ (added isotope tracer) in original water from site KSN subjected to natural sunlight (experiment #1). Error bars denote ±SD for triplicates. Cumulative PAR was corrected for attenuation by FEP and DOM. The initial MeHg concentration was 0.7 and 0.5 ng L^{-1} for ambient MeHg and for $Me^{198}Hg$, respectively.

First-order rate constants k_{pd} (d^{-1}) determined from the relationship between -ln ([Me^{198}Hg]/[Me^{198}Hg$_0$]) and time of sunlight exposure decreased in the order ANG > KSN > SKM (0.075, 0.048, 0.031 d^{-1}) (Table 6.3). As pointed out previously, first-order rate constants determined as a function of exposure time are not very useful for a comparison of results from different studies (Lehnherr & Louis, 2009; Black et al., 2012). This is because environmental conditions such as sun angle (time of day, latitude, season), temperature, air moisture and cloud cover varies and therefore the quantity of light is not proportional to time. Thus, first-order rate constants determined as a function of cumulative photon flux (E m^{-2}) are preferred.

Table 6.3. Photodemethylation first-order rate constants (k_{pd}) determined in the original water samples (experiment #1) at the three sites: Dystrophic lake (ANG), dystrophic lake – wetland (KSN), riparian wetland (SKM). Errors denote 95% confidence intervals (n=18). The chemical composition of the three waters is given in Table 6.1.

First-order constant	ANG	KSN	SKM
[a]k_{pd} (d^{-1})	0.075 ± 0.007	0.048 ± 0.004	0.031 ± 0.004
R^2	0.981	0.986	0.966
[b]k_{pd} (m^2 E^{-1})	0.0052 ± 0.0007	0.0033 ± 0.0004	0.0021 ± 0.0005
R^2	0.992	0.991	0.971
[c]k_{pd} (m^2 E^{-1})	0.0041 ± 0.0005	0.0030 ± 0.0004	0.0023 ± 0.0006
R^2	0.992	0.991	0.971
[d]$k_{pd\ Full\ Spectrum}$ (m^2 E^{-1})	0.0040 ± 0.0002	0.0029 ± 0.0002	0.0023 ± 0.0003
R^2	0.989	0.986	0.952

Constants were determined from the slope of the relationship between -ln ([Me^{198}Hg]/[Me^{198}Hg$_0$] and: [a]time of exposure to solar radiation in days, [b]cumulative incident PAR photon flux (E m^{-2}) of solar radiation corrected for FEP but not for actinic effects and light attenuation by DOM, [c]cumulative PAR$_{IN}$ photon flux (E m^{-2}) corrected for light attenuation by FEP and DOM, [d]cumulative 280-700 nm spectrum photon flux (E m^{-2}) corrected for wavelength-specific light attenuation by FEP and DOM as determined by Equation (6.2).

To enable a comparison with previous studies, photodegradation data were first related to incident cumulative photon flux of PAR (E m^{-2}) corrected for the attenuation by the bottles (FEP). As reported in Table 6.3, k_{pd} values determined in this way decreased in the order ANG > KSN > SKM (0.0052, 0.0033 and 0.0021 m^2 E^{-1},

respectively). These values are on the same order of magnitude as values determined the same way in boreal lakes: 0.0044 $m^2 E^{-1}$ (12.8 mg DOC L^{-1}) (Hines & Brezonik, 2007), and tundra wetland ponds: 0.0032-0.0036 (8-13 mg DOC L^{-1}) (Lehnherr et al., 2012).

To make the comparison of k_{pd} values among the three waters more relevant, light attenuation by DOM was corrected for. In a first step we used the photon flux measured as PAR inside the bottles (i.e. data corrected for attenuation of PAR by FEP and DOM), resulting in a k_{pd} of 0.0041, 0.0030 and 0.0023 $m^2 E^{-1}$ for ANG, KSN and SKM, respectively (Table 6.3). In the last step also the photon flux of UVA and UVB was considered, after correction for the wavelength-specific attenuation by FEP and DOM. The $k_{pd\ Full\ Spectrum}$ constant was determined as a function of the cumulative full spectrum photon flux (Equation 6.2), as illustrated by Figure 6.7 A. The value on this constant: 0.0040, 0.0029 and 0.0023 $m^2 E^{-1}$ for ANG, KSN and SKM, respectively, did not differ much from constants considering the transmission of PAR alone. The reason is the high concentrations of DOM in all three water samples, attenuating most of UVA and practically all of the UVB radiation.

We may compare values of $k_{pd\ Full\ Spectrum}$ for our three waters with data recalculated by Black and co-workers (2012), from boreal and tundra lakes, to yield first-order rate constants of ~0.005 $m^2 E^{-1}$ (for 4.0 and 15.6 mg DOC L^{-1}) (Hammerschmidt et al., 2006) and ~0.01 $m^2 E^{-1}$ (for 11.0 mg DOC L^{-1}) (Hines & Brezonik, 2007), respectively, and with coastal wetlands and sea water having constants of 0.0099 $m^2 E^{-1}$ (1.5–11.3 mg DOC L^{-1}) and 0.0032 $m^2 E^{-1}$, respectively (Black et al., 2012). These k_{pd} constants were expressed as a function of cumulative incident (330-700 nm) photon fluxes corrected for light attenuation by FEP and actinic scattering effects (applying a factor of 2.2 times incident light) in reaction bottles. It should, however, be noted that because the photon flux was not corrected for light attenuation by DOM and because the DOM concentration varied substantially among sites, the comparison of these k_{pd} constants (with each other and with those in this study) is not made on the same basis.
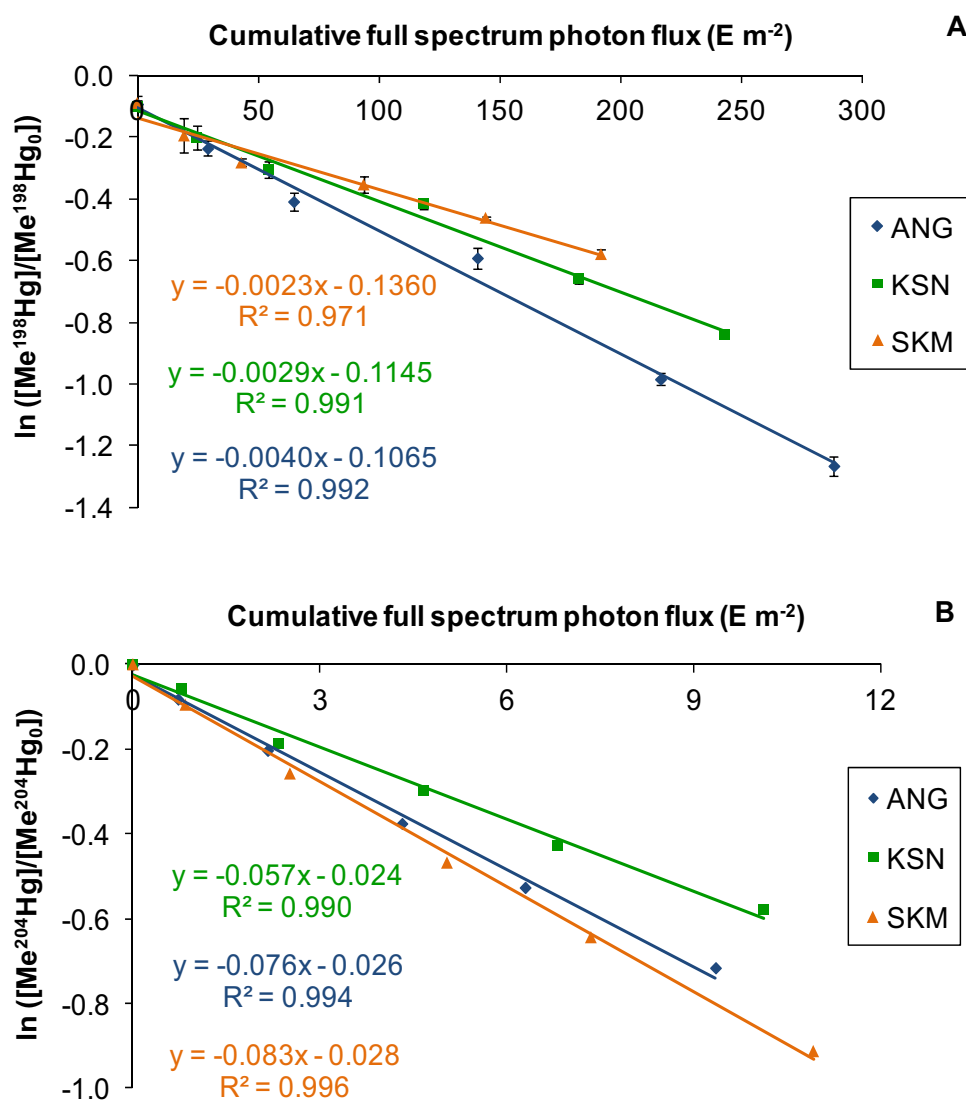
Figure 6.7. Relationships between ln([MeHg]/[MeHg$_0$]) and cumulative full spectrum photon flux corrected for wavelength-specific light attenuation by FEP and DOM. The $k_{pd\ Full\ Spectrum}$ (m^2 E^{-1}) was determined as the negative of the slope of the linear relationship. Data from experiment #1 (A), and experiment #2 (B) determined at the smallest MeHg/RSH ratio (Table 4). The order of the equations follows the order of the regression lines.

6.5.3 Determination of wavelength-specific photodegradation rate constants

Although the $k_{pd\ Full\ Spectrum}$ cover the total flux of photons in the spectral range 280-700 nm (corrected for attenuation by DOM), light of different wavelengths are equally weighed when it comes to the effect on MeHg degradation. This is obviously not correct since we know that UV light is much more potent to degrade MeHg than PAR

(Lehnherr & Louis, 2009). Therefore, to account for differences in the efficiency of MeHg degradation by PAR, UVA, and UVB, we determined rate constants for each of these three spectral regions. It should be noted that the degradation of MeHg can be expected to vary also with wavelength within each of these three light categories, and that the degradation (as well as the attenuation by FEP and DOM) therefore depends on the spectral composition of the light source within the three spectral ranges.

We determined first-order MeHg photodegradation rate constants: $k_{pd\ PAR}$, $k_{pd\ UVA}$ and $k_{pd\ UVB}$, which were corrected for wavelength-specific attenuation by FEP and DOM, using an iterative calculation procedure. Equations (6.3)-(6.5) were solved with values on $k_{pd\ Full\ Spectrum}$ determined in exp #1 and at the lowest MeHg to TOC ratio in exp #2. The lowest MeHg to RSH ratio was used in the calculations to be sure that MeHg was complexed by organic thiol groups (see discussion below in section 6.5.4). It was assumed that if the average photon flux of PAR, UVA and UVB, after correction for light attenuation by DOM, could be calculated, the values of $k_{pd\ PAR}$, $k_{pd\ UVA}$ and $k_{pd\ UVB}$ would be the same for water samples from a specific site involved in exp #1 and #2. The fact that the model converged to relatively small errors (merit-of-fit) for all three sites and for both experiments (Table 6.4), supports this assumption.

Table 6.4. Wavelength-specific first-order rate constants for MeHg photodegradation in water from the dystrophic lake (ANG), dystrophic lake–wetland (KSN), and riparian wetland (SKM).

		$k_{pd\ Full\ Spectrum}$	$k_{pd\ PAR}$	$k_{pd\ UVA}$	$k_{pd\ UVB}$	merit-of-fit[a]
ANG	exp#1	0.0040 ± 0.0001	0.0023 ± 0.00021	0.10 ± 0.024	7.1 ± 1.3	0.003
	exp#2	0.076 ± 0.0029	0.0023 ± 0.00021	0.10 ± 0.024	7.1 ± 1.3	0.001
KSN	exp#1	0.0029 ± 0.00009	0.0022 ± 0.00020	0.095 ± 0.023	6.8 ± 1.3	0.008
	exp#2	0.057 ± 0.0029	0.0022 ± 0.00020	0.095 ± 0.023	6.8 ± 1.3	0.013
SKM	exp#1	0.0023 ± 0.0001	0.0025 ± 0.00022	0.11 ± 0.026	7.8 ± 1.5	0.007
	exp#2	0.083 ± 0.0025	0.0025 ± 0.00022	0.11 ± 0.026	7.8 ± 1.5	0.012
					overall merit-of-fit[b]	0.0084

Values of $k_{pd\ PAR}$, $k_{pd\ UVA}$ and $k_{pd\ UVB}$ (m^2 E^{-1}) were calculated from an iterative procedure using equations (3), (4) and (5). Errors for the $k_{pd\ Full\ Spectrum}$ and calculated wavelength-specific k_{pd} values are reported as ±SE. The RSE of the k_{pd} values were estimated to be ±9%, ±24% and ±19% for $k_{pd\ PAR}$, $k_{pd\ UVA}$ and $k_{pd\ UVB}$, respectively.
[a]calculated as $(k_{pd\ Full\ Spectrum\ measured} - k_{pd\ Full\ Spectrum\ modelled})^2 / k_{pd\ Full\ Spectrum\ measured}^2$
[b]calculated as $\Sigma(k_{pd\ Full\ Spectrum\ measured} - k_{pd\ Full\ Spectrum\ modeled})^2 / \Sigma k_{pd\ Full\ Spectrum\ measured}^2$

In Table 6.4, data on $k_{pd\ PAR}$, $k_{pd\ UVA}$ and $k_{pd\ UVB}$ are reported. The three constants show a range of 0.0022-0.0025 $m^2\ E^{-1}$, 0.095-0.11 $m^2\ E^{-1}$ and 6.8-7.8 $m^2\ E^{-1}$, respectively, for the three sites. As noted, when the wavelength dependent light attenuation by FEP and DOM, as well as the wavelength-specific effect on MeHg degradation, are taken into full consideration, only small differences in the determined rate constants remained among the three sites. Considering an estimated RSE of ±9%, 24% and 19% of $k_{pd\ PAR}$, $k_{pd\ UVA}$ and $k_{pd\ UVB}$, respectively, it can be concluded that the wavelength-specific constants were indistinguishable for the three sites, despite differences in environmental settings and quantity and quality of DOM. Average values (±SE) calculated for the lake-wetland gradient (based on values from all three sites) were 0.0023 ± 0.0002, 0.10 ± 0.024 and 7.2 ± 1.3 $m^2\ E^{-1}$ for $k_{pd\ PAR}$, $k_{pd\ UVA}$ and $k_{pd\ UVB}$, respectively, resulting in a relative ratio of 1:43:3100 for the three constants.

This is the first time photodegradation rate constants have been determined separately for PAR, UVA and UVB, after taking into account wavelength-specific light attenuation by FEP and DOM. Previously reported constants have only considered the light attenuation by FEP, and are therefore site specific. For a water sample from a coastal wetland having 6.0 mg DOC L^{-1}, Black et al. (2012) reported wavelength-specific k_{pds} of 0.0025 $m^2\ E^{-1}$ for PAR, 0.092 $E^{-1}\ m^2$ for UVA (320-400 nm), 0.99 $E^{-1}\ m^2$ for UVB (290-320 nm). This corresponds to a relative ratio of 1:37:400 for PAR:UVA:UVB. These constants were not corrected for light attenuation by DOM. Such a correction would not change the value of the $k_{pd\ PAR}$, notably, whereas a significant attenuation of UV radiation would result in increased rate constants for this spectral range. A simple calculation using the UVA and UVB attenuation in our water samples suggest that about 55% of UVA and 85% of UVB would be attenuated by 6 mg DOC L^{-1}. This suggests that the k_{pd} for UVB would roughly be on the order of six times larger than the one reported, thus not too far away from our estimate. Black and co-workers determined the value of $k_{pd\ UVB}$ in sunlight with a small contribution from UVB (~0.5% of total photon flux). The fact that the UVB was indirectly extrapolated, and simply because of the difficulty of properly determining such a relatively small UVB photon flux, makes the $k_{pd\ UVB}$ value be more uncertain than $k_{pd\ PAR}$ and $k_{pd\ UVA}$. In this study, exp #2 provided a well-defined source with a significant UVB contribution, making the value

of the constant more robust. Similar to Black and co-workers, Lehnherr and St. Louis (2009) used combinations of UVA and UVB absorbing film to determine wavelength dependent constants. They reported a relative ratio of 1:10:3 for k_{pd} of PAR, UVA and UVB. In addition to not being corrected for light attenuation by DOM, these constants were calculated as a function of cumulative incident PAR, making the $k_{pd\ UVA}$ and $k_{pd\ UVB}$ much smaller than if determined as a function of UVA and UVB photon flux. Because the UVA and UVB composition of light was not reported, no recalculation can be done to enable a comparison with the results of this study.

6.5.4   The influence of the MeHg to RSH ratio and radical formation

In Table 6.5 values on $k_{pd\ Full\ Spectrum}$ can be compared at different MeHg to RSH molar ratios. As further illustrated by the linear regressions in Figure 6.8, the $k_{pd\ Full\ Spectrum}$ values are quite similar within sites at the three lowest MeHg to RSH ratios (0.0041-1.5). At sites KSN and SKM the constants were not significantly different (p > 0.1), whereas at site ANG values on $k_{pd\ Full\ Spectrum}$ determined at the MeHg to RSH molar ratios of 0.0041, 0.042 and 0.30 (0.076, 0.0064 and 0.0055 $m^2\ E^{-1}$) all were significantly different from each other (p < 0.001; Tukey's multiple comparison test). Thus, with the exception of ANG, values on $k_{pd\ Full\ Spectrum}$ showed no systematic pattern with the MeHg to RSH ratio for the three smallest MeHg to RSH ratios, despite a variation of the latter by about 2 orders of magnitude.

When the MeHg to RSH molar ratio was increased to reach values substantially above one (4.5–23, Table 6.5, Figure 6.8), there was a dramatic decrease in $k_{pd\ Full\ Spectrum}$ that was highly significant (p < 0.0001) at all three sites. We interpret this observation to be a consequence of MeHg bonding mainly to O and N moieties at the highest MeHg to RSH molar ratio (Qian et al., 2002). Thus, in line with results reported by Zhang and Hsu-Kim (2010), but without invoking any particular identity and mechanism behind the formation of organic radicals or ROS, we suggest that the strong bond between Hg and S in the H_3CHg-SR complex causes a weakening of the C-Hg bond of the MeHg molecule (Miller, 2007), making it susceptible to cleavage by

ROS. In contrast, the much weaker bond between Hg and O/N when concentrations of MeHg are in large excess of RSH, will have a less catalysing effect on the C-Hg bond cleavage. Because of an uncertainty in the estimate of the concentration of RSH groups of about ±50% in this study (Figure II.2, Annex II), the MeHg to RSH molar ratio of 1.5 in the SKM sample is not significantly different from 1.0.

Table 6.5. First-order MeHg photodegradation rate constants ($k_{pd\ Full\ spectrum}$) determined at four different MeHg (the sum of ambient MeHg and added Me^{204}Hg tracer) to RSH molar ratios in original water diluted in Milli-Q water to yield similar concentrations of TOC at the three sites. Errors denote ±95% confidence intervals (n=6 data points for each linear regression). Data from exp #2.

MeHg (nM)	TOC (mg L^{-1})	RSH (nM)	MeHg/RSH molar ratio	MeHg/spins molar ratio	[a]$k_{pd\ Full\ Spectrum}$ (m^2 E^{-1})
ANG					
676	2.26	150	4.5	139	0.010 ± 0.001
44	2.26	150	0.30	8.8	0.055 ± 0.004
6.2	2.26	150	0.042	1.3	0.064 ± 0.004
0.62	2.26	150	0.0041	0.1	0.076 ± 0.007
KSN					
676	2.45	110	6.1	198	0.019 ± 0.003
44	2.45	110	0.40	12.6	0.060 ± 0.005
6.3	2.45	110	0.057	1.8	0.049 ± 0.006
0.64	2.45	110	0.0058	0.2	0.057 ± 0.007
SKM					
677	2.89	30	23	256	0.012 ± 0.004
44	2.89	30	1.5	16.3	0.088 ± 0.009
6.4	2.89	30	0.21	2.4	0.096 ± 0.013
0.62	2.89	30	0.021	0.2	0.083 ± 0.006

[a]constant determined as the slope of the relationship between –ln ([Me^{204}Hg]/[Me^{204}Hg$_0$] and cumulative full spectrum irradiance corrected for light attenuation by FEP and DOM, as calculated by Equation (6.2).
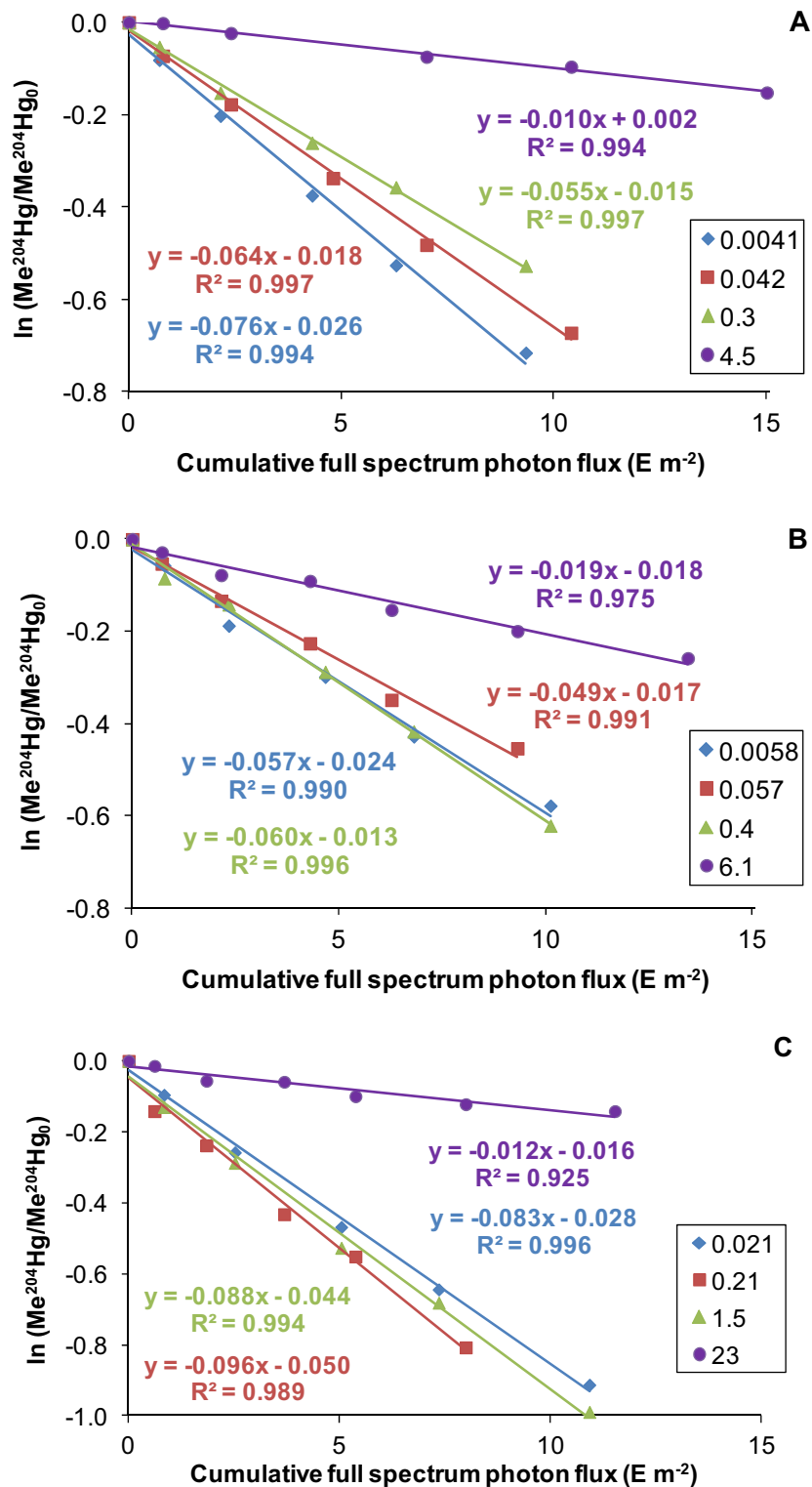
Figure 6.8. MeHg photodegradation by artificial light (experiment #2), as illustrated by relationships between ln ([$Me^{204}Hg$]/[$Me^{204}Hg_0$]) and cumulative full spectrum (PAR+UVA+UVB) photon flux at varying MeHg to RSH molar ratios (in legends) for water from site ANG (A), KSN (B) and SKM (C). The cumulative full spectrum photon flux was corrected for light attenuation by FEP and DOM.

The MeHg to organic radical spin molar ratio reported in Table 6.5 suggests that the added MeHg isotope was in excess of the concentration of organic radicals, except at the lowest MeHg to TOC ratio. However, because light absorbing chromophoric groups in dissolved organic matter (CDOM), and possibly other ROS precursors, were continuously sensitised and excited by radiation in the experiments, a "steady-state" concentration of organic radicals and ROS could be expected to build up in our experiments.

There is currently a lack of consensus regarding the mechanisms involved in the photolysis of MeHg in surface waters, and most likely a range of different organic radicals and ROS may be involved. Our general finding, in line with two recent studies (Lehnherr & Louis, 2009; Black et al., 2012), that MeHg degradation in presence of significant DOM is highly wavelength dependent (more so if the DOM light attenuation is accounted for), may point at the importance of CDOM as the primary process of radical formation. EPR studies of aquatic organic substances suggest that different types of organic radicals and ROS are formed at different spectral ranges. For quinoid type of moieties, radical formation mainly takes place at 280-340 nm, with maximum in the UVB range (Polewski et al., 2005). In this range CDOM have been shown to produce the ·OH radical (Vaughan & Blough, 1998). Given the significant concentrations of Fe in our three studied waters, also the photo-Fenton reaction, showing a maximum in the 300-320 nm spectral range (White et al., 2003), is likely to contribute to ·OH formation. In presence of DOM, Fe(III) complexed by DOM is photo-reduced to Fe(II) and subsequently reacts with hydrogen peroxide mainly formed by the action of CDOM (Southworth & Voelker, 2003; Karlsson & Persson, 2012). Obviously, the strong complexation of Fe(III) to DOM in these types of humic waters, which has been shown to almost completely suppress the hydrolysis of Fe(III) (Karlsson & Persson, 2012), is not sufficient to inhibit the photo-Fenton reaction. On the contrary, the coexistence of DOM and Fe likely enhance the formation of the very reactive ·OH (Vaughan & Blough, 1998; Southworth & Voelker, 2003; White et al., 2003). Complementary to ·OH formation, the production of hydrogen peroxide and $^1O_2$ by the action of CDOM is important also in the visual spectral range (Zepp et al., 1985; Southworth & Voelker, 2003).

Dioxygen was not measured in these experiments. In presence of bacteria and relatively high concentrations of DOM it cannot be excluded that dissolved O_2 was partly consumed. However, because of relatively small differences in organic and hydroxyl radical formation in presence of DOM and Fe under aerobic and anaerobic conditions (Vaughan & Blough, 1998; Southworth & Voelker, 2003; White et al., 2003; Polewski et al., 2005) the possible consumption of dioxygen is not expected to affect the MeHg degradation in our experiments.

Taken together, it may be suggested that the spectral dependence seen in the photolysis of MeHg is primarily due to a combination of different organic radicals and ROS covering a wide spectral range. The most reactive component (·OH) is produced in the low UVA and UVB ranges, whereas hydrogen peroxide and $^1O_2$ production extends more into the range of visual light. The opposing roles of DOM to both quench and possibly prolong the lifetime of certain ROS may also be a factor behind the wavelength dependent photolysis of MeHg in humic waters.

6.5.5   General discussion

Although much remains to be solved relative to the mechanisms of MeHg photodegradation in humic waters, a major step forward is the derivation of PAR, UVA and UVB specific first-order rate constants. These have in our experiments showed a consistency among different types of waters and waters subjected to dilution. We hypothesize that if the photon fluxes of PAR, UVA and UVB radiation are separately determined and the wavelength-specific light attenuation by DOM is corrected for, the first-order rate constants $k_{pd\ PAR}$, $k_{pd\ UVA}$ and $k_{pd\ UVB}$ can be considered universal, at least in waters dominated by DOM and in which MeHg is complexed by organic thiols. Our hypothesis build on the fact that CDOM gives rise to a complex pattern of wavelength dependent production of organic radicals and ROS, and most importantly, that DOM indirectly controls the photon flux through the attenuation of light. It could be argued that because the rate of MeHg degradation is driven by the photon flux, an increase in the concentration of any constituent giving rise to ROS formation (e.g., nitrate, Fe,

DOM) would contribute to an increased rate of MeHg photolysis. Although this is principally correct, our results (Figure 6.7, the water with the highest DOM level – SKM– shows the lowest photolysis rate) show that the anticipated increase in the rate of ROS formation with increasing concentrations of DOM are effectively counteracted by the effects of light attenuation, and possibly ROS quenching, by DOM. This also suggests that as long as the organic radical and ROS formation by CDOM exceeds ROS production generated by nitrate, Fe and possibly other components; variability in light attenuation and ROS quenching by DOM will control the rate of MeHg degradation and mask the possible influence from other ROS forming processes.

Future studies, extending the range of different types of waters, will show under which conditions this suggestion applies. For such waters, a set of established universal wavelength-specific photodegradation constants would be available for prediction of the rate of MeHg degradation, making additional experimental determinations of the rate of MeHg photodegradation unnecessary. The only input needed would be the wavelength-specific light absorption by DOM and the spectral composition of incident sunlight.

If Hg^0 is the principal product of MeHg photodegradation, as suggested by the literature (Chen et al., 2003), the photodemethylation process would highly contribute to Hg^0 evasion (Sellers et al., 1996; Krabbenhoft et al., 1998; Hammerschmidt & Fitzgerald, 2006b) and therefore, to Hg removal from aquatic ecosystems. On the other hand, the magnitude of the MeHg photodegradation in lakes and wetlands suggest that the reactions of demethylation promoted by sunlight could compete with the bioaccumulation of this species, and therefore inhibit its incorporation into aquatic trophic webs. Ultimately, the finding that photodegradation is an important MeHg removal pathway in lakes and wetlands, had great implications for the understanding of the Hg biogeochemical cycle in freshwater ecosystems. A good example of this is that, until the current moment, many studies on mass balance have probably underestimated methylation rates within the lake since MeHg photodegradation was unknown or not taken into account (Henry et al., 1995). The knowledge about this process can also be useful towards the design of methods to mitigate problems

derived from MeHg. For instance, when an industrial effluent has high a MeHg level, it could be dammed in shallow ponds before being dumped. Incidentally, this treatment may also diminish the concentration of inorganic Hg because of the photoreduction of Hg(II) to Hg^0 (Amyot et al., 1994).

Chapter 7

Study of MeHg photodegradation in freshwaters and its relationship with MeHg bioavailability

7 Study of MeHg photodegradation in freshwaters and its relationship with MeHg bioavailability

7.1 The DGT technique as a monitoring tool to assess the bioavailability of MeHg in water

The uptake of trace metals by aquatic organisms is primarily determined by the labile species able to cross biological membranes. Similarly, the DGT technique is based on the diffusion of labile species across a gel membrane followed by accumulation on an ion-exchange resin. Since the appearance of this technique in 1994, it has been used in numerous monitoring programs as an attempt to characterise the bioavailable fraction of trace metals in river, estuarine and sea water (Stark et al., 2006; Allan et al., 2008; Jordan et al., 2008; Schintu et al., 2008; Divis et al., 2012; Han et al., 2013).

However, in the case of Hg, the DGT technique is still in their first steps of development, and not too many studies on its ability to mimic the bioaccumulation of MeHg by biota have been performed to date. Liu et al. (2012) and Amirbahman et al. (2013) showed that DGT samplers are an effective proxy for assessing the MeHg uptake by rice plants and macroinvertebrates, respectively. Nevertheless, in both cases the DGT units were deployed in sediments to measure the MeHg in pore waters. Only Clarisse et al. (2012) performed a study comparing DGT and organisms uptake in water. The study demonstrated that DGT results reasonably predict MeHg uptake by clams from the aqueous phase and provide the basis for application of the DGT device as a surrogate for sentinel organism to monitor bioavailable MeHg. In addition, the reproducibility of DGT was higher than for clams (7% and 38%, respectively).

Compared to using biological organisms, the DGT technique is more reproducible and easier to handle. Only a few DGT units would be required to assess the bioavailability of MeHg, while a larger number of biosentinels would have to be deployed and analyzed to reach the same goal. Additionally, DGT devices do not have an MeHg background and can be deployed nearly anywhere, as long as there is water.

Thus, DGT appears to be a relatively inexpensive and promising monitoring tool for the assessment of bioavailability (i.e. measurement of the labile fraction of dissolved) of MeHg (Amirbahman et al. 2013; Clarisse et al 2012) in the environment, and thereby to describe the first step of MeHg biomagnification.

7.2   Objective of the study

The ultimate objective of the work enclosed in this chapter was to study the photodegradation of dissolved and colloidal MeHg in different natural and artificial freshwaters and the possible relationship between this process and MeHg bioavailability. MeHg photodegradation rates in six different types of freshwater with different DOC content and characteristics were obtained, and the labile fraction of MeHg in those same waters was measured by the DGT technique, in order to assess bioavailability.

7.3   Description of the study waters

Six different types of water were used: MilliQ water (NaCl 0.01M) (MQW), MilliQ water (NaCl 0.01M) with organic matter (10 mg OC L^{-1}) from a Nordic Reservoir (IHSS, 1R108N) (MQO), water from the Ebro River at Flix reservoir –Catalonia, Spain– (FLX) and water taken at three sites along a freshwater wetland–lake gradient in Boreal Sweden.

FLX water was collected at the Flix reservoir (41° 14' 01", 0° 32' 41") on the course of the Ebro River. The presence of Hg in the study area is attributable to emissions from an electrochemical factory (Montuori et al., 2006; Cotin et al., 2012) that has been producing chlorinated solvents for decades employing Hg electrodes. Therefore, there is a high motivation to study photodegradation processes and Hg bioavailability in Flix reservoir, in comparison with those Boreal Swedish waters, that have been thoroughly studied in a previous work (Chapter 6).

The three Swedish sites were a dystrophic lake –Ängessjön (ANG)–, a mixed *Sphagnum/Carex* peatland-dystrophic lake with approximately 30% open water – Kroksjön (KSN)–, and a riparian zone wetland created by artificial damming of a small stream –Stor-Kälsmyran (SKM)–. These three sites have been previously described in section 6.3.

7.4   Experimental methodology

7.4.1   Materials and equipments

All experiments were conducted in acid-washed 500 mL wide-mouth Teflon® FEP bottles (Thermo scientific-Nalgene, Rochester, NY, USA) (see the acid cleaning procedure in section 6.4.1). MeHg photodegradation in water samples was performed using SUNTEST CPS flatbed xenon exposure system from Atlas (Chicago, USA). It is equipped with 1500B NrB4 Xenon lamp that was operated at the potential of 250 W m^{-2} whose UV-Vis spectra is close to sunlight. A Varian Cary® 300 UV-visible spectrophotometer (Varian, CA, USA) was used to measure the DOC in the solutions. The system was calibrated for the range from 1 to 100 mg L^{-1}, and the absorbance was measured at 254 nm (Mattson et al., 1974). The pH in the solutions and samples was measured using a GLP 22 CRISON pHmeter (Barcelona, Spain). For the MeHg bioavailability assessment, the in-house manufactured P-DGT devices (described in section 4.2.1.1) and an incubator shaker Innova 40R (New Brunswick Scientific, Edison, NJ, USA) were used. The rest of the reagents and equipments used for this work are described in section 4.2.4.1.

7.4.2   Analytical determination of MeHg

The analytical methodology to determine MeHg both in the DGT resin gel discs and in the water samples is described in section 4.2.4.2.

7.4.3 Experiment to study MeHg photodegradation

Two 500 mL FEP bottles were filled with every water type; one replicate being used for the photodegradation process and the other as the dark control. In the case of the Swedish waters, since they had very high DOC levels, they were diluted to roughly 10 mg L^{-1} of DOC. Every bottle was filled to the top, added 250 pg of MeHgCl (as Hg) solution in acetone, shaken vigorously, wrapped with aluminium foil and left to equilibrate overnight at room temperature. The following morning, the six bottles were unwrapped and placed in the SUNTEST (Figure 7.1 A) for 7.5 hours. Before light exposure (0 h) and at different time intervals along the experiment (i.e. 0.5, 1.5, 3.5 and 7.5 h), pH, conductivity and DOC were determined. Moreover, at every interval of time, 2 mL of water were taken and preserved from light in an aluminium foil-wrapped glass vial, acidified to 0.4% with HCl, added 20 μL of EtHgCl (230 pg mL^{-1}) as internal standard and stored at 4 °C until analysis. At the end of photodegradation experiment, the bottle was double wrapped with aluminium foil and kept in the fridge until the bioavailability experiment started. The six dark controls followed the same procedure as described above, except from the fact that the bottles were double wrapped with aluminium foil also when placed inside the SUNTEST equipment and aliquots were taken only at three time intervals (i.e. 0, 3.5 and 7.5 h).

7.4.4 Experiment to study MeHg lability by means of the DGT technique

Two P-DGT units were introduced in each of the bottles (Figure 7.1 B), that previously underwent the MeHg photodegradation experiment (n = 12, six dark controls and six exposed to light). The bottles, which were double wrapped with aluminium foil, were placed in an incubator shaker at 25 °C and 30 rpm (Figure 7.1 C). After 23 hours, the DGT units were retrieved and stored in the fridge (4 °C). In order to monitor the MeHg concentration in the water throughout the experiment, 2 mL aliquots of water were taken from each bottle before and after DGT deployment.
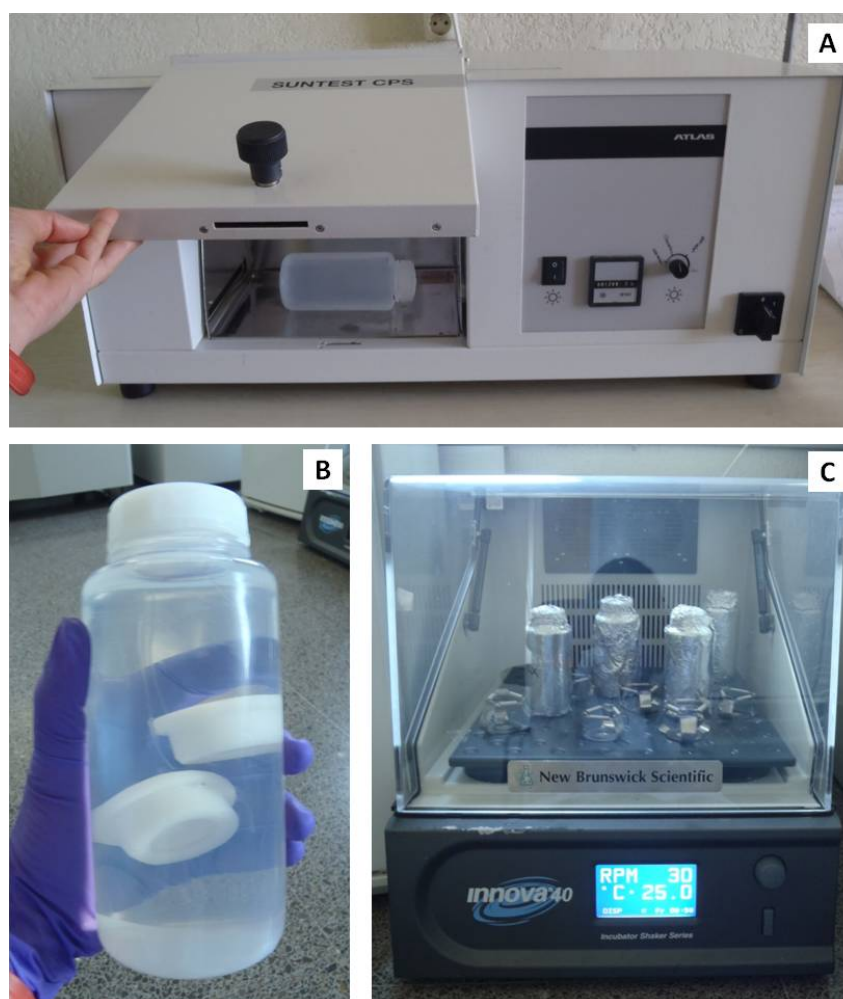
Figure 7.1. Equipment used in the experiments: (A) SUNTEST CPS flatbed xenon exposure system, (B) FEP Teflon bottle with water and two DGT units inside, and (C) aluminium foil wrapped bottles in the incubator.

7.5   Results and discussion

7.5.1   MeHg photodegradation in water samples using a Xenon lamp

As shown in Figure 7.2, for all the six types of water, the pH remained fairly stable along the experiment. However, the DOC concentration decreased slightly due to the DOM photolysis (Mopper et al., 1991; Hongve, 1994).
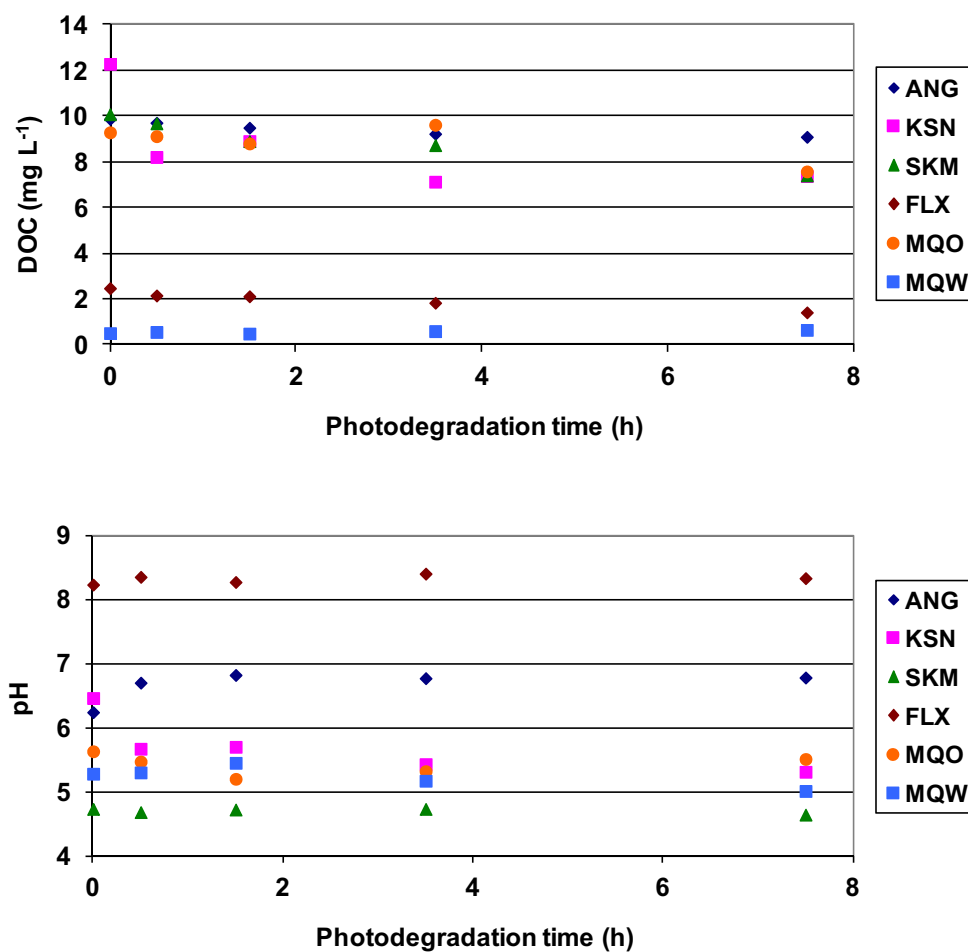
Figure 7.2. Changes in DOC and pH in the water samples exposed to the light during the course of the MeHg photodegradation experiment. The study waters (in the legend) are described in section 7.3.

In Figure 7.3, it can be observed that for all the waters the MeHg concentration diminished when the bottles were exposed to the Xenon lamp. On the contrary, the dark controls presented a constant MeHg level throughout the experiment.

The six aqueous matrices used in this experiment covered a wide range of pH (4.7-8.3). However, as reported previously, pH does not significantly affect the MeHg photodegradation rate constant (k_{pd}) (Sellers et al., 1996; Chen et al., 2003). Concerning the electrical conductivity, Chen et al. (2003) and Zepp et al. (1987) observed an enhancement in MeHg photodegradation rate with increasing chloride concentration, and proposed that it was due to the aqueous oxidation of chloride by hydroxyl radicals, producing chlorine radicals which may break the Hg-C bond. Taking

these findings into consideration, the higher k_{pd} in FLX water (0.254 h^{-1}), which is significantly different (t-student, α = 0.05) from the rest of k_{pd}s (see Table 7.1), might be explained by its high electrical conductivity (1010 µS cm^{-1}) in comparison with the Swedish waters (ANG, KSN and SKM, 11-40 µS cm^{-1}).
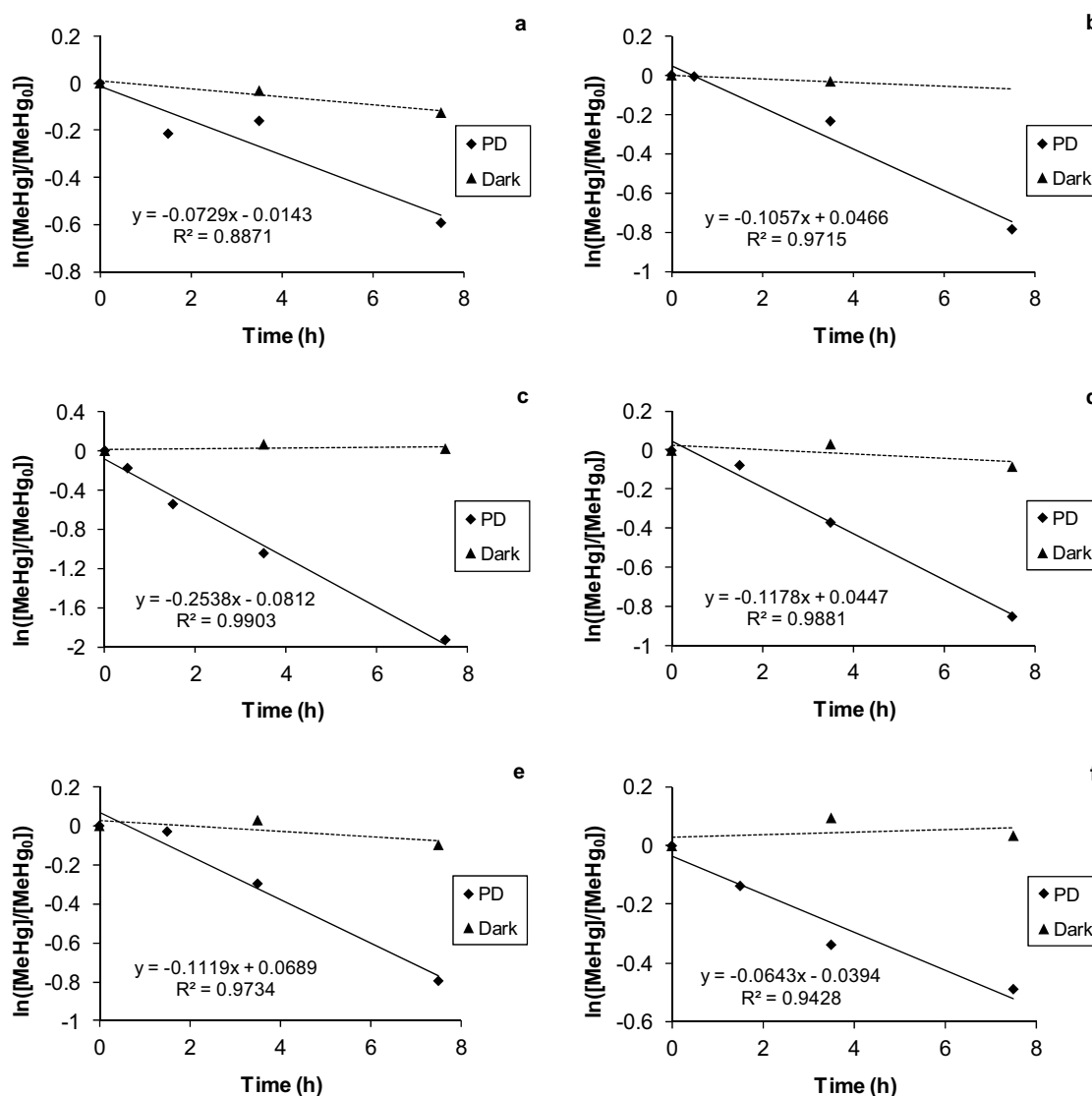
Figure 7.3. Relationships between ln([MeHg]/[MeHg$_0$]) and light exposure time (hours). The k_{pd} $_{Full\ Spectrum}$ (h^{-1}) was determined as the negative of the slope of the linear relationship. (a) MilliQ water (NaCl 0.01M) (MQW), (b) MilliQ water (NaCl 0.01M) with organic matter (MQO), (c) water from the Ebro River (FLX), (d) water from Ängessjön lake (ANG), (e) water from Kroksjön peatland-lake (KSN) and water from (f) Stor-Kälsmyran riparian zone wetland (SKM).

However, MQO and MQW waters, even having also a high conductivity (1150 µS cm^{-1}), presented lower k_{pd}s (0.106 and 0.073 h^{-1}, respectively). The poor linear lineariy

(R^2 = 0.89) in the photodegradation rate for MQW may likely be to the lack of organic matter, which has been shown to contribute to MeHg photodecomposition by means of oxygen reactive intermediates (·OH and $^1O_2$) (Alegria et al., 1997; Chen et al., 2003; Zhang & Hsu-Kim, 2010a) generated by the interaction of sunlight with DOM. Unlike previous works which suggested that MeHg photodegradation hardly occurs in the absence of DOM (Chen et al., 2003; Zhang & Hsu-Kim, 2010b), it has been recently reported that MeHg can be degraded by sunlight when is dissolved in plain ultra-pure water or in ultra-pure water in the presence of chlorides (Sun et al., 2013). In the same manner, we could observe a slight photodecomposition of MeHg even in our Milli-Q water with NaCl in solution (Figure 7.3 a, k_{pd} = 0.073 h^{-1}).

Table 7.1. Water quality and MeHg photodegradation kinetic parameters. Initial DOC concentration, average pH along the experiment, conductivity, MeHg photodegradation rate constant (k_{pd}) and the correlation coefficient of the regression line of the first order kinetics.

Water type	[DOC] (mg L^{-1})	pH	Cond. (µS cm^{-1})	k_{pd} (h^{-1})	R^2
ANG	9.9	6.7	40	0.118	0.99
KSN	12.3	5.7	11	0.112	0.97
SKM	10.1	4.7	12	0.064	0.94
FLX	2.1	8.3	1010	0.254	0.99
MQO	9.3	5.4	1150	0.106	0.97
MQW	≤ 0.010	5.2	1150	0.073	0.88

On the other hand, the lower k_{pd} found at MQO in comparison with FLX (Table 7.1) could be attributed to a higher DOM concentration than that measured at FLX (9.3 versus 2.1 mg OC L^{-1}), which attenuates more intensely the light penetrating in the bottle. This might confirm that unless the MeHg degradation reaction is not limited by the generation of free radicals or by the complexation of MeHg by thiol groups, the main effect of DOM on MeHg photodegradation seems to be light attenuation (section 6.5.5). To better explain the difference in the k_{pd} between FLX and MQO waters, the term "photodegradation yield" (*PDY*) has been created to be used in this concern. It is

not any real magnitude but just the result of a calculation made to give an estimate of relative amount of MeHg photodegraded in the middle of the bottle. The overall MeHg *PDY* is the addition of the *PDY* produced by UVB, UVA and visible light (Equation 7.1). For every of the three wavelength ranges, the *PDY* is calculated as the product (Equation 7.2) of the fraction of downwelling irradiance in the middle of the bottle (*fd*), the fraction of participation of that wavelength range in the photodegradation process (*fp*) and the fraction of that wavelength range in the spectrum of the light source used for the experiment (*fs*). The *fd*s were calculated using the diffuse attenuation coefficients (K_d) defined by Morris et al. (1995) and the downwelling irradiance equation described by Williamson et al. (1996), where *z* is the radius of the bottle (Equation 7.3). The *fp*s were obtained from the ratio $k_{pd\ PAR}$:$k_{pd\ UVA}$:$k_{pd\ UVB}$ (1:43:3100) reported in the section 6.5.3 of this thesis (Equation 7.4). The *fs*s of the Xenon lamp used in the experiment are unknown, but the global spectral distribution of the sunlight provided by the instrument supplier was used instead (0.4%, 5.6% and 50% of UVB, UVA and visible light, respectively) (Equation 7.5).

$$PDY_{overall} = PDY_{vis} + PDY_{UVA} + PDY_{UVB} \qquad (7.1)$$

$$PDY_{vis} = fd_{vis} \times fp_{vis} \times fs_{vis}$$
$$PDY_{UVA} = fd_{UVA} \times fp_{UVA} \times fs_{UVA}$$
$$PDY_{UVB} = fd_{UVB} \times fp_{UVB} \times fs_{UVB} \qquad (7.2)$$

$$fd_{vis} = \exp\,[-(K_{dvis})z)]$$
$$fd_{UVA} = \exp\,[-(K_{dUVA})z)]$$
$$fd_{UVB} = \exp\,[-(K_{dUVB})z)] \qquad (7.3)$$

$$fp_{vis} = \frac{1}{3144}; \quad fp_{UVA} = \frac{43}{3144}; \quad fp_{UVB} = \frac{3100}{3144} \qquad (7.4)$$

$$fs_{vis} = 50\%\ ; \quad fs_{UVA} = 5.6\%; \quad fs_{UVB} = 0.4\% \qquad (7.5)$$

The values of *PDY* were 0.0021 for MQO and 0.0041 for FLX water (Table 7.2), then the ratio PDY_{MQO}:PDY_{FLX} was 1:2.0. This can provide the most likely explanation of the

difference between the k_{pd} of those two waters, since the ratio $k_{pd\text{-}MQO}:k_{pd\text{-}FLX}$ was 1:2.4. Therefore, the main variable affecting the MeHg photodegradation might be the DOC concentration, which plays an important role in the attenuation of the different light wavelengths. Obviously, there were other variables that were not analyzed which could affect the photodecomposition process. Analogous results were obtained among the rest of our waters ($PDY_{ANG}:PDY_{FLX}$ = 1:2.1 vs. $k_{pd\text{-}ANG}:k_{pd\text{-}FLX}$ = 1:2.2; and $PDY_{KSN}:PDY_{FLX}$ = 1:2.7 vs. $k_{pd\text{-}ANG}:k_{pd\text{-}FLX}$ = 1:2.3).

Table 7.2. (a) Fraction of downwelling irradiance reaching the middle of the bottle with water (fd), (b) fraction of participation in the photodegradation process (fp), (c) fraction of contribution in the spectral composition of the lamp (fs) and (d) MeHg PD "quantity" for every light spectral range (UVB, UVA and visible light).

	UVB	UVA	Visible	Total
fd (2.1 mg OC L^{-1})[a]	0.825	0.924	0.982	-
fd (9.3 mg OC L^{-1})[a]	0.362	0.643	0.921	-
fp[b]	0.9860	0.0140	0.0003	-
fs[c]	0.004	0.056	0.500	-
MeHg *PDY* (2.1 mg OC L^{-1})[d]	0.0033	0.0007	0.0002	0.0041
MeHg *PDY* (9.3 mg OC L^{-1})[d]	0.0014	0.0005	0.0001	0.0021

Concerning the statistical comparison (t-student, α = 0.05) of the obtained k_{pd}s, all of them resulted not to be significantly different among each other, except in the case of FLX versus the rest of the waters (p-value ≤ 0.0008), and in the case of ANG versus SKM (p-value = 0.02).

To compare our k_{pd}s with other previously published is not possible since in this study we used a Xenon lamp, which has not been used for MeHg photodecomposition experiments before. Instead, the previously reported k_{pd}s were obtained by using natural sunlight. Moreover, the light spectrum of this lamp is unknown (although it is supposed to reproduce sunlight spectrum, it has a higher proportion of UV light) and

the radiation intensity in the exact location where the exposure to the lamp took place was not possible to measure due to practical reasons. That is another reason why we cannot calculate the cumulative photon flux (neither full spectrum nor wavelength specific) received by the samples during the experiment.

7.5.2   Lability of MeHg in the different types of water

As mentioned before, to accurately determine the labile fraction of Hg in water by DGT, a diffusion coefficient (D) obtained under similar conditions to those in the water in which the DGT units were deployed should be used. However, in this case we studied six different types of water with different characteristics, which makes difficult to have a DGT calibration (i.e. D acquisition) for each of them. Thus, to rigorously compare the lability of MeHg in those waters, we worked with the ratio between the MeHg mass accumulated by one DGT unit (M) and the average MeHg concentration (measured directly) in the deployment water during sampling (C) (Table 7.3). In this manner we did not have to deal with problems derived from the use of the same D for all the different waters.

The results were subjected to a Mann-Whitney test to statistically compare the MeHg lability indicator (M/C) in the water that underwent photodegradation and in the dark control. The significance level was set at $\alpha = 0.05$ and the statistical analysis was performed by using the SPSS 15.0 for Windows software (SPSS Inc., Chicago, IL, USA). The test showed no significant differences between the two treatments in any of the six types of water, therefore we can conclude that the action of sunlight does not affect the lability of MeHg.

Aside from the influence of the solar radiation on MeHg lability, the differences among the six waters can be discussed. The high values of the equilibrium binding constants (log K) for the association of MeHg with thiol-containing compounds or humic substances (12.6-16.9) (Reid & Rabenstein, 1981; Hintelmann et al., 1997b; Amirbahman et al., 2002; Qian et al., 2002) in comparison with the log K of MeHgCl

(5.25) (Schwarze & Schellen, 1965) at similar concentrations to those studied here, indicate that MeHg associates primarily with the thiol groups in the DOM. Thereby, in freshwater systems, when DOM concentration is sufficiently high, the MeHg-DOM complex should be more abundant than MeHgCl. Black et al. (2012) estimated that DOM bounds > 97% of the MeHg at a salinity of 25‰ and DOM concentration of 1.5 mg OC L^{-1} when MeHg concentration was 0.25-1.25 ng L^{-1}. Therefore, under our experimental conditions (salinity of 0.005-0.5‰ and DOM concentration of 2-12 mg OC L^{-1}) the MeHg-DOM binding should also be the predominant, although MeHg concentration was 500 ng L^{-1}. However, changes in the complexation of MeHg by DOM and chloride should be a function of DOM concentration, salinity and pH.

Table 7.3. Water quality parameters, lability and bioavailability information. Initial DOC concentration, average pH along the experiment, conductivity, ratios between the MeHg mass accumulated by one DGT unit (M) and the average MeHg concentration (measured directly) in the deployment water during sampling (C), and percentages of bioavailable MeHg in the dark control and in the water exposed to artificial sunlight.

Water type	[DOC] (mg L^{-1})	pH	Cond. (µS cm^{-1})	M/C (Dark) (cm^3)	M/C (Light) (cm^3)	% Bioav. MeHg (Dark)	% Bioav. MeHg (Light)
ANG	9.9	6.7	40	4.6 ± 0.4	4.8 ± 0.8	52 ± 5	55 ± 9
KSN	12.3	5.7	11	4.4 ± 0.4	5.1 ± 0.2	50 ± 5	58 ± 3
SKM	10.1	4.7	12	8.1 ± 1.7	8.9 ± 0.8	92 ± 20	101 ± 9
FLX	2.1	8.3	1010	6.7 ± 1.0	6.1 ± 0.5	76 ± 11	70 ± 5
MQO	9.3	5.4	1150	8.3 ± 1.5	7.8 ± 2.1	95 ± 17	88 ± 24
MQW	-	5.2	1150	6.9 ± 1.8	7.8 ± 1.0	53 ± 14	60 ± 8

Thereby, the lowest M/C ratios found in ANG (4.6-4.8) and KSN (4.4-5.1) waters (Table 7.3) could be explained by their high DOM concentration (~10 mg DOC L^{-1}) and their low conductivity (40 and 11 µS cm^{-1}, respectively), and hence by the prevalence of MeHg-DOM complexes in the solution. These complexes are bigger in size than the free MeHg ions (MeHg$^+$), what makes them diffuse at a slower rate through the DGT

diffusive layer, and they dissociate with more difficulty within the diffusive gel. Consequently, less amount of MeHg is bound to the thiol groups in the resin gel. A similar phenomenon happens also when working with living organisms. Some authors stated that an increase in DOM concentration leads to a decrease in MeHg bioavailability, as tested in algae, seston and hydropsychids or bacteria (Gorski et al., 2008; Tsui & Finlay, 2011; Luengen et al., 2012; Ndu et al., 2012), as the MeHg-DOM complexes are too large or hydrophilic to pass through the cell membrane. Furthermore, the slightly higher M/C ratio in FLX water (6.1-6.7) could be accounted for following the same behaviour. This water had a lower DOM concentration (2 mg DOC L^{-1}) and a notably higher conductivity (1010 µS cm^{-1}). In this manner, there could be a higher amount of MeHgCl, more easily dissociable. However, the value obtained for SKM water (8.1-8.9) is difficult to explain since its DOM concentration, pH and conductivity are almost equal to KSN (Table 7.3). The only possible explanation is that the quality or type of organic matter affects the lability of the MeHg-DOM complexes, controlling their availability for aquatic organisms, uptake and toxicity.

Concerning MQO and MQW waters, the only difference between them was that MQO had a DOM concentration of 9.3 mg/L and MQW was DOM-free. Although log K is substantially higher for MeHg associated with humic substances than for MeHgCl, MQO presented a similar MeHg lability (7.8-8.3) as MQW (6.9-7.8). Again, we observe as the presence of organic matter seems not to affect MeHg lability significantly, as showed by the similar D_{MeHg^+} and $D_{MeHg-DOM}$ obtained in section 4.3.2.1.

On the other hand, in order to estimate the fraction of MeHg that could be available for biota in all the water types, the following approach was done. The percentage of "bioavailable MeHg" (Table 7.3) was calculated as the quotient between the labile MeHg concentration (measured with DGT) and the average of the MeHg concentration (measured directly in the water before and after DGT deployment). The DGT-labile MeHg concentration was calculated using $D_{MeHg-DOM}$ for all the waters except for MQW, for which D_{MeHg^+} was employed (see section 4.3.2.1). The reason was that all the waters but MQW contained DOM, and MQW was just a solution of NaCl in Milli-Q water. As stated before, the D used for the DGT calculations should be obtained from a

calibration performed in water with similar or identical characteristics to those in the water in which the DGT units were deployed, if an accurate labile (and then, proxy for bioavailable) MeHg concentration determination is desired.

The high percentage of bioavailable MeHg in MQO (88-95%) versus that in MQW (53-60%) might be explained by the fact that DOC may enhance uptake, as Pickhardt and Fisher (2007) suggested. These authors showed that MeHg bioaccumulation in eukaryotic cells was greater in high DOC water. This uptake enhancement could happen through association of DOM with cell surfaces, which may facilitate uptake of Hg species to the cells and/or promote transport by influencing the permeability of the cell membrane (Vigneault et al., 2000; Boullemant et al., 2004). A similar phenomenom might occur in the DGT membrane filter and diffusion gel.

7.5.3 General discussion

Concerning the photodegradation study, it can be concluded that as long as there is organic matter in the solution, which favours the photodegradation process, the k_{pd} is mainly affected by the light attenuation effect by DOM.

On the other hand, the action of sunlight seems not to change the lability of MeHg and therefore, its bioavailability; however, the DOM quality could be the main variable affecting it. Future works should be focused on studying the influence of the type of DOM or humic substances present in the water on the bioavailability of MeHg, since several authors also suggested that DOM composition may determine site-specific bioavailability of MeHg (Gorski et al., 2008; Luengen et al., 2012; Ndu et al., 2012).

No studies on this photodegradation-bioavailability topic have been done to date, so I wanted to make a first approach by performing a simple experiment. These results demonstrated that in the experimental conditions (using a Xenon lamp) there is no direct connection between the two phenomena, but further research should be carried out with natural sunlight. Nevertheless, differences among the different types

of water were observed. This could serve as a first step to continue investigating the influence of different parameters on the availability of the MeHg present in water for living organisms.

PART IV

Chapter 8

Conclusions

8 Conclusions

8.1 Analytical methods

The conclusions of this thesis concerning analytical development of the **DGT technique** are the following:

- The commercial specific-for-Hg DGT devices were proven to effectively measure the concentration of dissolved labile Hg in water under laboratory conditions. However, under environmental conditions, and mainly in eutrophic waters, these samplers did not show a substantial uptake. The reason is their poor performance (tested in laboratory) when there is DOM present in solution. Some other problems were found in the field, such as the presence of biofouling and particulate matter, which clogged the filter.

- 3-mercaptopropyl functionalized silica gel was satisfactorily used as the binding agent in the DGT resin gel for THg measurements (previously, it had been used only for MeHg measurements).

- Polyacrylamide diffusive gel was shown not to compete with the resin for binding Hg(II) ions.

- Both in-house DGT samplers with polyacrylamide (P-DGT) or agarose as a diffusive gel (A-DGT) have been proven to be adequate for measuring the labile fraction of Hg in water. Nevertheless, the best choice to measure THg, considering that polyacrylamide diffusive gel did not accumulate Hg, the uptake rate in the resin gel was the most linear with time and its resin blanks were very low, was the P-DGT. This type of samplers is also considered the most suitable for MeHg determination, due to its higher uptake rate and its higher discrimination ability between MeHg species in solution.

- For the application of the DGT technique to monitor Hg concentration in natural waters, the calibration of the DGT units in the presence of DOM is necessary. Hg-DOM complexes diffuse at a lower rate through the diffusive gel, thus, a diffusion coefficient for these Hg species is needed in order not to underestimate the labile Hg fraction. In this manner, it is crucial to accurately simulate the natural water conditions when calibrating the DGT devices.

- The diffusion coefficient of MeHg obtained in the presence of DOM ($D_{MeHg-DOM}$) was higher than that of Hg(II) ($D_{Hg(II)-DOM}$), which suggests that MeHg-DOM complexes are more labile than Hg(II)-DOM complexes. This fact also shows the importance of calibrating the DGT samplers using the target Hg species.

- The DGT technique was satisfactorily used to measure labile THg and MeHg concentrations in a case study in which Hg removal and methylation in a constructed wetland (CW) pilot scale plant for wastewater treatment were assessed.

8.2 Environmental conclusions

The conclusions with respect to **Hg removal in a CW experimental plant for wastewater treatment** are as following:

- The experimental treatment plant seems to effectively remove the THg present in the wastewater as proven by the 75% removal, as long as there is not Hg saturation of the system. The removal of the DGT-labile THg was 90%, which is a very high efficiency regarding the most worrying fraction of Hg since it is the fraction susceptible to be uptaken by biota.

- The percentage of MeHg removal was 92-96%, whereas the labile MeHg was removed in a lesser extent (66%).

- The Hg removal capacity of this CW design was demonstrated, although several adjustments should be done depending on the Hg load of the influent. For such a high Hg load as the one injected into the treatment line, the dimensions of the CWs should be bigger or the inflow lower to avoid its breakhthorugh. However, with the low Hg loads commonly found in urban wastewater, this CW design could work suitably for long periods of time.

The main conclusions regarding the **MeHg photodegradation** studies are the ones exposed below:

- The MeHg photodegradation rate constant ($k_{pd\ Full\ Spectrum}$) varied significantly among sites, but the wavelength-specific rate constants ($k_{pd\ PAR}$, $k_{pd\ UVA}$ and $k_{pd\ UVB}$) were indistinguishable for the same sites.

- When the MeHg to thiol groups (RSH) molar ratio was increased to reach values substantially above one, there was a dramatic decrease in $k_{pd\ Full\ Spectrum}$. This might be a consequence of MeHg bonding mainly to O and N moieties when MeHg is in excess of RSH. On the contrary, when RSH are in excess, the strong bond between Hg and S in the MeHg-thiol complex causes a weakening effect of the C-Hg bond of the MeHg molecule, making it susceptible to cleavage by ROS.

- Light attenuation and ROS quenching by DOM will control the rate of MeHg degradation and mask the possible influence from other ROS forming processes, as long as organic radical and ROS formation by DOM exceeds ROS production generated by nitrate, Fe and possibly other components.

- $k_{pd\ PAR}$, $k_{pd\ UVA}$ and $k_{pd\ UVB}$, can be considered universal, at least in waters dominated by DOM and in which MeHg is complexed by organic thiols, if

the photon fluxes of PAR, UVA and UVB radiation are separately determined and the wavelength-specific light attenuation by DOM is corrected for.

- The ratio $k_{pd\ PAR}:k_{pd\ UVA}:k_{pd\ UVB}$ was 1:43:3100, showing the much higher MeHg photodegradation power of UVB radiation.

- These wavelength-specific rate constants allow the prediction of the rate of MeHg degradation, making additional experimental determinations of the MeHg photodegradation rate unnecessary. The only input needed would be the wavelength-specific light absorption by DOM and the spectral composition of incident sunlight.

Finally, the major conclusion in reference to the **effect of photodegradation on MeHg lability** is as following:

- The action of sunlight seems not to change the lability of MeHg and therefore, its bioavailability. However, the DOM quality could be the main variable affecting it.

RESUMEN DE LA TESIS EN CASTELLANO

Nuevos puntos de vista sobre el ciclo biogeoquímico del mercurio en aguas continentales. Desarrollo y aplicación de la técnica DGT para evaluación de la biodisponibilidad y estudios de fotodegradación de metilmercurio

Introducción

El **mercurio (Hg)** es un metal pesado caracterizado por ser el único en estado líquido a temperatura y presión ambiente. El Hg es ubicuo y puede aparecer en tres estados de oxidación: mercurio metálico o elemental (Hg^0), mercurio monovalente (Hg(I), cuya principal forma inorgánica es el ión mercurioso: Hg_2^{2+}) y mercurio divalente (Hg(II), principal forma inorgánica: ión mercúrico, Hg^{2+}). Excepto en la atmósfera, donde la mayor parte del Hg es vapor de Hg^0, en el resto de los compartimentos ambientales el Hg se encuentra fundamentalmente como sales inorgánicas ($HgCl_2$, $Hg(OH)_2$, HgS) y formas orgánicas (metilmercurio, $MeHg^+$; dimetilmercurio, Me_2Hg; y en menor medida, etilmercurio, $EtHg^+$; y fenilmercurio, $PhHg^+$) de Hg(II).

El mercurio y su principal mineral, el cinabrio (HgS), son conocidos y usados desde la antigüedad. Ya en el Paleolítico Superior, el bermellón (polvo de cinabrio) se usaba como pigmento rojo en pinturas rupestres. Sin embargo, los usos del Hg se han diversificado enormemente desde entonces y las principales **aplicaciones** de este metal han sido las siguientes: biocida en la industria papelera, en pinturas y en depósitos de semillas, formulaciones fitosanitarias, antiséptico en fármacos y cosméticos, extracción de oro y plata (minería artesanal), producción de disolventes clorados y otros derivados del cloro, catalizador para la síntesis de acetaldehído y acetato de vinilo, componente en termómetros, barómetros, manómetros, lámparas fluorescentes, baterías y otros aparatos eléctricos, y en amalgamas para empastes dentales.

Existen diferentes **fuentes de emisión** de Hg. Por un lado encontramos fuentes naturales, que son aquellas que emiten Hg de origen geológico a través de procesos naturales como erupciones volcánicas, actividad geotérmica, desorción gradual de los suelos o erosión natural de rocas enriquecidas con Hg. También existen fuentes antropogénicas, las cuales se dividen en primarias y secundarias. Las fuentes antropogénicas primarias son aquellas en las que Hg de origen geológico es liberado por acción del ser humano: minería, extracción de combustibles fósiles, producción de cemento o combustión de carbón. Las fuentes antropogénicas secundarias son aquellas que emiten Hg debido a un uso intencional del metal: fabricación de productos con Hg como componente, industria o minería artesanal del oro. Las principales actividades industriales que emplean Hg son la producción de monómero de cloruro de vinilo (precursor de PVC) y la industria de cloro-álcali (que emplea la tecnología de celda de Hg para la producción de cloro y sosa cáustica), siendo esta última la tercera actividad que más Hg consume mundialmente. La minería artesanal y en pequeña escala del oro es la mayor fuente de emisión de Hg por uso intencional, correspondiéndole también el mayor consumo de este metal.

El flujo continuo del Hg entre los distintos compartimentos ambientales es llamado ciclo del mercurio. El Hg comienza su **ciclo biogeoquímico** emanando desde la corteza terrestre o los océanos en forma de Hg^0. Una vez en la atmósfera, el Hg^0 puede ser oxidado a Hg(II) por la acción de O_3, ·OH or Br. Este Hg(II) puede pasar al agua y a los suelos por medio de deposición húmeda o seca. En el suelo, el Hg puede estar en forma de compuestos inorgánicos como $HgCl_2$ y $Hg(OH)_2$, formas menos reactivas como HgS y HgO o fuertemente unido a grupos de azufre reducido de la materia orgánica. El Hg adsorbido permanece en el suelo, mientras que el que está en disolución puede sufrir metilación o escorrentía hacia una masa de agua. En lo que respecta a la vegetación, el Hg en las partes aéreas proviene principalmente de la atmósfera, y el presente en las raíces proviene del suelo. Posteriormente, este Hg incorporado en los tejidos vegetales regresa al suelo vía caída de hojarasca y precipitaciones bajo la cubierta arbórea. El Hg puede volver a la atmósfera mediante la reducción a Hg^0, mediada principalmente por Fe^{2+} y compuestos húmicos y fúlvicos. En ambientes acuáticos, una porción del Hg(II) puede ser transformada en MeHg,

226

principalmente por la acción de bacterias sulfato-reductoras y metanogénicas. Sin embargo, el MeHg también puede generarse por metilación abiótica: transmetilación por parte de especies organometálicas de otros metales como Pb, As o Sn. El proceso inverso, la desmetilación, también puede ser biótica o abiótica (fotodegradación o reacción con sulfuro). Tanto el MeHg como el Hg(II) pueden ser captados por diferentes seres vivos y concentrados en sus tejidos (bioacumulación), aunque solo el MeHg tiene el potencial de biomagnificarse a lo largo de la cadena trófica.

Debido a esta bioacumulación y biomagnificación en la cadena alimentaria, los ecosistemas acuáticos son especialmente sensibles, y por ello se deben regular los **niveles de Hg en aguas**. La Directiva Marco del Agua (Directiva 2000/60/EC) recomienda a los estados miembros de la Unión Europea alcanzar un buen estado cualitativo y cuantitativo de todas las masas de agua antes de 2021, e incluye al Hg y sus compuestos como sustancias peligrosas prioritarias. La Directiva relativa a las normas de calidad ambiental en el ámbito de la política de aguas (Directiva 2008/105/EC) establece límites para la concentración de las sustancias prioritarias en aguas superficiales, y ha sido recientemente enmendada por la Directiva 2013/39/EC: la concentración máxima permitida de Hg en agua es de 0.07 µg L^{-1}, y el nivel de calidad establecido para biota es 20 µg kg^{-1}. El Real Decreto 60/2011 transpuso a la legislación española todos los aspectos contenidos en la Directiva 2008/105/EC, manteniendo las normas de calidad ambiental establecidas por la directiva europea para el Hg y sus compuestos. En cuanto al agua potable, la Directiva 98/83/EC relativa a la calidad del agua para consumo humano, estableció en 1 µg L^{-1} la concentración máxima permitida de Hg.

Los materiales más adecuados para la **toma y almacenamiento de muestras** cuyo contenido en Hg va a ser determinado son el PTFE (politetrafluoroetileno ó teflón), el PET (polietilen-tereftalato) y el vidrio. Para su reutilización, los contenedores de PTFE y vidrio deben limpiarse con disoluciones de ácido o BrCl, mientras que los de PET, más baratos, suelen ser de un solo uso. Las aguas naturales suelen filtrarse inmediatamente tras el muestreo para separar la fracción disuelta de la particulada. Se emplean filtros de distintos materiales (e.g. nylon, cuarzo) y tamaños de poro (0.45 µm es el más

común). La estabilización de las muestras para determinación de Hg disuelto se lleva a cabo mediante la adición de ácido (HCl o HNO$_3$) u oxidante (BrCl). Si el analito de interés es el MeHg, se recomienda la acidificación con HCl o la congelación de la muestra para preservar esta especie en agua. Si se usan contenedores de vidrio, deben ser de color ámbar para evitar la fotodegradación.

En **muestras sólidas**, la extracción de **Hg total (THg)** se suele llevar a cabo mediante digestión con ácidos fuertes (HNO$_3$, HNO$_3$/HCl, HNO$_3$/HCl/HF o HNO$_3$/H$_2$SO$_4$) en el caso de matrices como suelo o sedimentos, o con reactivos oxidantes (H$_2$O$_2$) en el caso de biota. Tras la digestión, se emplean los métodos para muestras líquidas que se describen más adelante. En general, las metodologías que conllevan digestión de la muestra son laboriosas y poco respetuosas con el medio ambiente. Como alternativa, el THg en muestras sólidas puede ser medido directamente con instrumentos automáticos (AMA-254 y el DMA-80), basados en la combustión catalítica de la muestra, preconcentración por amalgamación en una trampa de oro, desorción térmica y detección mediante espectrometría de absorción atómica (AAS). La ventaja de estos analizadores radica en que no se requiere pretratamiento de la muestra, el tiempo de análisis es muy corto y no se usan reactivos peligrosos.

En el caso de **muestras líquidas**, se puede emplear la detección mediante AAS también, aunque el sistema de detección más común es la espectrometría de fluorescencia atómica de vapor frío (CVAFS). Como pretratamiento para CVAFS, las muestras acuosas son digeridas con oxidantes fuertes para transformar todas las especies en Hg(II). Posteriormente, el Hg(II) se reduce mediante SnCl$_2$ o NaBH$_4$ a Hg^0, que es purgado de la disolución mediante un gas inerte y transportado al detector o preconcentrado en una trampa de oro. En este último caso, el Hg se libera calentando la trampa y se transporta a la celda de detección donde la fluorescencia se mide a una longitud de onda de 253.7 nm. Este procedimiento es recomendado por la EPA (método 1631) y la UE (EN 13506) para la determinación de THg en aguas naturales. Otros sistemas de detección empleados para el THg son la espectrometría de emisión atómica con plasma de acoplamiento inductivo (ICP-AES) y la espectrometría de masas con plasma de acoplamiento inductivo (ICP-MS).

La forma química de un contaminante afecta a su movilidad, biodisponibilidad, bioacumulación e impacto ecotoxicológico; por ello es importante conocer qué especies del elemento y en qué cantidad están presentes. En este contexto, el término **"análisis de especiación"** hace referencia a la actividad analítica de identificar y medir especies. Los métodos analíticos destinados al análisis de especiación deben comprender las siguientes fases: 1) **extracción** de las especies de interés de la muestra ambiental, asegurando la integridad de la forma química y la concentración de dichas especies; 2) **preconcentración** de las especies con el objetivo de alcanzar una concentración detectable por la técnica elegida; 3) **separación** de las especies sin variar sus concentraciones relativas originales; y 4) **detección** y determinación individual de cada especie. Además, dependiendo de la técnica de separación empleada, es necesario un paso adicional de **derivatización** para convertir las especies de Hg en formas volátiles.

La **extracción** debe ser llevada a cabo de tal manera que el analito se separe de la matriz sin pérdidas, contaminación o transespeciación, y con las menores interferencias posibles. Las técnicas más comúnmente empleadas son la extracción ácida (usando HNO_3 o HCl/ HNO_3 como extractantes), la extracción básica (usando KOH-metanol o hidróxido de tetrametilamonio), la destilación (tratando la muestra con H_2SO_4 y NaCl o KCl, y posteriormente separando las especies volátiles a 150 °C) y la extracción con fluidos supercríticos.

Para la **preconcentración**, tradicionalmente se han empleado la extracción líquido-líquido y la extracción en fase sólida. Sin embargo, en los últimos años se han buscado alternativas que reduzcan costes y residuos y fáciles de automatizar, como es el caso de la microextracción en fase sólida (SPME) y la purga y trampa (P&T). La SPME se basa en la extracción no exhaustiva de compuestos orgánicos volátiles o semivolátiles desde una matriz acuosa o gaseosa a una fibra de sílice fundida con una cubierta de una fase estacionaria apropiada. Los analitos son transportados desde la matriz a la fase estacionaria hasta que se alcanza el equilibrio (la cantidad de analito extraido llega a un estado estacionario). Existen dos modalidades: directa y *headspace* (la fibra se coloca en la capa de aire sobre la muestra), siendo esta última la más empleada. Las

fibras más comunes para especiación de Hg son las recubiertas con polidimetilsiloxano (PDMS), dada su alta estabilidad. La P&T permite la extracción y preconcentración de especies de Hg orgánicas mediante la derivatización y purga de la muestra acuosa con un flujo de gas (N_2) que arrastra los derivados volátiles hacia una columna (trampa) con un relleno adsorbente (Tenax, Chromosorb o Carbotrap).

La SPME, la P&T, así como la separación mediante cromatografía de gases, requieren que los analitos sean volátiles. Dado que el MeHg y otras especies orgánicas de Hg no son volátiles, se deber proceder a su transformación mediante reacciones de **derivatización**. La técnica tradicional es la reacción de Grignard, generalmente usando cloruro de butilmagnesio como reactivo. Sin embargo, dado que los reactivos de Grignard son muy sensibles al agua, se tienen que usar disolventes orgánicos para la extracción, y la preparación de la muestra es larga y tediosa; se ha optado por otros métodos como la generación de hidruros usando $NaBH_4$ o la alquilación (etilación, propilación o fenilación usando tetraetilborato de sodio ($NaBEt_4$), tetrapropilborato de sodio ($NaBPr_4$) o tetrafenilborato de sodio ($NaBPh_4$), respectivamente). En todos los casos la reacción tiene lugar en medio acuoso y el tiempo de análisis se reduce.

Aunque la cromatografía es la técnica más empleada para la **separación** de especies de Hg, existen métodos no cromatográficos que pueden separar adecuadamente una o dos especies en función de su diferente comportamiento físico o químico (i.e. solubilidad, volatilidad o potencial redox). Algunas de estas técnicas son la destilación, la P&T, la reducción selectiva a Hg^0, extracción selectiva en fase sólida o la electroforesis capilar. Sin embargo, la cromatografía de gases (GC) es la técnica más usada para la especiación de Hg debido a su fácil manejo, alto poder de resolución y fácil acoplamiento a un gran número de detectores; y se emplean tres tipos de columnas: empaquetadas, capilares y multicapilares. La cromatografía de líquidos de alta resolución (HPLC) es una técnica muy apropiada para la separación de especies polares o iónicas, así que también es una buena alternativa para la especiación de Hg. Ofrece mayor versatilidad que la GC, pero la sensibilidad conseguida es mucho menor debido los grandes volúmenes de disolvente empleado y el efecto dilución. Por último, la cromatografía iónica (IC) también ha sido empleada para separar especies de Hg.

Las características que deber reunir el sistema de **detección** ideal para especiación de metales traza son los siguientes: alta sensibilidad y especificidad, posibilidad de acoplamiento a GC o HPLC, operación continua on-line con la columna de separación, información en tiempo real, amplio rango de linealidad, y capacidad multielemental y multiisotópica. Las principales técnicas de detección empleadas para la especiación de Hg son la ICP-AES, la espectrometría de emisión atómica con plasma inducido por microondas (MIP-AES), la espectrometría de fluorescencia atómica (AFS), la AAS y la ICP-MS, cuyas características quizás sean las más próximas a las del detector ideal y ofrece la posibilidad de trabajar con diferentes isótopos estables (dilución isotópica).

La **"biodisponibilidad"** de un metal es un concepto difícil de definir. Podría incluir (1) la disponibilidad fisicoquímica del metal en el medio de exposición, (2) la demanda real de la biota y (3) el comportamiento toxicológico del metal dentro del cuerpo de los organismos. En esta tesis, consideraremos la biodisponibilidad como aquella propiedad del metal que puede ser estimada y evaluada por la técnica "gradientes de difusión en película fina" (DGT), una técnica de muestreo pasivo que supuestamente mimetiza las membranas biológicas y mide la fracción lábil de metales disueltos.

El muestreo puntual seguido de la medida de un amplio rango de contaminantes es el procedimiento más común para el monitoreo de metales pesados y especies organometálicas en ambientes acuáticos. Sin embargo, esta estrategia presenta desventajas como el gran número de muestras que deben tomarse para establecer la calidad de la masa de agua y que revela solo niveles instantáneos. Para superar estas limitaciones, se han desarrollado distintos tipos de **muestreadores pasivos** que presentan los siguientes beneficios: proporcionan concentraciones medias de contaminantes para periodos de muestreo de horas a semanas, sirven como procedimientos de enriquecimiento in situ, y protegen a los analitos de la descomposición durante el transporte y el almacenamiento. Las principales técnicas de muestreo pasivo para medir contaminantes orgánicos en agua son: (1) la diálisis in situ, (2) la diálisis con resinas receptoras, (3) dispositivos de membrana líquida, (4) el Chemcatcher, (5) el muestreador pasivo integrante de Hg (PIMS), (6) el Sorbicell, (7) el

equilibrio de difusión en película fina (DET) y (8) los gradientes de difusión en capa fina (DGT).

La **técnica DGT** surgió a mediados de los 90 para determinar in situ especies metálicas lábiles en sistemas acuáticos, y se basa en el transporte por difusión de solutos a través de un gradiente de concentración bien definido establecido dentro de una capa de hidrogel y un filtro de membrana, permitiendo obtener datos cuantitativos de la concentración del analito en periodos de horas a semanas. Los muestreadores DGT comprenden un agente ligante (resina) inmovilizado en un gel y separado de la solución que va a ser analizada por un gel permeable y un filtro, todo ensamblado en un dispositivo plástico consistente en un pistón y una tapa con una abertura (ver esquema en Figura 1). Una vez los solutos difunden através de las capas externas, se unen irreversiblemente al agente ligante. En base a la primera ley de difusión de Fick, la masa de analito (M) acumulada por la resina depende de su concentración en la disolución (C), del coeficiente de difusión (D) del analito en el gel de difusión, del grosor (Δg) de la capa de difusión, del área de exposición (A) y del tiempo de muestreo (t).

$$M = \frac{DAtC}{\Delta g}$$

Con esta técnica se puede muestrear cualquier especie lábil para la cual exista un agente ligante que pueda ser embebido en el gel receptor. La mayor parte de los metales pesados son usualmente medidos usando la resina de intercambio iónico Chelex 100, sin embargo para las especies de Hg se usan resinas más específicas que contienen grupos tiol. Las aplicaciones de esta técnica en aguas incluyen (1) medidas de especiación, (2) estudios de biodisponibilidad y (3) monitoreo ambiental de rutina.

Debido a la alta toxicidad y capacidad de bioacumulación y biomagnificación del MeHg, el estudio de sus vías de eliminación es crucial para controlar su presencia en el medio acuático. El MeHg puede ser desmetilado bien por la acción de microorganismos en la columna de agua o por **fotodegradación** en aguas superficiales, siendo este último el principal mecanismo de eliminación de MeHg en lagos oligotróficos. Aunque la fotólisis directa fue observada por Inoko (1981) en una

232

disolución acuosa de MeHgCl a la longitud de onda de absorción del Hg (253.7 nm), la fotolisis producida por la luz solar es esencialmente indirecta. La radiación visible y ultravioleta, al incidir en la materia orgánica disuelta (DOM) en el agua, tienen la capacidad de generar especies reactivas de oxígeno (ROS) (e.g. radical hidroxilo, ·OH; oxígeno singlete, $^{1}O_2$) que actúan como catalizadores en la desmetilación del MeHg.

Objetivos generales

Visto el tan marcado carácter contaminante del Hg en el medioambiente y especialmente en ecosistemas acuáticos, su distribución global y el creciente interés científico y social en el tema, esta tesis establece dos objetivos generales:

- Desarrollar la técnica DGT para la determinación del mercurio lábil en agua y, por extensión, para la evaluación de la biodisponibilidad de este metal en ecosistemas acuáticos.
- Estudiar la fotodegradación del MeHg en aguas continentales y su posible relación con la biodisponibilidad de dicha especie.

Evaluación de la técnica DGT para monitoreo de Hg disuelto en aguas continentales

El primer objetivo de este trabajo fue validar bajo condiciones de laboratorio un tipo de muestreador de DGT comercial (Exposmeter AB, Suecia) para la determinación de Hg en aguas. Posteriormente, se quiso evaluar la eficiencia de acumulación de Hg de dichos muestreadores bajo condiciones ambientales y tratar de medir in situ la concentración de Hg en ciertos tramos de los ríos Gállego y Ebro, ambos con un largo historial de contaminación por Hg debido a la existencia de plantas de cloro-álcali en sus márgenes.

El muestreador DGT comercial se compone de un pistón de plástico con una tapa con una abertura de 2 cm de diámetro, resina Spheron-thiol inmovilizada en un gel de poliacrilamida como gel receptor, un gel de difusión de agarosa y un filtro de

membrana con un tamaño de poro de 0,45 µm (ver disposición de las distintas capas en la Figura 1). Para la consecución del primer objetivo de este trabajo, se realizó un experimento de serie temporal sumergiendo varios muestreadores DGT en un contenedor con una disolución acuosa de NaCl y MeHgCl. Los muestreadores se extrajeron tras distintos intervalos de tiempo para poder obtener una cinética de acumulación. El D del MeHg en la capa de difusión del muestreador empleado se obtuvo a partir de la pendiente de la recta obtenida al representar la masa de MeHg acumulada en el gel receptor frente al tiempo de muestreo. En los tests realizados en el campo, se colocaron muestreadores DGT en distintos tramos de un mismo río (aguas arriba y aguas abajo del foco de contaminación por Hg) empleando distintos dispositivos para en un caso suspenderlos en la columna de agua del río y en otro posicionarlos muy próximos a los sedimentos del fondo. También se trató de realizar un experimento de serie temporal en el río Ebro de 8 semanas de duración, empleando un triplicado de muestreadores para cada uno de los 4 intervalos de muestreo. El THg, tanto en los geles receptores como en el agua, fue medido con el AMA-254.
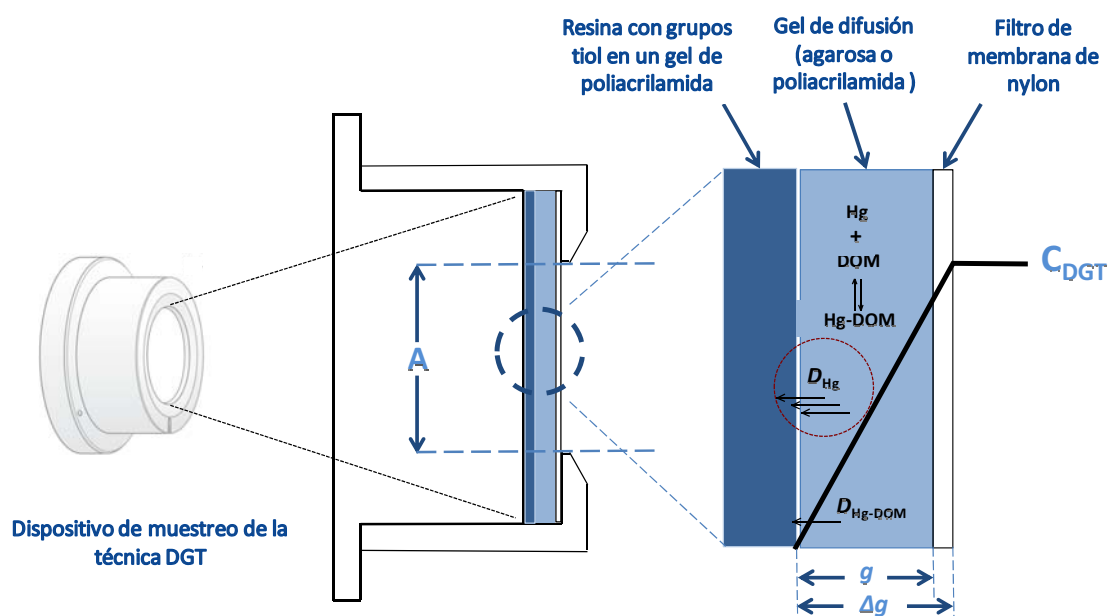
Figura 1. Esquema de un muestreador DGT genérico para determinación de Hg. A es el área de la ventana de exposición a la disolución, C_{DGT} es la concentración de Hg lábil en la disolución acuosa, g es el grosor del gel de difusión y Δg el grosor de la capa de difusión. D_{Hg} representa el coeficiente de difusión del Hg iónico libre, y D_{Hg-DOM}, el coeficiente de difusión del Hg complejado con materia orgánica disuelta. D_{Hg} está rodeado por un círculo para indicar que su valor es mayor.

Este estudio demostró la capacidad de estos muestreadores comerciales específicos para Hg para medir la concentración del Hg lábil disuelto en una disolución de NaCl en agua Milli-Q y verificó que se ajustaban a los principios de DGT. El D obtenido para MeHg en el gel de difusión de agarosa ($8,50 \times 10^{-6}$ cm^2 s^{-1}) puede compararse al de Hg(II) en agarosa ($8,86 \times 10^{-6} \times 10^{-6}$ cm^2 s^{-1}) (Docekalova y Divis, 2005), al de Hg(II) en agua ($8,47 \times 10^{-6}$ cm^2 s^{-1}), y en menor medida al de MeHg en gel de poliacrilamida ($5,1 \times 10^{-6}$ cm^2 s^{-1} at 20 °C) (Clarisse y Hintelmann, 2006). Sin embargo, bajo condiciones ambientales, y sobre todo en aguas eutróficas, se encontraron problemas como la presencia de biofouling y materia particulada que bloqueaba el filtro y la insignificante acumulación de Hg en los muestreadores. Además, se identificó la necesidad de obtener un D para especies de Hg complejadas con DOM, tal como se encuentran en las aguas naturales. Los complejos Hg-DOM, de mayor tamaño, difunden a menor velocidad, y por tanto, para no subestimar la fracción lábil de Hg, se necesita conocer el D de estas especies en la capa de difusión de DGT. Simular las características del agua a muestrear es fundamental para una exacta calibración de los DGT.

Desarrollo de la técnica DGT para determinación de Hg en agua dulce: Comparación de tres tipos de muestreadores en ensayos de laboratorio

El objetivo de este estudio fue evaluar la tasa de acumulación de Hg por parte de tres tipos de muestreadores DGT (el comercial y otros dos manufacturados internamente) y obtener el D del Hg(II) en sus respectivas capas de difusión, tanto en ausencia como en presencia de DOM. Posteriormente se evaluó la acumulación de MeHg por parte de los dos tipos de DGT auto-manufacturados y también se obtuvo la D de esta especie en ausencia y presencia de DOM.

Los muestreadores DGT (esquema en la Figura 1) estudiados fueron los siguientes:
- C-DGT: el muestreador comercial descrito en el apartado anterior.

- A-DGT: compuesto por gel de sílice funcionalizado con grupos 3-mercaptopropil embebido en un gel de poliacrilamida como agente ligante, un gel de difusión de agarosa y un filtro de membrana de nylon.

- P-DGT: con los mismos componentes que el A-DGT, excepto que en este caso el gel de difusión era de poliacrilamida.

En este estudio también se realizaron experimentos de serie temporal (Figura 2) con disoluciones acuosas de NaCl y Hg(II) o MeHg, según el caso, y en presencia o ausencia de un material de referencia de DOM de un embalse (IHSS, 1R108N) en disolución.

Figura 2. Montaje de los experimentos de serie temporal en ausencia (izquierda) y en presencia de DOM (derecha).

A partir de estas pruebas se pretendía decidir qué tipo de muestreador era el más adecuado para determinación de Hg inorgánico y MeHg en aguas dulces. Para el análisis de THg, tanto en agua como en el gel receptor de DGT, se siguió el Método 1631 de la US EPA (oxidación con BrCl, reducción con $SnCl_2$, preconcentración de doble etapa en trampa de oro y detección por CVAFS). En el caso del gel receptor, se llevó a cabo la optimización de la digestión ácida para dicha matriz como pretratamiento para

el análisis de THg, resultando ser el *aqua regia* la mejor opción como reactivo para la digestión. Para la determinación de MeHg en agua se realizó derivatización con NaBPh$_4$, extracción con SPME en espacio de cabeza (usando una fibra de PDMS 100 µM) y separación y detección mediante GC-CVAFS. En el caso de los geles receptores, primero se llevó a cabo una extracción con una disolución ácida de tiourea y luego se siguió el mismo procedimiento que para las muestras de agua.

El gel de sílice funcionalizado con grupos 3-mercaptopropil fue usado satisfactoriamente como agente ligante en el gel receptor para medidas de Hg(II) - previamente sólo había sido usado para determinación de MeHg (Clarisse y Hintelmann, 2006)-. Se demostró que el gel de difusión de poliacrilamida no compite con la resina en la unión con Hg(II), contrariamente a lo manifestado por Doceckalova y Divis (2005). Aunque los dos tipos de DGT auto-manufacturados con poliacrilamida (P-DGT) y agarosa (A-DGT) como gel de difusión parecen ser adecuados para medir la fracción lábil de Hg en agua, el P-DGT parece la mejor opción para determinación de Hg(II), ya que su tasa de acumulación se ajustó muy bien a un modelo lineal y presentó blancos muy bajos (denotados por el término independiente de la ecuación de las rectas en la Figura 3).
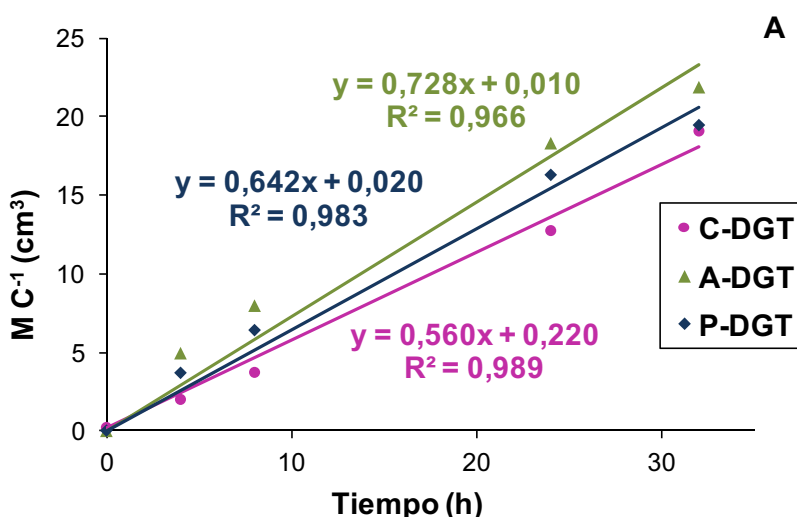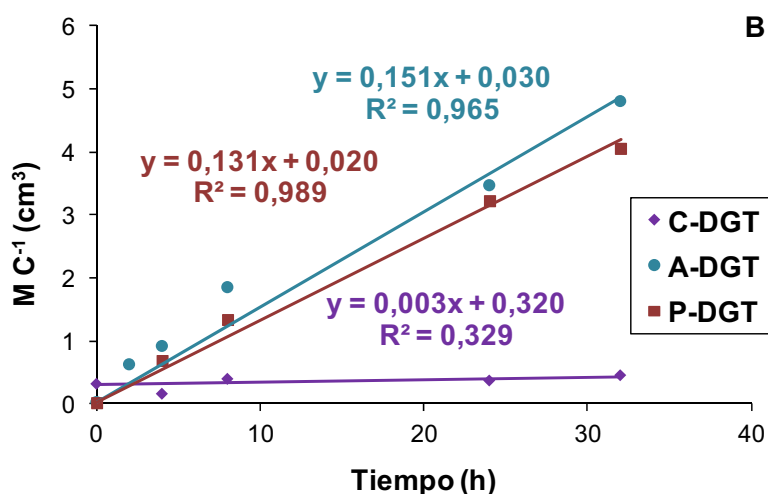
Figura 3. Cinéticas de acumulación de Hg(II): (A) en ausencia y (B) en presencia de DOM. Se representa la masa de Hg acumulada en el gel receptor (M) normalizada por la concentración de Hg presente en la disolución (C) para varios periodos de tiempo y tres tipos de muestreadores de DGT (C-DGT, A-DGT y P-DGT).

Los muestreadores comerciales (C-DGT) también mostraron una alta linealidad en la acumulación en ausencia de DOM (Figura 3 A). Sin embargo presentaron unos blancos muy altos, y en presencia de DOM, su acumulación de Hg(II) fue prácticamente nula a lo largo del tiempo (Figura 3 B). El P-DGT también parece ser el más apropiado para determinación de MeHg debido a su mayor velocidad de acumulación y su mayor capacidad de discriminación entre especies de MeHg (Figura 4).

El coeficiente de difusión obtenido en presencia de 10 mg L^{-1} de DOM tanto para Hg(II) ($D_{Hg(II)-DOM}$) como para MeHg ($D_{MeHg-DOM}$) fue menor que en ausencia de DOM ($D_{Hg^{2+}}$ y $D_{MeHg^{+}}$, respectivamente), debido a que los complejos de Hg con materia orgánica, de mayor tamaño, difunden a través de la capa de difusión más lentamente que los iones libres. Por otra parte, $D_{MeHg-DOM}$ fue mayor que $D_{Hg(II)-DOM}$, lo que sugiere que los complejos MeHg-DOM son más lábiles que los Hg(II)-DOM. Este hecho pone de manifiesto la importancia de calibrar los muestreadores de DGT usando la especie de Hg que posteriormente será analizada.
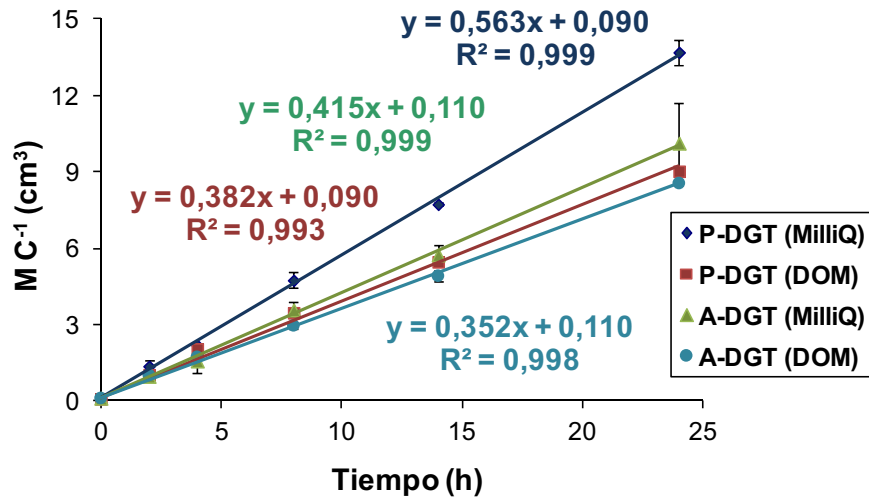
Figura 4. Cinéticas de acumulación de MeHg. Se representa la masa de MeHg acumulada en el gel receptor (M) normalizada por la concentración de MeHg presente en la disolución (C) para varios periodos de tiempo y dos tipos de muestreadores de DGT (P-DGT y A-DGT), tanto en ausencia (MilliQ) como en presencia (DOM) de DOM.

Inyección de Hg(II) en un humedal construido a escala experimental para tratamiento de aguas residuales. Aplicación de muestreadores de DGT para evaluar la eliminación, labilidad y metilación del Hg

Este estudio se llevó a cabo con el objetivo de evaluar la eficiencia de eliminación de Hg de un sistema alternativo para tratamiento de aguas residuales consistente en tres humedales construidos a escala experimental (humedal de flujo vertical, VF-CW; humedal horizontal de flujo subsuperficial, HF-CW; y humedal de flujo libre, FWS-CW) en serie (Figura 5). También se pretendía examinar la metilación de Hg en las diferentes etapas del tratamiento, puesto que los humedales son ecosistemas donde se produce MeHg vía biometilación
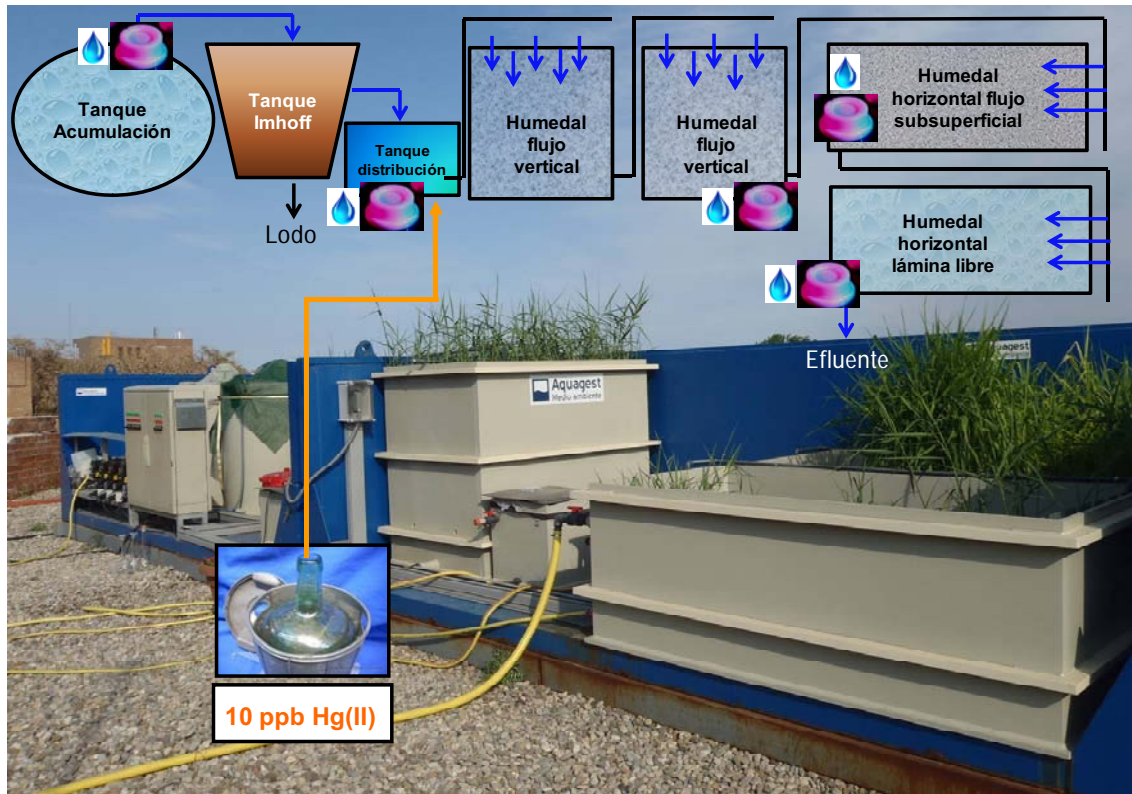
Figura 5. Fotografía y esquema de la planta de tratamiento experimental. Las imágenes de una gota y de un muestreador DGT indican los puntos en los que se han tomado muestras de agua y se ha empleado DGT, respectivamente. La flecha naranja indica el punto en el que se ha realizado la inyección de Hg(II).

Se aplicó la técnica DGT para determinar la fracción lábil de Hg y MeHg en el agua a lo largo de la línea de tratamiento (se colocó un cuadriplicado de muestreadores durante 5 días en los tanques que recogen el efluente de cada humedal) y se comparó con los niveles medidos directamente en el agua (disuelto total) (puntos de muestreo indicados en la Figura 5). El interés en medir la fracción lábil en este caso radica en el hecho de que el agua residual tratada es vertida en ríos o reutilizada para riego, donde esta fracción es susceptible de ser captada por distintos organismos. En este estudio, el THg en agua y en geles receptores de DGT se midió con el AMA-254, y el MeHg con SPME-GC-CVAFS.

Los resultados demostraron que la técnica DGT midió satisfactoriamente el Hg y el MeHg lábil en prácticamente todos los puntos de la línea de tratamiento muestreados durante los 5 días, a pesar que algún punto la concentración de Hg (en Imhoff y VF-

CW) y MeHg (en VF-CW) lábil resultó ser mayor que la de Hg y MeHg disuelto total (Figura 6).
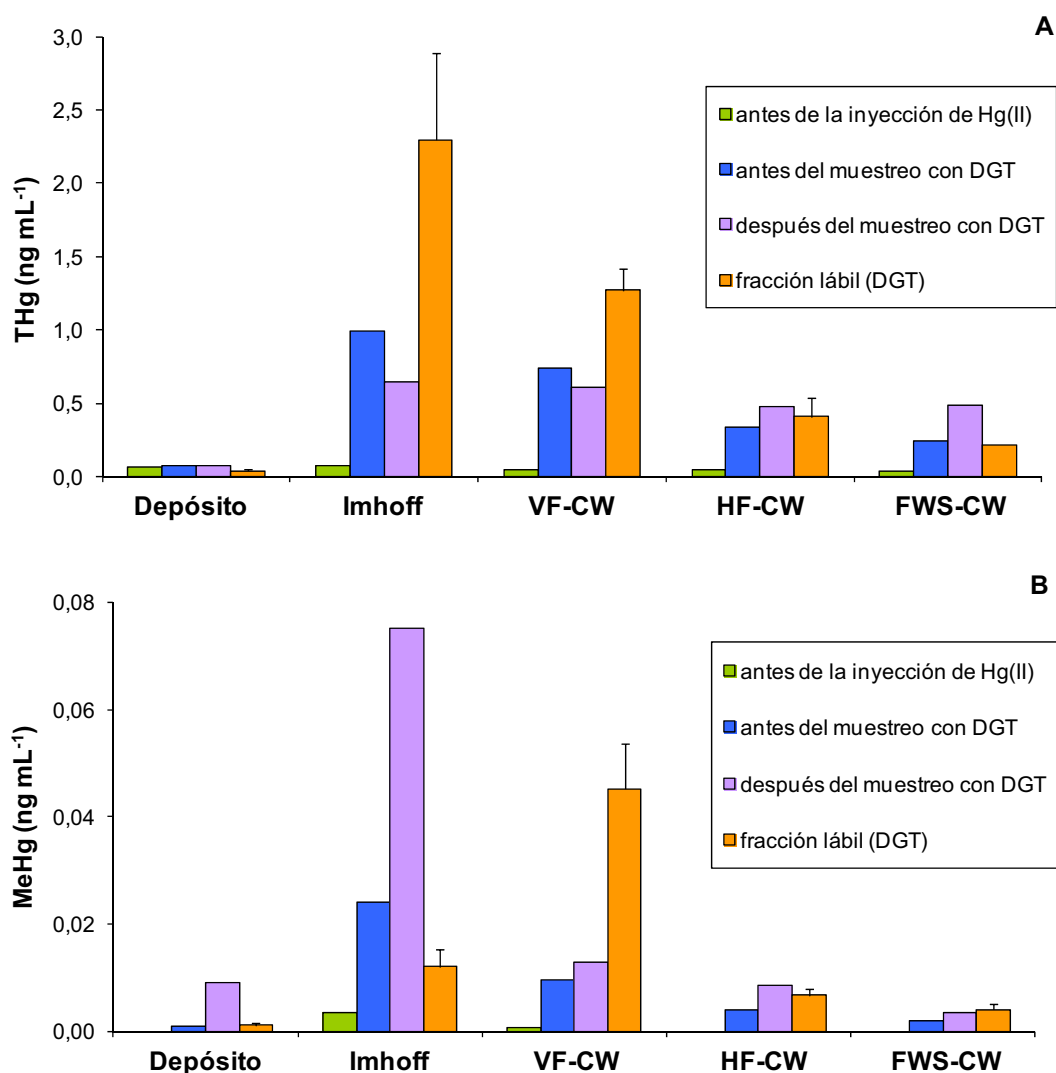
Figura 6. Concentración de (A) THg y (B) MeHg en la fase disuelta del agua medida directamente antes de la inyección de Hg(II); antes y después del muestreo con DGT; y determinada a partir de medidas con DGT (concentración lábil).

Esto se puede atribuir al hecho de que las medidas de Hg disuelto total corresponden a muestras puntuales, mientras que las unidades de DGT estuvieron muestreando durante 5 días para ofrecer la concentración media durante ese periodo. La planta de tratamiento es capaz de eliminar el 75% del Hg disuelto, mientras que no haya saturación del sistema, y el 90% del Hg lábil. Los porcentajes de eliminación fueron calculados a partir de los niveles obtenidos en el efluente del FWS-CW respecto

a los niveles en el efluente del tanque Imhoff, que fue el punto de inyección de Hg(II). En cuanto al MeHg, el porcentaje de eliminación de MeHg disuelto fue 92-96%, mientras que el MeHg lábil fue eliminado en menor medida (66%). Para la alta carga hidráulica (y de Hg) utilizada en este estudio, las dimensiones de los humedales construidos deberían ser mayores para evitar la saturación. También se recomienda la limpieza y drenaje del sistema de forma periódica para eliminar la acumulación de materia particulada y vegetación saturadas en Hg. Sin embargo, para las cargas de Hg comúnmente encontradas en aguas residuales urbanas, el diseño de esta planta podría funcionar adecuadamente durante largos periodos de tiempo.

Fotodegradación de MeHg en la fase acuosa de un gradiente laguna-humedal en la Suecia boreal

El objetivo de este estudio fue determinar la tasa de fotodegradación de MeHg en aguas con alto contenido en DOM (húmicas) de tres localizaciones en la Suecia boreal: un lago (ANG), un humedal (KSN) y una zona ribereña-humedal (SKM) (Figura 7); mediante la adición de un isótopo estable (Me^{198}Hg o Me^{204}Hg, dependiendo del experimento). Tras introducir el agua en botellas de teflón y añadir un trazador marcado isotópicamente, las botellas se expusieron a la luz (Figura 7 D). La radiación fotosintéticamente activa (PAR) se midió a lo largo del experimento. Según el experimento, las botellas completas o las muestras de una misma botella, se retiraron de la luz a distintos intervalos de tiempo, y tras la adición de un estándar interno (Me^{200}Hg) se almacenaron en la oscuridad a 19 °C. A partir de la concentración de MeHg de las muestras correspondientes a cada intervalo de exposición y de la radiación acumulada, se realizó una cinética de primer orden de fotodegradación de MeHg, que permitió la obtención de una constante de tasa de fotodegradación (k_{pd}).
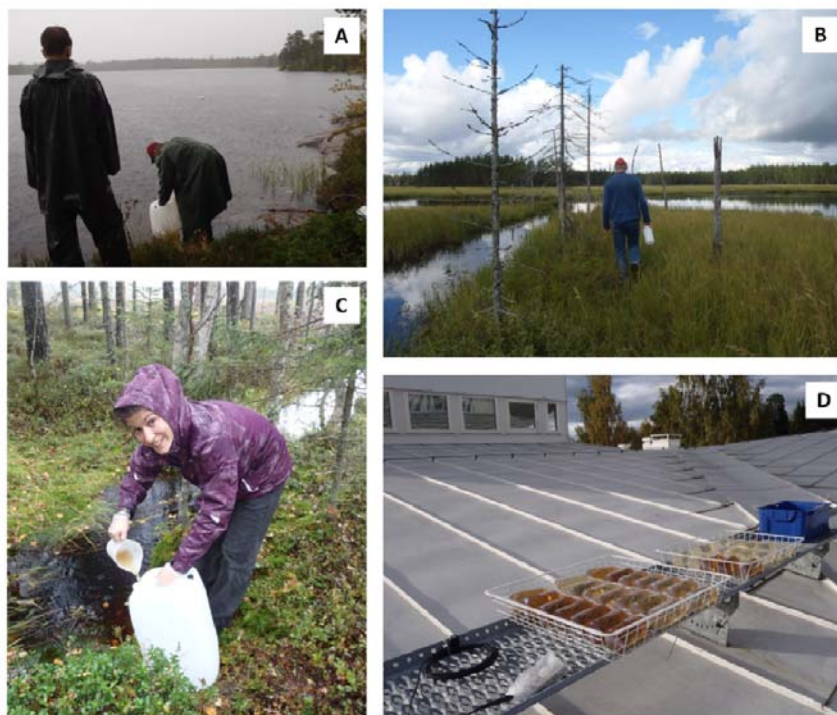
Figura 7. Imágenes de los puntos de muestreo en (A) un lago distrófico –ANG–, (B) un lago distrófico-humedal –KSN– y (C) un bosque ribereño-humedal en el norte de Suecia (área de Umeå); y (D) disposición de un experimento de fotodegradación de MeHg en el tejado de la universidad.

Se combinaron datos de dos experimentos en los que se empleó diferente composición espectral (luz solar natural y una fuente de luz UV artificial) para calcular constantes de tasa de fotodegradación de primer orden específicas para cada longitud de onda ($k_{pd\ PAR}$, $k_{pd\ UVA}$, $k_{pd\ UVB}$), corregidas por la atenuación de la luz por parte de la DOM y el teflón de las botellas. También se examinó la influencia del ratio molar MeHg/grupos tiol (RSH) en la velocidad de fotodegradación. La metodología seguida para determinar la concentración de MeHg en agua fue derivatización con NaBEt$_4$, concentración con P&T (Tenax) y separación y detección mediante GC-ICP-MS. La concentración de MeHg fue calculada usando el análisis de dilución isotópica. También se empleó espectroscopía de resonancia paramagnética electrónica (EPR) y *sulfur X-ray absorption near-edge spectroscopy* (S XANES) para cuantificar la formación de radicales y grupos tiol orgánicos, respectivamente.

Se observó que la constante de tasa de fotodegradación de MeHg teniendo en cuenta todo el espectro de la luz solar ($k_{pd\ Full\ Spectrum}$) variaba significativamente entre

las tres aguas estudiadas, mientras que k_{pdPAR}, k_{pdUVA} and k_{pdUVB} (calculadas mediante un procedimiento iterativo) eran indistinguibles para las tres aguas (Tabla 1).

Tabla 1. Constantes de tasa de fotodegradación de MeHg en agua de un lago distrófico (ANG), un lago distrófico-humedal (KSN) y una zona ribereña-humedal (SKM) para el experimento #1 (aguas sin diluir y luz solar) y el experimento #2 (aguas diluidas para alcanzar la misma concentración de DOC y fuente de luz UV artificial).

		$k_{pd\,Full\,Spectrum}$	$k_{pd\,PAR}$	$k_{pd\,UVA}$	$k_{pd\,UVB}$
ANG	exp#1	0,0040 ± 0,0001	0,0023 ± 0,00021	0,10 ± 0,024	7,1 ± 1,3
	exp#2	0,076 ± 0,0029	0,0023 ± 0,00021	0,10 ± 0,024	7,1 ± 1,3
KSN	exp#1	0,0029 ± 0,00009	0,0022 ± 0,00020	0,095 ± 0,023	6,8 ± 1,3
	exp#2	0,057 ± 0,0029	0,0022 ± 0,00020	0,095 ± 0,023	6,8 ± 1,3
SKM	exp#1	0,0023 ± 0,0001	0,0025 ± 0,00022	0,11 ± 0,026	7,8 ± 1,5
	exp#2	0,083 ± 0,0025	0,0025 ± 0,00022	0,11 ± 0,026	7,8 ± 1,5

Los errores para las k_{pd}s están reportados como ±SE

Por otra parte, se comprobó que cuando el ratio molar MeHg/RSH se incrementaba hasta alcanzar valores sustancialmente superiores a 1, había una marcada disminución de $k_{pd\,Full\,Spectrum}$ (Figura 8). Esto podría ser una consecuencia de la unión mayoritaria del MeHg a grupos moleculares de O y N, cuando el MeHg está en exceso respecto a los RSH. Al contrario, cuando los RSH están en exceso, la fuerte unión entre Hg y S en el complejo MeHg-tiol causaría un debilitamiento del enlace C-Hg de la molécula de MeHg, haciéndolo susceptible de ruptura por la acción de ROS.

A la luz de los resultados, se postula que mientras que la formación de radicales orgánicos y ROS por parte de la DOM exceda la producción de ROS generada por NO_3^-, Fe y posiblemente otros componentes, la atenuación de la luz y de ROS por parte de la DOM controlarán la tasa de fotodegradación de MeHg. Así, $k_{pd\,PAR}$, $k_{pd\,UVA}$ and $k_{pd\,UVB}$ pueden ser consideradas universales en aguas con altos contenidos en DOM siempre que la PAR, la radiación UVA y la radiación UVB incidentes en la muestra sean determinadas separadamente y se corrijan por la atenuación por DOM específica para cada longitud de onda. El ratio k_{pdPAR}:k_{pdUVA}:k_{pdUVB} fue de 1:43:3100, dejando patente el alto poder de fotodegradación de la radiación UVB. Estas constantes específicas para

cada longitud de onda permiten la predicción de la tasa de degradación de MeHg sin necesidad de determinaciones experimentales adicionales. Los únicos datos necesarios son la absorción de la luz específica para cada longitud de onda por parte de la DOM y la composición espectral de la luz incidente.
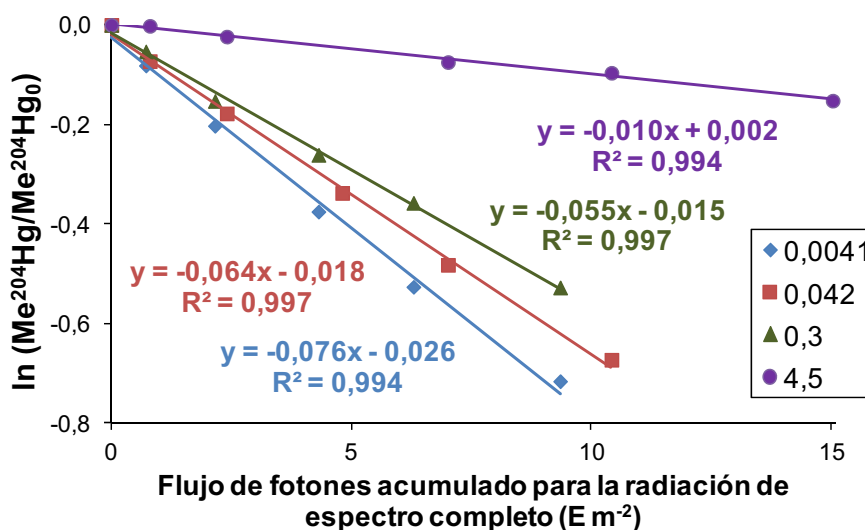
Figura 8. Cinética de primer orden para la fotodegradación de MeHg mediante luz artificial. Se representa la relación entre ln ([Me^{204}Hg]/[Me^{204}Hg$_0$]) y la radiación (PAR+UVA+UVB) acumulada a varios ratios molares MeHg/RSH (en la leyenda) para el agua de ANG. KSN y SKM presentan un comportamiento similar.

Estudio de la fotodegradación de MeHg en aguas continentales y su relación con la biodisponibilidad

El objetivo definitivo de este trabajo fue examinar la relación entre la fotodegradación y la biodisponibilidad del MeHg en agua. Para este fin, se obtuvieron las tasas de fotodegradación de MeHg en seis tipos de agua (natural y artificial) con diferentes características empleando una lámpara de Xenon, y posteriormente se midió la fracción de MeHg lábil mediante la técnica DGT para evaluar la biodisponibilidad. La técnica usada para la determinación de MeHg fue de nuevo SPME-GC-CVAFS.

245

La acción de la luz parece no alterar la labilidad del MeHg (tal como podemos apreciar comparando las columnas M/C (Oscuridad) y M/C (Luz) de la Tabla 2), y consideramos que por extensión, tampoco su biodisponibilidad. Sin embargo, la calidad de la DOM podría ser la principal variable con efecto sobre ella. En lo que refiere a la fotodegradación, este experimento podría confirmar que mientras haya materia orgánica en disolución, la k_{PD} se ve mayoritariamente afectada por la atenuación de la luz debido a la DOM. En cuanto a la labilidad, se han visto diferencias entre las aguas estudiadas, las cuales podrían atribuirse fundamentalmente al tipo de materia orgánica presente en disolución y que se asocia con el MeHg. Ningún estudio sobre el tema de fotodegradación-biodisponibilidad de MeHg había sido llevado a cabo hasta la fecha, por ese motivo se planteó éste como primera aproximación. Aunque los resultados no mostraron una conexión aparente entre los dos fenómenos, permitirán orientar investigaciones futuras en esta línea de trabajo.

Tabla 2. Parámetros de calidad del agua e información sobre la labilidad y biodisponibilidad del MeHg. Concentración de DOC inicial, pH medio a lo largo del proceso de fotodegradación, conductividad, ratios entre la masa de MeHg acumulada por una unidad de DGT (M) y la concentración media de MeHg medida directamente en el agua durante el muestreo (C) y porcentajes de MeHg biodisponible en el control (en oscuridad) y en la muestra expuesta a la luz.

Tipo de agua	[DOC] (mg L^{-1})	pH	Cond, (μS cm^{-1})	M/C (Oscuridad) (cm^3)	M/C (Luz) (cm^3)	% MeHg biodisponible (Oscuridad)	% MeHg biodisponible (Luz)
ANG	9,9	6,7	40	4,6 ± 0,4	4,8 ± 0,8	52 ± 5	55 ± 9
KSN	12,3	5,7	11	4,4 ± 0,4	5,1 ± 0,2	50 ± 5	58 ± 3
SKM	10,1	4,7	12	8,1 ± 1,7	8,9 ± 0,8	92 ± 20	101 ± 9
FLX	2,1	8,3	1010	6,7 ± 1,0	6,1 ± 0,5	76 ± 11	70 ± 5
MQO	9,3	5,4	1150	8,3 ± 1,5	7,8 ± 2,1	95 ± 17	88 ± 24
MQW	-	5,2	1150	6,9 ± 1,8	7,8 ± 1,0	53 ± 14	60 ± 8

Conclusiones

Las conclusiones de esta tesis en lo referente al desarrollo de la técnica DGT son las siguientes:

- Se probó que los muestreadores DGT comerciales específicos para Hg miden de forma efectiva la concentración de Hg disuelto lábil en condiciones de laboratorio. Sin embargo, bajo condiciones ambientales y principalmente en aguas eutróficas, estos muestreadores no mostraron una acumulación sustancial. La razón es su deficiente rendimiento cuando hay DOM presente en la disolución (testado en laboratorio).

- El gel de sílice funcionalizado con grupos 3-mercaptopropil fue satisfactoriamente usado como agente ligante en el gel receptor para la determinación de THg.

- Se demostró que el gel de difusión de poliacrilamida no compite con el gel receptor en la unión de iones de Hg(II).

- Se ha probado que tanto los muestreadores DGT manufacturados en el laboratorio con gel de poliacrilamida (P-DGT) como con gel de agarosa (A-DGT) como gel de difusión, son adecuados para la determinación de la fracción lábil de Hg en agua dulce. Sin embargo, la mejor opción para medir THg y MeHg, considerando su tasa de acumulación, sus blancos y su capacidad discriminatoria entre las especies en disolución, fue el tipo P-DGT.

- La calibración de los muestreadores DGT en presencia de DOM y simulando las características del agua que será muestreada, es necesaria para la aplicación de los mismos para el correcto monitoreo de la concentración de Hg lábil en aguas naturales.

- El coeficiente de difusión obtenido en la presencia de DOM para MeHg (DMeHg-DOM) fue mayor que para Hg(II) (DHg(II)-DOM), lo que sugiere que los complejos MeHg-DOM son más lábiles que los Hg(II)–DOM. Este hecho, confirma la importancia de calibrar los muestreadores DGT usando las especies de interés.

- La técnica DGT fue usada satisfactoriamente para determinar la concentración de THg y MeHg lábil en un estudio en el cual se trataba de evaluar la eliminación y metilación de Hg en una planta experimental para el tratamiento de agua residual urbana conformada por varios humedales construidos en serie.

Las conclusiones respecto a la eliminación de Hg en la planta experimental para tratamiento de aguas residuales son las que siguen:

- La planta de tratamiento parece eliminar eficientemente el THg disuelto (75% de eliminación) y el Hg lábil (90%) del agua residual tratada.
- La eliminación del MeHg disuelto total fue del 92-96%, y la del MeHg lábil, del 66%.
- Se demostró la capacidad de eliminación de Hg por parte de configuración de planta de tratamiento, aunque se deberían hacer varios ajustes en el diseño dependiendo de la carga de Hg del influente.

Las principales conclusiones en lo que concierne a los estudios de fotodegradación de MeHg son las expuestas a continuación:

- Mientras que la constante de velociadad de fotodegradación de MeHg (kpd Full Spectrum) varió significativamente entre las aguas estudiadas, las constantes específicas para cada longitud de onda (kpd PAR, kpd UVA and kpd UVB) fueron indistinguibles para las mismas aguas.
- Cuando el ratio molar MeHg/grupos tiol (RSH) se aumentó hasta alcanzar valores superiores a uno, se observó una disminución drástica en kpd Full Spectrum.
- Mientras que la formación de radicales orgánicos y ROS por parte de la DOM exceda la producción de ROS generada por otros compuestos, la atenuación de la luz y de ROS por parte de la DOM controlarán la tasa de fotodegradación de MeHg.

- $k_{pd\ PAR}$, $k_{pd\ UVA}$ y $k_{pd\ UVB}$ pueden ser consideradas universales en aguas con altos contenidos en DOM siempre que la PAR, la radiación UVA y la radiación UVB sean determinadas separadamente y se corrijan por la atenuación por DOM específica para cada longitud de onda.

- El ratio $k_{pd\ PAR}$:$k_{pd\ UVA}$:$k_{pd\ UVB}$ fue 1:43:3100, demostrando el alto poder de fotodegradación de la radiación UVB.

- Estas $k_{pd\ PAR}$, $k_{pd\ UVA}$ y $k_{pd\ UVB}$ permiten la predicción de la tasa de degradación de MeHg sólo conociendo la absorción de la luz específica para cada longitud de onda por parte de la DOM y la composición espectral de la luz incidente.

Finalmente, la principal conclusión en referencia al efecto de la fotodegradación en la labilidad del MeHg es la siguiente:

- La acción de la luz solar parece no afectar a la labilidad del MeHg, y por tanto, a su biodisponibilidad.

ANNEXES

ANNEX I

I   MeHg determination in sediments

I.1   Extraction of MeHg

The sediment sample was weighed (~100 mg) in a 30 mL Teflon vial. Subsequently, 10 ml of Milli-Q water, 0.5 ml of 9M H_2SO_4 aqueous solution and 0.2 ml of KCl (20% w/v) aqueous solution were added and the vial was capped. 5 ml of Milli-Q water were added to another vial (receiving vial). The sample vial was placed in the heating block (140 °C) and connected with the corresponding receiving vial using Teflon tubing. A N_2 gas flow (50-60 Ml min^{-1}) carried the distillate to the receiving vial until the 85-90% of the original volume was distilled. Then, the receiving vial was closed with a Teflon cap, covered with aluminium foil and stored at 4 °C in darkness until analysis (within a week). Two distillation blanks were prepared for each batch of analysis in the same manner as the samples. 50-100 mg of CRM for trace elements and MeHg in estuarine sediment IAEA-405 (IAEA, Vienna, Austria) were distilled in triplicate in order to establish the recovery of the method, that resulted to be of 79%.

I.2   Pre-concentration in Tenax traps and detection by GC-Py-AFS

In order to accomplish the MeHg determination, the distillate was ethylated using NaBEt$_4$. Ethylated Hg species are volatile, and therefore EtMeHg was purged from the solution at room-temperature and collected on a Tenax trap. After thermal release, individual mercury compounds are separated by GC.

Milli-Q water and an aliquot of the distillate (approx. 100 mL in total) were added to a bubbler (glass flask). Acetate buffer (2M, 200 µL) and NaBEt$_4$ (1%, 100 µL) were added directly into the bubbler. NaBEt$_4$ was stored in the freezer in darkness, and was allowed to reach room temperature a few minutes before use. A fresh vial of reagent was used for each batch of analysis and the aliquot was added as quickly as possible.

The bubbler was sealed at the gas inlet with a cap and gently swirled to ensure sample homogenisation, and a Tenax (20/35 mesh, Mandel, Alltech) trap was attached to the exit port. The mixture was allowed to react for 20 minutes. Later, a N_2 gas line (100-150 mL min^{-1}) was connected to the bubbler for 20 minutes. After that, the trap was removed and brought to the GC. One bubbler blank using only Milli-Q water and the reagents was prepared with each bubbling batch. A six-point calibration curve from 50 to 1000 pg of MeHg (as Hg) was prepared with a MeHgCl standard.

The Tenax trap was placed in line with the GC packed column, filled with with 15% OV-3 on Chemosorb W-AW (DMCS) 80/100 and kept at 105 °C. The trap was heated for 30 seconds (to reach a peak temperature of 200 ºC) and an argon stream (40 mL min^{-1}) carried the Hg species through the GC column –to be separated– and the pyrolyser –to be reduced to Hg^0– to the AFS detector.

The MeHg mass in the sample was quantified and corrected by the recovery yield by the CRM analysis. The MeHg concentration in the sediments was calculated after the correction by the moisture content of the samples.

Table I.1. Concentration of THg and MeHg in sediments and the percentage of total Hg as MeHg.

	THg ($\mu g\ g^{-1}$)[a]	MeHg ($ng\ g^{-1}$)	% MeHg/THg
Búbal (BU)	0.0375 ± 0.0013	0.250 ± 0.002	0.67
Sabiñánigo (SA)	1.657 ± 0.036	5.59 ± 0.28	0.34
Jabarrella (JB)	0.308 ± 0.011	22.18 ± 1.47	7.19
Flix wastes (FW)	49.4 ± 2.0	59.6 ± 17.0	0.12
Ascó (AS)	1.05 ± 0.04	2.11 ± 0.60	0.20

[a]measurements done with AMA-254

ANNEX II

II   Supplementary work for the MeHg photodegradation study

In this annex, I wanted to include all the additional work done to complete the study reported in chapter 6. Although I participated in the majority of the tasks described below, most of the work was done by other researchers: Solomon Tesfalidet (section II.1), Ulf Skyllberg and Andreas Drott (sections II.2 and II.4), and Anders Lindfors (section II.3).

II.1   Determination of organic radical concentration by EPR

Electron spin resonance spectroscopy (EPR) was used to measure the organic radicals content of humic substances. This method has previously been used as a measure of the quinone content in humic substances (Senesi and Steelink, 1989). The measurements were carried out using a Bruker Elexys E 500 spectrometer. The EPR signals were recorded at room temperature with the following settings: microwave power 0.6 mW; sweep time 20.97 s; sweep width 500 G; center field 3497 G; conversion time 10.24 ms; modulation frequency 100 KHz; modulation amplitude 5G; microwave frequency 9.789 GHz. A standard, 3-Carbamoyl-2,2,5,5-tetramethyl-3-pyrrolin-1-oxyl, was used to determine the g coefficient (g = 2.006) and concentration of spins. The total mass of freeze dried material obtained form 1 L of original water sample was dissolved in 0.1M NaOH and filled in glass capillaries. The capillaries were inserted into a standard EPR cavity and irradiated with a lamp (Repti Glo* 10.0 UVB, 20 W, 60 cm, Exoterra), which was hold at a distance of 45 cm from the cavity. Measurements were made every 5 minutes for a total of 30 minutes while irradiating with the fluorescent lamp.
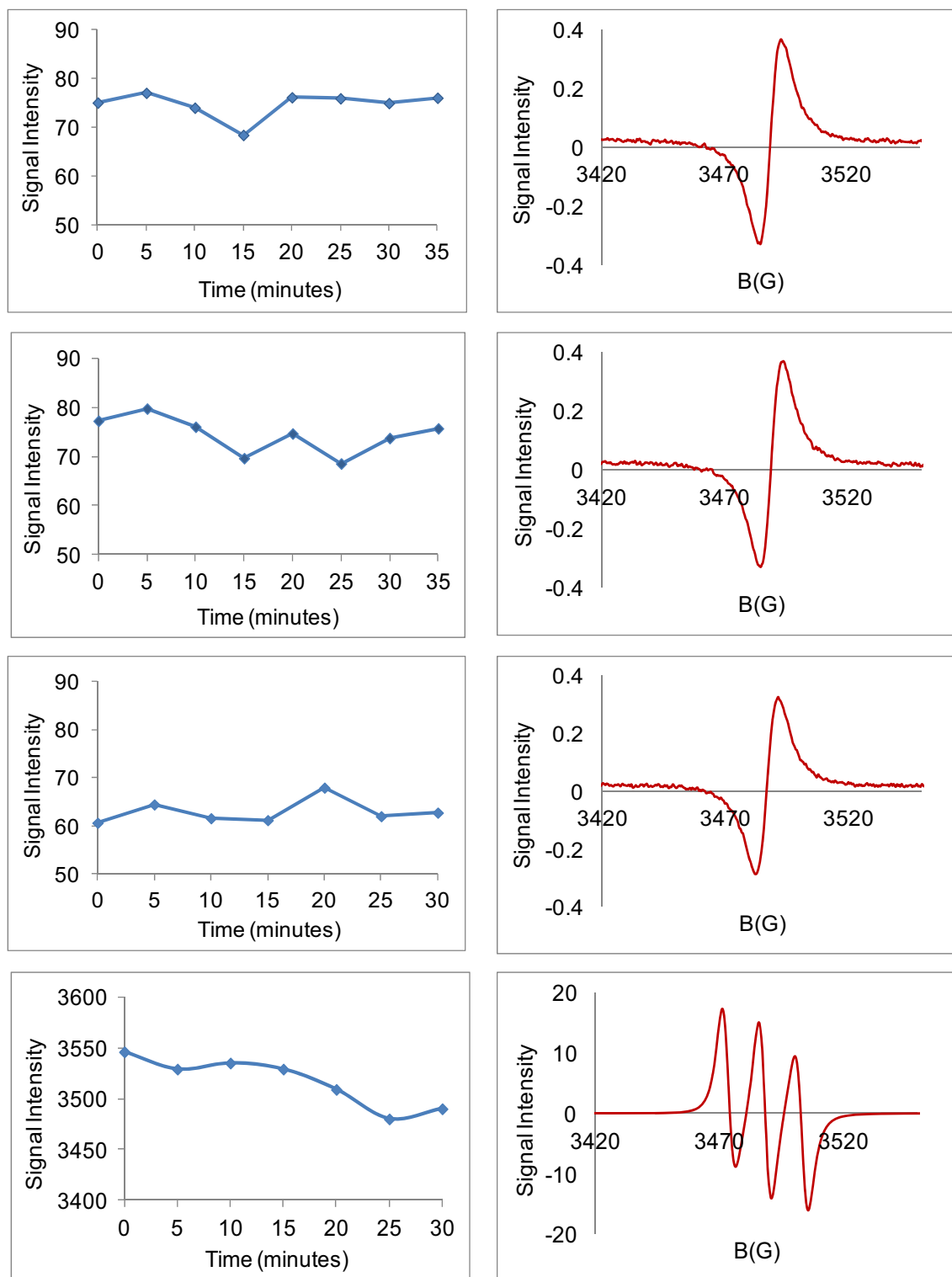
Figure II.1. EPR signal intensity versus time and magnetic field (B) with the units in Gauss. From top to bottom: site ANG, KSN, SKM and the 3-carbamoyl-2,2,5,5-tetramethyl-3-pyrrolin-1-oxyl model compound.

II.2 Determination of organic thiol groups by sulfur K-edge XANES

Freeze dried material from the original water samples was characterised by sulfur K-edge XANES at beamline i811 at MAX-lab, Lund, Sweden. Data were collected in fluorescence mode using a PIPS detector and each spectrum was an average of at least 10 scans collected in a quick scan mode covering the energy range of 2460 to 2500 eV. The maximum of the first peak of the $Na_2S_2O_3$ S XANES spectrum was set to 2472.0 eV. The method of spectral deconvolution as described by Yekta et al. (2012) and the relationship between X-ray absorption cross section and electronic oxidation state as reported by Xia et al. (1998) were used to calculate the relative composition of major sulfur forms in the freeze dried samples. Absolute concentrations of sulfur forms were then obtained by multiplication by total S (as determined by LECO analyzer). In agreement with Qian et al. (2002) the concentration of thiol groups (RSH) with a high affinity for MeHg was calculated as 30% of reduced organic S functionalities represented by gaussian peaks with a maximum between 2472 and 2474 eV. Finally, in order to calculate the concentration of RSH (mol L^{-1}) in the original water sample, the ratio of total organic C (as determined by LECO analyzer) and sulfate (as determined by S XANES) in the freeze dried sample was used an related to the measured TOC to sulfate ratio in the water sample.
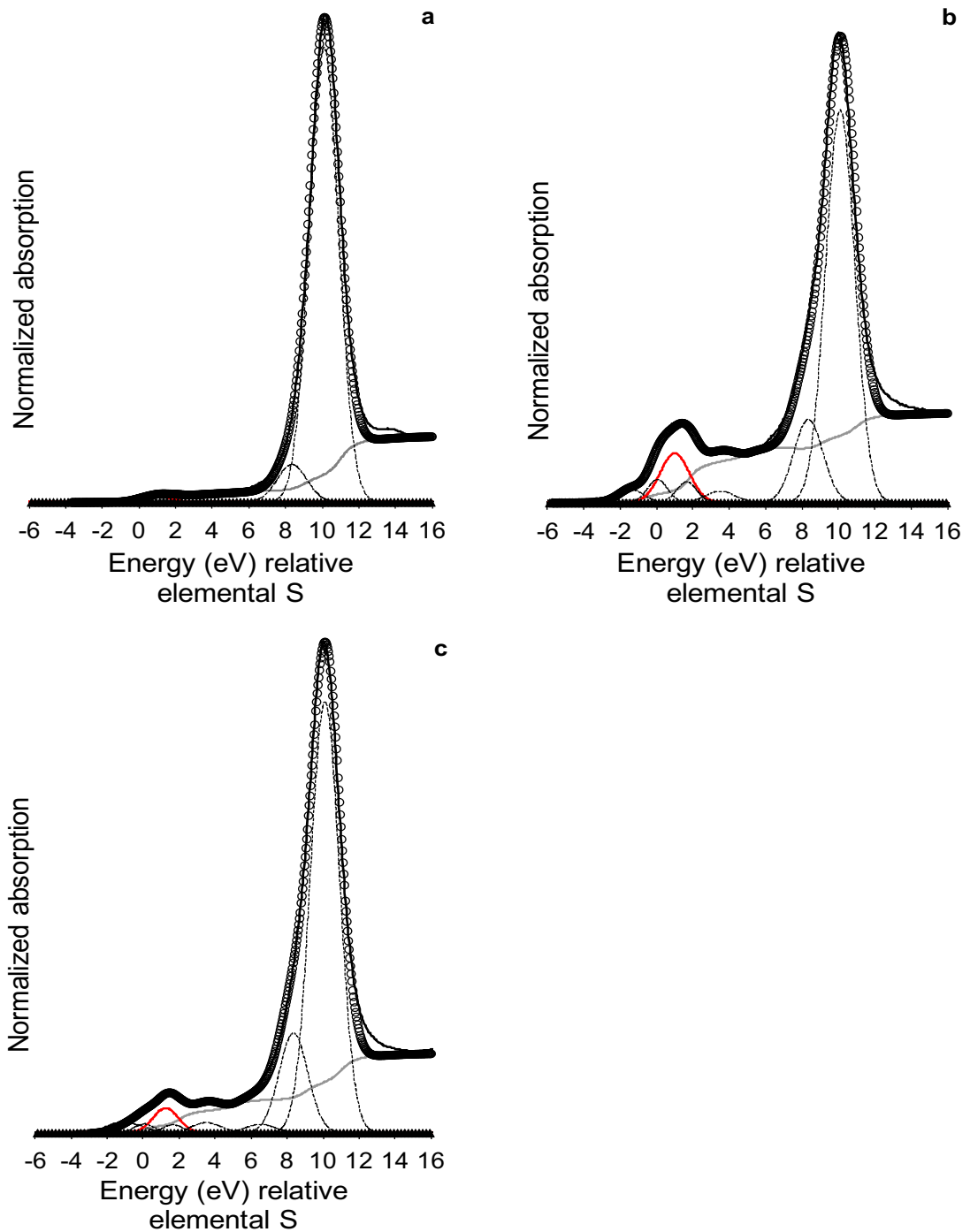
Figure II.2. Sulfur K-edge XANES spectra for site ANG (a), KSN (b) and SKM (c). The red Gaussian curve represents organically reduced S, 30% of which is estimated to be RSH (thiols). Because of a dilution of organic S (in DOM) by inorganic sulfate in the original water sample, the relative error in the estimate of RSH is about ±50%.

II.3   Modelling of spectral composition of sunlight in experiment #1

We performed radiative transfer simulations similar to those of Lindfors et al. (2009) in order to estimate the contribution by PAR (400–700 nm), UVA (320–400 nm) and UVB (280–320 nm) to the radiation received at the surface. The method of Lindfors et al. (2009) was originally developed for estimating the spectral UV radiation at the surface based on (1) the effective cloud optical depth as inferred from pyranometer measurements of global radiation (solar surface radiation, integrated over 300–3000 nm); (2) the total ozone column; (3) the surface albedo as estimated from measurements of snow depth; and (4) the total water vapor column. Here, we have extended the method to cover wavelengths from the UV up to 800 nm. We set all input parameters to values representative for Umeå in October: the total ozone column was chosen to be 290 DU, the water vapor column was set to 12 kg m^{-2}, and the surface albedo to 0.05 representative for snow-free conditions.

Previous validation results of the method show a good agreement with spectral UV measurements at the surface: the correlation coefficient for daily cumulative irradiances is around 0.99 or higher, while the mean percentage difference is mostly within ±8% (Morris et al., 1995). In contrast to Lindfors et al. (2009), we did not use pyranometer measurements for estimating the effective cloud optical depth and therefore we do not account for the true cloud effect in our calculations. Instead, we performed two separate radiative transfer simulations: (i) assuming cloud-free skies, and (ii) assuming a cloud attenuation roughly typical for the time of the year. Therefore, the absolute radiation level cannot be thought to realistically represent the radiation conditions at the surface. However, the relative contribution by PAR, UVA and UVB is much less sensitive to variations in cloudiness, and therefore is expected to be fairly accurate. Figure II.3 shows the simulated spectra for Umeå in October assuming cloud-free skies (upper panel) and with a typical cloud cover (lower panel).
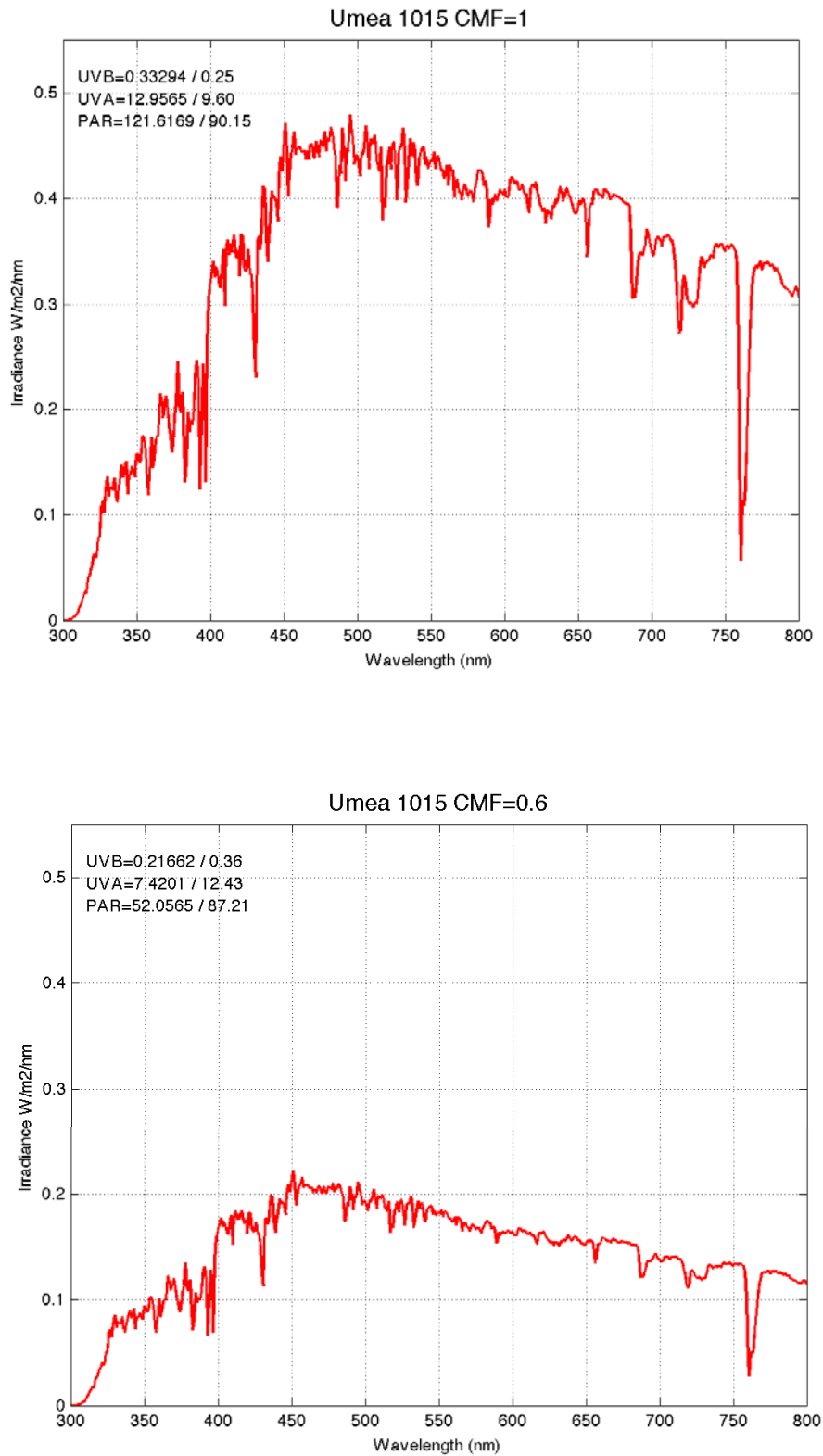
Figure II.3. Average sunlight spectra calculated for Umeå in October, 2011 with no clouds (top) and with tyoical cloud cover (bottom). Data recalculated to photon flux resulted in an average relative photon flux of PAR (400–700 nm), UVA (320–400 nm) and UVB (280–320 nm) of 92.3%, 7.5% and 0.17%, respectively.

II.4 Spectral composition of the lamp in experiment #2

The spectrum of the artificial UV lamp used in experiment #2 was determined by a ILT 900-R spectroradiometer (Internatinal Light Technologies, Peabody, MA, USA). The data was recalculated to photon flux (E m^{-2}) and integrated for the three spectral regions correspond to 91.6% PAR (400-700 nm), 6.3% UVA (320-400 nm) and 2.1% UVB (280-320 nm).
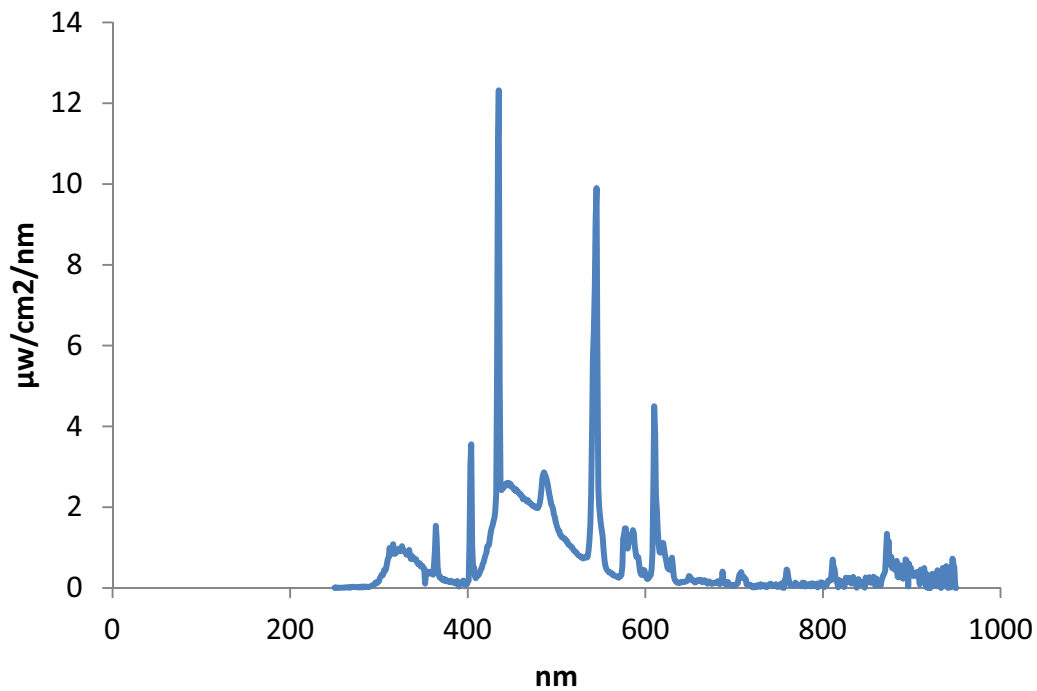
Figure II.4. Power spectrum of artificial UV lamp used in experiment #2.

II.5 Changes in UV absorbance and pH during the course of experiment #2

pH and SUVA$_{254nm}$ were measured in the water samples as described in section 6.4.3. In experiment #2, the high UVB intensity caused a loss of absorbance at 254 nm during the course of the experiment. Also, a slight decrease of pH can be noted in several cases.

(a)

(b)

(c)

(d)
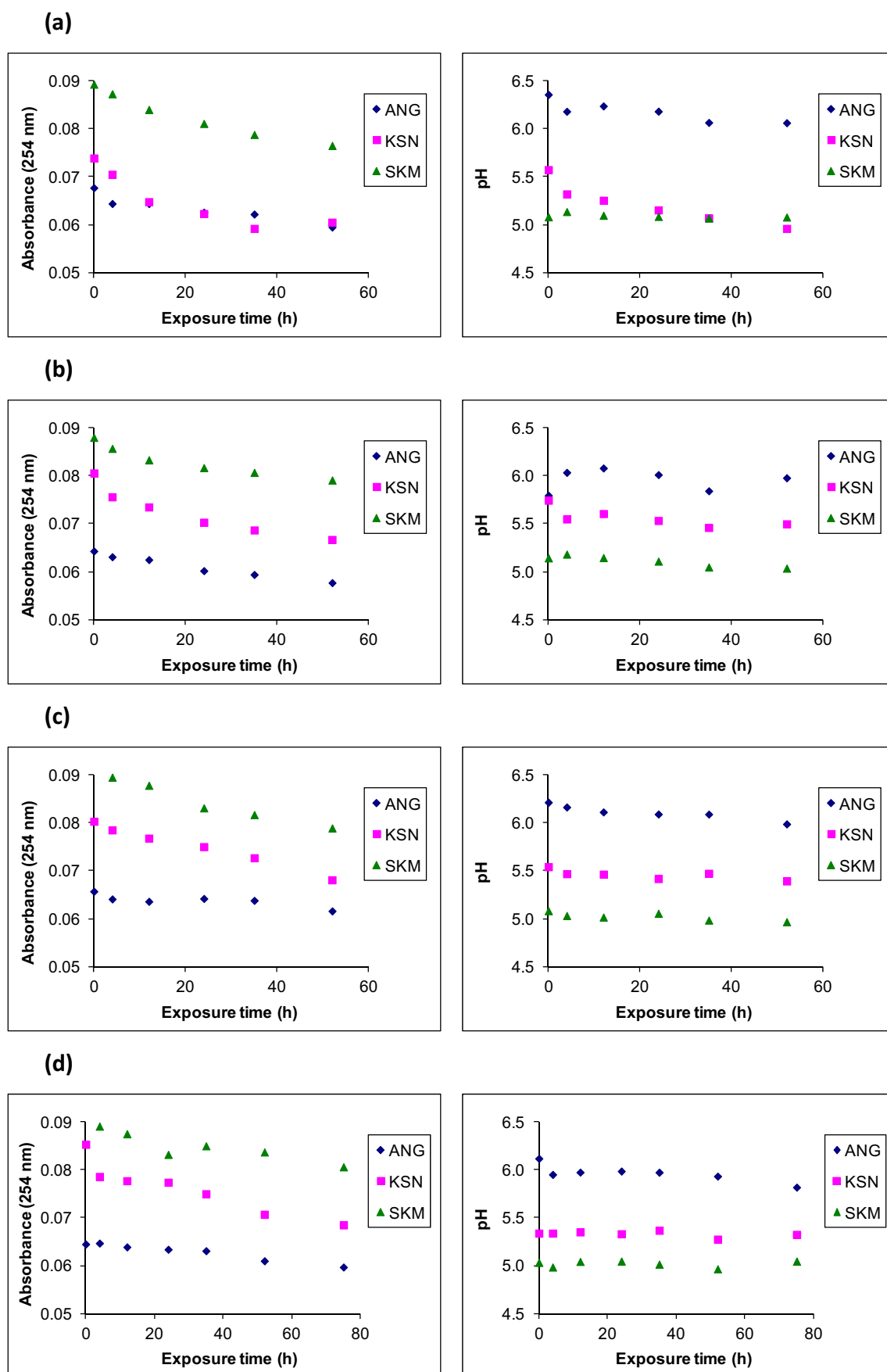
Figure II.5. Changes in UV absorbance and pH during the course of experiment #2 at MeHg to RSH molar ratios of: 0.0041 – 0.021 (a), 0.042 – 0.21 (b), 0.3 – 1.5 (c), and 4.5 – 23 (d).

ANNEX III: LIST OF PUBLICATIONS

Development of the DGT technique for Hg measurement in water:
Comparison of three different types of samplers in laboratory assays

C. Fernández-Gómez, B. Dimock, H. Hintelmann, S. Díez

Abstract

The Diffusive Gradients in Thin films (DGT) technique is an operationally defined method to determine the dissolved fraction of trace elements in water. The aim of this study was to develop this technique for the measurement of the bioavailable mercury species in natural waters. For that purpose, three types of DGT units (commercial, manufactured with agarose diffusive gel (DG) and manufactured with polyacrylamide DG) were tested under controlled conditions using an Hg(II) solution both with and without dissolved organic matter (DOM). An acid digestion method using aqua regia was optimised to efficiently digest the resin gel discs prior to analysis. A good performance was obtained for the three DGT types when deployed in a DOM-free mercury solution in the laboratory, and it was demonstrated that polyacrylamide gel can be used as diffusive layer for mercury sampling. However, when the DGT units were deployed in a mercury solution containing DOM, performance differences were observed. Furthermore, the mass of background mercury (blanks) varied among the different DGT types. In the light of the results, the devices manufactured with polyacrylamide DG seemed to be the best choice for dissolved mercury determination.

Laboratory and field evaluation of diffusive gradient in thin films (DGT) for monitoring levels of dissolved mercury in natural river water

Cristal Fernández-Gómez, Josep M. Bayona and Sergi Díez

Abstract

The diffusive gradient in the thin films (DGT) technique was tested to measure dissolved mercury (Hg) both in laboratory aqueous solutions and in situ in river water. For this purpose, a commercial ready-to-use and specific-for-Hg DGT device was used. Each sampler consisted of a filter membrane-agarose gel as the diffusive layer and a Spheron-Thiol resin in polyacrylamide gel as the binding agent. Basic performance assays at the laboratory with this type of DGT unit confirmed the applicability of Fick's first law for DGT measurements. The diffusion coefficient of MeHg in the agarose diffusive gel was 8.50×10^{-6} cm^2 s^{-1} at 25 °C. Several field studies were also carried out in two different rivers of the Ebro River basin (NE Spain) affected by Hg wastes released by the chlor-alkali industry. Hg concentrations determined by DGT were generally much lower than the results obtained through direct measurements of the river water. In addition, the results of a time series experiment also performed in the field show that the amount of Hg accumulated in the resin does not increase at all with the exposure time. This may be explained by the underestimation of the truly dissolved Hg fraction due to the formation of a biofilm layer on the surface of the samplers, thus clogging the filter and preventing Hg species from diffusing through it. Consequently, it was demonstrated that the DGT technique presents important limitations for measuring Hg in polluted rivers characterised by a high biomass load (eutrophic), whereas its performance was demonstrated to be correct in oligotrophic waters.

264

Fotodegradació de metilmercuri en llacs i aiguamolls

Photodegradation of methylmercury in lakes and wetlands

Cristal Fernández-Gómez, Josep M. Bayona i Sergi Díez

Abstract

El metilmercuri (MeHg) és un contaminant perillós, atesa la seva demostrada neurotoxicitat, i és actualment motiu d'una gran preocupació ambiental en sistemes aquàtics de tot el món. La degradació del MeHg en l'aigua és un procés crucial en el cicle biogeoquímic del mercuri, però avui dia no tots els mecanismes implicats es coneixen en profunditat. Encara que s'ha observat desmetilació microbiana tant en sediments com a la columna d'aigua, generalment es considera que la fotodegradació és la via d'eliminació de MeHg dominant en aigües continentals exposades a la llum solar. En el present article, repassarem les troballes més importants en aquest àmbit i discutirem els diferents factors que afecten la fotodegradació de MeHg en llacs i aiguamolls.

Methylmercury (MeHg) is a hazardous pollutant due to its proved neurotoxicity, so it is a subject of increasing environmental concern in aquatic systems all around the world. MeHg degradation in water is a crucial process in the mercury biogeochemical cycle but not all the mechanisms involved are as yet fully known. Although microbial demethylation of MeHg was observed both in sediment and water column, photodegradation is commonly considered to be the main pathway of MeHg removal in continental waters exposed to sunlight. In this paper the most significant findings on this issue are reviewed and the different factors affecting MeHg photodecomposition in lakes and wetlands are discussed.

Towards Universal Wavelength-Specific Photodegradation Rate Constants for Methyl Mercury in Humic Waters, Exemplified by a Boreal Lake-Wetland Gradient

Cristal Fernández-Gómez, Andreas Drott, Erik Björn, Sergi Díez, Josep M. Bayona, Solomon Tesfalidet, Anders Lindfors, and Ulf Skyllberg

Abstract

We report experimentally determined first-order rate constants of MeHg photolysis in three waters along a Boreal lake-wetland gradient covering a range of pH (3.8–6.6), concentrations of total organic carbon (TOC 17.5–81 mg L^{-1}), total Fe (0.8–2.1 mg L^{-1}), specific UV254 nm absorption (3.3–4.2 L mg^{-1} m^{-1}) and TOC/TON ratios (24–67 g g^{-1}). Rate constants determined as a function of incident sunlight (measured as cumulative photon flux of photosynthetically active radiation, PAR) decreased in the order dystrophic lake > dystrophic lake/wetland > riparian wetland. After correction for light attenuation by dissolved natural organic matter (DOM), wavelengthspecific (PAR: 400–700 nm, UVA: 320–400 nm and UVB: 280–320 nm) firstorder photodegradation rate constants (kpd) determined at the three sites were indistinguishable, with average values (±SE) of 0.0023 ± 0.0002, 0.10 ± 0.024 and 7.2 ± 1.3 m^2 E^{-1} for kpdPAR, kpdUVA, and kpdUVB, respectively. The relative ratio of k_{pdPAR}, k_{pdUVA}, and k_{pdUVB} was 1:43:3100. Experiments conducted at varying MeHg/TOC ratios confirm previous suggestions that complex formation with organic thiol groups enhances the rate of MeHg photodegradation, as compared to when O and N functional groups are involved in the speciation of MeHg. We suggest that if the photon fluxes of PAR, UVA, and UVB radiation are separately determined and the wavelength-specific light attenuation is corrected for, the first-order rate constants kpdPAR, kpdUVA, and kpdUVB will be universal to waters in which DOM (possibly in concert with Fe) controls the formation of ROS, and the chemical speciation of MeHg is controlled by the complexation with DOM associated thiols.

Passive sampling for inorganic contaminants in water. Chapter 1.15 in

Comprehensive Sampling and Sample Preparation

C. Fernández-Gómez, H. Hintelmann and S. Díez

Abstract

The current state of the art in passive sampling technology for environmental monitoring of inorganic pollutants (e.g., trace elements and nutrients) in aqueous matrices is discussed. Since they were invented almost four decades ago for monitoring air quality, passive dosimeters have found widespread use in monitoring organic and inorganic contaminants in air, water, sediments, and soils. This chapter describes major evolutionary milestones in passive sampling technology and focuses on its application for unique monitoring of inorganic pollutants in aqueous environments. An overview of sampling theory is provided, strategies for sampler design are examined, and calibration schemes are discussed. Passive sampling approaches using biosamplers and intrinsic advantages and challenges are discussed. A description of the most important passive sampling devices, with special attention to diffusive gradient in thin films, is followed by applications for group and individual speciation. The chapter concludes with a discussion on field study considerations, speciation, and future trends.

REFERENCES

Aberg, B., Ekman, L., Falk, R., Greitz, U., Persson, G. and Snihs, J. O. **1969**. Metabolism of methyl mercury (203Hg) compounds in man – Excretion and distribution, *Archives of Environmental Health 19*, 478.

Abuin, M., Carro, A. M. and Lorenzo, R. A. **2000**. Experimental design of a microwave-assisted extraction-derivatization method for the analysis of methylmercury, *Journal of Chromatography A 889*, 185-193.

Aguilar-Martínez, R. **2010**. Desarrollo del muestreador pasivo Chemcatcher para la monitorización y cuantificacion mediante GC-ICP-MS de mercurio y compuestos organoestánnicos en medios acuáticos. Tesis Doctoral, Universidad Complutense de Madrid, Madrid.

Aguilar-Martinez, R., Greenwood, R., Mills, G. A., Vrana, B., Palacios-Corvillo, M. A. and Gomez-Gomez, M. M. **2008**. Assessment of Chemcatcher passive sampler for the monitoring of inorganic mercury and organotin compounds in water, *International Journal of Environmental Analytical Chemistry 88*, 75-90.

Alegria, A. E., Ferrer, A. and Sepulveda, E. **1997**. Photochemistry of water-soluble quinones. Production of a water-derived spin adduct, *Photochemistry and Photobiology 66*, 436-442.

Allan, I. J., Knutsson, J., Guigues, N., Mills, G. A., Fouillac, A.-M. and Greenwood, R. **2008**. Chemcatcher (R) and DGT passive sampling devices for regulatory monitoring of trace metals in surface water, *Journal of Environmental Monitoring 10*, 821-829.

Alli, A., Jaffe, R. and Jones, R. **1994**. Analysis of organomercury compounds in sediments by capillary GC with atomic fluorescence detection, *Hrc-Journal of High Resolution Chromatography 17*, 745-748.

Alvarez, D. A., Stackelberg, P. E., Petty, J. D., Huckins, J. N., Furlong, E. T., Zaugg, S. D. and Meyer, M. T. **2005**. Comparison of a novel passive sampler to standard water-column sampling for organic contaminants associated with wastewater effluents entering a New Jersey stream, *Chemosphere 61*, 610-622.

Alvarez, R., Ordonez, A., Loredo, J. and Younger, P. L. **2013**. Wetland-based passive treatment systems for gold ore processing effluents containing residual cyanide, metals and nitrogen species, *Environmental Science-Processes & Impacts 15*, 2115-2124.

Amirbahman, A., Massey, D. I., Lotufo, G., Steenhaut, N., Brown, L. E., Biedenbach, J. M. and Magar, V. S. **2013**. Assessment of mercury bioavailability to benthic

macroinvertebrates using diffusive gradients in thin films (DGT), *Environmental science. Processes & impacts 15*, 2104-14.

Amirbahman, A., Reid, A. L., Haines, T. A., Kahl, J. S. and Arnold, C. **2002**. Association of methylmercury with dissolved humic acids, *Environmental Science & Technology 36*, 690-695.

Amos, H. M., Jacob, D. J., Streets, D. G. and Sunderland, E. M. **2013**. Legacy impacts of all-time anthropogenic emissions on the global mercury cycle, *Global Biogeochemical Cycles 27*, 410-421.

Amouroux, D., Tessier, E., Pecheyran, C. and Donard, O. F. X. **1998**. Sampling and probing volatile metal(loid) species in natural waters by in-situ purge and cryogenic trapping followed by gas chromatography and inductively coupled plasma mass spectrometry (P-CT-GC-ICP/MS), *Analytica Chimica Acta 377*, 241-254.

Amyot, M., Lean, D. and Mierle, G. **1997**. Photochemical formation of volatile mercury in high Arctic lakes, *Environmental Toxicology and Chemistry 16*, 2054-2063.

Amyot, M., Mierle, G., Lean, D. R. S. and McQueen, D. J. **1994**. Sunlight-induced formation of dissolved gaseous mercury in lake waters, *Environmental Science & Technology 28*, 2366-2371.

Amyot, M., Southworth, G., Lindberg, S. E., Hintelmann, H., Lalonde, J. D., Ogrinc, N., Poulain, A. J. and Sandilands, K. A. **2004**. Formation and evasion of dissolved gaseous mercury in large enclosures amended with (HgCl2)-Hg-200, *Atmospheric Environment 38*, 4279-4289.

Anjum, N. A., Ahmad, I., Valega, M., Pacheco, M., Figueira, E., Duarte, A. C. and Pereira, E. **2012**. Salt marsh macrophyte Phragmites australis strategies assessment for its dominance in mercury-contaminated coastal lagoon (Ria de Aveiro, Portugal), *Environmental Science and Pollution Research 19*, 2879-2888.

APHA. **2001**. *Standard Methods for the Examination of Water and Wastewater*; American Public Health Association: Washington, DC, USA.

Arroyo, P., Ansola, G. and Saenz de Miera, L. E. **2013**. Effects of substrate, vegetation and flow on arsenic and zinc removal efficiency and microbial diversity in constructed wetlands, *Ecological Engineering 51*, 95-103.

Arthur, C. L. and Pawliszyn, J. **1990**. Solid-phase microextraction with thermal-desorption using fused-silica optical fibers, *Analytical Chemistry 62*, 2145-2148.

Atallah, R. H. and Kalman, D. A. **1993**. Selective determination of inorganic mercury and methylmercury in tissues by continuous-flow and cold vapour atomic-absorption spectrometry, *Journal of Analytical Toxicology 17*, 87-92.

ATSDR. **1999**. *Toxicological profile for mercury*; Agency for toxic substances and disease registry. United States Department of Health and Human Services.

Avila, C., Matamoros, V., Reyes-Contreras, C., Piña, B, Casado, M., Mita, L., Rivetti, C., Barata. C., García, J., Bayona, J. M. **2014.** Attenuation of emerging organic contaminants in a hybrid constructed wetland system under different hydraulic loading rates and their associated toxicological effects in wastewater, *Science of the Total Environment 470-471*, 1272-1280.

Azaizeh, H., Linden, K. G., Barstow, C., Kalbouneh, S., Tellawi, A., Albalawneh, A. and Gerchman, Y. **2013**. Constructed wetlands combined with UV disinfection systems for removal of enteric pathogens and wastewater contaminants, *Water Science and Technology 67*, 651-657.

Bade, R., Oh, S. and Shin, W. S. **2012**. Diffusive gradients in thin films (DGT) for the prediction of bioavailability of heavy metals in contaminated soils to earthworm (Eisenia foetida) and oral bioavailable concentrations, *Science of the Total Environment 416*, 127-136.

Benes, P. and Steinnes, E. **1974**. Insitu dialysis for determination of state of trace-elements in natural-waters, *Water Research 8*, 947-953.

Benoit, J. M., Gilmour, C. C. and Mason, R. P. **2001**. The influence of sulfide on solid phase mercury bioavailability for methylation by pure cultures of Desulfobulbus propionicus (1pr3), *Environmental Science & Technology 35*, 127-132.

Bertilsson, S. and Tranvik, L. J. **2000**. Photochemical transformation of dissolved organic matter in lakes., *Limnology and Oceanography 45*, 753-762.

Bhatia, M. and Goyal, D. **2014**. Analyzing Remediation Potential of Wastewater Through Wetland Plants: A Review, *Environmental Progress & Sustainable Energy 33*, 9-27.

Biester, H., Gosar, M. and Covelli, S. **2000**. Mercury speciation in sediments affected by dumped mining residues in the drainage area of the Idrija mercury mine, Slovenia, *Environmental Science & Technology 34*, 3330-3336.

Bisinoti, M. C., Junior, E. S. and Jardim, W. F. **2007**. Seasonal behavior of mercury species in waters and sediments from the Negro river Basin, Amazon, brazil, *Journal of the Brazilian Chemical Society 18*, 544-553.

Bjorklund Blom, L., Morrison, G. M., Segura Roux, M., Mills, G. and Greenwood, R. **2003**. Metal diffusion properties of a Nafion-coated porous membrane in an aquatic passive sampler system, *J Environ Monit 5*, 404-9.

Bjorn, E., Larsson, T., Lambertsson, L., Skyllberg, U. and Frech, W. **2007**. Recent advances in mercury speciation analysis with focus on spectrometric methods and enriched stable isotope applications, *Ambio 36*, 443-451.

Black, F. J., Conaway, C. H. and Flegal, A. R. **2009**. Stability of Dimethyl Mercury in Seawater and Its Conversion to Monomethyl Mercury, *Environmental Science & Technology 43*, 4056-4062.

Black, F. J., Poulin, B. A. and Flegal, A. R. **2012**. Factors controlling the abiotic photo-degradation of monomethylmercury in surface waters, *Geochimica Et Cosmochimica Acta 84*, 492-507.

Blom, L. B., Morrison, G. M., Kingston, J., Mills, G. A., Greenwood, R., Pettersson, T. J. R. and Rauch, S. **2002**. Performance of an in situ passive sampling system for metals in stormwater, *Journal of Environmental Monitoring 4*, 258-262.

Bloom, N. **1989**. Determination of picogram levels of methylmercury by aqueous phase ethylation, followed by cryogenic gas-chromatography with cold vapor atomic fluorescence detection, *Canadian Journal of Fisheries and Aquatic Sciences 46*, 1131-1140.

Bloom, N. S. **1992**. On the chemical form of mercury in edible fish and marine invertebrate tissue, *Canadian Journal of Fisheries and Aquatic Sciences 49*, 1010-1017.

Boullemant, A., Vigneault, B., Fortin, C. and Campbell, P. G. C. **2004**. Uptake of neutral metal complexes by a green alga: Influence of pH and humic substances, *Australian Journal of Chemistry 57*, 931-936.

Bradac, P., Behra, R., Sigg, L. **2009.** Accumulation of Cadmium in Periphyton under Various Freshwater Speciation Conditions. *Environmental Science & Technology.* **2009,** *43*, 7291-7296.

Brandt, K. K., Holm, P. E. and Nybroe, O. **2008**. Evidence for bioavailable copper-dissolved organic matter complexes and transiently increased copper bioavailability in manure-amended soils as determined by bioluminescent bacterial biosensors, *Environmental Science & Technology 42*, 3102-3108.

Brezonik, P. L. and Fulkerson-Brekken, J. **1998**. Nitrate-induced photolysis in natural waters: Controls on concentrations of hydroxyl radical photo-intermediates by natural scavenging agents, *Environmental Science & Technology 32*, 3004-3010.

Brix, H. **1987**. Treatment of waste-water in the rhizosphere of wetland plants – The root-zone method, *Water Science and Technology 19*, 107-118.

Brown, S., Gustin, M. and Saito, L. **2005**. Characterization of mercury and water quality in Steamboat Creek and Wetland mesocosm, *Nevada Water Resources Association 3*, 41-63.

Brumbaugh, W. G., Petty, J. D., Huckins, J. N. and Manahan, S. E. **2002**. Stabilized liquid membrane device (SLMD) for the passive, integrative sampling of labile metals in water, *Water Air and Soil Pollution 133*, 109-119.

Brumbaugh, W. G., Petty, J. D., May, T. W. and Huckins, J. N. **2000**. A passive integrative sampler for mercury vapor in air and neutral mercury species in water, *Chemosphere: Global Science Change 2*, 1-9.

Brun, L. A., Maillet, J., Hinsinger, P. and Pepin, M. **2001**. Evaluation of copper availability to plants in copper-contaminated vineyard soils, *Environmental Pollution 111*, 293-302.

Buffle, J., Parthasarathy, N., Djane, N. K. and Matthiasson, L. Permeation liquid membrane for field analysis and speciation of trace compounds in waters. In *In-situ monitoring of aquatic systems: chemical analysis and speciation*, Buffle, J. and Horvai, G., Eds. Wiley: Chichester, **2000**; Vol. 3, pp 408 – 493.

Bulska, E., Baxter, D. C. and Frech, W. **1991**. Capillary column gas-chromatography for mercury speciation, *Analytica Chimica Acta 249*, 545-554.

Cai, Y. and Bayona, J. M. **1995**. Determination of methylmercury in fish and river water samples using in-situ sodium tetraethylborate derivatization following by solid-phase microextraction and gas-chromatography mass-spectrometry, *Journal of Chromatography A 696*, 113-122.

Cai, Y., Jaffe, R. and Jones, R. **1997**. Ethylmercury in the soils and sediments of the Florida Everglades, *Environmental Science & Technology 31*, 302-305.

Cai, Y., Monsalud, S. and Furton, K. G. **2000a**. Determination of methyl- and ethylmercury compounds using gas chromatography atomic fluorescence spectrometry following aqueous derivatization with sodium tetraphenylborate, *Chromatographia 52*, 82-86.

Cai, Y., Monsalud, S., Jaffe, R. and Jones, R. D. **2000b**. Gas chromatographic determination of organomercury following aqueous derivatization with sodium tetraethylborate and sodium tetraphenylborate - Comparative study of gas chromatography coupled with atomic fluorescence spectrometry, atomic emission spectrometry and mass spectrometry, *Journal of Chromatography A 876*, 147-155.

Calvert, J. G. and Lindberg, S. E. **2005**. Mechanisms of mercury removal by O-3 and OH in the atmosphere, *Atmospheric Environment 39*, 3355-3367.

Cambrolle, J., Redondo-Gomez, S., Mateos-Naranjo, E. and Figueroa, M. E. **2008**. Comparison of the role of two Spartina species in terms of phytostabilization and bioaccumulation of metals in the estuarine sediment, *Marine Pollution Bulletin 56*, 2037-2042.

Canario, J., Vale, C. and Caetano, M. **2005**. Distribution of monomethylmercury and mercury in surface sediments of the Tagus Estuary (Portugal), *Marine Pollution Bulletin 50*, 1142-1145.

Capelo, J. L., Lavilla, I. and Bendicho, C. **2000**. Room temperature sonolysis-based advanced oxidation process for degradation of organomercurials: Application to determination of inorganic and total mercury in waters by flow injection-cold vapor atomic absorption spectrometry, *Analytical Chemistry 72*, 4979-4984.

Caricchia, A. M., Minervini, G., Soldati, P., Chiavarini, S., Ubaldi, C. and Morabito, R. **1997**. GC-ECD determination of methylmercury in sediment samples using a SPB-608 capillary column after alkaline digestion, *Microchemical Journal 55*, 44-55.

Carrasco, L., Diez, S. and Bayona, J. M. **2009**. Simultaneous determination of methyl- and ethyl-mercury by solid-phase microextraction followed by gas chromatography atomic fluorescence detection, *Journal of Chromatography A 1216*, 8828-8834.

Carrasco, L., Diez, S., Soto, D. X., Catalan, J. and Bayona, J. M. **2008**. Assessment of mercury and methylmercury pollution with zebra mussel (Dreissena polymorpha) in the Ebro River (NE Spain) impacted by industrial hazardous dumps, *Science of the Total Environment 407*, 178-184.

Cattani, I., Zhang, H., Beone, G. M., Del Re, A. A. M., Boccelli, R. and Trevisan, M. **2009**. The Role of Natural Purified Humic Acids in Modifying Mercury Accessibility in Water and Soil, *Journal of Environmental Quality 38*, 493-501.

Celo, V., Lean, D. R. S. and Scott, S. L. **2006**. Abiotic methylation of mercury in the aquatic environment, *Science of the Total Environment 368*, 126-137.

Centineo, G., Gonzalez, E. B. and Sanz-Medel, A. **2004**. Multielemental speciation analysis of organometallic compounds of mercury, lead and tin in natural water samples by headspace-solid phase microextraction followed by gas chromatography-mass spectrometry, *Journal of Chromatography A 1034*, 191-197.

Chang, L. Y., Davison, W., Zhang, H. and Kelly, M. **1998**. Performance characteristics for the measurement of Cs and Sr by diffusive gradients in thin films (DGT), *Analytica Chimica Acta 368*, 243-253.

Chavan, P. V., Dennett, K. E., Marchand, E. A. and Gustin, M. S. **2007**. Evaluation of small-scale constructed wetland for water quality and Hg transformation, *Journal of Hazardous Materials 149*, 543-547.

Chen, J., Pehkonen, S. O. and Lin, C. J. **2003**. Degradation of monomethylmercury chloride by hydroxyl radicals in simulated natural waters, *Water Research 37*, 2496-2504.

Chung, S. W.-c. and Chan, B. T.-p. **2011**. A reliable method to determine methylmercury and ethylmercury simultaneously in foods by gas chromatography with inductively coupled plasma mass spectrometry after enzymatic and acid digestion, *Journal of Chromatography A 1218*, 1260-1265.

Clarisse, O., Foucher, D. and Hintelmann, H. **2009**. Methylmercury speciation in the dissolved phase of a stratified lake using the diffusive gradient in thin film technique, *Environmental Pollution 157*, 987-993.

Clarisse, O. and Hintelmann, H. **2006**. Measurements of dissolved methylmercury in natural waters using diffusive gradients in thin film (DGT), *Journal of Environmental Monitoring 8*, 1242-1247.

Clarisse, O., Lotufo, G., Hintelmann, H. and Best, E. P. **2010**. DGT as biomonitoring tool to assess methylmercury exposure to *Macoma balthica*, *in preparation*.

Clarisse, O., Lotufo, G. R., Hintelmann, H. and Best, E. P. H. **2012**. Biomonitoring and assessment of monomethylmercury exposure in aqueous systems using the DGT technique, *Science of the Total Environment 416*, 449-454.

Clarkson, T. W. **1997**. The toxicology of mercury, *Critical Reviews in Clinical Laboratory Sciences 34*, 369-403.

Clarkson, T. W. **2002**. The three modern faces of mercury, *Environmental Health Perspectives 110*, 11-23.

Clarkson, T. W. and Magos, L. **2006**. The toxicology of mercury and its chemical compounds, *Critical Reviews in Toxicology 36*, 609-662.

Compeau, G. C. and Bartha, R. **1985**. Sulfate-reducing bacteria – Principal methylators of mercury in anoxic estuarine sediment, *Applied and Environmental Microbiology 50*, 498-502.

Conesa, H. M., Schulin, R. and Nowack, B. **2010**. Suitability of using diffusive gradients in thin films (DGT) to study metal bioavailability in mine tailings: possibilities and constraints, *Environmental Science and Pollution Research 17*, 657-664.

Cotin, J., Garcia-Tarrason, M., Jover, L. and Sanpera, C. **2012**. Are the toxic sediments deposited at Flix reservoir affecting the Ebro river biota? Purple heron eggs and nestlings as indicators, *Ecotoxicology 21*, 1391-1402.

Dahlqvist, R., Zhang, H., Ingri, J. and Davison, W. **2002**. Performance of the diffusive gradients in thin films technique for measuring Ca and Mg in freshwater, *Analytica Chimica Acta 460*, 247-256.

Davey, E. W. and Soper, A. E. **1975**. Apparatus for insitu concentration of trace-metals from seawater, *Limnology and Oceanography 20*, 1019-1023.

Davison, W. and Zhang, H. **1994**. In-Situ Speciation Measurements of Trace Components in Natural-Waters Using Thin-Film Gels, *Nature 367*, 546-548.

de Bolster, M. W. G., Cammack, R., Coucouvanis, D. N., Reedijk, J. and Veeger, C. **1997**. *Glossary of terms used in bioinorganic chemistry*; 6; IUPAC: Great Britain, pp 1251-1303.

De Jonge, H. and Rothenberg, G. **2005**. New device and method for flux-proportional sampling of mobile solutes in soil and groundwater, *Environmental Science & Technology 39*, 274-282.

de la Varga, D., Ruiz, I. and Soto, M. **2013**. Winery Wastewater Treatment in Subsurface Constructed Wetlands with Different Bed Depths, *Water Air and Soil Pollution 224*.

Deacon, G. B. **1978**. Volatilization of methylmercury chloride by hidrogen-sulfide, *Nature 275*, 344.

Deng, B., Xiao, Y., Xu, X., Zhu, P., Liang, S. and Mo, W. **2009**. Cold vapor generation interface for mercury speciation coupling capillary electrophoresis with electrothermal quartz tube furnace atomic absorption spectrometry: Determination of mercury and methylmercury, *Talanta 79*, 1265-1269.

Devries, C. R. and Wang, F. Y. **2003**. In situ two-dimensional high-resolution profiling of sulfide in sediment interstitial waters, *Environmental Science & Technology 37*, 792-797.

Dietz, C., Madrid, Y. and Camara, C. **2001**. Mercury speciation using the capillary cold trap coupled with microwave-induced plasma atomic emission spectroscopy, *Journal of Analytical Atomic Spectrometry 16*, 1397-1402.

Diez-Gil, C., Martinez, R., Ratera, I., Hirsh, T., Espinosa, A., Tarraga, A., Molina, P., Wolfbeis, O. S. and Veciana, J. **2011**. Selective picomolar detection of mercury(II) using optical sensors, *Chemical Communications 47*, 1842-1844.

Diez, S. Human Health Effects of Methylmercury Exposure. In *Reviews of Environmental Contamination and Toxicology, Vol 198*, Whitacre, D. M., Ed. **2009**; Vol. 198, pp 111-132.

Diez, S. and Bayona, J. M. **2002**. Determination of methylmercury in human hair by ethylation followed by headspace solid-phase microextraction-gas chromatography-cold-vapour atomic fluorescence spectrometry, *Journal of Chromatography A 963*, 345-351.

Diez, S. and Bayona, J. M. **2006**. Trace element determination by combining solid-phase microextraction hyphenated to elemental and molecular detection techniques, *Journal of Chromatographic Science 44*, 458-471.

Diez, S. and Bayona, J. M. **2008**. Determination of Hg and organomercury species following SPME: A review, *Talanta 77*, 21-27.

Diez, S., Montuori, P., Querol, X. and Bayona, J. M. **2007**. Total mercury in the hair of children by combustion atomic absorption spectrometry (Comb-AAS), *Journal of Analytical Toxicology 31*, 144-149.

Divis, P., Machat, J., Szkandera, R. and Docekalova, H. **2012**. In situ Measurement of Bioavailable Metal Concentrations at the Downstream on the Morava River using Transplanted Aquatic mosses and DGT Technique, *International Journal of Environmental Research 6*, 87-94.

Docekalova, H. and Divis, P. **2005**. Application of diffusive gradient in thin films technique (DGT) to measurement of mercury in aquatic systems, *Talanta 65*, 1174-1178.

Dombeck, G. D., Perry, M. W. and Phinney, J. T. **1998**. Mass balance on water column trace metals in a free-surface-flow-constructed wetlands in Sacramento, California, *Ecological Engineering 10*, 313-339.

Dotro, G., Castro, S., Tujchneider, O., Piovano, N., Paris, M., Faggi, A., Palazolo, P., Larsen, D. and Fitch, M. **2012**. Performance of pilot-scale constructed wetlands for secondary treatment of chromium-bearing tannery wastewaters, *Journal of Hazardous Materials 239*, 142-151.

Ebinghaus, R., Hintelmann, H. and Wilken, R. D. **1994**. Mercury-cycling in surface waters and in the atmosphere – Species analysis for the investigation of transformation and transport-properties of mercury, *Fresenius Journal of Analytical Chemistry 350*, 21-29.

Eckley, C. S. and Hintelmann, H. **2006**. Determination of mercury methylation potentials in the water column of lakes across Canada, *Science of the Total Environment 368*, 111-125.

Elferink, J. G. R. **1999**. Thimerosal - A versatile sulfhydryl reagent, calcium mobilizer, and cell function-modulating agent, *General Pharmacology 33*, 1-6.

Emteborg, H., Baxter, D. C., Sharp, M. and Frech, W. **1995**. Evaluation, mechanism and application of solid-phase extraction using a dithiocarbamate resin for the sampling and determination of mercury species in humic-rich natural-waters, *Analyst 120*, 69-77.

Emteborg, H., Bjorklund, E., Odman, F., Karlsson, L., Mathiasson, L., Frech, W. and Baxter, D. C. **1996**. Determination of methylmercury in sediments using supercritical fluid extraction and gas chromatography coupled with microwave-induced plasma atomic emission spectrometry, *Analyst 121*, 19-29.

Engstrom, D. R. **2007**. Fish respond when the mercury rises, *Proceedings of the National Academy of Sciences of the United States of America 104*, 16394-16395.

Escudero, L. B., Olsina, R. A. and Wuilloud, R. G. **2013**. Polymer-supported ionic liquid solid phase extraction for trace inorganic and organic mercury determination in water samples by flow injection-cold vapor atomic absorption spectrometry, *Talanta 116*, 133-140.

EU. **1998**. Council Directive 98/83/EC of 3 November 1998 on the quality of water intended for human consumption.

EU. **2000**. Directive 2000/60/EC of the European Parliament and of the Council of 23 October 2000 establishing a framework for Community action in the field of water policy.

EU. **2008**. Directive 2008/105/EC of the European Parliament and the Council of 16 December 2008 on environmental quality standards in the field of water policy.

EU. **2013**. Directive 2013/39/EU of the European Parliament and of the Council of 12 August 2013 amending Directives 2000/60/EC and 2008/105/EC as regards priority substances in the field of water policy

Fan, Z. and Liu, X. **2008**. Determination of methylmercury and phenylmercury in water samples by liquid-liquid-liquid microextraction coupled with capillary electrophoresis, *Journal of Chromatography A 1180*, 187-192.

Fay, L. and Gustin, M. S. **2007**. Investigation of mercury accumulation in cattails growing in constructed wetland mesocosms, *Wetlands 27*, 1056-1065.

Fernandez, C., Conceicao, A. C. L., Rial-Otero, R., Vaz, C. and Capelo, J. L. **2006**. Sequential flow injection analysis system on-line coupled to high intensity focused ultrasound: Green methodology for trace analysis applications as demonstrated for the determination of inorganic and total mercury in waters

and urine by cold vapor atomic absorption spectrometry, *Analytical Chemistry 78*, 2494-2499.

Ferrari, C. P., Gauchard, P. A., Aspmo, K., Dommergue, A., Magand, O., Bahlmann, E., Nagorski, S., Temme, C., Ebinghaus, R., Steffen, A., Banic, C., Berg, T., Planchon, F., Barbante, C., Cescon, P. and Boutron, C. F. **2005**. Snow-to-air exchanges of mercury in an Arctic seasonal snow pack in Ny-Alesund, Svalbard, *Atmospheric Environment 39*, 7633-7645.

Fischer, L., Brunner, M., Prohaska, T. and Hann, S. **2012**. Accurate quantification of mercury in river water by isotope dilution MC-ICP-SFMS and ICP-QMS detection after cold vapour generation, *Journal of Analytical Atomic Spectrometry 27*, 1983-1991.

Fitzgerald, W. F. and Gill, G. A. **1979**. Sub-nanogram determination of mercury by 2-stage gold amalgamation and gas-phase detection applied to atmospheric analysis, *Analytical Chemistry 51*, 1714-1720.

Fitzgerald, W. F. and Lamborg, C. H. Geochemistry of mercury in the environment. In *Treatise on Geochemistry*, Holland, E. D. and Turekian, K. K., Eds. Elsevier–Pergamon: Oxford, **2004**; pp 107–148.

Fleck, J. A., Gill, G., Bergamaschi, B. A., Kraus, T. E. C., Downing, B. D. and Alpers, C. N. **2013**. Concurrent photolytic degradation of aqueous methylmercury and dissolved organic matter, *Science of the Total Environment*.

Fleming, E. J., Mack, E. E., Green, P. G. and Nelson, D. C. **2006**. Mercury methylation from unexpected sources: Molybdate-inhibited freshwater sediments and an iron-reducing bacterium, *Applied and Environmental Microbiology 72*, 457-464.

Fones, G. R., Davison, W., Holby, O., Jorgensen, B. B. and Thamdrup, B. **2001**. High-resolution metal gradients measured by in situ DGT/DET deployment in Black Sea sediments using an autonomous benthic lander, *Limnology and Oceanography 46*, 982-988.

Fritsche, J., Obrist, D. and Alewell, C. **2008**. Evidence of microbial control of Hg-0 emissions from uncontaminated terrestrial soils, *Journal of Plant Nutrition and Soil Science-Zeitschrift Fur Pflanzenernahrung Und Bodenkunde 171*, 200-209.

Gabriel, M. C. and Williamson, D. G. **2004**. Principal biogeochemical factors affecting the speciation and transport of mercury through the terrestrial environment, *Environmental Geochemistry and Health 26*, 421-434.

Gaona, X. **2004**. El mercurio como contaminante global. Desarrollo de metodologías para su determinación en suelos contaminados y estrategias para la reducción de su liberación al medio ambiente. Tesis Doctoral, Universitat Autònoma de Barcelona, Barcelona.

García, J. and Corzo, A. *Depuración con humedales construidos*. Ediciones Universidad Politécnica de Cataluña: Barcelona, **2008**.

Garcia, J., Rousseau, D. P. L., Morato, J., Lesage, E., Matamoros, V. and Bayona, J. M. **2010**. Contaminant Removal Processes in Subsurface-Flow Constructed Wetlands: A Review, *Critical Reviews in Environmental Science and Technology 40*, 561-661.

García, J., Ruíz, A. and Junqueras, X. *Depuración de aguas residuales mediante humedales construidos. Tecnología del Agua*. **1997**; p 165. 58–65.

Gardfeldt, K., Sommar, J., Stromberg, D. and Feng, X. B. **2001**. Oxidation of atomic mercury by hydroxyl radicals and photoinduced decomposition of methylmercury in the aqueous phase, *Atmospheric Environment 35*, 3039-3047.

Geerdink, R. B., Breidenbach, R. and Epema, O. J. **2007**. Optimization of headspace solid-phase microextraction gas chromatography-atomic emission detection analysis of monomethylmercury, *Journal of Chromatography A 1174*, 7-12.

Gil, S., Lavilla, I. and Bendicho, C. **2006**. Ultrasound-promoted cold vapor generation in the presence of formic acid for determination of mercury by atomic absorption spectrometry, *Analytical Chemistry 78*, 6260-6264.

Gil, S., Lavilla, I. and Bendicho, C. **2007**. Green method for ultrasensitive determination of Hg in natural waters by electrothermal-atomic absorption spectrometry following sono-induced cold vapor generation and 'in-atomizer trapping', *Spectrochimica Acta Part B-Atomic Spectroscopy 62*, 69-75.

Gilmour, C. C., Henry, E. A. and Mitchell, R. **1992**. Sulfate stimulation of mercury methylation in fresh-water sediments, *Environmental Science & Technology 26*, 2281-2287.

Gilmour, C. C., Riedel, G. S., Ederington, M. C., Bell, J. T., Benoit, J. M., Gill, G. A. and Stordal, M. C. **1998**. Methylmercury concentrations and production rates across a trophic gradient in the northern Everglades, *Biogeochemistry 40*, 327-345.

Gimpel, J., Zhang, H., Hutchinson, W. and Davison, W. **2001**. Effect of solution composition, flow and deployment time on the measurement of trace metals by the diffusive gradient in thin films technique, *Analytica Chimica Acta 448*, 93-103.

Gochfeld, M. **2003**. Cases of mercury exposure, bioavailability, and absorption, *Ecotoxicology and Environmental Safety 56*, 174-179.

Gorecki, T. and Namiesnik, J. **2002**. Passive sampling, *Trac-Trends in Analytical Chemistry 21*, 276-291.

Gorski, P. R., Armstrong, D. E., Hurley, J. P. and Krabbenhoft, D. P. **2008**. Influence of natural dissolved organic carbon on the bioavailability of mercury to a freshwater alga, *Environmental Pollution 154*, 116-123.

Grandbois, M., Latch, D. E. and McNeill, K. **2008**. Microheterogeneous Concentrations of Singlet Oxygen in Natural Organic Matter Isolate Solutions, *Environmental Science & Technology 42*, 9184-9190.

Greenwood, R., Mills, G. A., Vrana, B., Allan, I., Aguilar-Martínez, R. and Morrison, G. Chapter 9 Monitoring of priority pollutants in water using chemcatcher passive sampling devices. In *Comprehensive Analytical Chemistry*, R. Greenwood, G. M. and Vrana, B., Eds. Elsevier: **2007**; Vol. Volume 48, pp 199-229.

Grigal, D. F. **2002**. Inputs and outputs of mercury from terrestrial watersheds: a review, *Environmental Reviews 10*, 1-39.

Grinberg, P., Campos, R. C., Mester, Z. and Sturgeon, R. E. **2003a**. A comparison of alkyl derivatization methods for speciation of mercury based on solid phase microextraction gas chromatography with furnace atomization plasma emission spectrometry detection, *Journal of Analytical Atomic Spectrometry 18*, 902-909.

Grinberg, P., Campos, R. C., Mester, Z. and Sturgeon, R. E. **2003b**. Solid phase microextraction capillary gas chromatography combined with furnace atomization plasma emission spectrometry for speciation of mercury in fish tissues, *Spectrochimica Acta Part B-Atomic Spectroscopy 58*, 427-441.

Gustin, M. S., Biester, H. and Kim, C. S. **2002**. Investigation of the light-enhanced emission of mercury from naturally enriched substrates, *Atmospheric Environment 36*, 3241-3254.

Gustin, M. S., Chavan, P. V., Dennett, K. E., Donaldson, S., Marchand, E. and Fernanadez, G. **2006**. Use of constructed wetlands with four different experimental designs to assess the potential for methyl and total Hg outputs, *Applied Geochemistry 21*, 2023-2035.

Hall, B. **1995**. The gas-phase oxidation of elemental mercury by ozone, *Water Air and Soil Pollution 80*, 301-315.

Hamelin, S., Amyot, M., Barkay, T., Wang, Y. and Planas, D. **2011**. Methanogens: Principal Methylators of Mercury in Lake Periphyton, *Environmental Science & Technology 45*, 7693-7700.

Hammerschmidt, C. R. and Fitzgerald, W. F. **2006a**. Methylmercury cycling in sediments on the continental shelf of southern New England, *Geochimica Et Cosmochimica Acta 70*, 918-930.

Hammerschmidt, C. R. and Fitzgerald, W. F. **2006b**. Photodecomposition of methylmercury in an arctic Alaskan lake, *Environmental Science & Technology 40*, 1212-1216.

Hammerschmidt, C. R. and Fitzgerald, W. F. **2010**. Iron-Mediated Photochemical Decomposition of Methylmercury in an Arctic Alaskan Lake, *Environmental Science & Technology 44*, 6138-6143.

Hammerschmidt, C. R., Fitzgerald, W. F., Lamborg, C. H., Balcom, P. H. and Tseng, C. M. **2006**. Biogeochemical cycling of methylmercury in lakes and tundra watersheds of Arctic Alaska, *Environmental Science & Technology 40*, 1204-1211.

Han, S., Naito, W., Hanai, Y. and Masunaga, S. **2013**. Evaluation of trace metals bioavailability in Japanese river waters using DGT and a chemical equilibrium model, *Water Research 47*, 4880-4892.

Harper, M. P., Davison, W., Zhang, H. and Tych, W. **1998**. Kinetics of metal exchange between solids and solutions in sediments and soils interpreted from DGT measured fluxes, *Geochimica Et Cosmochimica Acta 62*, 2757-2770.

Harris, H. H., Pickering, I. J. and George, G. N. **2003**. The chemical form of mercury in fish, *Science 301*, 1203-1203.

Hazen, R. M., Golden, J., Downs, R. T., Hystad, G., Grew, E. S., Azzolini, D. and Sverjensky, D. A. **2012**. Mercury (Hg) mineral evolution: A mineralogical record of supercontinent assembly, changing ocean geochemistry, and the emerging terrestrial biosphere, *American Mineralogist 97*, 1013-1042.

Hegazy, A. K., Abdel-Ghani, N. T. and El-Chaghaby, G. A. **2011**. Phytoremediation of industrial wastewater potentiality by Typha domingensis, *International Journal of Environmental Science and Technology 8*, 639-648.

Hempel, M., Hintelmann, H. and Wilken, R. D. **1992**. Determination of organic mercury species in soils by high-performance liquid-chromatography with ultraviolet detection, *Analyst 117*, 669-672.

Henry, E. A., Dodgemurphy, L. J., Bigham, G. N., Klein, S. M. and Gilmour, C. C. **1995**. Total mercury and methylmercury mass-balance in an alkaline, hypereutrophic urban lake (Onondaga lake, NY), *Water Air and Soil Pollution 80*, 509-517.

Heumann, K. G., Rottmann, L. and Vogl, J. **1994**. Elemental speciation with liquid-chromatography inductively-coupled plasma isotope-dilution mass-spectrometry, *Journal of Analytical Atomic Spectrometry 9*, 1351-1355.

Heyes, A., Mason, R. P., Kim, E.-H. and Sunderland, E. **2006**. Mercury methylation in estuaries: Insights from using measuring rates using stable mercury isotopes, *Marine Chemistry 102*, 134-147.

Hijosa-Valsero, M., Fink, G., Schluesener, M. P., Sidrach-Cardona, R., Martin-Villacorta, J., Ternes, T. and Becares, E. **2011**. Removal of antibiotics from urban wastewater by constructed wetland optimization, *Chemosphere 83*, 713-719.

Hines, N. A. and Brezonik, P. L. **2007**. Mercury inputs and outputs at a small lake in northern Minnesota, *Biogeochemistry 84*, 265-284.

Hintelmann, H., Falter, R., Ilgen, G. and Evans, R. D. **1997a**. Determination of artifactual formation of monomethylmercury (CH_3Hg^+) in environmental samples using stable Hg^{2+} isotopes with ICP-MS detection: Calculation of contents applying species specific isotope addition, *Fresenius Journal of Analytical Chemistry 358*, 363-370.

Hintelmann, H., Harris, R., Heyes, A., Hurley, J. P., Kelly, C. A., Krabbenhoft, D. P., Lindberg, S., Rudd, J. W. M., Scott, K. J. and St Louis, V. L. **2002**. Reactivity and mobility of new and old mercury deposition in a Boreal forest ecosystem during the first year of the METAALICUS study, *Environmental Science & Technology 36*, 5034-5040.

Hintelmann, H., Welbourn, P. M. and Evans, R. D. **1997b**. Measurement of complexation of methylmercury(II) compounds by freshwater humic substances using equilibrium dialysis, *Environmental Science & Technology 31*, 489-495.

Hoigne, J. and Bader, H. **1978**. Ozonation of water - Kinetics of oxidation of ammonia by ozone and hydroxyl radicals, *Environmental Science & Technology 12*, 79-84.

Hong, Y. S., Rifkin, E. and Bouwer, E. J. **2011**. Combination of Diffusive Gradient in a Thin Film Probe and IC-ICP-MS for the Simultaneous Determination of CH3Hg+ and Hg2+ in Oxic Water, *Environmental Science & Technology 45*, 6429-6436.

Hongve, D. **1994**. Sunlight degradation of aquatic humic substances, *Acta Hydrochimica Et Hydrobiologica 22*, 117-120.

Horvat, M. Mercury analysis and speciation in environmental samples. In *Global and Regional Mercury Cycles: Sources, Fluxes and Mass Balances*, Baeyens, W., Ebinghaus, R. and Vastiliev, O., Eds. Kluwer Academic Publishers: Dordrecht, The Netherlands, **1996**.

Horvat, M., Byrne, A. R. and May, K. **1990**. A modified method for the determination of methylmercury by gas-chromatography, *Talanta 37*, 207-212.

Horvat, M., Liang, L. and Bloom, N. S. **1993**. Comparison of distillation with other current isolation methods for the determination of methyl mercury-compounds in low-level environmental-samples. 2. Water, *Analytica Chimica Acta 282*, 153-168.

Hu, H. **2000**. Exposure to metals, *Primary Care 27*, 983.

Hursh, J. B., Clarkson, T. W., Cherian, M. G., Vostal, J. J. and Vandermallie, R. **1976**. Clearance of mercury (Hg-197, Hg-203) vapor inhaled by human subjects, *Archives of Environmental Health 31*, 302-309.

Huynh, T. T., Zhang, H., Laidlaw, W. S., Singh, B. and Baker, A. J. M. **2010**. Plant-induced changes in the bioavailability of heavy metals in soil and biosolids assessed by DGT measurements, *Journal of Soils and Sediments 10*, 1131-1141.

IARC. **1997**. *Beryllium, Cadmium, Mercury, and Exposures in the Glass Manufacturing Industry*; International Agency for Research on Cancer, WHO: pp 14-19.

Inoko, M. **1981.** Studies on the photochemical decomposition of organomercurials-methylmercury(II) chloride, *Environmental Pollution Series B − Chemical and physical 2*, 3-10.

Jaffe, D., Prestbo, E., Swartzendruber, P., Weiss-Penzias, P., Kato, S., Takami, A., Hatakeyama, S. and Kajii, Y. **2005**. Export of atmospheric mercury from Asia, *Atmospheric Environment 39*, 3029-3038.

Jansen, S., Blust, R. and Van Leeuwen, H. P. **2002**. Metal speciation dynamics and bioavailability: Zn(II) and Cd(II) uptake by mussel (Mytilus edulis) and carp (Cyprinus carpio), *Environmental Science & Technology 36*, 2164-2170.

Jensen, S. and Jernelov, A. **1969**. Biological methylation of mercury in aquatic organisms, *Nature 223*, 753.

Jian, W. and McLeod, C. W. **1992**. Simple oxidative pretreatment for determination of organomercury by cold vapor atomic fluorescence spectrometry, *Mikrochimica Acta 109*, 117-120.

Jiménez-Moreno, M. **2008**. Desarrollo de métodos analíticos para especiación de mercurio y su aplicación a la comarca de Almadén. Tesis doctoral, Universidad de Castilla-La Mancha, Ciudad Real.

Jimenez-Moreno, M., Perrot, V., Epov, V. N., Monperrus, M. and Amouroux, D. **2013**. Chemical kinetic isotope fractionation of mercury during abiotic methylation of Hg(II) by methylcobalamin in aqueous chloride media, *Chemical Geology 336*, 26-36.

Jitaru, P., Infante, H. G. and Adams, F. C. **2004**. Simultaneous multi-elemental speciation analysis of organometallic compounds by solid-phase microextraction and multicapillary gas chromatography hyphenated to inductively coupled plasma-time-of-flight-mass spectrometry, *Journal of Analytical Atomic Spectrometry 19*, 867-875.

Jonsson, J. A. and Mathiasson, L. **1992**. Supported liquid membrane techniques for sample preparation and enrichment in environmental and biological analysis, *Trac-Trends in Analytical Chemistry 11*, 106-114.

Jordan, M. A., Teasdale, P. R., Dunn, R. J. K. and Lee, S. Y. **2008**. Modelling copper uptake by Saccostrea glomerata with diffusive gradients in a thin film measurements, *Environmental Chemistry 5*, 274-280.

Karlsson, T. and Persson, P. **2012**. Complexes with aquatic organic matter suppress hydrolysis and precipitation of Fe(III). *Chemical Geology 322*, 19-27.

Kehrig, H. A., Palermo, E. F. A., Seixas, T. G., Santos, H. S. B., Malm, O. and Akagi, H. **2009**. Methyl and Total Mercury Found in Two Man-Made Amazonian Reservoirs, *Journal of the Brazilian Chemical Society 20*, 1142-1152.

Kelly, M. G. and Whitton, B. A. **1995**. Trophic diatom index - A new index for monitoring eutrophication in rivers, *Journal of Applied Phycology 7*, 433-444.

Kerin, E. J., Gilmour, C. C., Roden, E., Suzuki, M. T., Coates, J. D. and Mason, R. P. **2006**. Mercury methylation by dissimilatory iron-reducing bacteria, *Applied and Environmental Microbiology 72*, 7919-7921.

Kim, K. H., Lindberg, S. E. and Meyers, T. P. **1995**. Micrometeorological measurements of mercury-vapor fluxes over background forest soils in Eastern Tennessee, *Atmospheric Environment 29*, 267-282.

King, J. K., Harmon, S. M., Fu, T. T. and Gladden, J. B. **2002**. Mercury removal, methylmercury formation, and sulfate-reducing bacteria profiles in wetland mesocosms, *Chemosphere 46*, 859-870.

Kingston, J. K., Greenwood, R., Mills, G. A., Morrison, G. M. and Persson, L. B. **2000**. Development of a novel passive sampling system for the time-averaged measurement of a range of organic pollutants in aquatic environments, *Journal of Environmental Monitoring 2*, 487-495.

Kocman, D., Horvat, M. and Kotnik, J. **2004**. Mercury fractionation in contaminated soils from the Idrija mercury mine region, *Journal of Environmental Monitoring 6*, 696-703.

Kot-Wasik, A., Zabiegala, B., Urbanowicz, M., Dominiak, E., Wasik, A. and Namiesnik, J. **2007**. Advances in passive sampling in environmental studies, *Analytica Chimica Acta 602*, 141-163.

Kotnik, J., Horvat, M., Tessier, E., Ogrinc, N., Monperrus, M., Amouroux, D., Fajon, V., Gibicar, D., Zizek, S., Sprovieri, F. and Pirrone, N. **2007**. Mercury speciation in surface and deep waters of the Mediterranean Sea, *Marine Chemistry 107*, 13-30.

Krabbenhoft, D. P., Hurley, J. P., Olson, M. L. and Cleckner, L. B. **1998**. Diel variability of mercury phase and species distributions in the Florida Everglades, *Biogeochemistry 40*, 311-325.

Kraepiel, A. M. L., Keller, K., Chin, H. B., Malcolm, E. G. and Morel, F. M. M. **2003**. Sources and variations of mercury in tuna, *Environmental Science & Technology 37*, 5551-5558.

Krishna, M. V. B., Ranjit, M., Karunasagar, D. and Arunachalam, J. **2005**. A rapid ultrasound-assisted thiourea extraction method for the determination of inorganic and methyl mercury in biological and environmental samples by CVAAS, *Talanta 67*, 70-80.

Kropfelova, L., Vymazal, J., Svehla, J. and Stichova, J. **2009**. Removal of trace elements in three horizontal sub-surface flow constructed wetlands in the Czech Republic, *Environmental Pollution 157*, 1186-1194.

Lambertsson, L. and Bjorn, E. **2004**. Validation of a simplified field-adapted procedure for routine determinations of methyl mercury at trace levels in natural water samples using species-specific isotope dilution mass spectrometry, *Analytical and Bioanalytical Chemistry 380*, 871-875.

Landner, L. and Reuther, R. *Metals in Society and in the Environment: A Critical Review of Current Knowledge on Fluxes, Speciation, Bioavailability and Risk for Adverse Effects of Copper, Chromium, Nickel and Zinc*. **2004**; Vol. 8, p 407.

Latch, D. E. and McNeill, K. **2006**. Microheterogeneity of singlet oxygen distributions in irradiated humic acid solutions, *Science 311*, 1743-1747.

Lavado, R., Urena, R., Martin-Skilton, R., Torreblanca, A., del Ramo, J., Raldua, D. and Porte, C. **2006**. The combined use of chemical and biochemical markers to assess water quality along the Ebro River, *Environmental Pollution 139*, 330-339.

Lead, J. R., Balnois, E., Hosse, M., Menghetti, R. and Wilkinson, K. J. **1999**. Characterization of Norwegian natural organic matter: Size, diffusion coefficients, and electrophoretic mobilities, *Environment International 25*, 245-258.

Lee, B. G., Griscom, S. B., Lee, J. S., Choi, H. J., Koh, C. H., Luoma, S. N. and Fisher, N. S. **2000**. Influences of dietary uptake and reactive sulfides on metal bioavailability from aquatic sediments, *Science 287*, 282-284.

Lee, Y. H. and Mowrer, J. **1989**. Determination of methylmercury in natural-waters at the sub-nanograms per liter level by capillary gas-chromatography after adsorbent preconcentration, *Analytica Chimica Acta 221*, 259-268.

Leermakers, M., Baeyens, W., Quevauviller, P. and Horvat, M. **2005**. Mercury in environmental samples: Speciation, artifacts and validation, *Trac-Trends in Analytical Chemistry 24*, 383-393.

Lehnherr, I. and Louis, V. L. S. **2009**. Importance of Ultraviolet Radiation in the Photodemethylation of Methylmercury in Freshwater Ecosystems, *Environmental Science & Technology 43*, 5692-5698.

Lehnherr, I., St Louis, V. L., Emmerton, C. A., Barker, J. D. and Kirk, J. L. **2012**. Methylmercury Cycling in High Arctic Wetland Ponds: Sources and Sinks, *Environmental Science & Technology 46*, 10514-10522.

Lehto, N. J., Davison, W., Zhang, H. and Tych, W. **2006**. An evaluation of DGT performance using a dynamic numerical model, *Environmental Science & Technology 40*, 6368-6376.

Leng, G., Feng, L., Li, S.-B., Yang, P. and Dan, D.-Z. **2013**. Speciation Analysis of Mercury in Sediments Using HPLC Hyphenated to Vapor Generation Atomic Fluorescence Spectrometry Following Microwave-Assisted Extraction, *Spectroscopy 28*, 54-67.

Leopold, K., Foulkes, M. and Worsfold, P. J. **2009**. Gold-Coated Silica as a Preconcentration Phase for the Determination of Total Dissolved Mercury in Natural Waters Using Atomic Fluorescence Spectrometry, *Analytical Chemistry 81*, 3421-3428.

Leopold, K., Harwardt, L., Schuster, M. and Schlemmer, G. **2008**. A new fully automated on-line digestion system for ultra trace analysis of mercury in natural waters by means of FI-CV-AFS, *Talanta 76*, 382-388.

Li, Y., Mao, Y., Liu, G., Tachiev, G., Roelant, D., Feng, X., Cai, Y. **2010.** Degradation of methylmercury and its effects on mercury distribution and cycling in the Florida Everglades, *Environmental Science & Technology 44,* 6661-6666.

Liao, C. H., Kang, S. F. and Wu, F. A. **2001**. Hydroxyl radical scavenging role of chloride and bicarbonate ions in the H2O2/UV process, *Chemosphere 44*, 1193-1200.

Lide, D., Ed., *CRC Handbook of Chemistry and Physics*, 85th ed. CRC Press, New York, **2004-2005**.

Lin, C. J. and Pehkonen, S. O. **1999**. The chemistry of atmospheric mercury: a review, *Atmospheric Environment 33*, 2067-2079.

Linak, E. **2009**. *Chemical Economics Handbook on VCM. Chap. 1*; SRI Consulting.

Lindberg, S. E., Meyers, T. P., Taylor, G. E., Turner, R. R. and Schroeder, W. H. **1992**. Atmosphere-surface exchange of mercury in a forest - Results of modeling and gradient approaches, *Journal of Geophysical Research-Atmospheres 97*, 2519-2528.

Lindfors, A., Heikkila, A., Kaurola, J., Koskela, T. and Lakkala, K. **2009**. Reconstruction of Solar Spectral Surface UV Irradiances Using Radiative Transfer Simulations, *Photochemistry and Photobiology 85*, 1233-1239.

Lomonte, C., Gregory, D., Baker, A. J. M. and Kolev, S. D. **2008**. Comparative study of hotplate wet digestion methods for the determination of mercury in biosolids, *Chemosphere 72*, 1420-1424.

Lorenzo, R. A., Vazquez, M. J., Carro, A. M. and Cela, R. **1999**. Methylmercury extraction from aquatic sediments - A comparison between manual, supercritical fluid and microwave-assisted techniques, *Trac-Trends in Analytical Chemistry 18*, 410-416.

Luengen, A. C., Fisher, N. S. and Bergamaschi, B. A. **2012**. Dissolved organic matter reduces algal accumulation of methylmercury, *Environmental Toxicology and Chemistry 31*, 1712-1719.

Luider, C. D., Crusius, J., Playle, R. C. and Curtis, P. J. **2004**. Influence of natural organic matter source on copper speciation as demonstrated by Cu binding to fish gills, by ion selective electrode, and by DGT gel sampler, *Environmental Science & Technology 38*, 2865-2872.

Lv, T., Wu, S., Hong, H., Chen, L. and Dong, R. **2013**. Dynamics of nitrobenzene degradation and interactions with nitrogen transformations in laboratory-scale constructed wetlands, *Bioresource Technology 133*, 529-536.

Lyman, S. N. and Jaffe, D. A. **2012**. Formation and fate of oxidized mercury in the upper troposphere and lower stratosphere, *Nature Geoscience 5*, 114-117.

Ma, X., Yin, Y.-g., Shi, J.-b., Liu, J.-f. and Jiang, G.-b. **2014**. Species-specific isotope dilution-GC-ICP-MS for accurate and precise measurement of methylmercury in water, sediments and biological tissues, *Analytical Methods 6*, 164-169.

Maderova, L., Watson, M. and Paton, G. I. **2011**. Bioavailability and toxicity of copper in soils: Integrating chemical approaches with responses of microbial biosensors, *Soil Biology & Biochemistry 43*, 1162-1168.

Madrid, Y., Cabrera, C., Perezcorona, T. and Camara, C. **1995**. Speciation of methylmercury and Hg(II) using bakers-yeast biomass (*Saccharomyces-cerevisiae*) - Determination by continuous-flow mercury cold vapor generation atomic-absorption spectrometry, *Analytical Chemistry 67*, 750-754.

Maldonado Santoyo, M., Landero Figueroa, J. A., Wrobel, K. and Wrobel, K. **2009**. Analytical speciation of mercury in fish tissues by reversed phase liquid chromatography-inductively coupled plasma mass spectrometry with Bi3+ as internal standard, *Talanta 79*, 706-711.

Mao, Y., Liu, G., Meichel, G., Cai, Y. and Jiang, G. **2008**. Simultaneous speciation of monomethylmercury and monoethylmercury by aqueous phenylation and purge-and-trap preconcentration followed by atomic spectrometry detection, *Analytical Chemistry 80*, 7163-7168.

Marvin-Dipasquale, M. C. and Oremland, R. S. **1998**. Bacterial methylmercury degradation in Florida Everglades peat sediment, *Environmental Science & Technology 32*, 2556-2563.

Mason, R. P. and Fitzgerald, W. F. **1993**. The distribution and biogeochemical cycling of mercury in the equatorial Pacific-ocean, *Deep-Sea Research Part I-Oceanographic Research Papers 40*, 1897-1924.

Mason, R. P. and Lawrence, A. L. **1999**. Concentration, distribution, and bioavailability of mercury and methylmercury in sediments of Baltimore Harbor and Chesapeake Bay, Maryland, USA, *Environmental Toxicology and Chemistry 18*, 2438-2447.

Mason, R. P., Reinfelder, J. R. and Morel, F. M. M. **1995**. Bioaccumulation of mercury and methylmercury, *Water Air and Soil Pollution 80*, 915-921.

Mason, R. P. and Sheu, G. R. **2002**. Role of the ocean in the global mercury cycle, *Global Biogeochemical Cycles 16*.

Matamoros, V., Jover, E. and Bayona, J. M. **2010**. Occurrence and fate of benzothiazoles and benzotriazoles in constructed wetlands, *Water Science and Technology 61*, 191-198.

Matheson, D. S., Clarkson, T. W. and Gelfand, E. W. **1980**. Mercury toxicity (*Acrodynia*) induced by long-term injection of gamma-globulin, *Journal of Pediatrics 97*, 153-155.

Matilainen, T. and Verta, M. **1995**. Mercury methylation and demethylation in aerobic surface waters, *Canadian Journal of Fisheries and Aquatic Sciences 52*, 1597-1608.

Mattson, J. S., Smith, C. A., Jones, T. T., Gerchakov, S. M. and Epstein, B. D. **1974**. Continuous monitoring of dissolved organic-matter by uv-visible photometry, *Limnology and Oceanography 19*, 530–535.

Mburu, N., Tebitendwa, S. M., Rousseau, D. P. L., van Bruggen, J. J. A. and Lens, P. N. L. **2013**. Performance Evaluation of Horizontal Subsurface Flow-Constructed Wetlands for the Treatment of Domestic Wastewater in the Tropics, *Journal of Environmental Engineering-Asce 139*, 358-367.

McGeer, J., Henningsen, G., Lanno, R., Fisher, N., Sappington, K., John Drexler, J. and Beringer, M. **2004**. *Issue paper on the bioavailability and bioaccumulation of metals*; U.S. Environmental Protection Agency: Washington, DC.

Menendez-Garcia, A., Fernández-Sanchez, M. L., Sanchez-Uria, J. E. and Sanz-Medel, A. **1996**. Speciation of mercury by continuous flow liquid-liquid extraction and inductively coupled plasma atomic emission spectrometry detection, *Mikrochimica Acta 122*, 157-166.

Menetrey, N., Oertli, B., Sartori, M., Wagner, A. and Lachavanne, J. B. **2008**. Eutrophication: are mayflies (Ephemeroptera) good bioindicators for ponds?, *Hydrobiologia 597*, 125-135.

Mergler, D., Anderson, H. A., Chan, L. H. M., Mahaffey, K. R., Murray, M., Sakamoto, M. and Stern, A. H. **2007**. Methylmercury exposure and health effects in humans: A worldwide concern, *Ambio 36*, 3-11.

Mester, Z., Sturgeon, R. E. and Lam, J. W. **2000**. Sampling and determination of metal hydrides by solid phase microextraction thermal desorption inductively coupled plasma mass spectrometry, *Journal of Analytical Atomic Spectrometry 15*, 1461-1465.

Miller, C. L., Southworth, G., Brooks, S., Liang, L. and Gu, B. **2009**. Kinetic controls on the complexation between mercury and dissolved organic matter in a contaminated environment, *Environmental Science & Technology 43*, 8548-8553.

Miller, S. M. **2007**. Cleaving C-Hg bonds: two thiolates are better than one, *Nature Chemical Biology 3*, 537-538.

Monperrus, M., Tessier, E., Point, D., Vidimova, K., Amouroux, D., Guyoneaud, R., Leynaert, A., Grall, J., Chauvaud, L., Thouzeau, G. and Donard, O. F. X. **2007**. The biogeochemistry of mercury at the sediment-water interface in the Thau Lagoon. 2. Evaluation of mercury methylation potential in both surface

sediment and the water column, *Estuarine Coastal and Shelf Science 72*, 485-496.

Montuori, P., Jover, E., Diez, S., Ribas-Fito, N., Sunyer, J., Triassi, M. and Bayona, J. M. **2006**. Mercury speciation in the hair of pre-school children living near a chlor-alkali plant, *Science of the Total Environment 369*, 51-58.

Mopper, K. and Zhou, X. L. **1990**. Hydroxyl radical photoproduction in the sea and its potential impact on marine processes, *Science 250*, 661-664.

Mopper, K., Zhou, X. L., Kieber, R. J., Kieber, D. J., Sikorski, R. J. and Jones, R. D. **1991**. Photochemical degradation of dissolved organic-carbon and its impact on the oceanic carbon-cycle, *Nature 353*, 60-62.

Morel, F. M. M., Kraepiel, A. M. L. and Amyot, M. **1998**. The chemical cycle and bioaccumulation of mercury, *Annual Review of Ecology and Systematics 29*, 543-566.

Moreno, F., Garcia-Barrera, T. and Gomez-Ariza, J. L. **2013**. Simultaneous speciation and preconcentration of ultra trace concentrations of mercury and selenium species in environmental and biological samples by hollow fiber liquid phase microextraction prior to high performance liquid chromatography coupled to inductively coupled plasma mass spectrometry, *Journal of Chromatography A 1300*, 43-50.

Morris, D. P., Zagarese, H., Williamson, C. E., Balseiro, E. G., Hargreaves, B. R., Modenutti, B., Moeller, R. and Queimalinos, C. **1995**. The attentuation of solar UV radiation in lakes and the role of dissolved organic carbon, *Limnology and Oceanography 40*, 1381-1391.

Morrison, G. M. P. **1987**. Bioavailable metal uptake rate determination in polluted waters by dialysis with receiving resins, *Environmental Technology Letters 8*, 393-402.

Morton, J. D., Hayes, K. F. and Semrau, J. D. **2000**. Bioavailability of chelated and soil-adsorbed copper to Methylosinus trichosporium OB3b, *Environmental Science & Technology 34*, 4917-4922.

Munksgaard, N. C. and Lottermoser, B. G. **2010**. Mobility and potential bioavailability of traffic-derived trace metals in a 'wet-dry' tropical region, Northern Australia, *Environmental Earth Sciences 60*, 1447-1458.

Murdock, C., Kelly, M., Chang, L. Y., Davison, W. and Zhang, H. **2001**. DGT as an in situ tool for measuring radiocesium in natural waters, *Environmental Science & Technology 35*, 4530-4535.

Myers, G. J., Davidson, P. W., Cox, C., Shamlaye, C. F., Tanner, M. A., Marsh, D. O., Cernichiari, E., Lapham, L. W., Berlin, M. and Clarkson, T. W. **1995**. Summary of the Seychelles Child Development Study on the relationship of fetal methylmercury exposure to neurodevelopment, *Neurotoxicology 16*, 711-715.

Nagase, H., Ose, Y., Sato, T., Ishikawa, T. and Mitani, K. **1980**. Differential determination of alkylmercury and inorganic mercury in river sediment, *International Journal of Environmental Analytical Chemistry 7*, 261-271.

Namiesnik, J., Zabiegala, B., Kot-Wasik, A., Partyka, M. and Wasik, A. **2005**. Passive sampling and/or extraction techniques in environmental analysis: a review, *Analytical and Bioanalytical Chemistry 381*, 279-301.

Navarro, A., Quiros, L., Casado, M., Faria, M., Carrasco, L., Benejam, L., Benito, J., Diez, S., Raldua, D., Barata, C., Bayona, J. M. and Pina, B. **2009**. Physiological responses to mercury in feral carp populations inhabiting the low Ebro River (NE Spain), a historically contaminated site, *Aquatic Toxicology 93*, 150-157.

Ndu, U., Mason, R. P., Zhang, H., Lin, S. and Visscher, P. T. **2012**. Effect of Inorganic and Organic Ligands on the Bioavailability of Methylmercury as Determined by Using a mer-lux Bioreporter, *Applied and Environmental Microbiology 78*, 7276-7282.

Obrist, D. **2007**. Atmospheric mercury pollution due to losses of terrestrial carbon pools?, *Biogeochemistry 85*, 119-123.

Obrist, D., Tas, E., Peleg, M., Matveev, V., Fain, X., Asaf, D. and Luria, M. **2011**. Bromine-induced oxidation of mercury in the mid-latitude atmosphere, *Nature Geoscience 4*, 22-26.

Olsen, S. **1950**. Aquatic plants and hydrospheric factors. I. Aquatic plants in Switzerland, Arizona., *Svensk Botanisk Tidskrift 44*, 1-34.

Ortiz, A. I. C., Albarran, Y. M. and Rica, C. C. **2002**. Evaluation of different sample pre-treatment and extraction procedures for mercury speciation in fish samples, *Journal of Analytical Atomic Spectrometry 17*, 1595-1601.

Padberg, S., Burow, M. and Stoeppler, M. **1993**. Methyl mercury determination in environmental and biological reference and other materials by quality-control with certified reference materials (CRMs), *Fresenius Journal of Analytical Chemistry 346*, 686-688.

Pal, B. and Ariya, P. A. **2004**. Gas-phase HO center dot-Initiated reactions of elemental mercury: Kinetics, product studies, and atmospheric implications, *Environmental Science & Technology 38*, 5555-5566.

Park, C. J. and Do, H. **2008**. Determination of inorganic and total mercury in marine biological samples by cold vapor generation inductively coupled plasma mass spectrometry after tetramethylammonium hydroxide digestion, *Journal of Analytical Atomic Spectrometry 23*, 997-1002.

Park, M., Yoon, H., Yoon, C. and Yu, J.-Y. **2011**. Estimation of mercury speciation in soil standard reference materials with different extraction methods by ion chromatography coupled with ICP-MS, *Environmental Geochemistry and Health 33*, 49-56.

Parker, J. L. and Bloom, N. S. **2005**. Preservation and storage techniques for low-level aqueous mercury speciation, *Science of the Total Environment 337*, 253-263.

Parks, J. M., Johs, A., Podar, M., Bridou, R., Hurt, R. A., Jr., Smith, S. D., Tomanicek, S. J., Qian, Y., Brown, S. D., Brandt, C. C., Palumbo, A. V., Smith, J. C., Wall, J. D., Elias, D. A. and Liang, L. **2013**. The Genetic Basis for Bacterial Mercury Methylation, *Science 339*, 1332-1335.

Peijnenburg, W. and Jager, T. **2003**. Monitoring approaches to assess bioaccessibility and bioavailability of metals: Matrix issues, *Ecotoxicology and Environmental Safety 56*, 63-77.

Pellet, B., Geffard, O., Lacour, C., Kermoal, T., Gourlay-France, C. and Tusseau-Vuillemin, M. H. **2009**. A model predicting waterborne cadmium bioaccumulation in gammarus pulex: the effects of dissolved organic ligands, calcium, and temperature, *Environmental Toxicology and Chemistry 28*, 2434-2442.

Pereira, M. E., Duarte, A. C., Millward, G. E., Abreu, S. N. and Vale, C. **1998**. An estimation of industrial mercury stored in sediments of a confined area of the Lagoon of Aveiro (Portugal), *Water Science and Technology 37*, 125-130.

Persson, L. B., Morrison, G. M., Friemann, J. U., Kingston, J., Mills, G. and Greenwood, R. **2001**. Diffusional behaviour of metals in a passive sampling system for monitoring aquatic pollution, *Journal of Environmental Monitoring 3*, 639-645.

Pichette, C., Zhang, H., Davison, W. and Sauve, S. **2007**. Preventing biofilm development on DGT devices using metals and antibiotics, *Talanta 72*, 716-722.

Pickhardt, P. C. and Fisher, N. S. **2007**. Accumulation of inorganic and methylmercury by freshwater phytoplankton in two contrasting water bodies, *Environmental Science & Technology 41*, 125-131.

Pirrone, N., Cinnirella, S., Feng, X., Finkelman, R. B., Friedli, H. R., Leaner, J., Mason, R., Mukherjee, A. B., Stracher, G. B., Streets, D. G. and Telmer, K. **2010**. Global mercury emissions to the atmosphere from anthropogenic and natural sources, *Atmospheric Chemistry and Physics 10*, 5951-5964.

Polewski, K., Slawinska, D., Slawinski, J. and Pawlak, A. **2005**. The effect of UV and visible light radiation on natural humic acid EPR spectral and kinetic studies, *Geoderma 126*, 291-299.

Qian, J., Skyllberg, U., Frech, W., Bleam, W. F., Bloom, P. R. and Petit, P. E. **2002**. Bonding of methyl mercury to reduced sulfur groups in soil and stream organic matter as determined by X-ray absorption spectroscopy and binding affinity studies, *Geochimica Et Cosmochimica Acta 66*, 3873-3885.

Qvarnstrom, J. and Frech, W. **2002**. Mercury species transformations during sample pre-treatment of biological tissues studied by HPLC-ICP-MS, *Journal of Analytical Atomic Spectrometry 17*, 1486-1491.

Raldua, D. and Pedrocchi, C. **1996**. Mercury concentrations in three species of freshwater fishes from the Lower Gallego and Cinca Rivers, Spain, *Bulletin of Environmental Contamination and Toxicology 57*, 597-602.

Ramalhosa, E., Segade, S. R., Pereira, E., Vale, C. and Duarte, A. **2001**. Simple methodology for methylmercury and inorganic mercury determinations by high-performance liquid chromatography-cold vapour atomic fluorescence spectrometry, *Analytica Chimica Acta 448*, 135-143.

Ramos, L., Fernandez, M. A., Gonzalez, M. J. and Hernandez, L. M. **1999**. Heavy metal pollution in water, sediments, and earthworms from the Ebro River, Spain, *Bulletin of Environmental Contamination and Toxicology 63*, 305-311.

Ravichandran, M. **2004**. Interactions between mercury and dissolved organic matter - a review, *Chemosphere 55*, 319-331.

Rehman, A., Shakoori, F. R. and Shakoori, A. R. **2010**. Resistance and Uptake of Heavy Metals by Vorticella microstoma and Its Potential Use in Industrial Wastewater Treatment, *Environmental Progress & Sustainable Energy 29*, 481-486.

Reid, R. S. and Rabenstein, D. L. **1981**. Nuclear magnetic-resonance studies of the solution chemistry of metal-complexes. 17. Formation-constants for the complexation of methylmercury by sulfhydryl-containing amino-acids and related molecules, *Canadian Journal of Chemistry-Revue Canadienne De Chimie 59*, 1505-1514.

Reyes-Contreras, C., Hijosa-Valsero, M., Sidrach-Cardona, R., Bayona, J. M. and Becares, E. **2012**. Temporal evolution in PPCP removal from urban wastewater by constructed wetlands of different configuration: A medium-term study, *Chemosphere 88*, 161-167.

Rezaee, A., Derayat, J., Mortazavi, S. B., Yamini, Y. and Jafarzadeh, M. T. **2005**. Removal of mercury from chlor-alkali industry wastewater using *Acetobacter xylinum* cellulose, *American Journal of Environmental Sciences 1*, 102-105.

Rezende, M. D. R., Campos, R. C. and Curtius, A. J. **1993**. Speciation of mercury in fish samples by solvent-extraction, methyl-mercury reduction directly in the organic medium and cold vapor atomic-absorption spectrometry, *Journal of Analytical Atomic Spectrometry 8*, 247-251.

Ribeiro, A. S., Vieira, M. A., Willie, S. and Sturgeon, R. E. **2007**. Ultrasound-assisted vapor generation of mercury, *Analytical and Bioanalytical Chemistry 388*, 849-857.

Ridal, J. J., Yanch, L. E., Fowlie, A. R., Razavi, N. R., Delongchamp, T. M., Choy, E. S., Fathi, M., Hodson, P. V., Campbell, L. M., Blais, J. M., Hickey, M. B. C., Yumvihoze, E. and Lean, D. R. S. **2010**. Potential causes of enhanced transfer of mercury to St. Lawrence River Biota: implications for sediment management strategies at Cornwall, Ontario, Canada, *Hydrobiologia 647*, 81-98.

Romaní, A. M., Sabater, S. and Muñoz, I. The Physical Framework and Historic Human Influences in the Ebro River. In *The Ebro River Basin. The Handbook of Environmental Chemistry*, Barceló, D. and Petrovic, M., Eds. Springer-Verlag: Berlin Heidelberg, **2011**; Vol. 13, pp 1-20.

Rosenkranz, B. and Bettmer, J. **2002**. Rapid separation of elemental species by multicapillary GC, *Analytical and Bioanalytical Chemistry 373*, 461-465.

Roulier, J. L., Tusseau-Nuillemin, M. H., Coquery, M., Geffard, O. and Garric, J. **2008**. Measurement of dynamic mobilization of trace metals in sediments using DGT and comparison with bioaccumulation in Chironomus riparius: First results of an experimental study, *Chemosphere 70*, 925-932.

Rozemeijer, J., van der Velde, Y., de Jonge, H., van Geer, F., Broers, H. P. and Bierkens, M. **2010**. Application and Evaluation of a New Passive Sampler for Measuring Average Solute Concentrations in a Catchment Scale Water Quality Monitoring Study, *Environmental Science & Technology 44*, 1353-1359.

Rudd, J. W. M. **1995**. Sources of methyl mercury to fresh-water ecosystems - A review, *Water Air and Soil Pollution 80*, 697-713.

Rumbold, D. G. and Fink, L. E. **2006**. Extreme spatial variability and unprecedented methylmercury concentrations within a constructed wetland, *Environmental Monitoring and Assessment 112*, 115-135.

Safavi, A., Maleki, N. and Doroodmand, M. M. **2010**. Fabrication of a selective mercury sensor based on the adsorption of cold vapor of mercury on carbon nanotubes:

Determination of mercury in industrial wastewater, *Journal of Hazardous Materials 173*, 622-629.

Sánchez-Uria, J. E. and Sanz-Medel, A. **1998**. Inorganic and methylmercury speciation in environmental samples, *Talanta 47*, 509-524.

Sani, A., Scholz, M. and Bouillon, L. **2013**. Seasonal assessment of experimental vertical-flow constructed wetlands treating domestic wastewater, *Bioresource Technology 147*, 585-596.

Santner, J., Prohaska, T., Luo, J. and Zhang, H. **2010**. Ferrihydrite Containing Gel for Chemical Imaging of Labile Phosphate Species in Sediments and Soils Using Diffusive Gradients in Thin Films, *Analytical Chemistry 82*, 7668-7674.

Sanz, J., Raposo, J. C., Larreta, J., Martinez-Arkarazo, I., de Diego, A. and Madariaga, J. M. **2004**. On-line separation for the speciation of mercury in natural waters by flow injection-cold vapour-atomic absorption spectrometry, *Journal of Separation Science 27*, 1202-1210.

Sarica, D. Y. and Turker, A. R. **2012**. Speciation and Determination of Inorganic Mercury and Methylmercury by Headspace Single Drop Microextraction and Electrothermal Atomic Absorption Spectrometry in Water and Fish, *Clean-Soil Air Water 40*, 523-530.

Scally, S., Davison, W. and Zhang, H. **2006**. Diffusion coefficients of metals and metal complexes in hydrogels used in diffusive gradients in thin films, *Analytica Chimica Acta 558*, 222-229.

Schaefer, J. K., Yagi, J., Reinfelder, J. R., Cardona, T., Ellickson, K. M., Tel-Or, S. and Barkay, T. **2004**. Role of the Bacterial Organomercury Lyase (MerB) in Controlling Methylmercury Accumulation in Mercury-Contaminated Natural Waters, *Environmental Science & Technology 38*, 4304-4311.

Scheulhammer, A. M., Meyer, M. W., Sandheinrich, M. B. and Murray, M. W. **2007**. Effects of environmental methylmercury on the health of wild birds, mammals, and fish, *Ambio 36*, 12-18.

Schintu, M., Durante, L., Maccioni, A., Meloni, P., Degetto, S. and Contu, A. **2008**. Measurement of environmental trace-metal levels in Mediterranean coastal areas with transplanted mussels and DGT techniques, *Marine Pollution Bulletin 57*, 832-837.

Schwarze, G. and Schellen, M. **1965**. Die Komplexchemie des Methylquecksilber-Kations, *Helvetica Chimica Acta 48*, 28.

Scott, D. T., McKnight, D. M., Blunt-Harris, E. L., Kolesar, S. E. and Lovely, D. R. **1998**. Quinone moities act as electron acceptors in the reduction of humic substances

by humics-reducing microorganisms, *Environmental Science & Technology 32*, 2984-2989.

Seethapathy, S., Gorecki, T. and Li, X. J. **2008**. Passive sampling in environmental analysis, *Journal of Chromatography A 1184*, 234-253.

Seidel, K. **1966**. Reinigung von Gewassern Durch Hohere Pflanzen, *Naturwissenschaften 53*, 289.

Selin, N. E. **2009**. Global Biogeochemical Cycling of Mercury: A Review, *Annual Review of Environment and Resources 34*, 43-63.

Selin, N. E., Jacob, D. J., Yantosca, R. M., Strode, S., Jaegle, L. and Sunderland, E. M. **2008**. Global 3-D land-ocean-atmosphere model for mercury: Present-day versus preindustrial cycles and anthropogenic enrichment factors for deposition, *Global Biogeochemical Cycles 22*.

Sellers, P., Kelly, C. A. and Rudd, J. W. M. **2001**. Fluxes of methylmercury to the water column of a drainage lake: The relative importance of internal and external sources, *Limnology and Oceanography 46*, 623-631.

Sellers, P., Kelly, C. A., Rudd, J. W. M. and MacHutchon, A. R. **1996**. Photodegradation of methylmercury in lakes, *Nature 380*, 694-697.

Senesi, N. and Schnitzer, M. **1977**. Effects of pH, reaction time, cehmical reduction and irradiation on ESR spectra of fulvic acid, *Soil Science 132*, 224-234.

Serafimovski, I., Karadjova, I., Stafilov, T. and Cvetkovic, J. **2008**. Determination of inorganic and methylmercury in fish by cold vapor atomic absorption spectrometry and inductively coupled plasma atomic emission spectrometry, *Microchemical Journal 89*, 42-47.

Sheoran, A. S. and Sheoran, V. **2006**. Heavy metal removal mechanism of acid mine drainage in wetlands: A critical review, *Minerals Engineering 19*, 105-116.

Shi, J. B., Liang, L. N., Jiang, G. B. and Jin, X. L. **2005**. The speciation and bioavailability of mercury in sediments of Haihe River, China, *Environment International 31*, 357-365.

Sinclair, K. A., Xie, Q. and Mitchell, C. P. J. **2012**. Methylmercury in water, sediment, and invertebrates in created wetlands of Rouge Park, Toronto, Canada, *Environmental Pollution 171*, 207-215.

Skyllberg, U., Qian, J., Frech, W., Xia, K. and Bleam, W. F. **2003**. Distribution of mercury, methyl mercury and organic sulphur species in soil, soil solution and stream of a boreal forest catchment, *Biogeochemistry 64*, 53-76.

Slaveykova, V. I., Karadjova, I. B., Karadjov, M. and Tsalev, D. L. **2009**. Trace Metal Speciation and Bioavailability in Surface Waters of the Black Sea Coastal Area Evaluated by HF-PLM and DGT, *Environmental Science & Technology 43*, 1798-1803.

Slaveykova, V. I., Parthasarathy, N., Buffle, J. and Wilkinson, K. J. **2004**. Permeation liquid membrane as a tool for monitoring bioavailable Pb in natural waters, *Science of the Total Environment 328*, 55-68.

Slemr, F., Brunke, E. G., Ebinghaus, R., Temme, C., Munthe, J., Wangberg, I., Schroeder, W., Steffen, A. and Berg, T. **2003**. Worldwide trend of atmospheric mercury since 1977, *Geophysical Research Letters 30*.

Slemr, F. and Langer, E. **1992**. Increase in global atmospheric concentrations of mercury inferred from measurements over the Atlantic-ocean, *Nature 355*, 434-437.

Southworth, B. A. and Voelker, B. M. **2003**. Hydroxyl radical production via the photo-Fenton reaction in presence of fulvic acid, *Environmental Science & Technology 37*, 1130-1136.

Spain. **2011**. Real Decreto 60/2011, de 21 de enero, sobre las normas de calidad ambiental en el ámbito de la política de aguas.

Stamenkovic, J., Gustin, M. S. and Dennett, K. E. **2005**. Net methyl mercury production versus water quality improvement in constructed wetlands: Trade-offs in pollution control, *Wetlands 25*, 748-757.

Stark, J. S., Johnstone, G. J., Palmer, A. S., Snape, I., Larner, B. L. and Riddle, M. J. **2006**. Monitoring the remediation of a near shore waste disposal site in Antarctica using the amphipod Paramoera walkeri and diffusive gradients in thin films (DGTs), *Marine Pollution Bulletin 52*, 1595-1610.

Stoichev, T., Amouroux, D., Martin-Doimeadios, R. C. R., Monperrus, M., Donard, O. F. X. and Tsalev, D. L. **2006**. Speciation analysis of mercury in aquatic environment, *Applied Spectroscopy Reviews 41*, 591-619.

Suda, I., Suda, M. and Hirayama, K. **1993**. Degradation of methyl and ethyl mercury by singlet oxygen generated from sea-water exposed to sunlight or ultraviolet-light, *Archives of Toxicology 67*, 365-368.

Suda, I., Totoki, S. and Takahashi, H. **1991**. Degradation of methyl and ethyl mercury into inorganic mercury by oxygen free radical-producing systems - Involvement of hydroxyl radical, *Archives of Toxicology 65*, 129-134.

Sun, R., Wang, D., Zhang, Y., Mao, W., Zhang, T., Ma, M. and Zhang, C. **2013**. Photo-degradation of monomethylmercury in the presence of chloride ion, *Chemosphere 91*, 1471-1476.

Sun, Y. C., Chung, Y. T. and Mierzwa, J. **2001**. Study of matrix influence on supercritical fluid extraction of polar mercury species from solid samples, *Analyst 126*, 1694-1699.

Syversen, T. and Kaur, P. **2012**. The toxicology of mercury and its compounds, *Journal of Trace Elements in Medicine and Biology 26*, 215-226.

Tao, S. and Liang, T. **1997**. Long-term monitoring of bioavailable copper in the aquatic environment using a resin-filled dialysis membrane, *Bulletin of Environmental Contamination and Toxicology 58*, 712-719.

Tchounwou, P. B., Ayensu, W. K., Ninashvili, N. and Sutton, D. **2003**. Environmental exposure to mercury and its toxicopathologic implications for public health, *Environmental Toxicology 18*, 149-175.

Teasdale, P. R., Hayward, S. and Davison, W. **1999**. In situ, high-resolution measurement of dissolved sulfide using diffusive gradients in thin films with computer-imaging densitometry, *Analytical Chemistry 71*, 2186-2191.

Telmer, K. and Stapper, D. *A Practical Guide: Reducing Mercury Use in Artisanal and Small-scale Gold Mining*. UNEP: Nairobi, Kenya and Geneva, Switzerland, **2012**.

Telmer, K. H. and Veiga, M. M. World Emissions of Mercury from Artisanal and Small Scale Gold Mining. In *Mercury Fate and Transport in the Global Atmosphere: Emissions, Measurements and Models*, Pirrone, N. and Mason, R., Eds. Springer: New York, **2009**.

Templeton, D. M., Ariese, F., Cornelis, R., Danielsson, L. G., Muntau, H., Van Leeuwen, H. P. and Lobinski, R. **2000**. Guidelines for terms related to chemical speciation and fractionation of elements. Definitions, structural aspects, and methodological approaches (IUPAC Recommendations 2000), *Pure and Applied Chemistry 72*, 1453-1470.

Thayer, J. S. **1989**. Methylation: Its role in the environmental mobility of heavy elements, *Applied Organometallic Chemistry 3*, 123-128.

Tien, C. J. and Chen, C. S. **2013**. Patterns of Metal Accumulation by Natural River Biofilms During Their Growth and Seasonal Succession, *Archives of Environmental Contamination and Toxicology 64*, 605-616.

Tjerngren, I., Karlsson, T., Bjorn, E. and Skyllberg, U. **2012a**. Potential Hg methylation and MeHg demethylation rates related to the nutrient status of different boreal wetlands, *Biogeochemistry 108*, 335-350.

Tjerngren, I., Meili, M., Bjorn, E. and Skyllberg, U. **2012b**. Eight Boreal Wetlands as Sources and Sinks for Methyl Mercury in Relation to Soil Acidity, C/N Ratio, and Small-Scale Flooding, *Environmental Science & Technology 46*, 8052-8060.

Torrens, A., Molle, P., Boutin, C. and Salgot, M. **2009**. Impact of design and operation variables on the performance of vertical-flow constructed wetlands and intermittent sand filters treating pond effluent, *Water Research 43*, 1851-1858.

Truitt, R. E. and Weber, J. H. **1981**. Determination of complexing capacity of fulvic-acid for copper(II) and cadmium(II) by dialysis titration, *Analytical Chemistry 53*, 337-342.

Tseng, C. M., Amouroux, D., Brindle, I. D. and Donard, O. F. X. **2000**. Field cryofocussing hydride generation applied to the simultaneous multi-elemental determination of alkyl-metal(loid) species in natural waters using ICP-MS detection, *Journal of Environmental Monitoring 2*, 603-612.

Tseng, C. M., deDiego, A., Martin, F. M. and Donard, O. F. X. **1997**. Rapid and quantitative microwave-assisted recovery of methylmercury from standard reference sediments, *Journal of Analytical Atomic Spectrometry 12*, 629-635.

Tsui, M. T. K. and Finlay, J. C. **2011**. Influence of Dissolved Organic Carbon on Methylmercury Bioavailability across Minnesota Stream Ecosystems, *Environmental Science & Technology 45*, 5981-5987.

Ullrich, S. M., Tanton, T. W. and Abdrashitova, S. A. **2001**. Mercury in the aquatic environment: A review of factors affecting methylation, *Critical Reviews in Environmental Science and Technology 31*, 241-293.

UNEP. **2002**. *Global Mercury Assessment*; UNEP Chemicals. Inter-organization programme for the sound management of chemicals.

UNEP. **2008**. *The Global Atmospheric Mercury Assessment: Sources, Emissions and Transport.*; UNEP Chemicals Branch: Geneva, Switzerland.

UNEP. **2010**. *Study on the possible effects on human health and the environment in Asia and the Pacific of the trade of products containing cadmium, lead and mercury.*; UNEP Chemicals Branch: Geneva, Switzerland.

UNEP. **2013**. *Global Mercury Assessment 2013: Sources, Emissions, Releases and Environmental Transport.*; UNEP Chemicals Branch: Geneva, Switzerland.

USEPA. **2000**. *Constructed wetlands treatment of municipal wastewaters. EPA 625-R-99-010.*

USEPA. **2002**. *Method 1631, Revision E: Mercury in Water by Oxidation, Purge and Trap and Cold Vapor Atomic Fluorescence Spectrometry*.

Van der Veeken, P. L. R., Chakraborty, P. and Van Leeuwen, H. P. **2010**. Accumulation of Humic Acid in DET/DGT Gels, *Environmental Science & Technology 44*, 4253-4257.

Vaughan, P. P. and Blough, N. V. **1998**. Photochemical formation of hydroxyl radical by constituents of natural waters, *Environmental Science & Technology 32*, 2947-2953.

Vermillion, B. R. and Hudson, R. J. M. **2007**. Thiourea catalysis of MeHg ligand exchange between natural dissolved organic matter and a thiol-functionalized resin: a novel method of matrix removal and MeHg preconcentration for ultratrace Hg speciation analysis in freshwaters, *Analytical and Bioanalytical Chemistry 388*, 341-352.

Vigneault, B., Percot, A., Lafleur, M. and Campbell, P. G. C. **2000**. Permeability changes in model and phytoplankton membranes in the presence of aquatic humic substances, *Environmental Science & Technology 34*, 3907-3913.

von Canstein, H., Li, Y., Timmis, K. N., Deckwer, W. D. and Wagner-Dobler, I. **1999**. Removal of mercury from chloralkali electrolysis wastewater by a mercury-resistant Pseudomonas putida strain, *Applied and Environmental Microbiology 65*, 5279-5284.

Vrana, B., Mills, G. A., Allan, I. J., Dominiak, E., Svensson, K., Knutsson, J., Morrison, G. and Greenwood, R. **2005**. Passive sampling techniques for monitoring pollutants in water, *Trac-Trends in Analytical Chemistry 24*, 845-868.

Vymazal, J. **2011**. Constructed Wetlands for Wastewater Treatment: Five Decades of Experience, *Environmental Science & Technology 45*, 61-69.

Vymazal, J., Brix, H., Cooper, P. F. and Green, M. B. *Constructed Wetlands for Wastewater Treatment in Europe*. Backhuys Publishers: Leiden, The Netherlands, **1998**; p 366.

Vymazal, J., Kropfelova, L., Svehla, J., Chrastny, V. and Stichova, J. **2009**. Trace elements in Phragmites australis growing in constructed wetlands for treatment of municipal wastewater, *Ecological Engineering 35*, 303-309.

Vymazal, J., Kropfelova, L., Svehla, J. and Stichova, J. **2010**. Can multiple harvest of aboveground biomass enhance removal of trace elements in constructed wetlands receiving municipal sewage?, *Ecological Engineering 36*, 939-945.

Waples, J. S., Nagy, K. L., Aiken, G. R. and Ryan, J. N. **2005**. Dissolution of cinnabar (HgS) in the presence of natural organic matter, *Geochimica Et Cosmochimica Acta 69*, 1575-1588.

Warnken, K. W., Davison, W. and Zhang, H. **2008**. Interpretation of in situ speciation measurements of inorganic and organically complexed trace metals in freshwater by DGT, *Environmental Science & Technology 42*, 6903-6909.

Warnken, K. W., Davison, W., Zhang, H., Galceran, J. and Puy, J. **2007**. In situ measurements of metal complex exchange kinetics in freshwater, *Environmental Science & Technology 41*, 3179-3185.

Watras, C. J., Morrison, K. A., Kent, A., Price, N., Regnell, O., Eckley, C., Hintelmann, H. and Hubacher, T. **2005**. Sources of methylmercury to a wetland-dominated lake in northern Wisconsin, *Environmental Science & Technology 39*, 4747-4758.

Weiner, J. G., Krabbenhoft, D. P., Heinz, G. H. and Scheuhammer, A. M. Ecotoxicology of mercury. In *Handbook of Ecotoxicology*, Hoffman, D. J., Rattner, B. A., Burton, G. A. and Cairns, J., Eds. Lewis Publishers: Boca Raton, FL, USA, **2003**; pp 409-463.

Weishaar, J. L., Aiken, G. R., Bergamaschi, B. A., Fram, M. S., Fujii, R. and Mopper, K. **2003**. Evaluation of specific ultraviolet absorbance as an indicator of the chemical composition and reactivity of dissolved organic carbon, *Environmental Science & Technology 37*, 4702-4708.

Westoo, G. **1966**. Determination of methylmercury compounds in foodstuffs. I. Methylmercury compounds in fish identification and determination, *Acta Chemica Scandinavica 20*, 2131.

White, E. M., Vaughan, P. P. and Zepp, R. G. **2003**. Role of the photo-Fenton reaction in the production of hydroxyl radicals and photobleaching of colored organic matter in a cosatal river of the southeast United States, *Aquatic Sciences 65*, 402-414.

WHO. **1989**. *Environmental Health Criteria 86: Mercury-Environmental Aspect*; Seventh Wolrd Health Organization Convention.

WHO. **1990**. *Environmental Helth Criteria 101. Methylmercury*; International Program on Chemical Safety.

WHO. **1993**. *Guidelines for Drinking-water Quality. Second edition*; World Health Organization: Geneva, Switzerland.

WHO. **2008**. *Guidelines for Drinking-water Quality. Third edition*; World Health Organization: Geneva, Switzerland.

Williamson, C. E., Stemberger, R. S., Morris, D. P., Frost, T. M. and Paulsen, S. G. **1996**. Ultraviolet radiation in North American lakes: Attenuation estimates from DOC measurements and implications for plankton communities, *Limnology and Oceanography 41*, 1024-1034.

Wolfe, M. F., Schwarzbach, S. and Sulaiman, R. A. **1998**. Effects of mercury on wildlife: A comprehensive review, *Environmental Toxicology and Chemistry 17*, 146-160.

Worms, I., Simon, D. F., Hassler, C. S. and Wilkinson, K. J. **2006**. Bioavailability of trace metals to aquatic microorganisms: importance of chemical, biological and physical processes on biouptake, *Biochimie 88*, 1721-1731.

Wu, R. S. S. and Lau, T. C. **1996**. Polymer-ligands: A novel chemical device for monitoring heavy metals in the aquatic environments, *Marine Pollution Bulletin 32*, 391-396.

Wurl, O., Elsholz, O. and Ebinghaus, R. **2000**. Flow system device for the on-line determination of total mercury in seawater, *Talanta 52*, 51-57.

Yin, X.-B. **2007**. Dual-cloud point extraction as a preconcentration and clean-up technique for capillary electrophoresis speciation analysis of mercury, *Journal of Chromatography A 1154*, 437-443.

Yu, L. P. and Yan, X. P. **2003**. Factors affecting the stability of inorganic and methylmercury during sample storage, *Trac-Trends in Analytical Chemistry 22*, 245-253.

Zabiegala, B., Kot-Wasik, A., Urbanowicz, M. and Namiesnik, J. **2010**. Passive sampling as a tool for obtaining reliable analytical information in environmental quality monitoring, *Analytical and Bioanalytical Chemistry 396*, 273-296.

Zachariadis, G. A., Anthemidis, A. N., Daftsis, E. I. and Stratis, J. A. **2005**. On-line speciation of mercury and methylmercury by cold vapour atomic absorption spectrometry using selective solid phase extraction, *Journal of Analytical Atomic Spectrometry 20*, 63-65.

Zepp, R., Faust, B. C. and Holgné, J. **1992a**. Hydroxyl radical formation in aqueeous reactions (pH 3-8) of iron(II) with hydrogen peroxide. The photo-Fenton reaction., *Environmental Science & Technology 26*, 313-319.

Zepp, R., Faust, B. C. and Holgné, J. **1992b**. Hydroxyl radical formation in aqueeous reactions (pH 3-8) of iron(II) with hydrogen peroxide. The photo-Fenton reaction., *Environmental Science & Technology 26*, 313-319.

Zepp, R. G., Hoigne, J. and Bader, H. **1987**. Nitrate-induced photooxidation of trace organic-chemicals in water, *Environmental Science & Technology 21*, 443-450.

Zepp, R. G., Schlotzhauer, P. F. and Sink, R. M. **1985**. Photosensitized transformations involving electronic energy transfer in natural waters: Role of humic substances, *Environmental Science & Technology 19*, 74-81.

Zhang, H. and Davison, W. **1995**. Performance-Characteristics of Diffusion Gradients in Thin-Films for the in-Situ Measurement of Trace-Metals in Aqueous-Solution, *Analytical Chemistry 67*, 3391-3400.

Zhang, H. and Davison, W. **1999**. Diffusional characteristics of hydrogels used in DGT and DET techniques, *Analytica Chimica Acta 398*, 329-340.

Zhang, H. and Davison, W. **2000**. Direct in situ measurements of labile inorganic and organically bound metal species in synthetic solutions and natural waters using diffusive gradients in thin films, *Analytical Chemistry 72*, 4447-4457.

Zhang, H., Davison, W., Gadi, R. and Kobayashi, T. **1998**. In situ measurement of dissolved phosphorus in natural waters using DGT, *Analytica Chimica Acta 370*, 29-38.

Zhang, H., Davison, W. and Ottley, C. **1999**. Remobilisation of major ions in freshly deposited lacustrine sediment at overturn, *Aquatic Sciences 61*, 354-361.

Zhang, T. and Hsu-Kim, H. **2010a**. Photodegradation of methylmercury is enhanced by complexation with thiol-containing natural organics, *Geochimica Et Cosmochimica Acta 74*, 1213.

Zhang, T. and Hsu-Kim, H. **2010b**. Photolytic degradation of methylmercury enhanced by binding to natural organic ligands, *Nature Geoscience 3*, 473-476.

Zheng, C. B., Li, Y., He, Y. H., Ma, Q. and Hou, X. D. **2005**. Photo-induced chemical vapor generation with formic acid for ultrasensitive atomic fluorescence spectrometric determination of mercury: potential application to mercury speciation in water, *Journal of Analytical Atomic Spectrometry 20*, 746-750.

Zibordi, G., Hooker, S. B., Mueller, J. and Lazin, G. **2004**. Characterization of the immersion factor for a series of in-water optical radiometers, *Journal of Atmospheric and Oceanic Technology 21*, 501-514.

Zierhut, A., Leopold, K., Harwardt, L. and Schuster, M. **2010**. Analysis of total dissolved mercury in waters after on-line preconcentration on an active gold column, *Talanta 81*, 1529-1535.